# Modelling the Thermal Performance of Complex Glazing Systems

**PhD Thesis**

**Anastasia Mylona**

**Welsh School of Architecture**
**Cardiff University**

May 2007




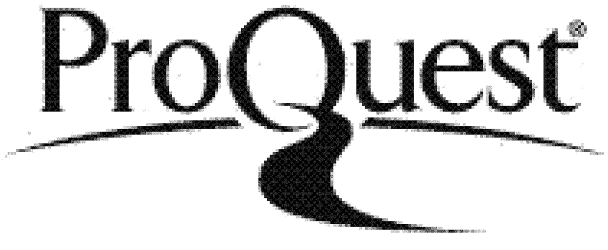


ProQuest LLC
789 East Eisenhower Parkway
P.O. Box 1346
Ann Arbor, MI 48106-1346

Form: PG/R/06/09

CARDIFF UNIVERSITY
PRIFYSGOL CAERDYDD

**APPENDIX 1:**
**Specimen Layout for Thesis Summary and Declaration/Statements page to be included in a Thesis**

**DECLARATION**

This work has not previously been accepted in substance for any degree and is not concurrently submitted in candidature for any degree.

Signed ..... (candidate) Date 24/5/2007

**STATEMENT 1**

This thesis is being submitted in partial fulfillment of the requirements for the degree of PhD (insert MCh, MD, MPhil, PhD etc, as appropriate)

Signed ..... (candidate) Date 24/5/2007

**STATEMENT 2**

This thesis is the result of my own independent work/investigation, except where otherwise stated.
Other sources are acknowledged by explicit references.

Signed ..... (candidate) Date 24/5/2007

**STATEMENT 3**

I hereby give consent for my thesis, if accepted, to be available for photocopying and for inter-library loan, and for the title and summary to be made available to outside organisations.

Signed ..... (candidate) Date 24/5/2007

**STATEMENT 4 - BAR ON ACCESS APPROVED**

I hereby give consent for my thesis, if accepted, to be available for photocopying and for inter-library loans **after expiry of a bar on access** approved by the Graduate Development Committee.

Signed ..... (candidate) Date 24/5/2007

## Summary

The aim of this research is to investigate the thermal performance of various shaded glazing options through the use of thermal modelling in order to reduce solar gains and as a result cooling loads in buildings.
The review of early and recent research on the study of the radiation transport through glazing systems with slat-type blinds, and the more recent development of prediction tools, identified the elements affecting the thermal performance of various glazing systems, as well as the current needs in the calculation of the performance of such complex systems. The review demonstrated that no established and validated methodology is offering the flexibility that the study of the thermal performance of complex glazing systems with integrated slat-type shading is requiring. In order to serve the objectives of this work two existing simulation packages were selected and modified in order to better represent the properties of the various glazing systems and to examine their performance in a more holistic approach.
The review of the calculation of the total solar transmittance, g-value, currently used as a representation of the performance of the various glazing systems, revealed that the variables that influence the g-value and so the thermal performance of a glazing system are the incident solar radiation, the optical and thermal properties of the glazing system and its components, and the temperature difference between internal and external environment, while it excludes any heat losses through the system. Introduced was a steady-state G-value to describe the thermal performance of different glazing systems under steady-state conditions and a dynamically calculated $\hat{g}_d$ value under real climate conditions.

The selected prediction tools were validated by comparing results against a validated reference model and measurements under real climate conditions. Results showed that although there is scope for further improvements in the calculation of the transmission characteristics of slat-type blind configurations, the prediction tools were able to distinguish between basic design alternatives, in the choice of similar shaded glazing options, in a sufficient to many applications in the design industry level of accuracy.

The tools were applied to a variety of shaded glazing systems, under both steady-state and real climate conditions for three locations. The results showed that lower g-values could be achieved by higher slat angles (e.g. 70°) and light colour blind material, while externally positioned blinds seem to be performing thermally better. Examples demonstrated that the above trends could be reversed if the performance of the various glazing systems is not carefully examined. The g-value also showed a high dependency on the angle of incidence, with higher values presented at angles of incident closer to normal and lower values at higher angles of incident. The above dependency of the g-value on solar angles revealed also the $\hat{g}_d$ value's seasonal and latitude dependency.
Comparisons undertaken between the steady-state G and the dynamically calculated $\hat{g}_d$, and also between predicted cooling loads, for keeping desirable internal temperatures in an office space, and both G and $\hat{g}_d$, highlighted the potential of the steady-state G to misinform the designer on the choice of glazing system, while the dynamically calculated $\hat{g}_d$ is a more reliable indicator of the thermal performance of the various glazing systems, in practice.
Examined was also the influence of various glazing systems on the performance of an energy efficient cooling system (chilled ceiling) in keeping desirable internal temperatures and preventing condensation levels, in a case study application. The performance of the chilled ceiling cooling system showed to be affected by the choice of glazing/blind option, but greater, in terms of both condensation and temperature control, was the effect of infiltration rates.

# Acknowledgements

First of all I would like to thank my two supervisors, Professor Phil Jones and Mr Don Alexander of the Welsh School of Architecture, for their constant support, direction and faith in this research project, even when things were not going so well. Their knowledge and ideas had a great influence on this work.

I would also like to thank Lund University and especially Bengt Hellstrom from the Department of Construction and Architecture (Energy and Building Design, Lund Institute of Technology) for providing the weather data for the simulations undertaken during the validation of the tool used in this work.

It was a great pleasure to work with everybody in the Welsh School of Architecture. A big thanks to Katrina Lewis and Annie Pitchford for making the extra effort when help was needed, to Sylvia Harris for being a great librarian and to Julie Gwilliam for being a great friend, colleague and "boss", always looking out for me.

I would also like to say a great thank you to the Alumni office of Cardiff University for being my "home" for three years, and especially to Sarah Price for being much more than a boss, always showing understanding when the research had to come first.

Many thanks to my current work colleagues at UK Climate Impacts Programme, Oxford University, for their constant support over the last year and for believing in me much more than I believed in myself and also to Dr Vic Crisp for reading the thesis and giving me very valuable feedback.

Last but not least I would like to thank my friends and family for their patience and constant faith in me and most of all Steve for enjoying life together with me. I wouldn't have made it without him.

# Contents

# Symbol Index

The symbols used within this work are defined as follows:

A: fixed background infiltration flow rate ($m^3/s$) (e.g. for mechanically aided ventilation),

a: absorption of glazing system

Abs: absorption of blind

$A_v'$: effective area of openings calculated by the equation: $A_v' = (1/A_1^2 + 1/A_2^2)^{-0.5}$

$A_v$: total area of openings calculated by the equation: $A_v = A_1 + A_2$ ($m^2$)

$A_w$: window area ($m^2$)

$A_1$: area of air inlet ($m^2$)

$A_2$: area of air outlet ($m^2$)

B: wind component of the cavity flow rate

C: stack effect component of the cavity flow rate

$C_d$: theoretical value of the discharge coefficient

D: multiplier that can be varied depending on the control strategy of the glazing system, (If D is set to 0 there is no ventilation and the cavity behaves as a normal cavity)

$\Delta T$: temperature difference between the cavity mean temperature and the entering air (K)

E: incident solar radiation ($W/m^2$)

$E_{h,s}$ : heating load for the month with incident solar radiation through the window glass area ($W/m^2$)

$E_{h,n}$ : heating load for the month without incident solar radiation ($W/m^2$)

$E_{c,s}$ : cooling load for the month with incident solar radiation through the window glass area ($W/m^2$)

$E_{c,n}$ : cooling load for the month without incident solar radiation ($W/m^2$)

$\Phi$: transmitted total energy flow ($W/m^2$)

G: incident solar radiation on the window glass area ($W/m^2$)

Gs: incident solar radiation ($W/m^2$)

G-value: total solar transmittance calculated under steady-state conditions

g: acceleration due to gravity (9.8 $m/s^2$)

g-value: total solar transmittance or solar factor

$\hat{g}_d$ values: total solar transmittance dynamically calculated under real climate conditions

$g_{eff}$: effective total solar transmittance

$g_{exp}$: experimental estimate of total solar transmittance

H: window height (m)

HG: heat gain to the room ($W/m^2$)

$\tau_s$: g-value (ISO standard)

$I_s$: incident solar radiation ($W/m^2$)

$I_G$: global solar radiation on the window ($W/m^2$)

I: total radiant solar gain through the glazing (direct and diffuse) ($W/m^2$)

Is: external solar irradiance normal to the glazing ($W/m^2$)

i: angle of incidence of the solar radiation (for vertical openings: $\cos(i) = \cos(\gamma) \cos(a-\varphi)$, where $\varphi$ is the azimuth of the normal to the window)

Le(γ,a): amount of radiation, per unit solid angle, coming from direction (γ,a) during the time of year for which there is an overheating risk. It includes radiation that comes directly from the sun (for the given (γ,a)) and that is diffused from the sky

Q: air flow rate through a cavity ($m^3/s$)

$Q_{capacity}$: correction term for the heat capacity of the box with respect to changes in the box temperature during the measurement period (W)

$Q_{cool}$: measured cooling energies (W) (for keeping the temperature in the experimental box steady)

$Q_{el.heat}$: measured heating energies (W) (for keeping the temperature in the experimental box steady)

$Q_s$: convective and long-wave radiant heat exchange from the internal surface of the glazing as a result of solar incidence ($W/m^2$)

$Q_s'$: convective and long-wave radiant heat exchange from the internal surface of the glazing under identical conditions except with no solar irradiance, achieved through a second simulation ($W/m^2$)

$Q_{sun}$ : heat balance of the experimental box (W)

$Q_{room}$: heat losses from the experimental box to the room (W) (where the box was placed)

$Q_v$: ventilative heat flow inside the room due to ventilated layer as a result of solar incidence ($W/m^2$), and

$Q'_v$: ventilative heat flow inside the room due to ventilated layer without solar incidence ($W/m^2$)

$Q_w$: ventilation rates in the cavity due to stack effect ($m^3/s$)

$Q_{window}$: heat losses through the window (W)

$q_i$: secondary heat transfer factor

$q_{int}$: net density of heat flow rate through the glazing system to the internal environment ($W/m^2$)

$q_{int}$ ($I_s = 0$): net density of heat flow rate through the glazing system to the internal environment, but without incident solar radiation ($W/m^2$)

RH: relative humidity

$R_{diff}$: diffuse reflection of blind system

$R_{spec}$: specular reflection of blind system

r: altitude of the patch of sky under consideration and a its azimuth

$r_{dif,dif}$: diffuse radiation reflected (diffuse to diffuse reflection)

$r_{dir,dif}$: reflected towards the outside solar radiation (direct to diffuse reflection)

$r_{dir,dir}$: reflected towards the outside solar radiation (direct to direct reflection) for perfectly specular surfaces

SHGC: solar heat gain coefficient

SC: shading coefficient

T: direct solar transmittance

T(γ,a): transmittance of the window (with shading device) to radiation from this direction (it is a directional/hemispherical transmittance)

$T_c$: cavity mean temperature (K)

$T_{diff}$: diffuse transmittance of blind system

$t_e$: solar direct transmittance

$\tau_{dif,dif}$: diffuse radiation transmitted (diffuse to diffuse transmittance)

$\tau_{dir,dif}$: transmitted after reflection solar radiation (direct to diffuse transmittance)

$\tau_{dir,dir}$: directly transmitted solar radiation (direct to direct transmittance)

U-value: thermal transmittance ($W/m^2K$)

u: wind speed (m/s)

# Chapter 1

# Research Overview

## *1.1 Overview*

Chapter 1 presents the problem this research is going to address. The historical background of glass as a building material and its use in highly glazed buildings will be reviewed briefly, including problems associated with such buildings and how this research will attempt to approach them. This chapter will also present the aim and objectives of this research and the proposed methodology for their achievement. The outline of the structure of the thesis with a summary of all the chapters and their individual sections will also be briefly reviewed in this chapter.

## *1.2 Historical Background and Necessity of the Current Research*

Glass is a material widely used today in office buildings (figures 3 & 4). Due to its aesthetic qualities and its transparency, glass offers visual contact with the outside and daylight during the working hours of the day, creating a healthy and stimulating living and working environment for the occupants (figures 1 & 2) (Bell and Burt, 1996; Littlefair et al, 2001; Muneer et al, 2000).

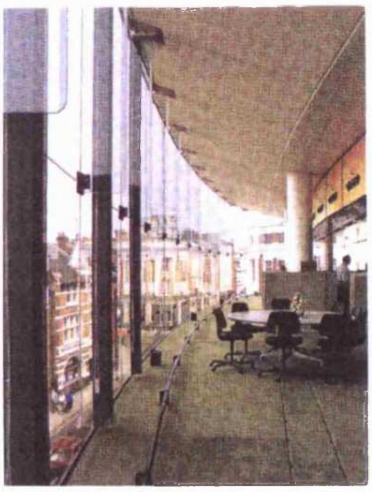

Figures 1 & 2: Interior of highly glazed buildings

Figure 3: Commerz Bank HQ

Figure 4: RWE HQ

Since the beginning of the nineteenth century, when framed building structures were introduced (figures 5 & 6), glass has become a material widely used in the external

envelop of buildings. Even though glass has many advantages as a material (daylight, low cost construction, open plans, modern aesthetics), soon highly glazed buildings had to face constrains imposed by building physics and comfort. Glass's low thermal resistance as a material increased the permeability of the building's envelope to heat transfer, creating an internal environment directly dependant to the external climatic conditions. This had as a result the increasing use of air conditioning for cooling and heating in order to achieve acceptable environmental conditions and as a result high energy consumption in highly glazed buildings. Furthermore, the acoustical performance was poor while air, water and a general lack of weather tightness of the connections between glass and metal frame, caused high infiltration rates as well as condensation and corrosion of the glass and the metal elements.

Figure 5: Reliance Building, Chicago, 1894

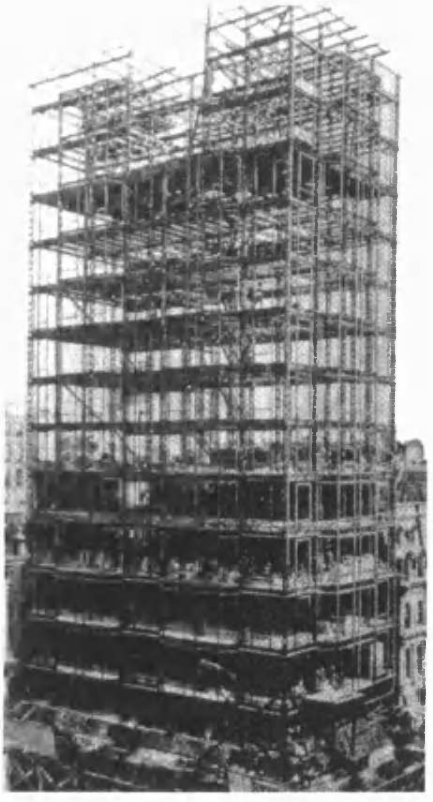

Figure 6: Steel construction

Advanced construction and material technology introduced new glazing systems resistant to fire, wind and thermal stress, condensation and noise proof sealed double pane window systems, low-E glass coatings, integrated shading techniques with manual or automatic controls and gas filled gaps. Due to the above technological advances glass has become a popular material towards energy efficient buildings. The development of windows with low U-values and thus low energy losses made possible the use of large glazed surfaces in buildings avoiding problems such as draughts and high heating costs during the winter months. Also the exploitation of the sun as a renewable energy source for natural lighting during the day, all year round, minimises the use of energy for electric lighting and improves the quality of the indoor environment (Kristensen and Rodot, 1994). The above is especially true in commercial buildings (Lewis and Rodot, 1994) where large window areas and atria are being increasingly introduced and fully glazed facades are being designed as the building's external skin in order to make the most of the natural lighting during daytime.

However, there are still problems associated with highly glazed buildings such as high solar gains which can result in overheating and excessive use of air conditioning (Littlefair, 2005 and CIBSE, 2006).

The use of advanced glazing such as tinted, laminated or patterned glass can reduce solar gains but also reduce the amount of natural light coming into the room, especially in overcast conditions (figures 7 & 8) (Littlefair, 1999; Pfrommer et al, 1995). The use of flexible shading techniques integrated in the glazing system can provide solutions towards controlling the solar gains while maximising the availability of natural daylight (figure 9 & 10) (Littlefair, 1999; Littlefair, 2005; Bell & Burt, 1996), but they are usually considered as an emergency measure after the occurrence of overheating problems and high cooling loads.

Figures 7 & 8: Glazed façade with tinted glass

Figure 9: TAD HQ

Figure 10: Siemens Pavilion

In order to avoid overheating and high energy consumption in highly glazed buildings, the knowledge of the thermal performance of the external envelop of the building is of a primary importance during the design stage. Advanced tools are needed to predict the thermal performance of a variety of glazing options available in the market under real climate conditions and throughout the year, and taking under consideration the environmental system of the building.

This work investigates the thermal performance of various multilayered shaded glazing options by the use of computerised prediction tools also developed and validated as part of this research. The thermal performance of the various glazing systems will be illustrated as embodied by their total solar transmittance or solar factor, g-value. The total solar transmittance g-value incorporates both the direct and diffuse solar radiation transmitted through the glass and the secondary heat transmitted to the inside of the room as a result of radiation, convective and long-wave (EN 410, 1998). The g-values of various glazing systems are often published by glazing manufacturers (Saint-Gobain, 2000 and Pilkington, 2000) and they are determined through simulation or are measured in laboratory facilities according to international standards in order to provide a standardized value that can describe and compare different glazing systems.

## *1.3 Aim, objectives and methodology*

### 1.3.1 Research question

This research intent to give an answer to the following question: "How is it possible for designers to examine the impact of glazing/shading solutions on solar gains and cooling loads?"

### 1.3.2 Aim

The overall aim of this work is to investigate the thermal performance of various shaded glazing options through the use of thermal modelling in order to reduce solar gains and as a result cooling loads in buildings. To achieve that goal a series of objectives were set:

### 1.3.3 Objectives

- Through the review of past and recent research identify the elements most important in shaping the thermal performance of various glazing systems and the

current needs in the calculation of such performance in order to be used as a designer's tool in the choice of glazing solution.

- Select the prediction tools most suitable for this research and, where applicable, modify them in order to reach the objectives of this research.
- Review the way currently the thermal performance of various glazing systems is described and compared and identify a calculation method for its representation to be used for this study, both steady-state and dynamic (under real climate conditions).
- Validate the selected and modified prediction tools.
- Apply the prediction tools in order to examine the thermal performance of various shaded multilayered glazing options, under both steady-state and real climate conditions and identify the variables that the thermal performance of the various glazing options depends on. Also, identify differences between the steady-state and dynamic thermal performance.
- Examine the connection between the thermal performance representation of a glazing system and the cooling needs of a space. Also examine how the thermal performance of various glazing systems could affect the thermal state of a space when coupled with the same capacity energy efficient cooling system.

### 1.3.4 Methodology

For the completion of the above objectives the following steps were identified:

- Review early and recent research on the study of the radiation transport through glazing systems with slat-type blinds and the more recent development of prediction tools used for the calculation of the thermal and optical properties of multilayered glazing systems and their elements.

- Present the main features of the tools selected for the prediction of the thermal performance of various complex glazing systems under both steady-state and real climate conditions and describe any modifications the tools had to undergo.

- Present the theory of the total solar transmittance, g-value, and review the ways it is currently used in order to produce a standard comparable value that would

describe the thermal performance of different glazing systems. Also introduce a way to calculate a total solar transmittance that describes the thermal performance of various glazing systems under more realistic scenarios, using real climate data sets, and introduce the benefits of such a value.

- Validate the selected prediction tools and the selected calculation method by comparing results against other validated reference models and measurements under real climate conditions.

- Apply the prediction tools to:
    - examine a variety of similar shaded glazing systems, under both steady-state and real climate conditions, in order to identify the variables that the g-value depends on and demonstrate the classification of optimum shading solutions and the prediction tools' utility to assist in the choice of shading options,
    - compare between the results from the calculations under steady-state and real climate conditions in order to identify differences and/or inconsistencies between the two ways of representation, possible failure scenarios when a steady-state representation is used and the benefits of a more realistic approach in the choice of glazing system,
    - examine the efficiency of the steady-state and dynamically calculated g-values as indicators of the thermal performance of different glazing systems by comparing them with the energy consumption for cooling in a typical office space,
    - examine the effectiveness of an energy efficient cooling system in regards to keeping acceptable thermal conditions in the space when coupled with the various glazing systems under consideration.

## *1.4 Structure of Thesis*

### Chapter 1: Research Overview

Chapter 1 explains the problem this work is going to address. The aim and objectives of this research are presented along with the suggested methodology for their achievement. The outline of the structure of the thesis with a summary of all the chapters and their individual sections is also being reviewed in this chapter.

1.1 Gives an overview of chapter 1.

1.2 Presents briefly the historical background of the glass as a building material and its use in highly glazed buildings, including problems associated with such buildings and how this research will attempt to approach them.

1.3 Presents the research question that this work will try to answer along with the aims and objectives and the proposed methodology for their achievement.

1.4 Presents the structure of the thesis with a summary of all the chapters and their individual sections.

### Chapter 2: Origins of Research

Chapter 2 identifies gaps and shortcomings in the ways the thermal performance of complex glazing systems has been assessed by reviewing early and recent research on the study of radiation transport through shaded glazing systems with slat-type blinds and the more recent development of simulation tools used for the calculation of the thermal and optical properties of shaded glazing systems.

2.1 Gives an overview of chapter 2

2.2 Explores the benefits of using slat-type blinds

2.3 Reviews early approach in solving the complex solar transmission through the widely used slat-type blinds, in order to give designers general guidelines for the choice of shading based on its position, colour, angle of tilt and a combination of the above or empirical ways to calculate the optical properties of different glazing systems. Also shows how research gradually developed a way to produce a value that would characterise the thermal performance of different glazing systems, the total solar transmittance or g-value.

2.4 Reviews recent research on the thermal performance of complex glazing systems such as measurements of the optical properties of shading and/or glazing systems (§2.4.1), the use of the Monte Carlo & Geometric Optics approach on the definition of the optical properties of glazing systems (§2.4.2), the ALTSET project which included calculations and measurements of the g-value of various glazing systems (§2.4.3), the "Solar Protection in Buildings" project at Lund University which also included calculations and measurements (§2.4.4) and a more recent BRE research suggesting a manual calculation of an effective g-value that would incorporate angle of incidence (§2.4.5).

2.5 Reviews the various prediction tools currently available for the calculation of the thermal performance of complex glazing systems such as the European tool WIS (§2.5.1), the tool derived from the Solar Protection in Buildings project undergone at Lund University, ParaSol (§2.5.2) and the WINDOW5 tool developed by the Windows and Daylight Group of the Lawrence Berkeley Laboratory in California (§2.5.3). Main features of the above tools are described and various aspects related to their operation and the results provided are discussed.

## Chapter 3: Description of Prediction Tools Used in this Research

Two existing simulation packages were selected in order to be used in this research. A glazing simulation program modified from GLSIM (Pfrommer, 1995) calculates the optical solar properties for a defined glazing system and the dynamic thermal simulation model HTB2 (Alexander, 1997), which has been modified to accept this data. Chapter 3 presents the main features of both packages, more relevant to this work and also the

modifications the two simulation packages have undergone in order to reach the objectives of this research.

3.1 Gives an overview of chapter 3.

3.2 Describes the main features of the thermal model HTB2 at input and output level.

3.3 Describes the main features of the modified model GLSIM at both input and output level (§3.3.1) and also the theory of radiation transfer through blinds that the model is based on (§3.3.2).

3.4 Describes the modifications the two tools were undergone in order to work together and produce the data necessary for this research

**Chapter 4: Solar Radiation Transfer through Glazing & Review of Total Solar Energy Transmittance Theory and Practice**

Chapter 4 introduces the way the thermal performance of various glazing systems is currently described and compared by the use of their total solar transmittance or g-value, reviews the various ways is being currently calculated and presents the way the g-value of various glazing systems will be calculated in this research, under both steady-state and real climate conditions.

4.1 Gives an overview of chapter 4.

4.2 Describes the thermal processes involved in the transmission of solar radiation through a glazing system and defines the total solar transmittance as a value.

4.3 Reviews the various ways the calculation of the g-value has been defined by various standards, European (§4.3.1), American (§4.3.2) and International (§4.3.3), by research projects, ALTSET (§4.3.4), by models, WIS (§4.3.5) and ParaSol (§4.3.6), by measurements (§4.3.7) and by available guidance, BRE (§4.3.8).

4.4 Reviews the boundary conditions under which the steady-state g-value is being calculated. The review includes European (§4.4.1) and International Standards (§4.4.2).

4.5 Introduces the boundary conditions under which the steady-state g-value is calculated in this research (§4.5.1) and also the calculation method used for a g-value that would describe the various glazing systems under more realistic scenarios.

## Chapter 5: Evaluation of Prediction Tools

The selected and modified prediction tools were validated against other established and validated prediction tools and against measurements. The results from the validation are presented in this chapter.

5.1 Gives an overview of chapter 5.

5.2 Results, extracted using the prediction tools, are compared with the reference model WIS. Compared are the optical properties, direct transmittance, diffuse transmittance and absorption of the solar radiation, for a variety of angular dependent blind configurations (§5.2.1) and for a variety of glass-blind-glass configurations (§5.2.2). Also compared are steady-state g-values for glass-blind-glass configurations, with angular dependent blinds in a non-ventilated cavity (§5.2.3). The steady-state g-values for glass-blind-glass configurations with non angular dependent blinds but with ventilated cavity and for different ventilation rates are also compared against the reference model (§5.2.4).

5.3 Results, calculated using the prediction tools, are compared against measurements under real climate conditions for a variety of glass-blind-glass configuration.

5.4 Discusses the accepted levels of accuracy at thermal modelling results when it is used in order to assist the choice of the optimum glazing system.

## Chapter 6: Application to Shaded Glazing Systems

The prediction tools were applied, in this chapter, to various shaded glazing options in order to examine their thermal performance under both steady-state and real climate conditions. From the results, a classification of optimum shading solutions were identified. A comparison between the steady-state and the dynamically calculated g-values identified shortcomings in the use of a steady-state G-value and benefits in using a more dynamic representation of the thermal performance of the various glazing systems.

6.1 Gives an overview of chapter 6.

6.2 Describes the shaded glazing systems chosen for the application of the prediction tools. Blind cases tested here are angular dependent.

6.3 Presents the results from the simulations under the steady-state conditions.

6.4 Describes the environment conditions of the test cell used for the simulations under real climate conditions and presents the results for London.

6.5 Compares results between the steady-state and real climate calculations for London.

6.6 Presents results from the simulations under real climate conditions for two other European locations (Ostersund – Sweden and Athens – Greece).

6.7 Compares results between the steady-state and real climate calculations for the two locations (Ostersund – Sweden and Athens – Greece) and London.

6.8 Examines the sensitivity of g to ventilation when ventilation in the cavity between the two glass panes is considered. Blind cases tested here are non angular dependent.

### Chapter 7: Efficiency of the G-value and the $\hat{g}_d$ value as Indicators of Cooling Demand

This chapter compares the steady-state g-value and the dynamically calculated g-value of the various glazing systems under consideration with the cooling needs of a typical office space. The above comparison aims to examine the efficiency of these values as indicators of the thermal performance of different glazing systems when energy consumption for cooling is considered.

7.1 Gives an overview of chapter 7.

7.2 Compares the average cooling loads calculated over a hot day in the summer, for the three locations, with the steady-state and dynamically calculated g-values for the various glazing systems under consideration.

### Chapter 8: Application to a Case Study

This chapter studies the influence of various glazing systems on the performance of an energy efficient cooling system in a case study application. Examined is the way different window arrangements influence the internal temperature and condensation levels when coupled with a fixed capacity cooling system, for three locations.

8.1 Gives an overview of chapter 8.

8.2 Examines the efficiency of a chilled ceiling cooling system of certain power output when coupled with the various glazing systems under consideration, for the three locations (§8.2.1 Ostersund, §8.2.2 London, §8.2.3 Athens). Various infiltration rates are examined for each case and the results presented include environmental temperatures, relative humidity levels and condensation levels, where and when occurred.

**Chapter 9: Research Outcome and Proposed Future Research**

This chapter presents the outcome of this research with a chapter-to-chapter summary of findings. Overall conclusions are drawn based on the objectives of this research and recommendations for further research are given.

9.1 Gives an overview of chapter 9.

9.2 Presents a chapter-to-chapter summary of findings.

9.3 Presents recommendations for further research.

9.4 Presents the overall conclusions related to the objectives of the research.

## *1.5 References*

Alexander, D K (1997) 'A Model for the Thermal Environment of Building in Operation, Release 2.0c', Welsh School of Architecture, Cardiff University

Bell, J and Burt, W (1996) 'Designing Buildings for Daylight', BRE Report 288, BRE

CIBSE (2006) 'Design for Improved Solar Shading Control', CIBSE TM:37, CIBSE

European Standard EN 410:1998 (1998) 'Glass in Building - Determination of Luminous and Solar Characteristics of Glazing', European Committee for Standardization, Brussels

Kristensen, P E and Rodot, M (1994) 'Daylighting Technologies in Non-Domestic Buildings', International Journal of Solar Energy, Vol.15, pp.55-67

Lewis, J O and Rodot, M (1994) 'The applications of Renewable Energy Technologies in Buildings', International Journal of Solar Energy, Vol.15, pp.27-36

Littlefair, P J (1995) 'Designing with Innovative Daylight', BRE Report 305, BRE

Littlefair, P J (1999) 'Solar Shading of Buildings', BRE Report 364, BRE

Littlefair, P J (2005) 'Summertime Performance of Windows with Shading Devices', BRE Trust

Littlefair, P J, Slater, A, Perry, M, Graves, H and Jaunzens, D (2001) 'Office Lighting', BRE Report 415, BRE

Muneer, T, Abodahab, N, Weir, G and Kubie, J (2000) 'Windows in Buildings: Thermal, Acoustic, Visual and Solar Performance', Architectural Press

Pfrommer, P, Lomas, K J, Seale, C, and Kupke, Chr (1995) 'The Radiation Transfer through Coated and Tinted Glazing', Solar Energy, Vol.54, No.5, pp.287-299

Pilkington (2000) 'Glass', Pilkington UK Ltd

Saint-Gobain (2000) 'Glass Guide', Saint-Gobain Glass

## *1.6 Bibliography*

Behling, S & S (1999) 'Glass – Structure and Technology in Architecture', Prestel, New York

Button, D and Pye, B (1993) 'Glass in Building', Butterworth Architecture

Campagno, A (1996) 'Intelligent Glass Facades – Material, Practice, Design', Birkhauser, Germany

Glancey, J (2000) 'The Story of Architecture', Dorling Kindersley

Korn, A (1967) 'Glass in Modern Architecture', Barrie and Rockliff, London

Krewinkel, H W (1998) 'Glass Buildings: Material, Structure and Detail', Birkhäuser

Olgyay A & V (1957) 'Solar Control and Shading Devices', Princeton University Press, Princeton, New Jersey

Wigginton, M (1996) 'Glass in Architecture', Phaidon

Wigginton, M and Jude, H (2002) 'Intelligent Skin', Architectural Press

## *1.7 Figure Index*

Figures 1, 3, 4 and 6 were taken from 'Glass – Structure and Technology in Architecture'
Figure 5 was taken by 'The Story of Architecture'
Figure 2 was taken by 'Glass in Architecture'
Figures 7 and 8 were taken by 'Saint-Gobain' Glass Guide, 2000 Edition
Figures 9 and 10 were taken from 'Intelligent Glass Facades – Material, Practice, Design'

# Chapter 2

# Origins of Research

## *2.1 Overview*

This chapter presents early and more recent research that has been conducted on the study of the radiation transport through multilayered glazing systems with integrated shading devices and also the more recent development of prediction tools for the calculation of the thermal and optical properties of multilayered glazing systems and their elements. Through the review of past and recent research, this chapter will present the development of methods in predicting the thermal performance of multilayered glazing systems and their elements and identify gaps and shortcomings in the methods currently used for predicting their thermal performance.

## *2.2 Slat-Type Shading Devices*

As previously mentioned glass has become a material widely used towards energy efficient buildings, by maximising the use of natural daylight. Even though heat losses can be minimised by the choice of glazing systems with low U-value, there are still overheating problems associated with highly glazed buildings, especially during hot and sunny periods of the year, due to high solar heat gains entering the space. A form of shading is usually the measure recommended for the control of solar heat gains, with many different options available in the market to choose from.

Solar protective glass is largely used for the control of solar gains in highly glazed buildings, but even though it is easy to install and integrate to the façade design and low cost to maintain, at the same time reduces daylight transmission at all times, which means reduction of daylight even during overcast conditions when it is most wanted

(Littlefair, 1999; Littlefair, 2005; Bell & Burt, 1996). Also solar protective glass reduces the building's solar gains all through the day and all year round, which can result in an increase in the energy use for heating during the cold periods of the year. Furthermore, although advanced glazing technologies (smart glasses: photochromic, electrochromic, thermochromic etc) have shown considerable promise, technological problems and high cost have limited their impact so far (Littlefair, 1992; Roche, 1997; CIBSE, 2004).

Other forms of shading include overhangs, awnings and deep window seals. These shading options are permanently integrated to the façade of the building which means that they are obstructing the daylight all the time, even when there is no need for shading from direct sunlight (CIBSE, 2004).

Research has already shown that the use of slat-type blinds can considerably reduce the energy consumption for cooling in a building (Lute et al, 1990; Bordass et al, 1995; Lee et al, 1998). Furthermore, slat-type blinds are flexible and easy to use allowing user control, view out and protection from direct sunlight only when needed, maximising the availability of daylight. They are also low-cost to install and maintain and they offer the possibility of redirecting sunlight towards areas away from the window improving the daylight distribution in the space and thus improving the visual comfort of the occupants (Christoffersen, 1996).

Slat-type blinds offer a variety of material (aluminium, wood, plastic, steel; opaque or perforated), material finish (specular, diffusive), colour, position (internal, external and inter-pane) and geometry (range of width, spacing between slats and thickness) depending on the performance requirements.

## *2.3 Performance Prediction - Early Research*

Early research has examined the benefits of choosing double glazing for window openings as opposed to single glazing, (Parmelee and Aubele, 1948), but soon studies were focused on the effectiveness of shading strategies on reducing glare and heat gain through glazing while exploiting to the maximum the available daylight (Parmelee et al, 1953; Stephenson and Mitalas, 1965; Nicol, 1966; Mills and McCluney, 1993). The above research groups tried to calculate or measure the transmission, absorption and

reflection values of the incident solar radiation of shaded glazing systems by solving the complicated geometry of slat-type blind, as a widely used shading strategy for windows. A lot of the research until the early seventies was mainly focused on the benefits of using slat-type blinds related to the exploitation of the daylight (Stephenson and Mitalas, 1965; Nicol, 1966), while the effects of shading on dealing with overheating problems in highly glazed buildings started also to interest the research community (Parmelee and Aubele, 1952; Parmelee et al, 1953).

The earliest and most extensive studies related to solar shading as a method to control solar gains entering the space were carried out by the American Society of Heating and Ventilating Engineers (ASHVE), Cleveland laboratory, where the transmission, absorption and reflection characteristics of slat-type blinds and shaded single glass (slat-type blinds positioned internally and externally) were examined through mathematical and experimental analysis (various colours and angles of tilt were examined). The mathematical analysis for the determination of absorption, reflectance and transmittance of various slat-type blinds was based on the monochromatic incident radiation (ultra-violet and infrared) and considered the absorption characteristic of the slat surface, the angle of the incident radiation, the slat width and spacing and both specular and diffuse reflectance of the slat surfaces.

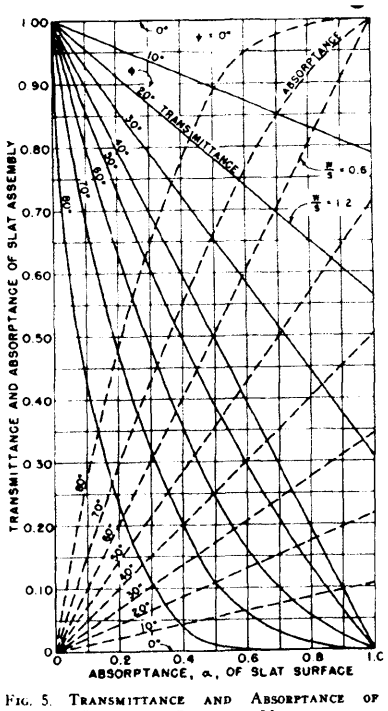


FIG. 5. TRANSMITTANCE AND ABSORPTANCE OF SPECULAR REFLECTING SLATS FOR MONOCHROMATIC RADIATION

Figure 2.1: Transmittance and absorption of specular slats for monochromatic radiation (Parmelee and Aubele, 1952)

Results were presented in a graphical way (Parmelee and Aubele, 1952) as in figure 2.1. The experimental analysis measured the absorption of the slat-type blinds using two methods (by the use of a calorimeter and by exposing the slats to direct sunlight), and the direct and diffuse transmittance of various glass - blind systems (by the use of a calorimeter) (Parmelee et al, 1953). Curves were presented showing the mathematical and experimental correlation of absorption, reflectance and transmittance of various blind systems and glass – blind combinations for

various slat angles, slat width to spacing ratios and profile angles[1] (figure 2.2).

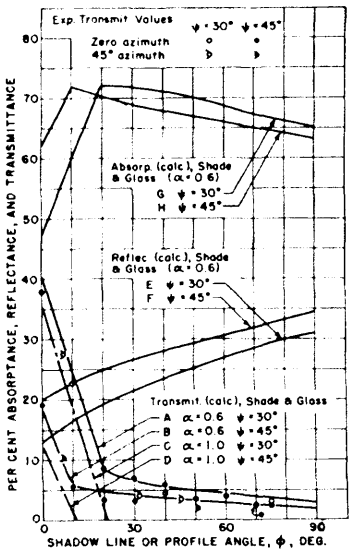


FIG. 6. ABSORPTANCE, REFLECTANCE, AND TRANSMITTANCE OF GREEN SLAT-TYPE SUN SHADES IN COMBINATION WITH GLASS NO. 9
*(Shades on outdoor side. W/S = 1.2)*

Figure 2.2: Absorption, reflection and transmittance of green slat-type sun shade in combination with glass (Parmelee et al, 1953)

Shade factors[2] for slat-type blinds (figure 2.3) and design data for slat-type blinds in combination with various types of single glass were given, using the theoretically and experimentally determined properties, as well as the percentage of absorbed energy (long-wave radiation) that enters the room (Parmelee and Vild, 1953), in order to be applied to published design data for un-shaded glass for the calculation of the total transmittance and shade factors of blind-glass combinations.

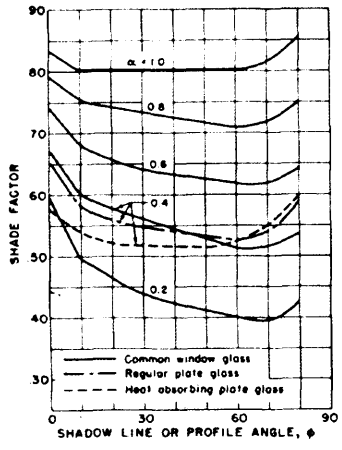


FIG. 3. SHADE FACTORS FOR INDOOR SLAT-TYPE SUNSHADES *vs.* PROFILE ANGLE, $\phi$, AND SLAT ABSORPTANCE, $\alpha$: SLAT ANGLE, $\psi = 45$ DEG; SPACING RATIO, $W/S = 1.2$

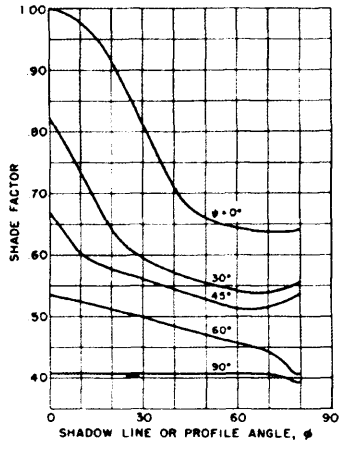


FIG. 4. SHADE FACTORS FOR INDOOR SLAT-TYPE SUNSHADES *vs.* PROFILE ANGLE, $\phi$, AND SLAT ANGLE, $\psi$: SLAT ABSORPTANCE, $\alpha = 0.4$; SPACING RATIO, $W/S = 1.2$

Figure 2.3: Shade factors for indoor slat-type sunshades vs profile angle, for various slat absorption and slat angles

[1] Profile angle in this research is defined as the sun angle that controls the performance of a given slat assembly in that it determines the position of the shadow line cast on one slat by the slat between it and the sun.

[2] Shade factor in this study is defined as the total gain from a shade-glass combination minus the convection and radiation gain from single un-shaded common window glass divided by the total incident solar radiation transmitted by single un-shaded common window glass.

The transmittance, reflectance and absorption values produced in the above research in combination with a theoretical model for the calculation of heat transfer due to convection and long wave radiation were used in order to calculate the solar heat gain of a double glazed system with internally positioned Venetian blind (Farber et al, 1963). The same theoretical model was further developed in order to include the calculation of the solar heat gain through double glazing with inter-pane Venetian blind (various colours of slat material were examined) (Smith and Pennington, 1964). Solar heat gains of the two glazing systems (double glazing with internally and double glazing with inter-pane positioned Venetian blind) were compared and it was shown that solar heat gains could be reduced by choosing the right position and colour of the shading device.

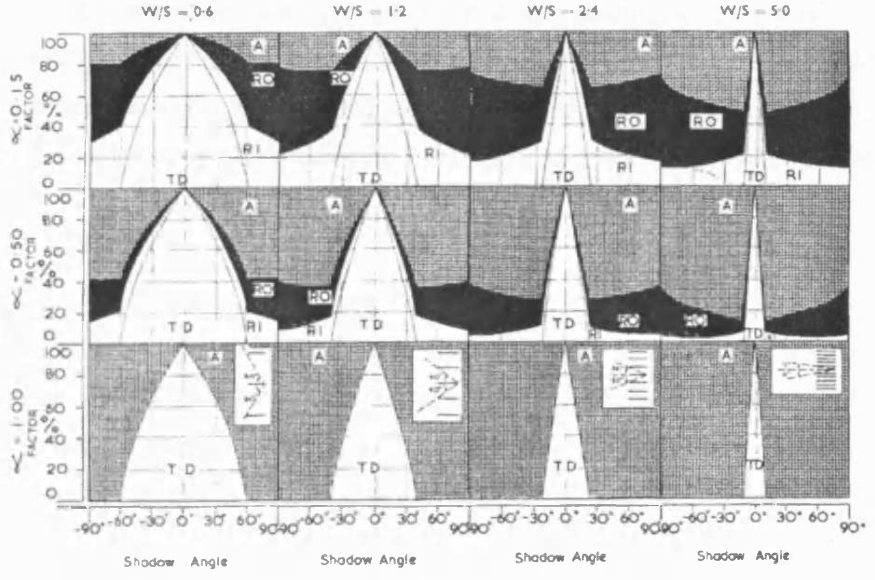


*Fig. 4. Transmission, reflection and absorption factors vs. shadow angle.*
Blade Angle $\Psi = 0°$. Range of $W/S$ and $\alpha$.
A. Absorbed in system. R.O. Reflected out. R.I. Reflected in.
T.D. Transmitted directly between blades.

Figure 2.4: transmission, absorption and reflection factors of slat-type shading systems for the 'cut off' angles of direct solar incidence (Nicol, 1966)

Further research, mainly interested in shading as a sunlight control method, was also based on the method developed by ASHVE (Parmelee and Aubele, 1952; Parmelee et al, 1953). It was aimed to provide designers with basic calculation data for slat-type shading systems based on their geometry and angle of incidence for sunlight control. That was achieved by calculating and presenting in a graphical way (figure 2.4) the transmission, absorption and reflection factors of slat-type shading systems for the 'cut

off' angles[3] of direct solar incidence that is not obstructed by the slats, for a variation of slat colour and viewing angles (angles that allow view out). The research is limited to light-colour slat-type blind (various angles of tilt were also examined) with no intergraded window glass, while is suggesting that data from this study could be used in order to calculate solar heat gains entering the room (Nicol, 1966).

Another research also interested in slat-type shading as a method to control sunlight used the O'Brien's method (each surface of a blind slat is subdivided into several strips, each having uniform luminance) in order to include reflections between shading and window glass (O'Brien, 1963), for the study of the radiation transfer through glazing systems with slat-type blinds. The slat luminance of a light-coloured, 45° tilted and internally positioned slat-type blind in a single glazing window was calculated based on the angle dependent (vertical angle of incident) transmittance and reflectance. The author pointed out the importance of the absorption factor of the blind, and its impact on the re-emitted radiation entering the space, to the air-conditioning designer (Stephenson and Mitalas, 1965).

Pilkington (1973) aimed to help designers on their choice of glazing systems by publishing a guide with the transmittance, reflectance and total solar energy transmittance (g-value) characteristics of various glazing system configurations (single and double glazing, solar control glass and single and double glazing with slat-type blinds) presented in a graphical way for normal and vertical angle of incidence (figure 2.5).

Furthermore, Owens (1974) faced the designers' problem of lack of technical information on the solar optical properties of various manufacturers' material by simplifying the choices of glazing systems. His theory was based on the assumption that when blinds are used they are adjusted so that there is no direct penetration of solar radiation. So the solar radiation entering the space is the diffused from the sky, the reflected diffused from the ground, part of the direct solar radiation penetrating the slats through inter-reflection and the transmittance of the material of the blind (when not opaque). He also limited the option of tilted slat angle at either closed or 45° (as sufficient to summarize the

[3] 'Cut off' angles in this study are defined as the limiting angles at which radiation can be directly transmitted between the slats.

performance of the blind) and the position of the blind to internally (for a single or double glazing) and inter-pane (for double glazing).

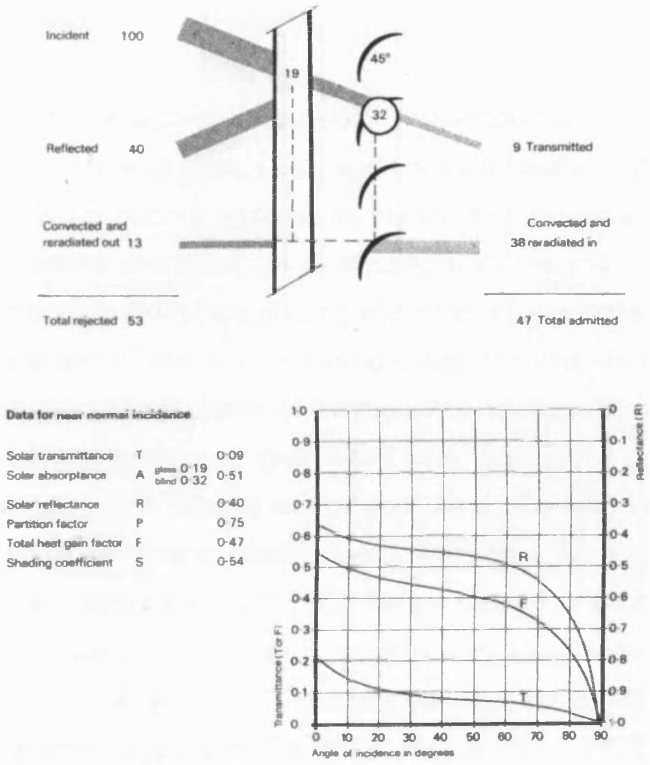


Figure 2.5: Transmittance and reflection factors of the direct solar radiation through a glass – blind configuration (Pilkington 1973)

The shading coefficients of the above combinations were presented (in a graphical way – figure 2.6) as a y against x correlation of the transmittance of the external glass against the reflectance of the blind for 45° tilted angle. The author also gave a series of tables, classifying blind performance based on their transmittance, absorption and reflectance for closed slats and 45° angle of tilted slat. Finally he suggested an empirical way for designers to measure the transmittance and reflectance of various blind materials based on their openness (Owens 1974).

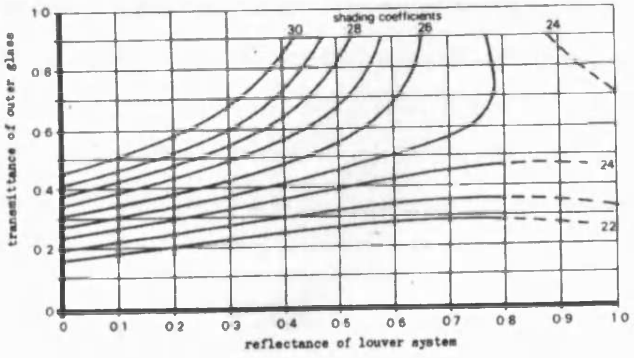


Figure 2.6: Shading coefficient of double glazing with opaque louvers at 45° between glazing panes (Owens 1974)

After the energy crisis of the seventies research focus turned more towards the control of solar gains entering a building for overheating prevention in order to provide a healthy

internal environment with low energy consumption. Mills & McCluney (McCluney, 1987; Mills & McCluney, 1993; McCLuney & Mills, 1993) pointed out the importance of energy saving for heating and cooling by the careful choice of glazing during the design stage of a building.

Their research was focused on the calculation of the shading coefficient (SC)[4] (McCLuney & Mills, 1993) and the solar heat gain coefficient (SHGC)[5] (Mills & McCluney, 1993) of glazing systems, for normal and vertical angle of incidence respectively. Their research examined planar shading solutions, mainly different roller blinds positioned internally to a single glazing and different types of tinted glass, as a way to control SC and SHGC and reduce cooling loads. The simplifications taken under consideration during the calculation of the thermal processes of the solar radiation transmission through the glazing system had as a result the limited use of this method to single glazing (with internal vertical and planar shading) systems, while made it inappropriate for multiple-pane glazing systems and generally systems that are thermally asymmetric. The authors are pointing out the importance of an angle dependent SC and a SHGC calculated under realistic conditions and also the importance of the development of mathematical models that could calculate the SHGC for multilayered and more complex shaded glazing systems (McCLuney & Mills, 1993).

Rheauly and Bilgen in Canada ventured to explore, by both a theoretical (Rheauly and Bilgen, 1987; Rheauly and Bilgen, 198A) and an experimental method (Rheauly and Bilgen, 1989B; Rheauly and Bilgen1990), the thermal behaviour of an advanced glazing system of a double glazing with an inter-pane Venetian blind (grey diffusive material) in a sealed cavity, covering the entire south wall of a standard office space. The heat exchange through the above glazing system was examined for a single cell formed by two slats and the surrounding glass panes. The results were compared with an un-shaded double glazing unit and presented in relation to the energy use of the office space for cooling in the summer and heating in the winter.

[4] The SC is the ratio of solar heat gain passing through a glazing system to the solar heat gain that occurs under the same conditions if the window was made of clear, standard, un-shaded glass. The lower the SC number, the better the solar control efficiency of the glazing system.

[5] The SHGC is the fraction of incident solar radiation admitted through a window, both directly transmitted and absorbed and subsequently released inward. SHGC is expressed as a number between 0 and 1. The lower a window's solar heat gain coefficient, the less solar heat it transmits.

## *2.4 Performance Prediction - Recent Research*

### 2.4.1 Measurement of the Spectral Properties of Glazing Systems

Further research on the thermal performance of shaded glazing systems was based on the calculation of their solar heat gain coefficient (see also §2.3: McCLuney & Mills, 1993). The thermal performance of an off-white non-specular Venetian blind was assessed in combination with clear double glazing, positioned internally and in between a double glazing system, embodied by the SHGC. The method included the measurement of the bidirectional transmittance and reflectance of the non-specular Venetian blind on a large-scale gonio-radiometer (method described in Klems and Warner, 1995) and the knowledge of the solar-optical properties of the glass layers of the system (published angular-dependent glass data by manufacturers). The properties of the glazing system were then built up computationally from the measured layer properties using a transmittance/multiple-reflection calculation analytically presented in Klems (1994B). The calculation produced the total directional-hemispherical[6] transmittance of the glazing system and the layer-by-layer absorption.

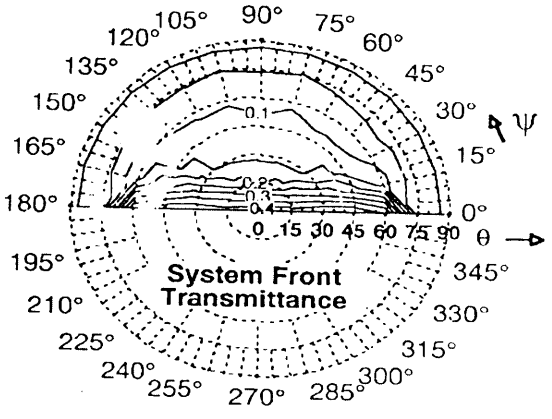


Figure 2.7: Directional-hemispherical transmittance of the glazing system with 45° slat angle (presented in half hemisphere). θ is the vertical incident radiation and ψ is the horizontal angle of incidence (Klems and Warner, 1997)

These properties were in turn combined with calorimetric measurements of the layers' inward-flowing parts of the absorbed solar energy for the particular geometric and thermal system configuration (Klems and Warner, 1992; Klems and Kelley, 1995) to produce the overall SHGC of the glazing system (Klems 1994A). The directional-hemispherical transmittance (figure 2.7) and absorption of the shading device and the directional-hemispherical SHGC (figure 2.8) of the glazing system were presented on a

[6] Directional-hemispherical indicates radiation incident from a small solid angle (direction) from outside the glazing system transmitted/reflected in all directions (i.e. over a hemisphere to the inside/outside).

3-dimentional spherical coordinate system for three angles of tilted slat (0°, 45° and 90°) (Klems and Warner, 1997) in order to show that the thermal performance of angular dependent glazing systems should consider the time of day, orientation and season, by providing a time and location varying value (SHGC) for the description of the thermal properties of complex glazing systems.

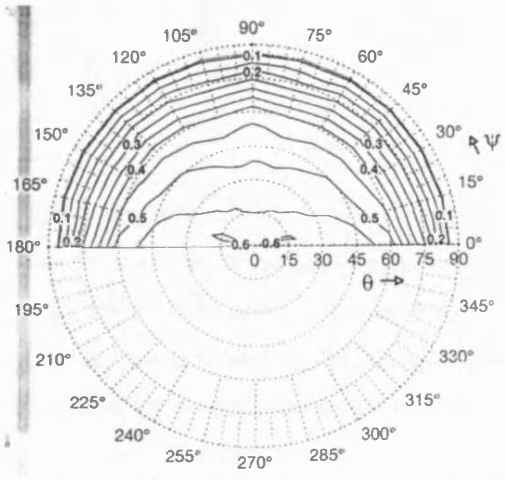


Figure 2.8: SHGC of the glazing system with 45° slat angle (presented in half hemisphere). θ is the vertical incident radiation and ψ is the horizontal angle of incidence (Klems and Warner, 1997)

An equivalent value to SHGC for characterising the thermal performance of different glazing systems developed in Europe is the g-value or total solar transmittance. An approach to measure the total solar transmittance g-value of a glazing system involved the use of calorimetric methods to calculate the g-value of the glazing system as a total (Rosenfeld et al, 1996) rather than through the measured optical and thermal properties of the glazing's components (see above study). Characteristic in this research is the suggestion of reference conditions, due to the lack of established EN and ISO standards at the time of this study, for the calculation of a $g_{exp}$ (experimental estimate of g-value), based on a predictive model (Rosenfeld, 1996), since the total solar transmittance as a glazing property would normally depend on the environmental conditions on both sides of the glazing and accurate estimate of the g-value by measurements is difficult and expensive. The authors suggest that the calculation of g under standard conditions would support the commercialisation of the new technologically advanced glazing systems.

The importance of the variation of the angle of incidence of the solar radiation on the optical and thermal properties of different shaded glazing systems was examined by means of measurements and calculations by Breitenbach et al (2001). The glazing systems examined were a double glazing system with an adjustable blind located in the cavity between the glass panes and another double glazing system with a fixed blind again positioned between the glass panes. The spectral bi-directional transmittance

functions were measured for each component of both systems for a range of incident angles using a gonio-spectrometer (figure 2.9) (Breitenbach et al, 2001), while the thermal properties were measured with an illuminated hot box (Marshall and Mason-Jones, 1995).

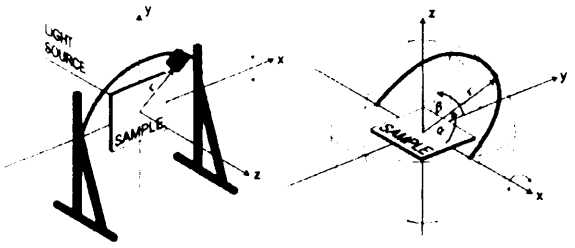


Figure 2.9: Co-ordinate system for the gonio-spectrometer (Breitenbach et al, 2001)

The total solar transmittance (g-value) and the direct transmittance of the two glazing systems were calculated by a model developed for the calculation of the total solar transmittance for glazing systems made of non-scattering components (Rosenfeld, 1996), for vertical and horizontal angle of solar incidence (figure 2.10). The variation of the direct transmittance and the total solar transmittance with slat angle was also examined for normal incidence for the double glazing system with the adjustable blind. The authors (Breitenbach et al, 2001) are pointing out the importance of a flexible calculation model, like the one used in this research (Rosenfeld, 1996), in order to allow studies of the effect of changing the properties of individual components without the need for extensive testing of all possible combinations.

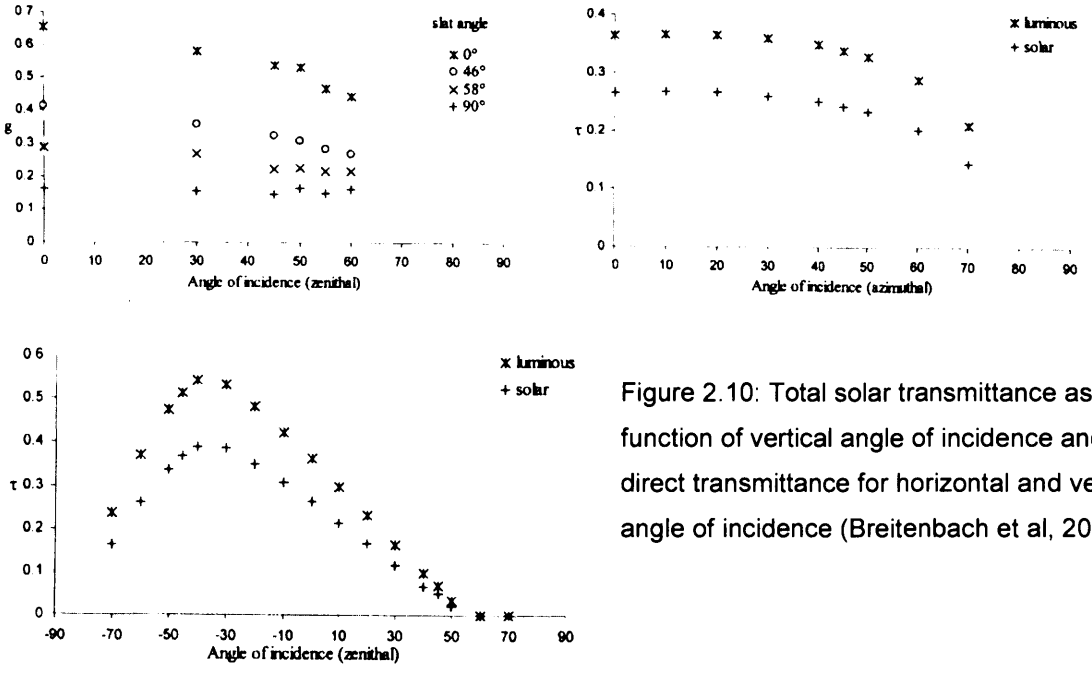


Figure 2.10: Total solar transmittance as a function of vertical angle of incidence and direct transmittance for horizontal and vertical angle of incidence (Breitenbach et al, 2001)

Research by Kuhn et al (Kuhn et al, 2000) involved the development of a methodology to assess the effectiveness of a sun-shading system together with an associated control strategy. Both calorimetric measurements in a control environment and calculations using ray-tracing techniques were used for acquiring an angle-dependent g-value of various glazing systems with integrated Venetian blinds. Knowing the angle-dependent g-value and the distribution of the incident radiation by modelling the sky radiance, they calculated the incident solar radiation and the solar radiation transmitted into the building for every hour of the year at a specific location. The effective $g_{eff}$[7] was calculated for the various glazing systems for three orientations (south, north and east) and for two different shading strategies and conclusions were drawn as to how important is orientation to the design of the shading strategy of the window and also the consideration of an angle-dependent g-value for a reliable evaluation of the overheating protection.

### 2.4.2 The Monte Carlo Methods and Geometric Optics Approach

Campell (Campbell and Whittle, 1997; Campell, 1998) used the Monte Carlo Methods / Geometric Optics approach, a combination of numerical stochastic process[8] (Monte Carlo Methods[9]) and ray-tracing techniques[10] (Geometric Optics), in order to create a "Simple Window Simulator" to explore the transport of solar radiation through complex glazing systems containing slat-type shading. That was achieved by the calculation of the transmission, absorption and reflection of the direct solar radiation through blind assemblies and glass-blind combinations.

---

[7] $g_{eff}$ in this research is the ratio of the monthly sums of the transmitted to the incident solar energy for this month and location.

[8] Radiation transport is a natural stochastic process – a sequence of random events – and therefore amenable to solution via a Monte Carlo Simulation, which is a numerical stochastic process.

[9] A Monte Carlo Method can be defined as any method used for solving a mathematical problem via an appropriate statistical sampling technique. Monte Carlo is a method of statistical simulation used to determine the average behavior of a modeled system (Campbell, 1998).

[10] Ray tracing (GO) is the technique where a ray/photon bundle (unspecified number of photons) is traced from emission at its parent surface through possible multiple scattering events (collisions) until it is finally absorbed by a body in the environment.

A double glazing system with external, inter-pane and internal Venetian blind of 45° slat angle and "idealised" blind materials (perfectly diffuse and perfectly specular) was examined. The solar factors for the above assemblies were calculated for the direct solar radiation, for vertical angle of beam incident radiation, and for the diffuse incident radiation (mean value). Thermal radiation, conduction and convection were not considered. Based on the results were given some general guidelines on the selection and use of the above shading options based on their position and material. Of particular focus was the effect of the slat curvature, in the transmittance and reflection of the assemblies, the inclination of the curved surface (upward or downward), as well as the importance of angle of incidence (Campell, 1998).

Since the Monte Carlo simulations only provided predictions of the distribution of incident solar radiation and not the total solar transmittance the Klems & Warner (1996) formulas and layer-specific inward-flowing fraction, $N_i$ (Klems & Warner, 1996) (see also §2.4.1), were used to calculate the solar heat gain coefficient directional ($SHGC_d$) for vertical angle of incidence and 77 altitude-azimuth pairs, and also the mean diffuse ($SHGC_D$) (sky diffused and ground reflected diffused). From both the directional and diffuse SHGC it is possible to calculate the overall heat gain ($W/m^2$) (Klems & Warner, 1996).

A study case of a specific location was examined where the seasonal variation of an instantaneous SHGC and total solar heat gain ($W/m^2$), calculated at noon for a south-facing façade, was presented (Campbell, 1998), while it was pointed out that the optimum choice of a blind will also depend on the design strategy of the building, the orientation of the window/façade etc, and that a calculation model should take the above under consideration (Campbell and Whittle, 1997; Campbell, 1998).

### 2.4.3 The ALTSET Project

The European project ALTSET (Angular-dependent Light and Total Solar Energy Transmittance) had as an objective the development of European standard laboratory test procedures for the determination of the angular dependent light and total solar transmittance g of complex glazing and integrated shading elements. The total solar transmittance for five different complex glazing products was measured by a group of scientific partners, each laboratory using their own solar calorimetric equipment and test

procedures (Platzer, 2000). From the comparison of the results produced by the different laboratories was concluded that the only way to acquire a measured comparable quantity that could sufficiently describe different glazing systems was by establishing common reference standard conditions (Platzer, 2000) for the measurement of a constant value g.

Even though the reference conditions achieved a common way to compare g-values of different complex glazing systems measured in different laboratories, simulations showed that, on the energy consumption for cooling or heating in a building, the difference between the results using angular data and the ones using constant value g (for normal angle of incidence) can be very significant depending on the glazing type (e.g. when there is an angle dependent shading device integrated in the glazing system, such as slat-type blind) (Platzer, 2000).

In parallel to the development of the test procedures there was also a development and validation of calculation models to predict the properties of a variety of complex glazing systems (Rosenfeld et al, 2000). The calculation models were based on the concept that a complex (multilayered) glazing can be represented by a stack of layers, each layer representing one of the component elements of the glazing. If the optical and thermal properties of each layer are known then it is possible to calculate the corresponding elements of the stack (Rosenfeld et al, 2000; also see Rosenfeld, 1996; Breitenbach et al, 1999; Breitenbach et al, 2001). Two models were used for the calculation of the total solar transmittance of a double glazing system with inter-pane Venetian blind. One was the European software WIS (Dijk and Goulding, 1996) developed as part of the ALTSET project and the other one was the calculation method described at Breitenbach et al, 2001 (see §2.4.1). The calculations using both methods showed that WIS is particular suitable for blinds of diffusive materials while the model described at Breitenbach et al, 2001 is operating better for specular materials. Comparison between measurements and calculations showed that the area that needs further investigation is an improved computer model for scattering components.

### 2.4.4 Lund University Measurements

The Solar Shading Project at Lund University was initiated in 1997, and concluded 2002, and aimed to increase the knowledge of the performance of shading devices (Wall and Bülow-Hübe, 2001; Wall and Bülow-Hübe, 2003). Within the project a wide range of shading devices was examined by means of measurements, in real climate (Bülow-Hübe and Lundh, 2002) and in a controlled environment, and calculations using a computer model (ParaSol), which was developed as part of the project (Bülow-Hübe et al, 2003). Main aims of the project were to measure the solar properties of a large variety of solar shading available in the market, in order to provide comparable g-values measured under similar conditions and also to provide designers with a tool for the prediction of the thermal performance of different glazing systems with integrated shading techniques for the choice of an optimum shading solution during the early design stage of a building.

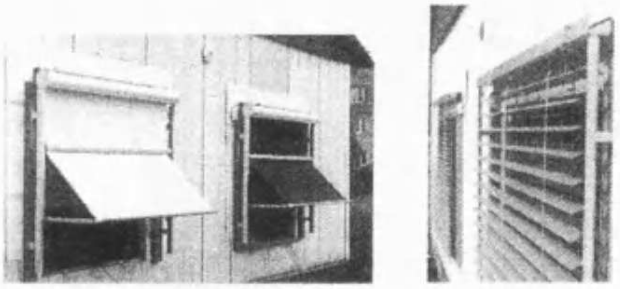

Figure 2.11: Twin-boxes with installed Italian awnings and external slat-type blinds (Wall and Bülow-Hübe, 2003)

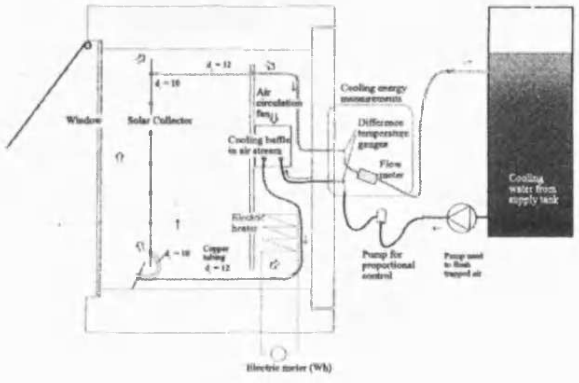


Figure 2.12: Hot box and measuring system (Wall and Bülow-Hübe, 2003)

The g-value of a wide range of shading devices positioned externally, inter-pane and internally to a standard double glazing system, was measured in real climate (Lund, Sweden) and during clear days (minimum global solar radiation: 100W/m$^2$), by the use of an installation composed by two well insulated boxes placed in a room of constant temperature (figures 2.11 & 2.12). The two boxes had each one a south facing window with the same glazing system with and without shading. By the use of a solar absorber behind the windows the total solar

energy transmittance was measured for the double glazing window, for each shading device and for each glazing system (double glazing and shading device) (Wall and Bülow-Hübe, 2001; Bülow-Hübe and Lundh, 2002; Wall and Bülow-Hübe, 2003).

The measurements were repeated but this time only the g-value of the variety of the shading devices was measured, depending on their position (external, inter-pane or internal to the double glazing unit), in a controlled laboratory environment by the use of a solar simulator and a calorimeter box (figure 2.13). The measurements using the solar simulator produced an angle dependent g-value for the shading devices presented, for vertical angle of incidence (Wall and Bülow-Hübe, 2001; Wall and Bülow-Hübe, 2003). In this way the research group aimed to provide a method of producing a comparable value that can be measured in a controlled environment as opposed to a climate dependant value measured in a much more complicated and costly outdoor set-up.

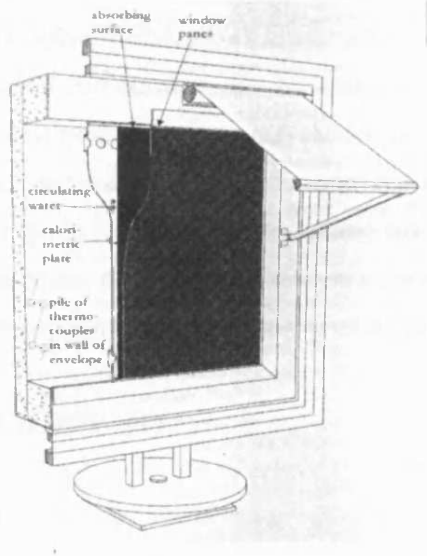


Figure 2.13: Drawing of a calorimeter box with calorimeter plate and installed sun shade on the window (Wall and Bülow-Hübe, 2003)

The design tool ParaSol was developed within the project in order to provide designers and generally those in the building industry with a simple but sufficiently advanced tool for the study of the potential of solar protection for different types of sunshades and also their influence on the building energy performance at an early design stage. The software provides monthly average values of T (direct solar transmittance) and g (total solar transmittance) for the window, the shading device and the system (window and shading) and maximum cooling and heating loads as well as yearly energy demands for a room with a window, with and without shading, by running yearly simulations for a variety of locations. An updated version of the software provides U-values, T and g-values for standard conditions and normal incidence of the solar radiation for the internal and inter-pane position of the shading devices (Wall and Bülow-Hübe, 2001; Wall and Bülow-Hübe, 2003; Bülow-Hübe et al, 2003; see also review of the Parasol tool in 2.5.2).

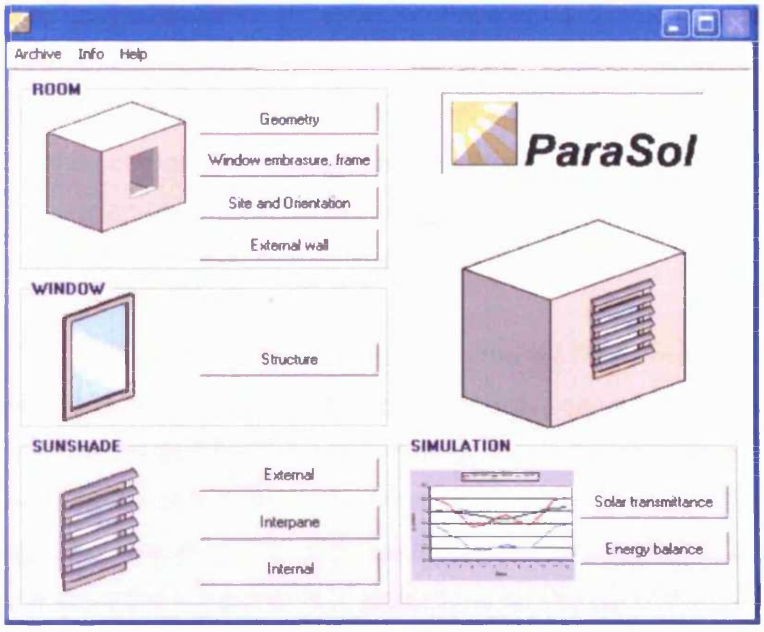


Figure 2.14: ParaSol start form, © Division of Energy and Building Design, Department of Construction and Architecture, Lund Institute of Technology, Lund University

Results from measurements, in real climate and in a controlled environment and ParaSol calculations were compared for the validation of the laboratory and simulation method (Wall and Bülow-Hübe, 2001; Wall and Bülow-Hübe, 2003; Bülow-Hübe et al, 2003). The produced g-values were not directly comparable, since measurements in real climate were done during one day, measurements in the controlled environment were done for vertical angle of incidence and calculations provided a monthly average (also for standard conditions and normal incidence for some of the cases). So the results compared were the g-values for normal incidence, provided by the measurements in controlled environment and ParaSol simulations, and the average daily, provided by the measurements in real climate.

### 2.4.5 BRE Guidance

BRE (Littlefair, 2005) lately published a guide for designers when choosing a glazing system in order to avoid overheating. The report separates the total solar transmittance into two categories; the standard g-value measured or calculated for normal incidence and the effective g-value ($g_{eff}$) that is calculated for different angles of incidence. The $g_{eff}$ in this research is defined as the solar gain in period of potential overheating through window with shading device, divided by the solar gain through un-shaded and unglazed opening for the same period. The period from May to August was chosen as the basis for the calculation of the solar gain. The whole 24 hour day was used rather than only the hours of solar radiation and only the 2.5% of peak days for radiation availability were included.

The calculation of the $g_{eff}$ defined above aim to include the effect of orientation and inclination of the window surface as well as the sun altitude (differentiation between seasons rather than months) in the total solar transmittance in order to provide a value for the comparison between shading techniques and also to be used as input in simple calculation methods (manual or computational) of solar gains, and as a result the heat gains and overheating risk, in a space.

The report is providing designers with the $g_{eff}$ for different glazing systems with various shading devices, positioned externally, inter-pane and internally, calculated for different orientations and for slat-type blinds also calculated for different inclinations of the slats. Also the $g_{eff}$ of the separate components (various glass and shading choices) are specified and a way to calculate the $g_{eff}$ of various glazing systems by the given $g_{eff}$ of the separate components. Calculations for the $g_{eff}$ of the glazing systems are based on the standard BS EN 13363-1. The report also provides a simple computer tool for the calculation of the $g_{eff}$ of glazing systems when the g-values of the separate components are provided by the manufacturers.

## *2.5 Prediction Tool Review*

As seen in 2.3 and 2.4, the theory of radiation transport through shaded glazing systems with slat-type blinds has been studied extensively in a number of research projects from the 1950's onwards, but the complexity of the theoretical models or measurement methods (real climate or calorimetric) proved to be time consuming and impractical when one had to choose between a variety of material and shading options. So the need for more flexible and accurate, computer generated, models was formed within the 1990's, when the following computer tool development was undertaken.

### 2.5.1 WIS

WIS (Advanced Window Information System) is the result of a EU project in order to develop a uniform European software for the calculation of thermal and optical solar properties of window systems under steady-state conditions (Dijk et al, 2002). Calculations are made according to the International Standard ISO 15099 (2003).

Different window systems are described as a combination of a transparent system (built up by layers of glass panes and shading options) (figure 2.15) and the structure of the window (frame and spacer).

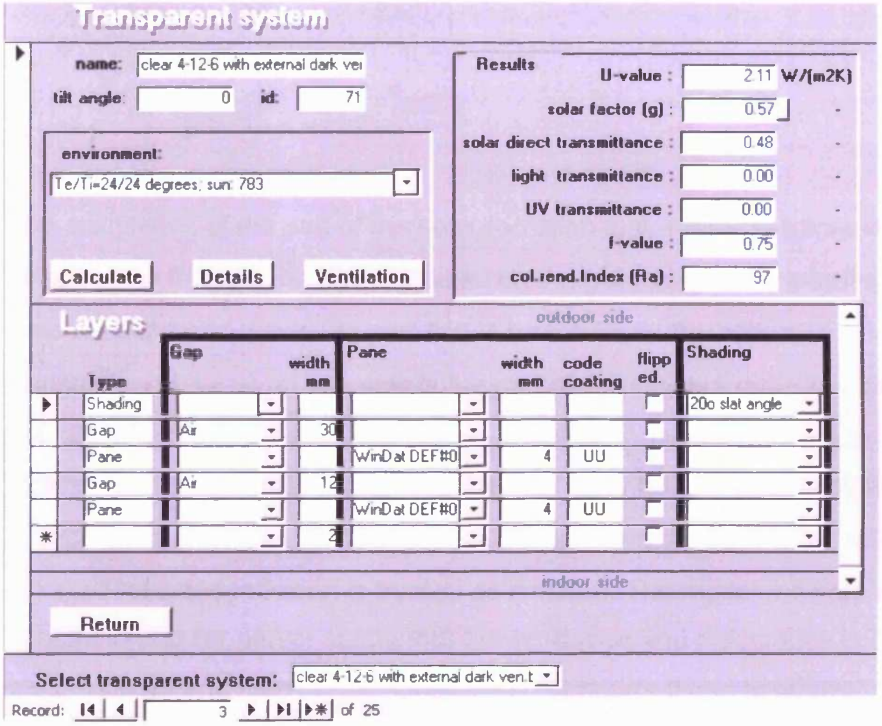


Figure 2.15: WIS, transparent system input stage, © 1994-2003 EU Thematic Network WinDat

Shading options examined by WIS are divided into two categories; panes (coatings and films) and layer type blinds (roller blinds and slat-type blinds). The model for the calculation of the slat-type blinds is based on the calculation of the solar properties of the blind from the measured optical characteristics of the material, the geometry of the blind layer and the angle of incidence (at present restricted to a vertical angle of incidence). The procedure is taken from a more detailed three-dimensional model, LAMAS, developed in the European project PASCOOL (Coronel et al, 1994). A single cell consisted of two adjacent slats and two virtual side layers, is considered, each slat divided into five equal elements (Figure 2.1). The virtual side layers are perfectly transparent.

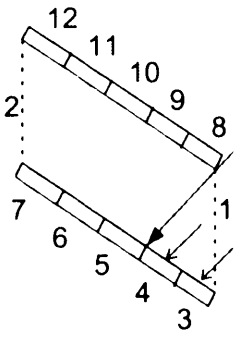


Figure 2.16: Simplified model for the calculation of the optical properties of a slat-type blind

The calculation of the part of the solar radiation that is directly transmitted (direct to direct, $\tau_{dir,dir}$) through the blind is based on the geometry of the shading device and the angle of incidence, while the part that is transmitted after reflection (direct to diffuse transmittance, $\tau_{dir,dif}$) on the slats is the part of the incident radiation, diffusely reflected by the slats, that leaves the blind from the struck side towards the inside. The part of the incident radiation passing through the virtual layer towards the outside is the reflectance (direct to diffuse, $r_{dir,dif}$) of the blind, while there is no direct to direct reflection ($r_{dir,dir}$) since all reflected radiation is treated as diffused. The model requires as input the spectral (specular and/or scattering) transmittance and reflectance or the solar transmittance and reflectance (direct to direct and/or direct to diffuse) characteristics of the blind material, measured at normal incidence, throughout the calculations. The absorption of the blind is obtained by difference ($1-\tau_{dir,dir} - \tau_{dir,dif} - r_{dir,dir} - r_{dir,dif}$). Diffuse radiation transmitted or reflected by the device is assumed to remain diffuse ($\tau_{dif,dif}$ and $r_{dif,dif}$)

For the calculation of the direct to diffuse transmittance and reflectance WIS is using the view factor approach. The view factors[11] between the five parts of each of the two slats (the outside surface of one and the inside surface of the other) and between the incident radiation and the irradiated parts are calculated, after identifying the slat parts struck by the solar incidence. Due to the assumption of non-specular reflection the view factors can be calculated by conventional view factor calculation methods for diffuse radiation

[11] Radiation view factor is the fraction of thermal energy leaving the surface of object 1 and reaching the surface of object 2, determined entirely from geometrical considerations. Stated in other words, radiation view factor is the fraction of object 2 visible from the surface of object 1, and ranges from zero to 1. (efunda: Engineering Fundamentals, Heat Transfer Glossary, www.efunda.com)

exchange. The same way are calculated the diffusely transmitted and reflected ($\tau_{dif,dif}$ and $r_{dif,dif}$) properties, but this time for diffuse incident radiation.

The blinds are semi-transparent to infrared (thermal) radiation. IR properties (transmittance and reflectance) of the shading device are calculated using the same model as for the calculation of diffuse transmission and reflection (diffuse – diffuse) of solar radiation, replacing the slat's solar optical properties by its thermal radiation properties (emissivity). From the thermal radiation properties of the slat and the view factors between the outside, the inside and the slat surfaces, the IR properties of the layer are calculated.

Thermal heat transfer through the glazing system is modelled in detail, considering radiation exchange, convection and conduction between the layers of the transparent system and the gaps formed by the various layers, for ventilated and non-ventilated cavities (both natural and forced ventilation are considered). All above calculations described are included in the Dijk et al (2002) and ISO 15099 (2003).

In case the type of shading device is not suitable for using the model described above (e.g. roller blind), WIS offers the possibility to direct input the transmittance and reflectance for each angle of incidence, data which could be provided from another model or from measurements in a gonio-photometer. In this case the same basic simplification is applied; the incident solar beam is assumed to be splited into a part which is transmitted directly (direct to direct transmittance) and a part which is diffusely transmitted isotropicly (direct to diffuse). The reflection is always considered as isotropicly diffused and diffuse radiation is transmitted always as diffused (diffuse to diffuse) (Dijk et al, 2002).

WIS is producing thermal and solar properties for vertical angle of incidence for various shading options and for the transparent system (composed by glass panes, gas or air layers and shading options) in an analytical report, while g-values are calculated only for normal incident for the transparent system. Every transparent system is composed through a selection of layers from existing materials or by the option of creating new slat-type blinds by entering the geometry, the optical properties for normal incident and the thermal properties (e.g. emissivity) of the blind. There is also a choice of ventilated or

non-ventilated cavities between the layers, while for ventilated cavities there is an option of natural or forced ventilation. At the time of this research WIS is restricted to two types of air flow; from outside to inside (e.g. through a ventilated cavity between two glass panes) and from inside to inside (e.g. through a ventilated cavity between a glass pane and an internally positioned blind). The program also offers a choice of the environment for the steady-state calculations for a CEN only calculations (all calculations are done according to EN 673 and EN 410) and expert mode, where WIS gives an option of entering other boundary conditions.

WIS is a flexible and easy to use tool for either professionals (designers, manufacturers etc) or researchers. At the time of completion of this research there has been no published quantitative representation of the uncertainty related to the tool. Currently WIS is the European reference software for the description and comparison of different glazing systems and it has been used in various research projects to validate other calculation models or methods of measurement in steady-state conditions (Rosenfeld et al, 2000; Kuhn et al, 2000). Outcomes from the above projects expressed some qualitative weaknesses related to WIS; it is particularly suitable for blinds made of material whose reflectance is diffuse and Lambertian, while it seems to underestimate the g-value for high specularly material (e.g. mirror finish or lamellae).

The current version of WIS is restricted to steady-state calculations (no real climate input option) and without taking under consideration the environmental conditions of the room/building (ventilation rates, internal loads etc). The g-value produced by the software can be used as a way to compare different glazing systems but it is not describing the thermal performance of the transparent system for a specific building in a specific location and under real climate conditions.

### 2.5.2 ParaSol

ParaSol is the prediction tool developed as part of the "Solar Protection in Buildings" project at Lund University (Wall and Bülow-Hübe, 2001; Wall and Bülow-Hübe, 2003). The graphical user interface of ParaSol was based on a dynamic energy simulation engine named DEROB-LTH. Physical solar radiation models for the combination of sunshades and glazing systems were developed in this project and implemented in the

DEBOR-LTH simulation engine. ParaSol can simulate different types of shading devices positioned externally, inter-pane and internally.

ParaSol calculates the solar transmittance of slat-type blinds from the slat optical (for normal incidence) and geometrical properties (figure 2.17). The solar properties, both directly and diffusely transmitted and reflected radiation, as well as absorbed radiation, of the slat-type blind layer are calculated by tracing an incoming beam between two adjacent slats through the layer (method based on the assumption of a single cell consisting of two plane slats and two virtual side layers - see also §2.5.1 WIS). The calculation of the diffused transmitted and reflected part of the radiation is based on the concept of dividing the slats of the above single cell system into five parts (see also §2.5.1 WIS).

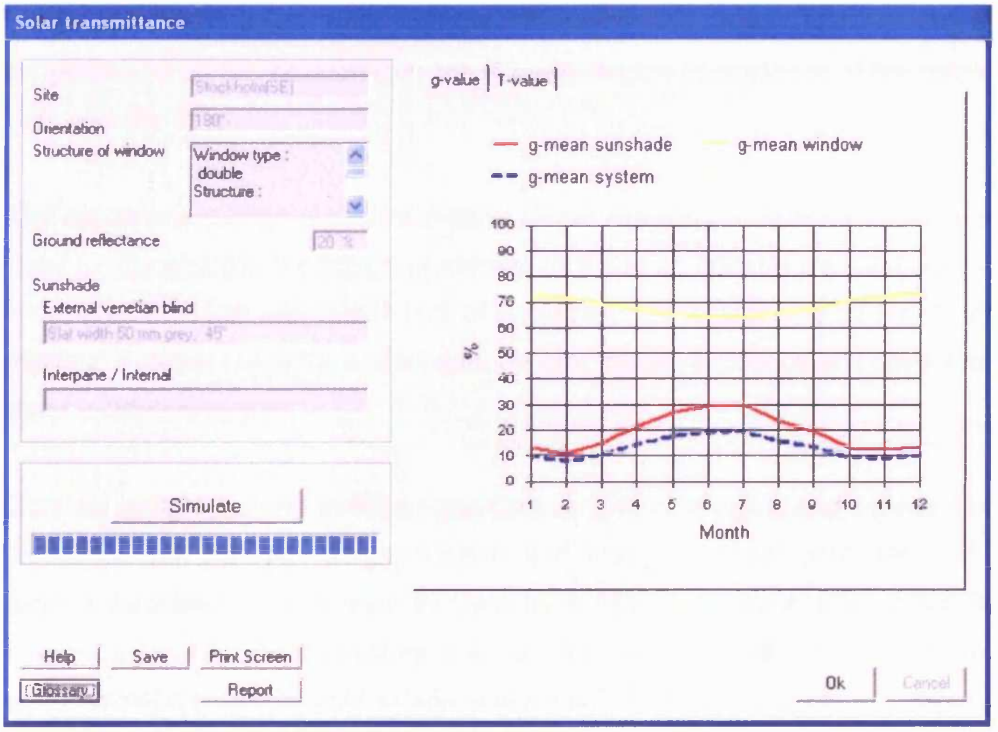


Figure 2.17: ParaSol, Solar Transmittance simulation output, © Division of Energy and Building Design, Department of Construction and Architecture, Lund Institute of Technology, Lund University

Heat transfer due to convection between the slat-type blind and the adjacent layers is treated with a simplified model based on the two extreme cases of totally open and closed slats. For all slat angles in between convection is assumed to be a mixture

between the two extreme cases. All calculations are described in detail in the 2nd report of the "Solar Protection in Buildings" project (Wall and Bülow-Hübe, 2003; Bülow-Hübe et al, 2003).

Plane shading devices such as roller blinds are treated as planar layers parallel to the glass panes. Although some planar shading devices are porous, all internal and inter-pane devices in ParaSol are calculated as non air permeable.

The optical properties of the glass panes (previously mentioned for the slat-type shading) are calculated (using Fresnel's formula[12] and Snell's law of refraction[13]) for different angles of incident (every 5th degree) and ParaSol uses these data to calculate the optical properties of the window (without shading) for the direct solar radiation. The optical properties of the window for the diffuse radiation are calculated by integrating the properties for direct radiation over the different angles of incidence of the hemisphere (diffused sky patches).

The cases where internal and inter-pane planar shading (no external choice available) is used for the window, the optical properties (diffused and direct) are calculated as for the window alone. However, due to lack of angle resolved optical data for planar shading material ParaSol reads the optical data only for normal incidence and uses it for all the other incidence angles.

Convective heat transfer in the air gap between planar shading and a glass pane is calculated as if between two glass panes and between an internal planar blind and the room is calculated as if for an inner glass pane (Wall and Bülow-Hübe, 2003; Bülow-Hübe et al, 2003). The convective heat transfer coefficient between the outside pane and external air is in ParaSol simulations set to 15W/m$^2$K.

[12] At the boundary between two objects with different indices of refraction (e.g. air and a scattering volume), some incident light is reflected back from the boundary and some of it is transmitted, depending on the angle of the incident light ray and the indices of refraction of the surfaces. The Fresnel formula describes this effect.

[13] Refraction is the bending of the path of a light wave as it passes across the boundary separating two media. Refraction is caused by the change in speed experienced by a wave when it changes medium.

ParaSol has two types of simulations. The first simulation type is the 'Solar Transmittance' which provides monthly average values of T (direct solar transmittance) and g (total solar transmittance) for the window, the shading device and the system (window and shading), in the form of graphs, and U-values, T and g-values for standard conditions and normal incidence of the solar radiation for glazing systems with internal and inter-pane shading devices (figure 2.17). The second simulation type is the 'Energy Balance' which provides the maximum cooling and heating loads as well as yearly energy demands for a room with a window, with and without shading, by running simulations with hourly data for a variety of locations (figure 2.18).

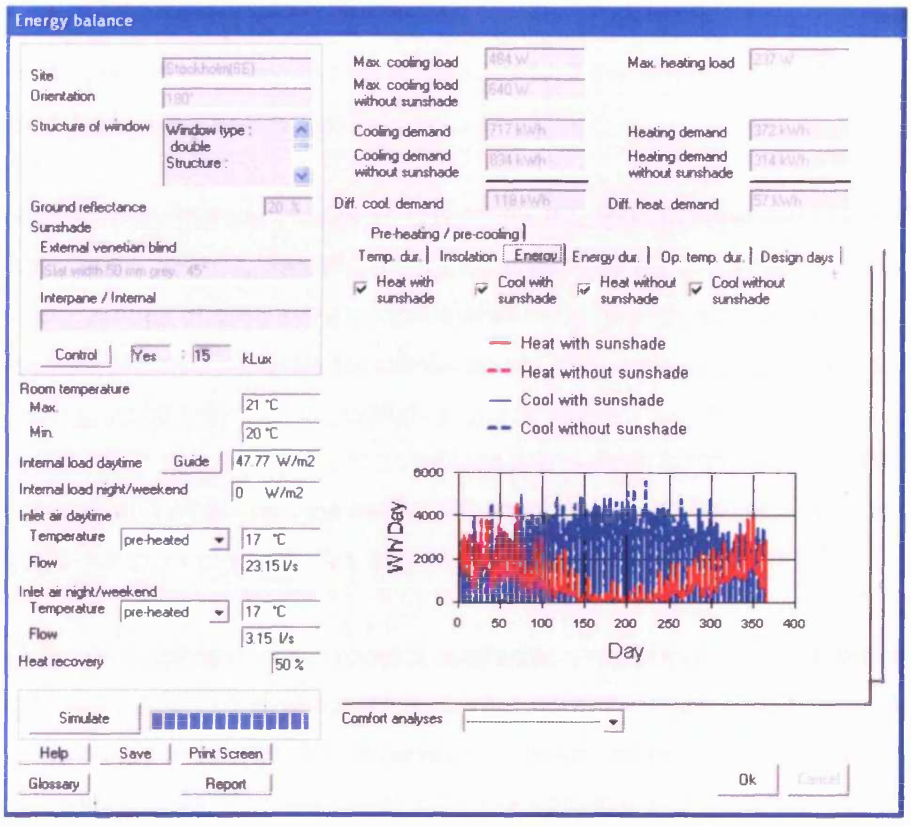


Figure 2.18: ParaSol, Energy Balance simulation output, © Division of Energy and Building Design, Department of Construction and Architecture, Lund Institute of Technology, Lund University

Input data includes the geometry, location and orientation of the room, choice of shading and its position and geometry, and structure of the window (composed by layers of glass panes and air gaps). For the 'Energy Balance' part of the simulation there are additional options of thermostat set-points for heating and cooling, internal loads, room

ventilation rates and inlet air temperatures during work hours and nights or weekends respectively. A simple control of the shading devices based on the solar radiation incident intensity on the window without external shading as well as a pre-heating unit to heat the inlet air have been implemented in ParaSol.

Version 2.0 of the ParaSol (available at the time of this research) treats all air gaps between the different layers of the various glazing systems as closed. This is important especially for cases such as windows with internally positioned blinds (usually mounted with an open air gap) or inter-pane blinds in a ventilated cavity. The g-value calculated by the program will not include the part of the absorbed by the blind solar radiation which is transmitted back into the room (or outside, if the ventilated cavity is connected to the outside) by air flow through the gap.

Furthermore, there are no input options for the optical properties of external slat-type blinds (they are only described geometrically) and the properties U-value, g-value and T of the various glazing systems calculated under steady-state conditions and for normal incident are only available for combinations of internal and inter-pane shading with glazing, while they are not available for any system with externally positioned shading device. Two sets of boundary conditions are chosen for steady-state calculations, for the summer and winter months set by ISO standards (ISO 15099, 2003), while there is no option for input of alternative sets of boundary conditions.

Only one geometry for the room is available; a rectangular office module with one external wall with one window and the temperature in the studied room is assumed the same as the temperature in adjacent rooms and corridors so there is no energy transfer between spaces. The wall construction description regarding heat storage is limited to a choice between lightweight and heavyweight while there is no option for floor and ceiling materials.

There is also lack of a detailed documentation of the input data and output results for every case that is being simulated in order to print or save as a report sheet or even use in more detailed energy simulation programs.

### 2.5.3 WINDOW5

WINDOW5 is a computer program developed by the Windows and Daylight Group of the Lawrence Berkeley Laboratory in California (Arashteh, 1986) for the calculation of solar and thermal properties of different glazing and window systems. U-value and solar heat gain coefficient (SHGC) calculations are performed by assuming a one-dimensional temperature profile in the centre of the glazing configuration. Thermal heat transfer is calculated by modelling the short-wave radiation, with fundamental radiative theory being used to calculate heat exchange between panes. Convective heat transfer between the panes is calculated using semi-empirical correlations (Arashteh, 1986; Robinson and Littler, 1993). Recently updated algorithms are consistent with ASHRAE SPC142 and ISO15099 (2003).

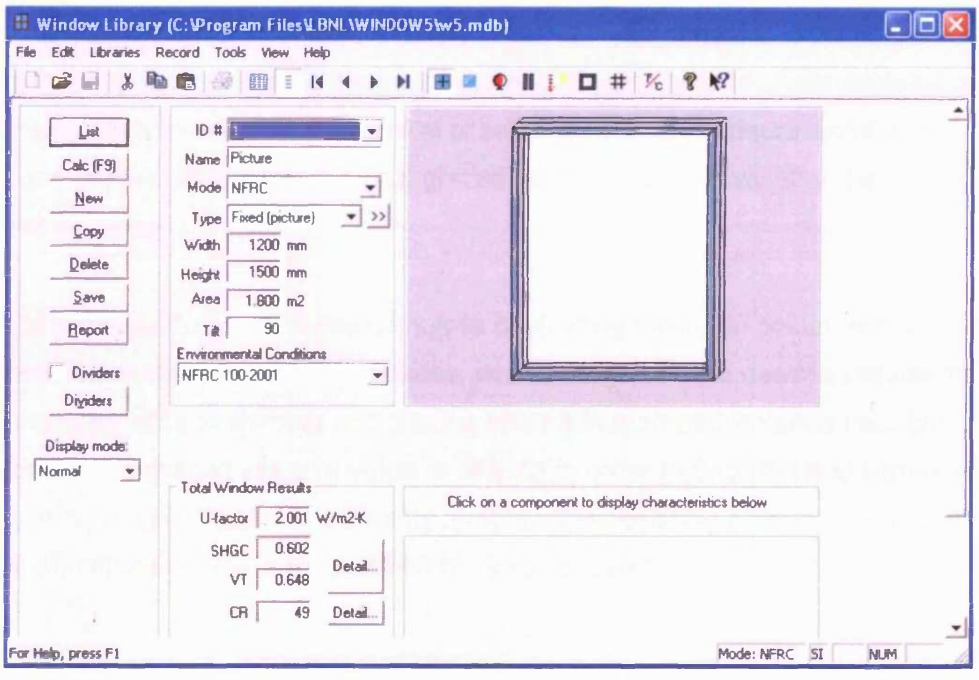


Figure 2.19: Window5 input stage for window system, © 1999-2005 Regents of the University of California

WINDOW5 allows the built up of the glazing system by adding layers of different glass panes and sealed cavities filled with gas (air, argon etc.). The selection of glazing system, frame and dividers form the choice of window system.

Calculations of the U-value and SHGC of various glazing and window systems are performed under a set of environmental conditions. The Environmental Conditions Library contains various options of boundary conditions but there is also the option of user's input. U-value and SHGC are calculated for normal angle of incidence for the window systems and for normal and vertical angle of incidence for the glazing options.

The current version of WINDOW5 does not include any type of shading (except solar control glasses) and also there is no option for ventilated cavities.

## *2.6 Conclusions*

This chapter showed how research, as early as the fifties, tried to solve the complex radiation transport through the widely used slat-type blinds, in order to give designers general guidelines for the choice of shading. Originally for daylight exploitation, research increasingly focused on the control of solar gains and the decrease of energy consumption for cooling in highly glazed buildings, especially after the energy crisis of the seventies.

Early research identified basic choices of shading based on colour, slat angle and position of slat-type shading devices, while recognised the need to include the thermal characteristics of shading and glazing options in their performance calculation. The need for a standardised value (g-value or SHGC) in order to describe and compare different glazing options, that would include direct and secondary solar transmittance characteristics, was also identified by early research.

On the downside, the oversimplified calculation methods and assumptions or the complexity of mathematical and experimental methods made the performance prediction restricted to the research community. Furthermore, the limited choices of shading and glazing options explored, the lack of thermal properties in the performance characterisation of various shading/glazing options and the resulted properties restricted to normal or vertical optical characteristics limited the use of the research outcome but helped in identifying the need for a more flexible and holistic approach in the prediction of glazing performance.

Either by real climate measurements, controlled environment laboratory measurements, theoretical model calculations or the combination of all three, most recent research included the thermal characteristics and long-wave radiation transmission of shading and glazing systems in their performance predictions. All three ways proved to be time consuming and impractical when a design decision had to be made, when one had to take under consideration a wide variety of material and shading options or when technology introduced advanced or new materials that needed description.

Recent research examined the thermal performance of various multilayered glazing systems as embodied by a standardised value (g-value or SHGC) in order to provide designers with a comparable measure that would characterise the various glazing options. Identified was the importance of the angle of solar incident, not only the vertical but also the sun altitude and azimuth dependant, in the thermal performance of the various glazing options.

Main outcome of recent research was the recognition of the need for flexible prediction tools that would calculate the thermal performance of various multilayered glazing options at an early design stage, also taking under consideration the location, the orientation and the environmental conditions of the individual building.

To address the above issues, flexible computer models were developed that would calculate the total solar transmittance and the solar properties of different glazing systems, with the possibility of integrated shading options, under steady-state conditions or under more realistic scenarios and with the prospect of updating the material library when new technology advances directed it. Such computer tools were described in section 2.5 of this chapter.

WIS and WINDOW5 calculate the g-value (or SHGC) of various glazing systems with and without shading (no shading option in the WINDOW5 software) for normal incidence and under steady-state conditions. Output data produced by these two computer models can be used as input data in subroutines in more detailed energy simulation programs in order to calculate the energy use in a building, while the g-value (or SHGC) produced can be used for comparing different glazing options. What the above tools (WIS and WINDOW5) can not offer at the moment of this study is the performance of different

glazing systems in more realistic scenarios where location and local climate affect the systems' thermal performance.

ParaSol was developed and validated within a wider project aimed to measure the solar transmission properties of a large variety of solar shading available in the market, in order to provide comparable g-values measured under similar conditions. ParaSol was introduced as a tool for designers to predict the thermal performance of different glazing systems with integrated shading techniques when choosing a shading solution, during the early design stage of a building. The prediction tool is producing a total solar transmittance g for different glazing options for both normal incident, under steady-state conditions (excluding external shading options) and a monthly average for local climate conditions and for various locations. Shortcomings of ParaSol are the exclusion of ventilated cavities for multilayered glazing systems, the lack of detailed output of the calculated optical properties of the glazing systems and the restriction of the building's environmental conditions in a single room.

The prediction tool review identified the need for a tool that would be able to provide a comparable value calculated under steady-state conditions as well as a more realistic value for the description of different glazing systems dynamically calculated under more realistic scenarios.

## *2.7 References*

Arashteh, D (1986) 'WINDOW 2.0 User and Reference Guide', Windows and Daylighting Group, Lawrence Berkeley Laboratory, Berkeley, Canada

Bell, J and Burt, W (1996) 'Designing Buildings for Daylight', BRE Report 288, BRE

Bordass, W T, Bromley, A K R and Leaman, A J (1995) 'Comfort, Control and Energy Efficiency in Offices', BRE Information Paper IP 3/95, BRE, Garston, UK

Breitenbach, J, Lart, S, Längle, I and Rosenfeld J L J (2001) 'Optical and Thermal Performance of Glazing with Integral Venetian Blinds', Energy and Buildings, Vol.33, pp.433-442

Breitenbach, J, Lart, S and Rosenfeld, J L J (1999) 'Optical Properties and Total Solar Energy Transmittance of Double-Glazing with Solar Control Film', Proceedings North Sun Conference, Edmonton, Canada, 11-14 August, pp.391-396, Solar Energy Society of Canada

Bülow-Hübe, H, Kvist, H and Hellström, B (2003) 'Estimation of the Performance of Sunshades Using Outdoor Measurements and the Software Tool ParaSol V 2.0', Proceedings at ISES Solar World Congress, Gothenburg, 14-19 June

Bülow-Hübe, H and Lundh, U (2002) 'Outdoor Measurements of G-values for External, Interpane and Internal Sunshades', Proceedings of EPIC 2002 AIVC Energy Efficienct and Healthy Building in Sustainable Cities, Lyon, 23-26 October, Vol.3, pp.795-800

Campbell, N S (1998) ' A Monte Carlo Approach to Thermal Radiation Distribution in the Built Environment', PhD Thesis, University of Nottingham

Campbell, N S and Whittle, J K (1997) 'Analysing Radiation Transport Through Complex Fenestration Systems', Proceedings of Building Simulation '97, Vol.1, pp.173-180

Christoffersen, J (1998) 'Daylight Utilisation in Office Buildings', PhD Thesis, Energy and Indoor Climate Division, Danish Building Research Institute & Thermal Insulation Laboratory, Technical University of Denmark

CIBSE (2004) 'Environmental Performance Toolkit for Glazed Facades', CIBSE Technical Manual TM345, Chartered Institution of Building Services Engineers, London

Clark, J P and McLean, D (1988) 'ESP – A Building and Plant Enrgy Simulation System', Version 6, Release 8, Energy Simulation Research Unit, University of Strathclyde and ABACUS Simulations Limited, Glasgow, UK

Coronel, J F, Alvarez, S and Molina, J L (1994) 'Solar, Optical and Thermal Performance of Louver Type Shading Devices', Proceedings of European Conference on Energy Performance and Indoor Climate in Buildings, Lyon, France

Datta, G (2001) 'Effect of Fixed Horizontal Louver Shading Devices on Thermal Performance of Building by TRNSYS Simulation', Renewable Energy, Vol.23, p.497-507

Dijk, van D, Kenny, P & Goulding, J (eds) (2002) 'WIS Reference Manual', available from http://windat.ucd.ie/wis/html/index.html

European Standard EN 13363-1:2003 (2003) 'Solar Protection Devices Combined with Glazing. Calculation of Solar and Light Transmittance. Simplified Method', European Committee for Standardization, Brussels

Farber, E A, Smith, W A, Pennington, C W and Reed, J C (1963) 'Theoretical Analysis of Solar Heat Gain Through Glass with Inside Shading', ASHRAE Transactions, Vol.69, pp.392-405

International Standard ISO 15099:2003 (2003) 'Thermal Performance of Windows, Doors and Shading Devices – Detailed Calculations', The International Organization for Standardization

Klein, S A et al (1988) 'TRNSYS, A Transient System Simulation Program', Manual, Solar Energy Laboratory, University of Wisconsin, Madison, USA

Klems, J H (1994A) 'A New Method for Predicting the Solar Heat Gain of Complex Fenestration Systems: I. Overview and Derivation of the Matrix Layer Calculation', ASHRAE Transactions, Vol.100, Part 1, pp.1065-1072

Klems, J H (1994B) 'A New Method for Predicting the Solar Heat Gain of Complex Fenestration Systems: II. Detailed Description of the Matrix Layer Calculation', ASHRAE Transactions, Vol.100, Part 1, pp.1073-1086

Klems, J H and Kelley, G O (1995) 'Calorimetric Measurements of Inward-Flowing Fraction for Complex Glazing and Shading Systems', ASHRAE Transactions, Vol.95, Part 1

Klems, J H and Warner J L (1992) 'A New Method for Predicting the Solar Heat Gain of Complex Fenestration Systems', Proceedings of ASHRAE/DOE/BTECC Thermal Performance of the Exterior Envelops of Buildings V Conference, Clearwater Beach, Florida, USA, December 7-10

Klems, J H and Warner J L (1995) 'Measurement of Bidirectional Optical Properties of Complex Shading Devices', ASHRAE Transactions, Vol.101, Part 1

Klems, J H and Warner J L (1997) 'Solar Heat Gain Coefficient of Complex Fenestrations with a Venetian Blind for Differing Slat Tilt Angles', ASHRAE Transactions, Vol.103, Part 1

Kuhn, T E, Bühler, C and Platzer, W J (2000) 'Evaluation of Overheating Protection with Sun-Shading Systems', Solar Energy, Vol.69, Nos.1-6, pp.59-74

Lee, E S, DiBartolomeo, DL and Selkowitz, S E (1998) 'Thermal and Daylighting Performance of an Automated Venetian Blind and Lighting System in a Full-Scale Private Office', Energy and Building, Vol.29, pp.47-63

Littlefair, P J (1992) 'Daylight Coefficients for Practical Computation of Internal Illuminances', Lighting Research and Technology, CIBSE, Vol.24, No.3, pp.127-135

Littlefair, P J (1999) 'Solar Shading of Buildings', BRE Report 364, BRE

Littlefair, P J (2005) 'Summertime Performance of Windows with Shading Devices', BRE Trust

Lute, P J, Liem, S H and Van Paassen, A H C (1990) 'Control of Passive Indoor Climate Systems with Adjustable Shutters, Shading Devices and Vent Windows', Faculty of

Mechanical Engineering and Marine Technology, Delft University of Technology, Netherlands

Maccari, A and Zinzi, M (2001) 'On the Influence of Angular Dependence Properties of Advanced Glazing Systems on the Energy Performance of Buildings', Proceedings of Seventh International IBPSA Conference, Rio de Janeiro, Brazil, August 13-15

Marshall, R H and Mason-Jones, A (1995) 'Thermal, Optical and Toatl Solar Energy Transmittance Measurements of Advanced Glazing Materials', Proceedings of Window Innovations '95, Toronto, Canada, pp.32-29

McCluney, R (1987) 'Determining Solar Radiation Heat Gain of Fenestration Systems', Passive Solar Journal, Vol.4, No.4, pp.439-487

McCluney, R and Mills, L (1993) 'Effect of Interior Shade on Window Solar Gain', ASHRAE Transactions, Vol.99, Part 2

Mills, L R and McCluney R (1993) 'The Benefits of Using Window Shades', ASHRAE Journal, Vol.35, Part 11, pp.20-27

Nicol, J F (1966) 'Radiation Transmission Characteristics of Louver Systems', Building Science, Vol.1, pp.167-182

O'Brien, P F (1963) 'Luminous Flux Transfer in Louvers', Illuminating Engineering, Vol. 58, No.5, p.346

Owens, P G T (1974) 'Solar Control Performance of Open and Translucent Louvre Systems', ASHRAE Transactions, Vol.80, Part 2, p.p.324-341

Parmelee, G V and Aubele, W W (1948) 'Solar and Total Heat Gain Through Double Flat Glass', A.S.H.V.E Research Report No.1348, ASHVE Transactions, p.407

Parmelee, G V and Aubele, W W (1952) 'The Shading of Sunlit Glass – An Analysis of the Effect of Uniformly Spaced Flat Opaque Slats', ASHVE Research Report No.1460, ASHVE Transactions, Vol.58, p.377

Parmelee, G V, Aubele, W W and Vild D J (1953) 'The Shading of Sunlit Glass – An Experimental Study of Slat-Type Sun Shades', A.S.H.V.E Research Report No.1474, ASHVE Transactions, Vol.59, p.221

Parmelee, G V and Vild D J (1953) 'Design Data for Slat Type Sun Shades for Use in Load Estimating', ASHVE Research Report No.1485, ASHVE Transactions, Vol.59, p.403

Pfrommer, P (1995) 'Thermal Modelling of Highly Glazed Spaces', PhD Thesis, De Montfort University, Leicester

Pilkington Glass (1973) 'Thermal Transmission of Windows', Environmental Advisory Service

Platzer, W J (2000) 'The ALTSET Project: Measurement of Angular Properties for Complex Glazings', Proceedings of the 3rd International ISES Europe Solar Congress, Copenhagen, Denmark, 19-22 June

Rheauly, S and Bilgen, E (1987) 'On the Heat Transfer through an Automated Venetian Blind Window System', ASME/JSME Conference, Solar Engineering, Honolulu, Hawaii, pp.745-755

Rheauly, S and Bilgen, E (1989A) 'Heat Transfer Analysis in an Automated Venetian Blind Window System', Journal of Solar Energy Engineering, Vol.111, pp.89-95

Rheauly, S and Bilgen, E (1989B) 'Experimental Study of the Thermal Performance of Automated Venetian Blind Windows', Solar and Wind Technology, Vol.6, No.5, pp.581-588

Rheauly, S and Bilgen, E (1990) 'Experimental Study of Full-size Automated Venetian Blind Windows', Solar Energy, Vol.44, No.3, pp.157-160

Robinson, P and Littler, J (1993) 'Thermal Performance Assessment of an Advanced Glazing System', Solar Energy, Vol.50, No.2, pp.129-134

Roche, L (1997) 'Smart Glass', Building Services, The CIBSE Journal, Vol.19, No.8, pp.27-29

Rosenfeld, J L J (1996) 'On the Calculation of the Total Solar Energy transmittance for Complex Glazing Systems', Proceedings of the 8th International Meeting on Transparent Insulation, Freiburg, Germany

Rosenfeld, J L J, Marshall, R H, Platzer, W J and Kuhn, T (1996) 'Calorimetric Determination of the Total Solar Energy Transmittance: Principles', Proceedings of the 8th International Meeting on Transparent Insulation Material, Freiburg, Germany

Rosenfeld, J L J, Platzer, W J, Van Dijk, H and Maccari, A (2000) 'Modelling the Optical and Thermal Properties of Complex Glazing: Overview of Recent Developments', Solar Energy, Vol. 69(suppl.), Nos.1-6, pp.1-13

Smith, W A and Pennington, C W (1964) 'Solar Heat Gain through Double Glass with Between-Glass Shading', ASHRAE Journal, Vol.6, Part 10, pp.50-52

Stephenson, D G and Mitalas, G P (April 1965) 'Solar Transmission through Windows with Venetian Blinds', Proceedings of the CIE International Conference, University of Newcastle upon Tyne

Wall, M, and Bülow-Hübe, H (eds) (2001) 'Solar Protection in Buildings', Report TABK--01/3060, Dept. of Construction & Architecture, Lund Institute of Technology, Lund University, Lund, Sweden

Wall, M, and Bülow-Hübe, H (eds) (2003) 'Solar Protection in Buildings. Part 2:2000-2002', Report EBD-R—03/1, Dept. of Construction & Architecture, Lund Institute of Technology, Lund University, Lund, Sweden

# Chapter 3

# Description of Prediction Tools Used in this Research

## *3.1 Overview*

As demonstrated in chapter 2 no established and validated methodology is offering the flexibility that this research is requiring in order to provide a holistic approach on the thermal performance of different glazing systems with integrated slat-type shading, in building design. In order to serve the objectives of this work a combination of two existing simulation packages has been modified and used for the estimation of the thermal performance of various complex glazing systems. A glazing simulation program calculates the solar properties for a defined glazing system and a dynamic thermal simulation model which has been modified to accept this data. This chapter presents the main features of both packages most relevant to this work and also the modifications the two simulation packages have undergone in order to reach the objectives of this study.

## *3.2 Dynamic Thermal Simulation Model HTB2*

### 3.2.1 Overview

The dynamic thermal simulation model HTB2 (Lewis & Alexander, 1985; Alexander, 1997) has been designed as an investigative model for the thermal performance of buildings. Its aim is to model and monitor the thermal environment of modern low energy buildings and to provide the user with a flexible tool for studying the detailed operation of the building, incorporating the many aspects of thermal transport and thermal gain. For that, HTB2 is written in a modular format in which each subsystem has been isolated and localised in specific subroutines. This means that any section of code which deals with any particular aspect may be quickly identified in order to allow the user to alter and extend the capabilities of the model with minimum of difficulty.

### 3.2.2 Features

The description of the glazing system is part of the building description in the model. A building is being described by its geographical location and by its spaces, linked to each other and to the outside by elements (window, wall, floor, ceiling and internal partitioning), through thermal exchanges and ventilation paths. Every element in the structure of the building is described as a sequence of layers and layer thickness or cavity. Each layer is composed by a choice of material, provided by the model (library file), each material in turn described by its conductivity, density and heat capacity.

For transparent elements, such as windows, the solar properties of the glazing system and absorption factors (%, for normal incident) for every layer are required. If the layer is a cavity (e.g. between two glass panes) the model provides various alternative options. The cavity can be either sealed or ventilated. For sealed cavities there is an option between a normal cavity (high emissivity cavity), low emissivity cavity and a cavity of fixed resistance (defined in the declared width of the layer), while a ventilated cavity is defined by the cavity ventilation factors. The cavity ventilation factors refer to parameters in the general equation for the flow through the cavity:

$$Q\ (m^3/s) = [A + B * u + C * (\sqrt{\Delta T})] * D \qquad (3.1)$$

where, A is a fixed background infiltration flow rate (e.g. for mechanically aided ventilation),
B is the wind component of the cavity flow rate,
u is the wind speed (m/s)
C is the stack effect component of the cavity flow rate,
$\Delta T$ is the temperature difference between the cavity mean temperature and the entering air, and
D is a multiplier that can be varied depending on the control strategy of the glazing system. If D is set to 0 there is no ventilation and the cavity behaves as a normal cavity.

The ventilation rates in the cavity (due to stack effect) are calculated according to ISO 15099 (2003) standard by the equation:

$$Q_w\ (m^3/s) = 0.61 * A_v' * [2\Delta T * g * H / T_c]^{0.5} \qquad (3.2)$$

where: 0.61 is the theoretical value of the discharge coefficient $C_d$, commonly used in calculations,

$A_v'$ refers to the effective area of openings (vents) and is calculated by the equation:

$$A_v' = (1/A_1^2 + 1/A_2^2)^{-0.5}$$

where, $A_1$ ($m^2$) is the area of air inlet and $A_2$ ($m^2$) the area of air outlet,

$\Delta T$ (K) is the temperature difference between the cavity mean temperature and the entering air,

g is the acceleration due to gravity (9.8 $m/s^2$),

H (m) is the window height,

and, $T_c$ (K) is the cavity mean temperature.

The cavity ventilated factor due to stack effect can be calculated by equation (3.1) if it is assumed A=B=0 and D=1:

$$Q_w\ (m^3/s) = C * \sqrt{\Delta T} \qquad (3.3)$$

From equations (3.2) and (3.3) C can be calculated by:

$$C = 0.61 * A_v' * (2 * g * H / T_c)^{0.5} \qquad (3.4)$$

The current version of ISO 15099 standard is not specifying a way to calculate the ventilation through a cavity due to the wind effect so the CIBSE (1999) approximation based on the calculation recommendation for single sided ventilation for a single opening is used here to calculate B:

$$B = 0.025 * A_v \qquad (3.5)$$

Where $A_v$ is the total area of openings ($m^2$): $A_v = A_1 + A_2$

The thermal forces acting on the building are the external climate, heating/cooling and ventilation control system and incidental heat sources (lighting, occupation levels and small power sources – e.g. computers). The result of these thermal forces acting on the building is to generate a set of heat fluxes and air movements, which in turn produce a set of temperatures for each space.

Output data are stored after every simulation in a form of a report, its format shaped according to the needs of the user. Time varying heat flows and solar gains in the space through the transparent system, internal gains (see chapter 6) as well internal temperatures, relative humidity levels and condensation levels (see chapter 7) are some of the predicted data more relative to this research.

HTB2 has been under development from the late 1980's and is in use in a number of research centres in the UK and abroad (Jones, 2001), and has been validated against ASHRAE Standard 140 (ASHRAE Standard 140-2001, 2001).

## *3.3 Glazing Simulation Program*

### 3.3.1 Features

The glazing simulation program, modified from GLSIM (Pfrommer, 1995), calculates the optical properties for a defined glazing system. Meeting the requirements of ISO 15099:2003 (International Standard ISO 15099:2003, 2003), this program determines the angular dependent solar transmission, for both direct and diffuse components, and the absorption for a multilayered glazing system and for each layer in the system. Each layer can be composed of glass, air or a shading material; e.g. horizontal or vertical slat-type blinds, fabric or perforated sheet. The data is calculated for a full hemisphere; angular transmission and absorption for both altitude and azimuth are determined. Figure 3.1 shows contour plots of direct transmission plotted against altitude and azimuth for sample horizontal and vertical blinds, both in a double glazed system. The plots are illustrating the difference between the two shading configurations, a feature which is not used by current modelling methods.

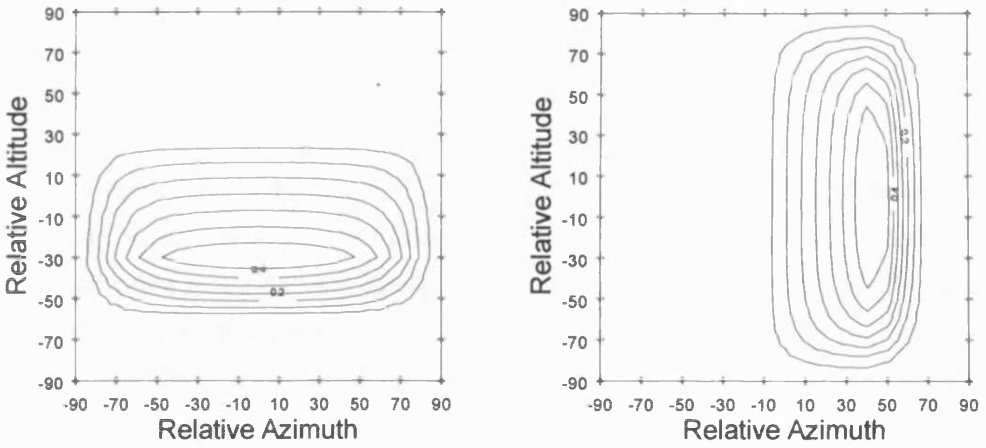


Figure 3.1: Graphical representation of a glazing optical transmission characteristic for a 4mm float double glazing unit with horizontal and vertical slatted blinds, as calculated by the glazing simulation program.

Input data in the glazing simulation program for the calculation of the transmittance characteristics of the glazing systems are:

*(a) For the glass panes*

For the glass panes the specification of the solar transmittance characteristics, transmittance - total of direct and diffuse - and absorption, for normal incidence and thickness are required. For many commercial glass panes total transmittance characteristics are available either through published data (glass guides) or through calculation by software such as WIS (Dijk and Oversloot, 2003) and WINDOW (Arashteh, 1986).

The glass simulation program also calculates the solar transmittance characteristics for multilayered glass panes from optical first principles (uses the wavelength dependent optical properties - complex refraction and absorption indices - for 20 wavelengths between 300nm and 2500nm) requiring a specification of glass and film material properties and thickness. A library with a collection of material files for the most common glass material and coatings is provided by the original GLSIM (Pfrommer, 1994; Pfrommer, 1995) even though in practice the "formula" for most commercial glasses is

not readily available to the end user. However, as mentioned previously, for many commercial glasses total solar transmittance characteristics are available (by manufacturers or other glass simulation models) and can be used in the model instead in order to characterise the glass pane in total.

Even though simple glass panes such as floated glass are used in this study, the program can calculate glazing systems with more complex glass panes such as glass with multi-layer coatings, with noble metal coatings and tinted glass. For complex multi-layer glass panes the specification of layer sequence and thickness can be proved to be complicated since they are not usually available to the end user by the manufacturers. Pfrommer (1994) and Pfrommer et al (1995) is providing a method in order to define the layer sequence and thickness for such glass panes using the library provided and standard manufacturers' data. The program can include panes with any number of sequence layers.

*(b) For the shading*

For the shading device the geometry of the slat-type blind (slat width, slat spacing, slat angle and slat curvature) is required, while slat thickness is considered very thin and slat length infinite. Curved slats[1] are treated by the program as surface-slices of a cylinder. The curvature of the slat is described by the radius of the cylinder (Pfrommer, 1995; Pfrommer et al, 1996). Roller blinds are treated as closed slat-type horizontal blinds (with 0° curvature).

Also required for the calculations are the slat material reflectance (total of specular and diffused), openness (direct transmittance), diffusion (diffuse transmittance) and specularity (or shinning factor[2]).

[1] More work on the influence of curved slats on the transmittance of the different radiation components was considered approximately using assumptions given by Pfrommer (1995).

[2] The shinning factor is defined as the relation between direct to diffuse reflection and specular (direct to direct) reflection and depends on the slat material. The shinning factor becomes 0 for pure diffuse reflection or 1 for ideal specular reflection (Pfrommer, 1994; Pfrommer, 1995).

### 3.3.2 Radiation Transfer through Blinds

The model for the calculation of the stat-type blinds is using a view factor calculation approach (Pfrommer, 1995; Pfrommer et al, 1996). The radiation transmission through blinds was divided into four parts: direct transmittance (the part of incident radiation that is transmitted without reflections), diffuse transmittance (the part of diffuse radiation that is transmitted without reflections), direct reflected transmittance (the part of incident radiation that is transmitted after reflections; can be direct to direct, or direct to diffuse depending on the material's specularity), diffuse reflected transmittance (the part of diffuse radiation that is transmitted after reflections).

The direct transmittance is calculated based on the geometry of the blind (see features 3.3.1) and the angle of incidence. The diffuse transmittance coming from a piece of the sky or the ground that enters the room through the open space between the slats is defined by the cut-off angles, which depend on the blind geometry and slat angle of tilt. The diffuse transmittance is calculated in a similar way as the direct transmittance but the sun angle this time is substituted by the profile angle (the corresponding angle which determines the effective incidence angle of a diffuse radiation portion from a certain sky, or ground, vault). The model is using an isotropic sky.

The direct reflected transmittance consists of two parts the direct to diffuse reflected radiation part and the direct to direct specular part (the correlation between the two parts depends on the material of the slat), while for the diffuse reflected transmittance the specular part is neglected and it is considered to be purely diffused. To calculate both direct and diffuse reflected radiation, the single cell method (also see chapter 2, §2.5.1) is used to calculate the view factors between the illuminated slat part and the inside, the illuminated slat part and the upper slat and the upper slat and the inside. Currently, the glass simulation program, considers all the slat surfaces (both sides of the slat) to have the same reflectance and the same material IR emissivity.

For the interaction between the blind and glazing, both multiple reflections (calculation steps up to the second reflection occurring between the blind and the glazing) and the effect of the blind on the beam direction, which modifies the angle at which solar radiation strikes the glass, are considered (Pfrommer, 1995; Pfrommer et al, 1996).

## *3.4 Modifications to the Models*

HTB2 was intended as a general-purpose simulation code for the examination of the energy and environmental performance of buildings (Lewis & Alexander, 1990). The treatment of glazing in HTB2 had remained essentially unchanged from its initial formulation in the late 1980's. Key features to the modelling of fabric elements were the separate treatment of surface radiant and convective heat exchange, and the specification, and explicit calculation, of the thermal state of material layers of fabric.

Glazing was intended to be treated in a flexible manner. Thermally, glazing was considered as other fabric elements, so heat flow and internal and surface temperatures were explicitly determined. In terms of transparency, solar characteristics (i.e. total transmission and absorption) for a glazing type were specified as look-up tables (for instance as illustrated in figure 3.2) detailed in steps of 10 degrees of incidence angle. Intermediate values were determined by linear interpolation. Shading devices were also specified by look-up tables, describing "masks" of the sky in 10 degree segments, in order to determine the blockage of direct and diffuse solar irradiance (Alexander, Ku Hassan & Jones, 1997). The combination of site and individual surface masks and of the glazing characteristic determined the direct and indirect solar gain to the space.

During an investigation into the modelling of highly glazed spaces Pfrommer et al, (1996) developed a more general glazing and shading model, which was able to be used in conjunction with HTB2 (Pfrommer, 1995).

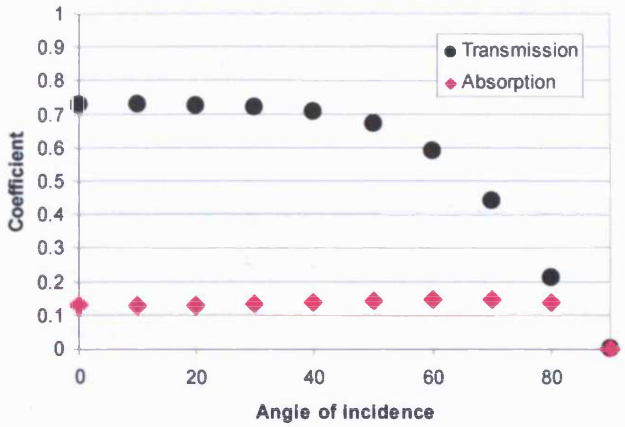


Figure 3.2: Graphical representation of an original HTB2 glazing characteristic of a 4mm float double glazing unit.

Modifications to both the glass simulation program and the thermal model HTB2 were undergone by Donald Alexander, co-creator and responsible for the development of the thermal model HTB2. The role of the author in the development of the prediction tool was to set the main objectives for its application in this research.

The modifications to the glass simulation program included adjustments in the treatment of optical characteristics to allow the production of transmission characteristics that would vary by altitude and azimuth, as opposed to only angle of incidence of 10° steps, and also adjustments to allow the option of inter-pane shading. The program was also modified in order to allow unlimited number of layers composing a glazing system, each layer being either glass pane or blind.

In determining solar transmission through transparent elements, the original algorithms of HTB2 operated only from the angle of incidence. As indicated by many researchers (e.g. Klems & Warner, 1997, Janák, 2003) this approach is insufficient to take into consideration asymmetrical optical characteristics such as those produced by slatted blinds. The treatment of solar characteristics was therefore extended to allow the specification and utilisation of (in the HTB2 code) transmission characteristics that vary in relative altitude and azimuth, generated through the Pfrommer model. An example of

the transmission through a horizontal and vertical slat-type blind system is illustrated in figure 3.1.

Following the original HTB2 methods, 10 degree segments were used to encapsulate the transmission characteristics, with simple linear interpolation used between key points. In addition to direct-beam transmission ($\tau_{dir\text{-}dir}$) and absorption ($\alpha$), a separate characteristic component for diffuse transmission (e.g. from slat inter-reflections) ($\tau_{dir\text{-}dif}$) was introduced. Where previously a global "diffuse transmission" coefficient was required for each glazing type, in the new code diffuse sky and ground transmission is calculated directly through integration of the direct transmission characteristics over the upper (sky) and lower (ground) radiance distributions. In this way, site obstructions and external shading can be explicitly taken into account. The approach can be used to specify horizontal or vertical blind systems without alteration. The model is using an isotropic sky distribution for the diffuse solar components, while research is currently being undergone in order to test the model with an anisotropic sky (Alexander, 2005).

In the thermal treatment of glazing in the modified model, a blind is considered as a thin plane layer (regardless of slat angle). A mid-pane blind thus creates two "half" cavities within the glazing unit, while an external or internal blind will create a new cavity before or after the glazing unit as appropriate. The blind layer may have material properties specified, so that thermal mass and resistance can be taken into consideration. Convective and radiant exchange across the "half" cavities are determined separately. Each cavity can be specified as un-ventilated or ventilated to internal or external spaces. The two cavities do not communicate thermally apart from through the blind material; there is no internal mixing taken into consideration. Further, as HTB2 contains a fundamentally 1-dimensional heat-flow model, the glass, cavity and blind material temperatures are each considered to be uniform across their respective areas.

## *3.5 Conclusions*

Two existing simulation packages have been selected in order to be used in this work for the study of the thermal performance of various glazing systems. This chapter reviewed their main features more related to the objectives of this work. The reviews of the computer tools currently available in the market for the designer (chapter 2, §2.5) and of the selected tools for this work have identified a number of modifications that the selected models should undergo before the investigation of the thermal performance of glazing systems could be undertaken.

The dynamic thermal simulation model HTB2 has been designed as an investigative model for the thermal performance of buildings. HTB2 was chosen for this research because of its flexibility in use and further developement, offering various options for the calculation environment (under steady-state or real climate conditions) and various options of building form, fabric and building systems. Modifications to the model, undertaken by the code authors, aimed to the more accurate representation of the different glazing systems and their treatment of optical and thermal properties and as a result to get a better understanding of their thermal performance.

The modifications to HTB2 concentrated in the treatment of glazing in order to allow the specification and utilisation of transmission characteristics that vary in relative altitude and azimuth, as opposed to vertical angle of incidence of 10° steps. Furthermore, a separate characteristic component for diffuse transmission was introduced, in addition to direct-beam transmission and absorption, and diffuse sky and ground transmission were modified to be calculated directly through integration of the direct transmission characteristics over the upper (sky) and lower (ground) radiance distributions. Finally a ventilated cavity (e.g. between a glazing and an internal blind) was added as an additional layer option, where applicable.

The glass simulation program calculates the solar transmittance characteristics, which vary in relative altitude and azimuth, of various glazing systems, composed by a series of layers, each layer being either glass or blind. The glass simulation program was chosen for this research because of its flexibility in calculating a wide range of glazing

options and its compatibility with the thermal model HTB2. Modifications to the program were undergone in order to further widen the options of glazing to be calculated and also produce a more realistic representation of their solar properties.

Modifications to the glass simulation program included adjustments in the treatment of optical characteristics to allow the production of transmission characteristics that would vary by altitude and azimuth, as opposed to vertical angle of incidence of 10° steps, and also adjustments to allow the option of inter-pane shading. The program was also modified in order to allow unlimited number of layers (glass or blind) in the composition of a glazing system.

The combined model after being modified as previously described will need to be tested and validated against available reference data before it can be applied with confidence.

## *3.6 References*

Alexander, D K (1997) 'A Model for the Thermal Environment of Building in Operation, Release 2.0c', Welsh School of Architecture, Cardiff University

Alexander, D K, Ku Hassan, K A & Jones, P J (1997) 'Simulation of Solar Gains through External Shading Devices', Proceedings of the 5th International IBPSA Conference, Prague, Czech Republic

Alexander, D K, Mylona, A & Jones, P J (2005) 'The Simulation of Glazing Systems in the Dynamic Thermal Model HTB2', Proceedings of the 9th International IBPSA Conference, Montreal, Canada

Arashteh, D (1986) 'WINDOW 2.0 User and Reference Guide', Windows and Daylighting Group, Lawrence Berkeley Laboratory, Berkeley, Canada

ASHRAE Standard 140-2001 (2001) 'Standard Method of Test for the Evaluation of Building Energy Analysis Computer Programs (ANSI approved)', AHRAE

CIBSE (1999) 'Environmental Design', CIBSE Guide, Vol. A, Chartered Institution of Building Services Engineers, London

Dijk, V H and Goulding, J (1996) 'Reference Manual WIS, Advanced Windows Information System', University College Dublin, Dublin, Ireland

International Standard ISO 15099:2003 (2003) 'Thermal Performance of Windows, Doors and Shading Devices – Detailed Calculations', The International Organization for Standardization

Jones, PJ, Kopitsis, D (2001) 'Modelling the Thermal Performance of Glazed Facades', Proceedings of the National Conference: The Whole-Life Performance of Facades, Bath

Lewis, PT, Alexander, DK (1990) 'HTB2: A Flexible Model for Dynamic Building Simulation', Building and Environment, Volume 25, No.1

Pfrommer, P (1994) 'GLSIM - Glazing Simulation Program', User Manual, Version 1.0, De Montfort University, Leicester

Pfrommer, P, Lomas, K J, & Kurke, CHR (1996) 'Solar Radiation Transport through Slat-Type Blinds: A New Model and its Application for Thermal Simulation of Buildings', Solar Energy, Vol.57, No.2, pp.77-91

Pfrommer, P, Lomas, K J, Seale, C & Kurke, CHR (1995) 'The Radiation Transfer through Coated and Tinted Glazing', Solar Energy, Vol.54, No.5, pp.287-299

Pfrommer, P (1995) 'Thermal Modelling of Highly Glazed Spaces', PhD Thesis, De Montfort University, Leicester

# Chapter 4

# Solar Radiation Transfer through Glazing & Review of Total Solar Transmittance Theory and Practice

## *4.1 Overview*

This chapter presents the thermal processes involved in the transmission of the solar radiation through a glazing system. Special attention is drawn to the calculation and definition of the total solar transmittance, g-value, a representation of the thermal performance of various glazing options, used in order to describe and compare different glazing systems. Finally, presented is the calculation method used in this research in order to produce both a steady-state and a more realistic representation of g-value.

## *4.2 Total Solar Transmittance through a Glazing System*

Figure 4.1 illustrates the thermal processes involved in the transmission of the solar radiation through a glazing system. Of the incident solar radiation that falls on the outside surface of a glazing system, some is reflected immediately and some transmitted directly to the interior (either as a direct, or as a diffused solar radiation depending on the nature of the glazing system). The remainder is absorbed into the glazing system which increases its temperature. Due to this increase in temperature, some of the absorbed solar radiation is eventually released into the building interior, as convective or long-wave radiation. This re-released energy can be significant and its amount depends on the details of the design of the glazing system.

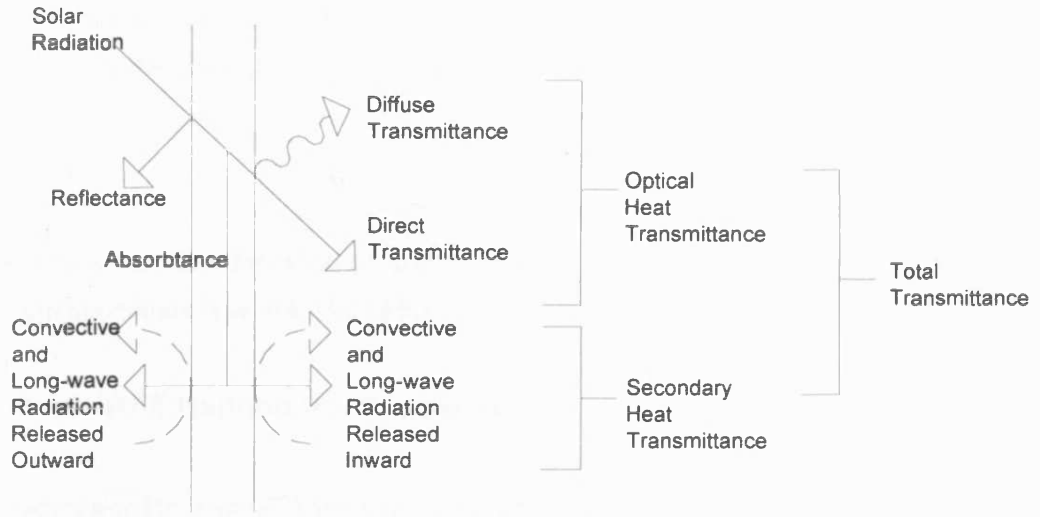


Figure 4.1: Division of the incident solar radiation

The total solar transmittance incorporates this "extra" heat gain, and is defined as the sum of the direct and diffuse solar radiation transmitted through the glass and the secondary heat transmitted to the inside of the room as a result of radiation, convective and long-wave.

## *4.3 Review of the g-value Definition*

The g-value (or solar factor) is a representation of the total solar transmittance through a glazing system and is currently used as a way to characterize and compare between different glazing systems available in the market. This paragraph presents a review of the g-value as defined by up to date European and International Standards and also as measured and/or calculated in recent studies and simulation tools.

### 4.3.1 EN 410:1998

EN 410 suggests a mathematical model for the calculation of the separate components of the transmitted solar radiation. According to EN 410 the total solar transmittance g is defined as the sum of solar direct transmittance and the secondary heat transfer factor

of the glazing towards the inside, the latter resulting from heat transfer by convection and long-wave IR-radiation of that part of the incident solar radiation which has been absorbed by the glazing:

$g = t_e + q_i$

where: $t_e$ is the solar direct transmittance and
$q_i$ is the secondary heat transfer factor

### 4.3.2 ASHRAE Handbook – Fundamentals

The equivalent to g-value American value is the solar heat gain coefficient (SHGC). According to ASHRAE (2005) the SHGC incorporates the directly transmitted solar radiation and the inward flowing portion of the absorbed solar radiation, and is conducted, convected and radiated to the interior:

$SHGC = T + N\mathcal{A}$

Where: T is the directly transmitted solar radiation and
$\mathcal{A}$ is the absorbed solar radiation
N is the fraction of the absorbed solar radiation flowing inwards

ASHRAE is providing a mathematical model for the calculation of the separate components of the transmitted solar radiation.

### 4.3.3 ISO 15099:2003

ISO 15099 is also suggesting a mathematical model for the calculation of the heat flow through the glazing. According to the most recent ISO standard (2003) the total solar transmittance g of a glazing system can be defined as the difference between the net heat flow rate into the internal environment with and without incident solar radiation.

$\tau_s = q_{int} - q_{int} (I_s = 0) / I_s$

where: $\tau_s$ is the g-value,

$q_{int}$ is the net density of heat flow rate through the glazing system to the internal environment ($W/m^2$)

$q_{int}$ ($I_s = 0$) is the net density of heat flow rate through the glazing system to the internal environment, but without incident solar radiation ($W/m^2$)

and $I_s$ is the incident solar radiation ($W/m^2$)

### 4.3.4 ALTSET Project

The ALTSET project measured the total energy flow through various glazing options by using the calorimetric method. The ALTSET defined the g-value of a window system or of the separate components as the difference between:

- the total net energy flow per unit of area into the internal environment, due to incident solar radiation on the system and heat loss by transmission through the system,
- and: the total net energy flow per unit of area into the internal environment, due to heat loss by transmission through the system with the same temperature and wind boundary conditions

That is the difference between the total net heat flow of the irradiated and dark state.

$$g = \Phi(E) - \Phi(E=0) / AE$$

where, $\Phi$ is the transmitted total energy flow ($W/m^2$),

E is the incident solar radiation for area A of the glazing system ($W/m^2$)

### 4.3.5 WIS

WIS is using the same mathematical model suggested by the ISO standard to calculate the heat flow through the glazing system. According to WIS the g-value is defined by the density of heat flow rate leaving the component at the inside surface, under steady-state conditions, caused by solar radiation at the outside surface, divided by the intensity of incident solar radiation on the component.

WIS is using the following formula to calculate the g-value of various glazing systems for normal incident:

g = HG(with Gs) – HG(without Gs) / Gs

where: HG is the Heat Gain towards the room ($W/m^2$)and
Gs is the incident solar radiation ($W/m^2$)

Heat Gain (HG) is defined here as the sum of the short wave radiation flow per $m^2$, the long wave heat flow per $m^2$ due to inner surface temperature of the transparent system, the long wave heat flow per $m^2$ due to transmission through IR transparent layers (such as Venetian blinds etc) the convective heat flow per $m^2$ due to the inner surface temperature of the transparent system and, where applicable, the ventilative heat flow per $m^2$ due to air layer connected with the room air via a air permeable layer, divided by the transparent system.

### 4.3.6 ParaSol

ParaSol is an energy model that calculates the cooling and heating loads in the space and uses them to calculate the g-value. ParaSol tool is calculating a more realistic representation of a monthly mean solar factor which takes under consideration the climate of the location of the glazing system. The above g-value is defined as the difference between the cooling and the heating loads with incident solar radiation, minus the same without incident solar radiation, divided by the incident solar radiation through the window:

$g = [(E_{c,s} – E_{h,s}) – (E_{c,n} – E_{h,n})] / G$ or $g = (E_{c,s} – E_{c,n} - E_{h,s} + E_{h,n}) / G$

where: $E_{c,s}$ is the cooling load for the month with incident solar radiation through the window glass area ($W/m^2$),
$E_{c,n}$ is the cooling load for the month without incident solar radiation ($W/m^2$),
$E_{h,s}$ is the heating load for the month with incident solar radiation through the window glass area ($W/m^2$),

$E_{h,n}$ is the heating load for the month without incident solar radiation ($W/m^2$) and
G is the incident solar radiation on the window glass area ($W/m^2$) (Wall and Bülow-Hübe, 2001; Wall and Bülow-Hübe, 2003).

### 4.3.7 Lund Measurements

Similarly, measurement under real climate conditions calculated the energy use for cooling and heating in order to achieve an energy balance in the test sell. The measurements of a total solar transmittance g at Lund University were based on the definition of the total transmitted solar energy $Q_{sun}$ divided by the global solar radiation on the window area:

$$g_{system} = Q_{sun} / I_G * A_w$$

where $I_G$ is the incident solar radiation on the window ($W/m^2$),
$A_w$ is the window area ($m^2$) and
$Q_{sun}$ is the heat balance for the box used for the experiment (W):

$$Q_{sun} = Q_{cool} - Q_{el.heat} + Q_{window} + Q_{room} + Q_{capacity}$$

$Q_{cool}$ and $Q_{el.heat}$ are the measured cooling and heating energies (W) (for keeping the temperature in the box steady),
$Q_{window}$ is the heat losses through the window (W),
$Q_{room}$ is the heat losses from the box to the room (W) (where the box was placed) and finally $Q_{capacity}$ is a correction term for the heat capacity of the box with respect to changes in the box temperature during the measurement period (W) (description of the experiment: Wall and Bülow-Hübe, 2001; Wall and Bülow-Hübe, 2003).

### 4.3.8 BRE Report

Littlefair, in the BRE report for the summertime performance of windows with shading devices, (Littlefair, 2005) is distinguishing between the g-value and the effective g-value. The g-value definition is in accordance with the EN 410, while the effective g-value or $g_{eff}$

is defined as the solar gain in period of potential overheating through window with shading device divided by the solar gain through unshaded, unglazed aperture for the same period. The period from May to August and the peak radiation days (2.5%) have been chosen for the calculation of the solar gains.

The calculation of the $g_{eff}$ defined above aims to include the effect of orientation and inclination of the window surface as well as the sun altitude (differentiation between seasons rather than months) in the total solar transmittance in order to provide a value for the comparison between shading techniques and also to be used as input in simple calculation methods (manual or computational) of solar gains, and as a result the heat gains and overheating risk, in a space.

The report provides a simple computer tool to calculate the $g_{eff}$ of a window system by knowing the steady-state g-values of the separate components given by the manufacturers. The same report also provides a method for a window plus blind calculation when the effective g values of its component are known, based on the standard BS EN 13363-1.

Additionally the report provides a calculation of the $g_{eff}$ which is based on directional transmittance data for the window, with or without a shading device, weighted by the amount of radiation reaching it from different directions:

$$g_{eff} = \iint Le(\gamma,a)\cos(i)\,T(\gamma,a)\cos(\gamma)\,d\gamma da \,/\, \iint Le(\gamma,a)\cos(i)\cos(\gamma)\,d\gamma da \qquad (4.1)$$

where: $\gamma$ is the altitude of the patch of sky under consideration and a its azimuth
$T(\gamma,a)$ is the transmittance of the window (with shading device) to radiation from this direction (it is a directional/hemispherical transmittance)
i is the angle of incidence of the solar radiation (for vertical openings: $\cos(i) = \cos(\gamma)\cos(a-\varphi)$, where $\varphi$ is the azimuth of the normal to the window)
$Le(\gamma,a)$ is the amount of radiation, per unit solid angle, coming from direction $(\gamma,a)$ during the time of year for which there is an overheating risk. It includes radiation that comes directly from the sun (for the given $(\gamma,a)$) and that is diffused from the sky.

The report provides data for the above calculation method and additionally refers briefly to a computer program that has been written to compute Le(γ,a) for 5° steps in (a) and 2° steps in (γ) and it uses a one minute time step from May the 1st until August the 31st inclusive.

## *4.4 Review of the Boundary Conditions for the Calculation of a Steady-state g-value*

The g-values of various glazing systems and their components are often published by glazing manufacturers. They are determined through simulation or are measured in laboratory facilities in order to provide a standardized value that can describe and compare different glazing systems. This paragraph will review the most commonly used sets of boundary conditions for the calculation of a steady-state g-value.

### 4.4.1 EN 410

According to the European standard EN 410 (British Standard EN 410:1998, 1998; also see boundary conditions for the calculation of the U-value at EN 673:1998), the g-value is determined under the following conditions:

- steady incident solar radiation, normal to the window
- the external convective heat transfer coefficient is 18.6 $W/m^2K$ (equivalent to a wind speed of 4m/s), and
- the internal convective heat transfer coefficient is 3.6 $W/m^2K$
- steady internal and external temperatures

### 4.4.2 ISO 15099

ISO 15099 (International Standard Organization ISO 15099:2003) suggests the following boundary conditions for the calculation of the g-value:

Winter conditions:

- internal temperature: 20 °C
- external temperature: 0 °C
- internal convective heat transfer coefficient is 3.6 $W/m^2K$
- external convective heat transfer coefficient is 20 $W/m^2K$
- solar irradiance is normal to the window surface, at 300 $W/m^2$

Summer conditions:

- internal temperature: 25 °C
- external temperature: 30 °C
- internal convective heat transfer coefficient is 2.5 $W/m^2K$
- external convective heat transfer coefficient is 8 $W/m^2K$
- solar irradiance is normal to the window surface, at 500 $W/m^2$

Even though the above sets of boundary conditions are suggested by standards (EN and ISO) they are acting only as suggestions and are not currently used explicitly. Various research (e.g. see ALTSET project §4.3.3) has used a variation or different sets from the above suggested sets and the various glass simulation programs in the market (e.g. WIS §2.5.1) provide the option of input alternative sets of boundary conditions.

## *4.5 Calculation of the Total Solar Transmittance in this Research*

### 4.5.1 Boundary Conditions for the Calculation of a Steady-State G-value

Even though this research is mainly interested in the thermal performance of glazing systems under realistic conditions, it was considered necessary to also calculate the steady-state G-values of the glazing systems under consideration in order to be used for validating the combined simulation method but also to show that the method could also be used in order to provide a standardized value for comparison with manufacturers' data.

The boundary conditions selected for the simulation of the steady-state G-value, under "laboratory" conditions are consistent to the EN410. Since solar irradiance and

internal/external values are not defined by EN410 the above values were adopted by the ALTSET project, set up for the calorimetric measurements of various advanced glazing systems.

- solar irradiance is normal to the window surface, at 783 $W/m^2$
- internal temperature: 24°C
- external temperature: 24°C
- the external convective heat transfer coefficient is 18.6 $W/m^2K$ (equivalent to a wind speed of 4m/s), and
- the internal convective heat transfer coefficient is 3.6 $W/m^2K$

Simulations in this research under the above boundary conditions are made for both normal and vertical angle of incidence.

### 4.5.2 Dynamic Calculation of an Hourly $\hat{g}_d$

The above boundary conditions can be used in order to provide a standardized value that can describe and compare different glazing systems. While this is advantageous to the designer for a coarse selection of glazing types (e.g. a glazing system with a G-value of 0.3 should be preferable to one of 0.8), the standardized value does not necessarily imply how the system may work in practice. Of particular concern is the omission of angular information as the steady-state G-value is determined only for normal incident radiation (according to the standards). Glazing systems which show a high angular dependency, such as venetian blinds, are not well served by the steady-state G-value (Platzer, 2000). The detailed selection of glazing options, e.g. the differentiation between systems of otherwise close G-values, which can behave significantly different in practice, will require more detailed parameters, more advanced simulation. Such simulations need to answer questions such as the effect of placement of blinds (e.g. internal, external or mid-pane), the effect of colour and shade, and the effect of location and climate, on the performance of the glazing system.

These simulations will test glazing specifications under time-varying conditions, under realistic meteorological conditions and coupled to the design fabric and servicing

strategies, in order to allow the designer to investigate the holistic performance in practice of available glazing options.

The dynamically calculated hourly g-value, termed here as $\hat{g}_d$, in order to differentiate it from the steady-state laboratory G-value, was estimated from the simulation output data as: the sum of the short-wave radiation (direct and diffuse), the secondary heat transmitted to the inside of the room as a result of radiation, convective and long-wave (the long-wave heat flow due to inner surface temperature of the transparent system and the convective heat flow due to the inner surface temperature of the transparent system) and, where applicable, the ventilative heat flow due to ventilated layer connected with the room, normalized by the incident solar radiation:

$$\hat{g}_d = I + [Q_s + Q_v] - [Q_s' + Q'_v] / Is \qquad (4.1)$$

where: $I$ (W/m$^2$) is the short-wave radiation through the glazing (direct and diffuse)
$Is$ (W/m$^2$) is the incident solar radiation on the window
$Q_s$ (W/m$^2$) is the convective and long-wave radiant heat exchange from the internal surface of the glazing as a result of solar incidence
$Q_s'$ (W/m$^2$) is the convective and long-wave radiant heat exchange from the internal surface of the glazing under identical conditions except with no incident solar radiation, achieved through a second simulation
$Q_v$ (W/m$^2$) is the ventilative heat flow inside the room due to ventilated layer as a result of solar incidence, and
$Q'_v$ (W/m$^2$) is the ventilative heat flow inside the room due to ventilated layer without solar incidence

The above formula for the calculation of the $\hat{g}_d$ was also used for the calculation of the steady-state G but for the boundary conditions previously described (§4.5.1).

## 4.6 Conclusions

Chapter 4 presented the thermal processes involved in the transportation of solar radiation through a glazing system and reviewed the way the total solar transmittance, g-value, is used in order to provide a thermal performance representation to describe and compare different glazing systems. The review of the calculation of the g-value, which included European and International standards and the most recent research and calculation tools, revealed that even though some differences are expressed in the way the g-value is measured or calculated, depending on the availability of resources and calculation methods used, the variables that influence the g-value and so the thermal performance of a glazing system are the same; the incident solar radiation, the optical and thermal properties of the glazing system and the temperature difference between internal and external environment (for the calculations/measurements under real climate conditions). All above variables influence the way the solar gains are transferred into the space. The review also showed that the calculation of g-value excludes any heat losses.

A distinction was made between the steady-state G-value and the dynamically calculated $\hat{g}_d$ value under real climate conditions. Taking under consideration all the variables that influence the total solar transmittance a calculation method was suggested to estimate both G-value and $\hat{g}_d$ value from simulation method.

## 4.7 References

ASHRAE (2005) 'ASHRAE Handbook - Fundamentals', ASHRAE

European Standard EN 410:1998 (1998) 'Glass in Building - Determination of Luminous and Solar Characteristics of Glazing', European Committee for Standardization, Brussels

International Standard ISO 15099:2003 (2003) 'Thermal Performance of Windows, Doors and Shading Devices – Detailed Calculations', The International Organization for Standardization

Littlefair, P (2005) 'Summertime Performance of Windows with Shading Devices', BRE Trust

European Standard EN 673:1998 (1998) 'Glass in building - Determination of thermal transmittance (U-value), Calculation method' European Committee for Standardization, Brussels

Wall, M, and Bülow-Hübe, H (eds) (2001) 'Solar Protection in Buildings', Report TABK--01/3060, Dept. of Construction & Architecture, Lund Institute of Technology, Lund University, Lund, Sweden

Wall, M, and Bülow-Hübe, H (eds) (2003) 'Solar Protection in Buildings. Part 2:2000-2002', Report EBD-R—03/1, Dept. of Construction & Architecture, Lund Institute of Technology, Lund University, Lund, Sweden

Platzer, W J (2000) 'The ALTSET Project: Measurement of Angular Properties for Complex Glazings', Proceedings of the 3rd International ISES Europe Solar Congress, Copenhagen, Denmark, 19-22 June

Van Dijk, H and Goulding, J (1996) 'Reference Manual WIS, Advanced Windows Information System', University College Dublin, Dublin, Ireland

# Chapter 5

# Evaluation of Prediction Tools

## *5.1 Overview*

In order to test the applicability of the combined calculation method developed from the requirements identified in chapter 3, it was considered necessary to compare results with measurements and validated tools.

First a comparison of the optical properties of glazing and shading was undertaken for a number of blinds and glass – blinds configurations in order to test the glazing simulation program. Properties examined were the transmittance (direct and diffuse) and the absorption of a series of blind configurations and for glass-blind-glass configurations for 90 to -90 angle of incidence. Results were compared with WIS as the standard reference model (Dijk & Oversloot, 2003). Even though the exact accuracy of the model through its validation process is not currently available (see also description in chapter 2) it is presently the best practical tool available for the examination of the optical and thermal properties of different glazing systems.

Secondly, a comparison of the steady-state G-value of a series of multilayered glass/blind configurations was undertaken this time including external and internal as well as inter-pane blinds. For the calculation of the steady-state G-value HTB2 was used as a steady-state model in order to model a simple space perfectly heated/cooled to a steady internal temperature and also to model the boundary conditions as further explained in chapter 4, §4.5. Results were again compared with the WIS reference model.

Finally, the dynamically calculated $\hat{g}_d$ value of a series of glass-blind-glass configurations was compared with field trial data taken by Lund University (Bülow-Hübe et al, 2003). Test facilities described further in chapter 2, §2.4.4. The thermal model HTB2 was used to model the test cell conditions and the simulations were run under hourly climate data provided by Lund. Even though some data for comparison were available through laboratory measurements, at the time of this research the Lund project was the only one to have undertaken real climate measurements of an hourly $\hat{g}_d$ value in field trial facilities.

## *5.2 Comparison to Reference Model*

Comparisons were made through evaluation of average (ME) and root-mean-square (RMSE) error between the reference standards (chapter 4, §4.5.1) and the modified model. Initial evaluations were made of the blind transmission model in isolation, of the blind transmission model in combination with glass panels, and of the total solar transmission of the glazed systems under steady-state conditions. The reference for each of these was the WIS software. An extensive description of WIS is presented in chapter 2 §2.5.1.

### 5.2.1 Blind Configurations

Slat-type blinds examined here are presented in table 5.1. The blind slats were 28mm deep with a 22mm pitch. The same blind samples and glass-blind-glass systems were used during detailed test-cell measurements during a test programme run by Lund University (Bülow-Hübe et al, 2003).

| Case | Slat reflectance | Slat Angle |
|---|---|---|
| W0 (white 0°) | 0.67 | 0° |
| W45 (white 45°) | 0.67 | 45° |
| W80 (white 80°) | 0.67 | 80° |
| B0 (white 0°) | 0.19 | 0° |
| B80 (white 80°) | 0.19 | 80° |

Table 5.1: Summary of comparison test data configurations

Considering the slat-type blind in isolation, compared to WIS calculations the calculation of direct beam transmission ($\tau_{dir\text{-}dir}$) was seen to be exact (as might be expected from a simple geometrical problem) (figure 5.1). Calculation of the diffusing beam transmission ($\tau_{dir\text{-}dif}$) was also good but not perfect, with a mean error of 0.0008 and a RMSE of 0.007 across the five configurations (figure 5.2, 5.3, 5.4 & 5.5).

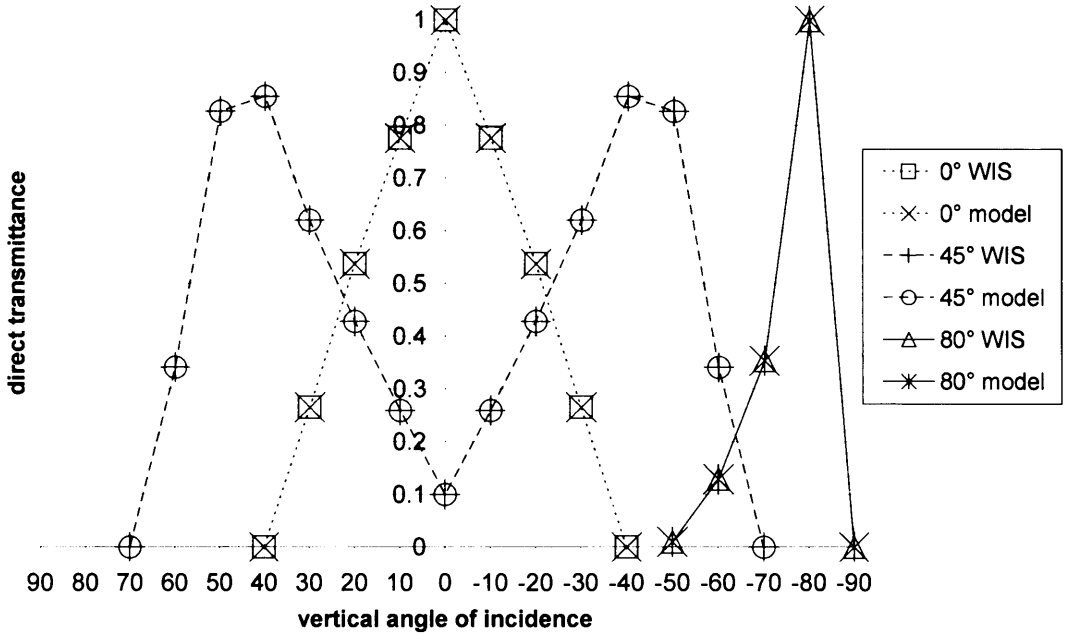


Figure 5.1: Comparison of direct transmittance ($\tau_{dir\text{-}dir}$) through slat-type blinds with various slat angle

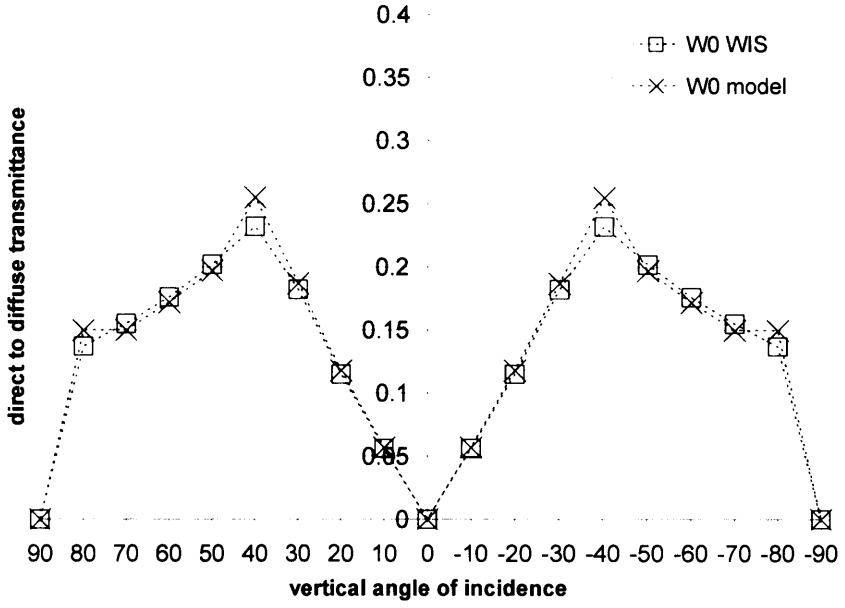


Figure 5.2: Comparison of diffuse transmittance ($\tau_{dir\text{-}dif}$) through slat-type blind for the W0 case

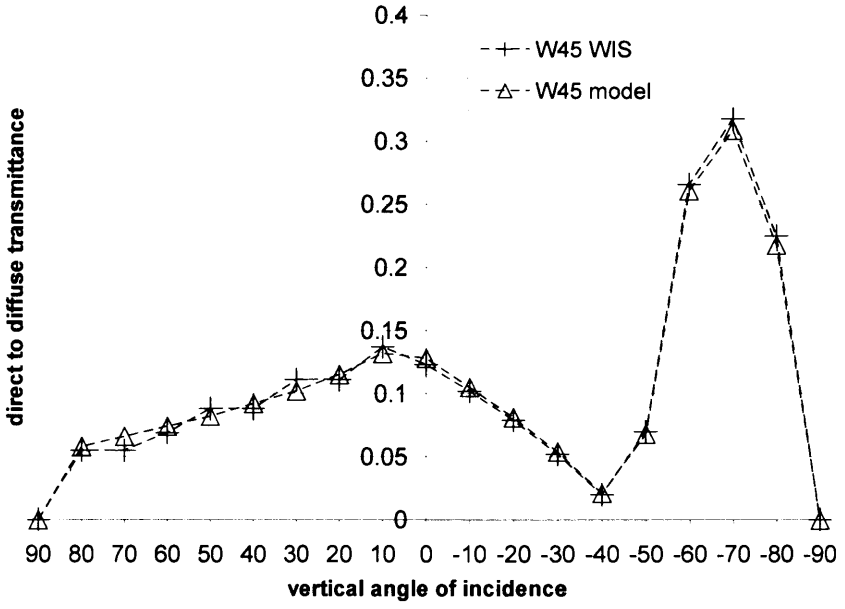


Figure 5.3: Comparison of diffuse transmittance ($\tau_{dir\text{-}dif}$) through slat-type blind for the W45 case

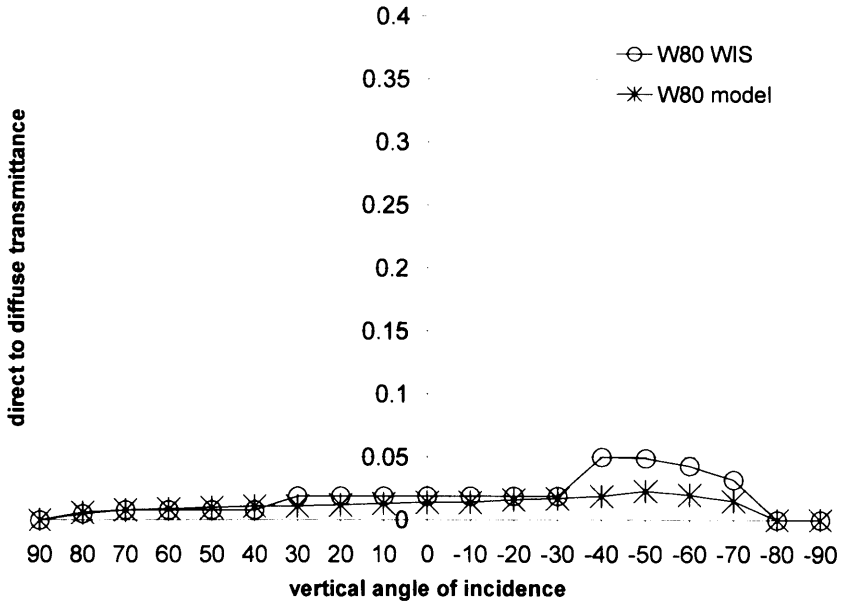


Figure 5.4: Comparison of diffuse transmittance ($\tau_{dir\text{-}dif}$) through slat-type blind for the W80 case

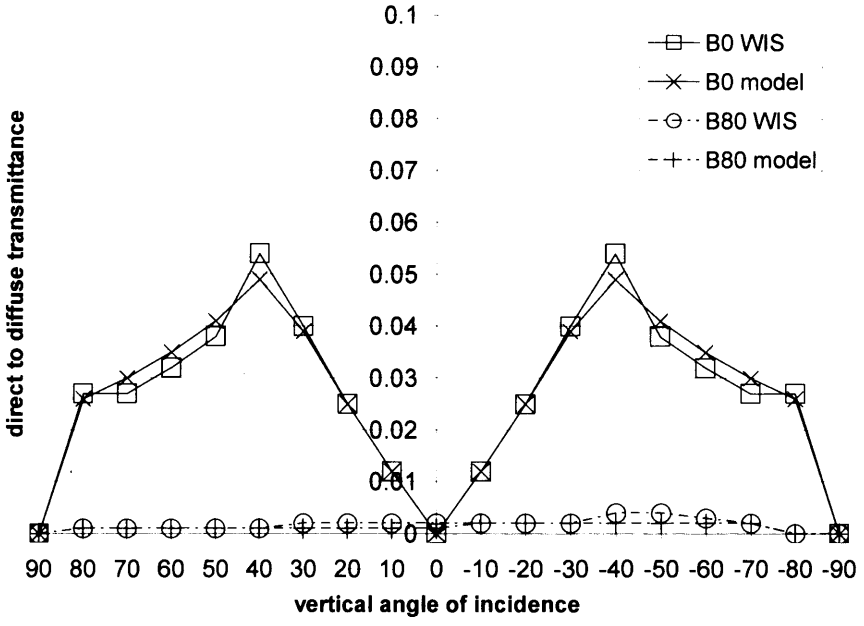


Figure 5.5: Comparison of diffuse transmittance ($\tau_{dir\text{-}dif}$) through slat-type blinds for the blue cases

There were found to be larger discrepancies in the absorption characteristic factors however, particularly for large slat angles; this component exhibited a RMSE of 0.025 and a mean error of 0.013 (figure 5.6, 5.7, 5.8 & 5.9). This is seen to indicate a

weakness in the view factor calculation, which at time of writing has not been identified and requires further investigation.

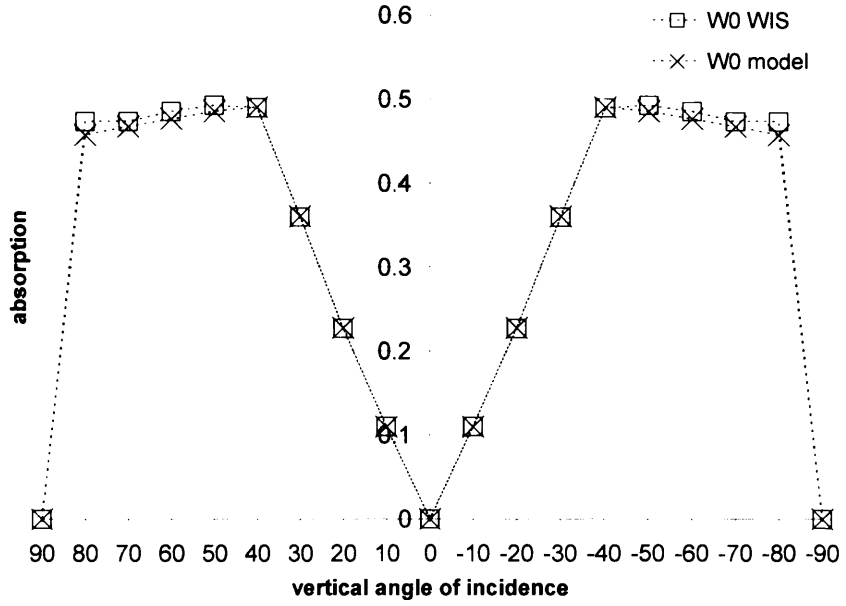


Figure 5.6: Comparison of absorption values for slat-type W0 blind case

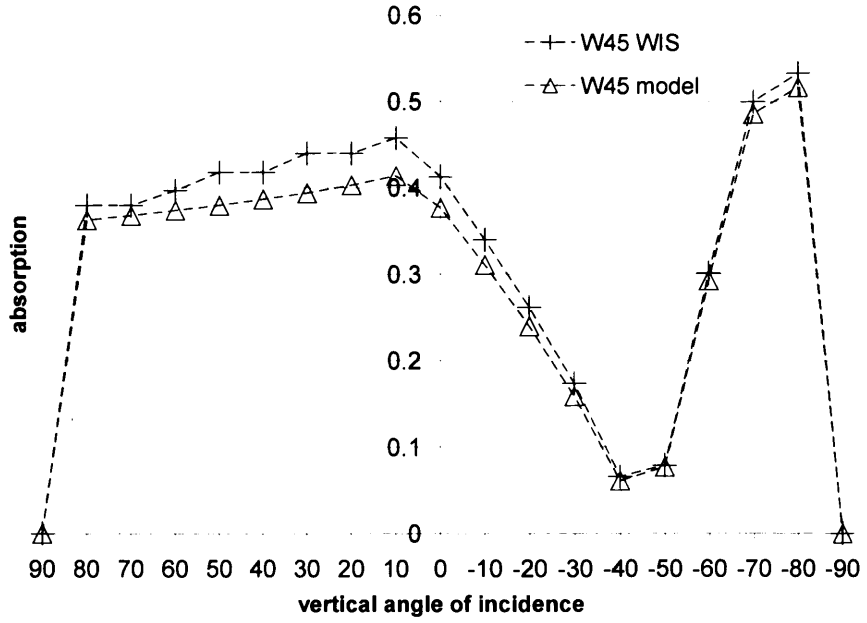


Figure 5.7: Comparison of absorption values for slat-type blind for the W45 case

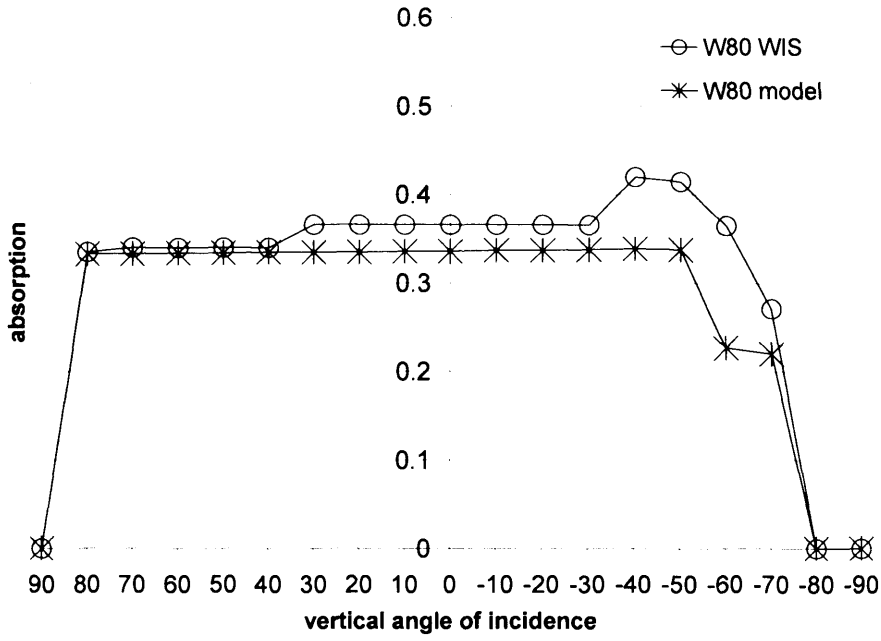


Figure 5.8: Comparison of absorption values for slat-type blind for the W80 case

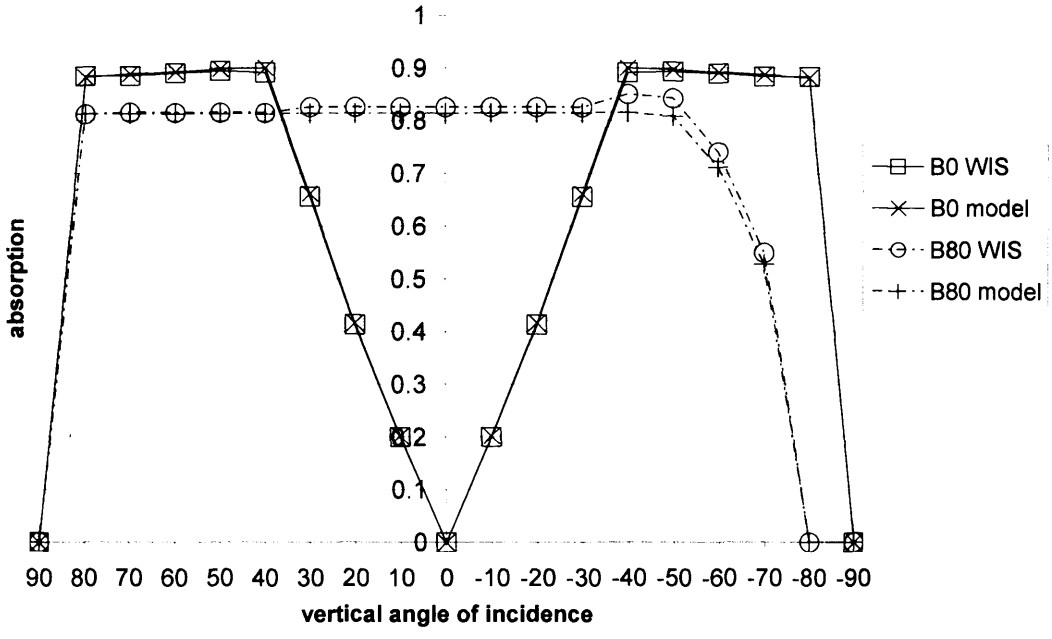


Figure 5.9: Comparison of absorption values for slat-type blinds for the blue cases

Table 5.2 summarises the results of the diffuse transmittance and absorption values of the blinds under consideration.

| Case | WIS mean values for 90 to -90 angle of incidence | | RMSE WIS-Model | |
|---|---|---|---|---|
| | Diffuse Transmittance | Absorption | Diffuse Transmittance | Absorption |
| W0 (white 0°) | 0.13 | 0.33 | 0.009 | 0.007 |
| W45 (white 45°) | 0.10 | 0.32 | 0.005 | 0.025 |
| W80 (white 80°) | 0.018 | 0.30 | 0.012 | 0.046 |
| B0 (white 0°) | 0.027 | 0.60 | 0.002 | 0.004 |
| B80 (white 80°) | 0.002 | 0.68 | 0.0008 | 0.015 |

Table 5.2: Summary of results from comparison of optical properties of blinds with reference model

### 5.2.2 Glass – Blind – Glass Configurations

The same slat-type blinds examined here (table 5.1) but this time for a glass-blind-glass system. The blinds were contained between 4mm clear float glass panes in a 30mm unventilated cavity. The blind slats were 28mm deep with a 22mm pitch.

For the slat-type blinds in combination with glass panes there is a further deterioration from the ideal. RMSE error in total transmission (direct and diffuse) of the system has now increased to 0.008 (figures 5.10, 5.11, 5.12, 5.13 & 5.14) and in absorption to 0.031 (figures 5.15, 5.16, 5.17 & 5.18). The cause of disagreement in the treatment of absorption in the combination algorithm could not be identified during this research but further investigation could be undertaken by the code authors in a later research.

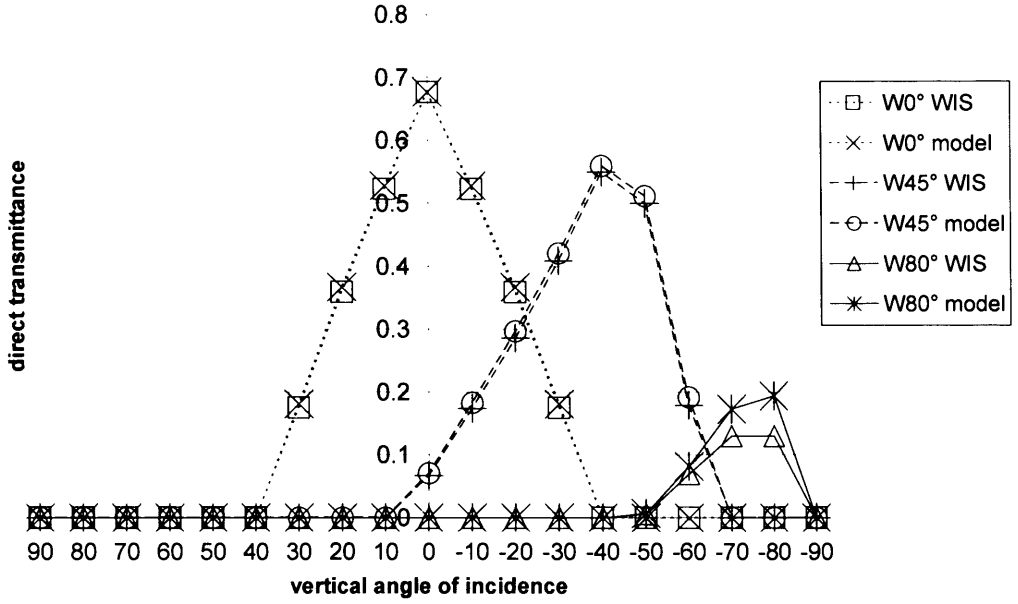


Figure 5.10: Comparison of system direct transmission of the white blind cases in a double glazed pane

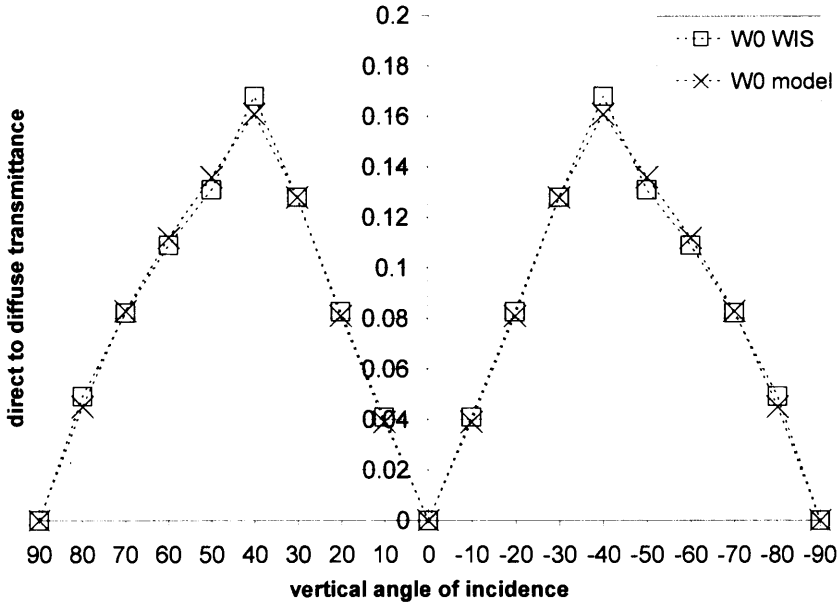


Figure 5.11: Comparison of system diffuse transmission of the W0 case in a double glazed panel

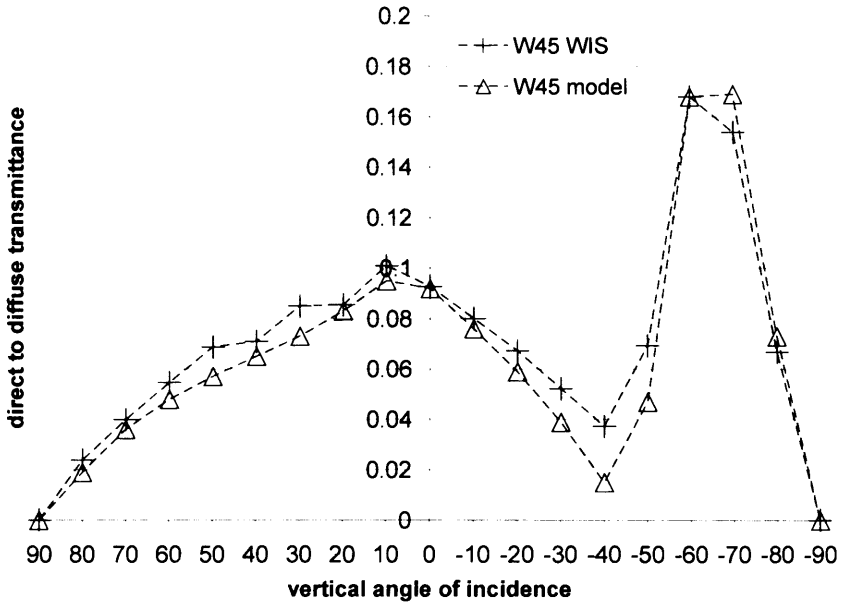


Figure 5.12: Comparison of system diffuse transmission of the W45 case in a double glazed panel

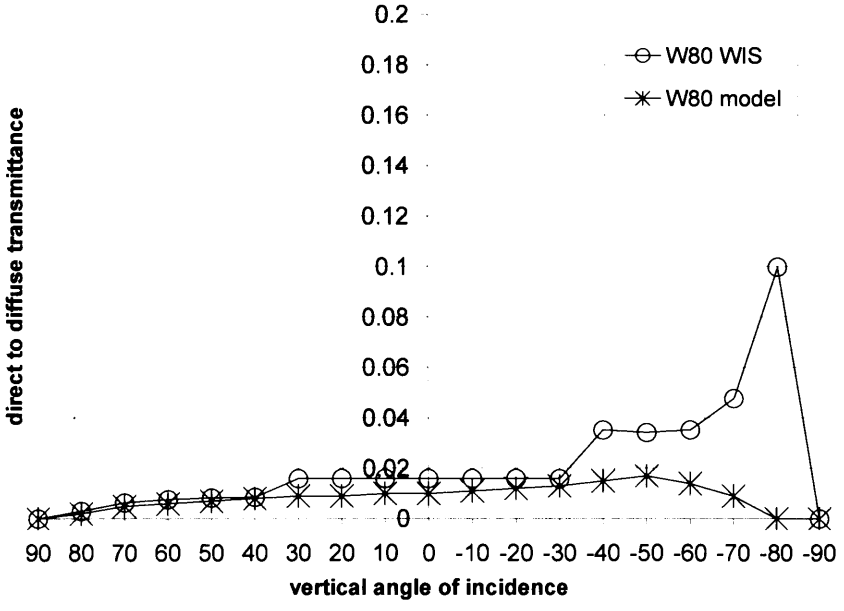


Figure 5.13: Comparison of system diffuse transmission of the W80 case in a double glazed panel

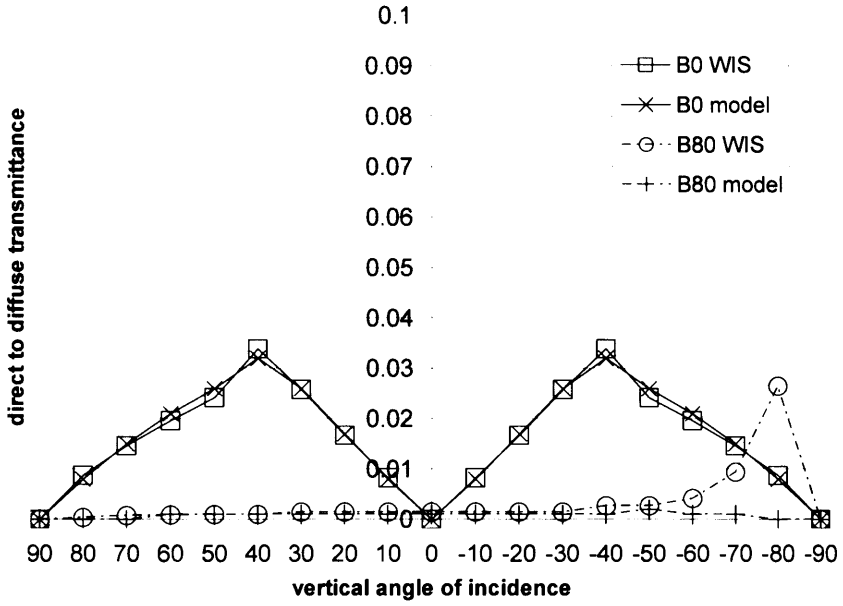


Figure 5.14: Comparison of system diffuse transmission of the blue blind cases in a double glazed panel

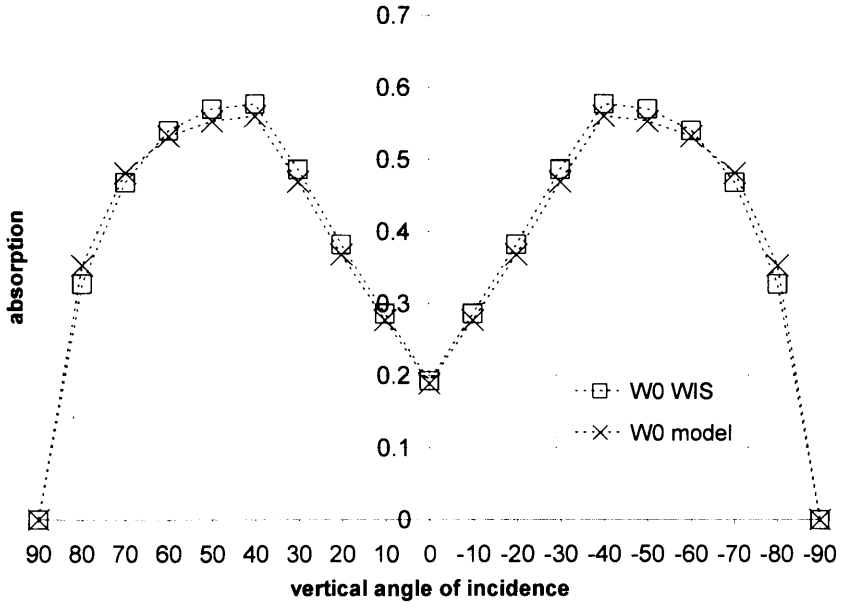


Figure 5.15: Comparison of system absorption of the W0 blind case in a double glazed panel

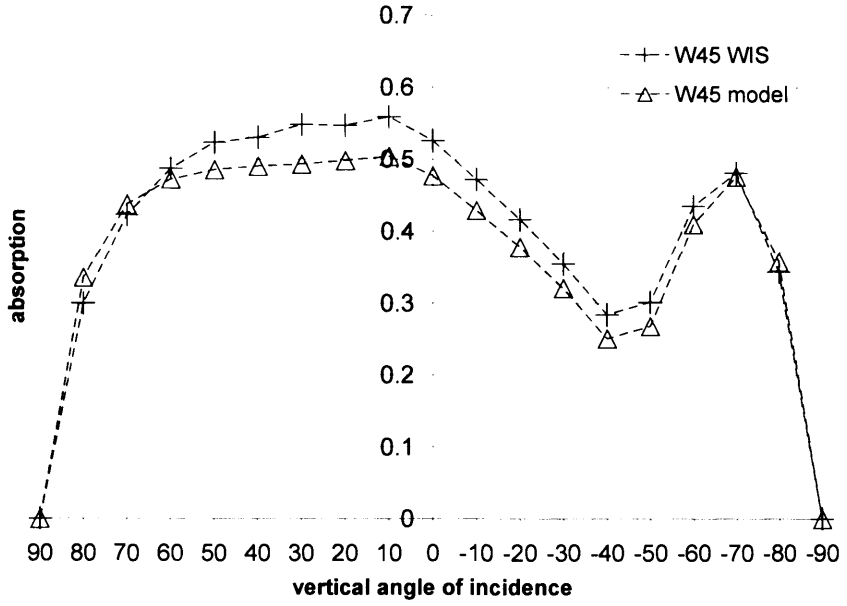


Figure 5.16: Comparison of system absorption of the W45 blind case in a double glazed panel

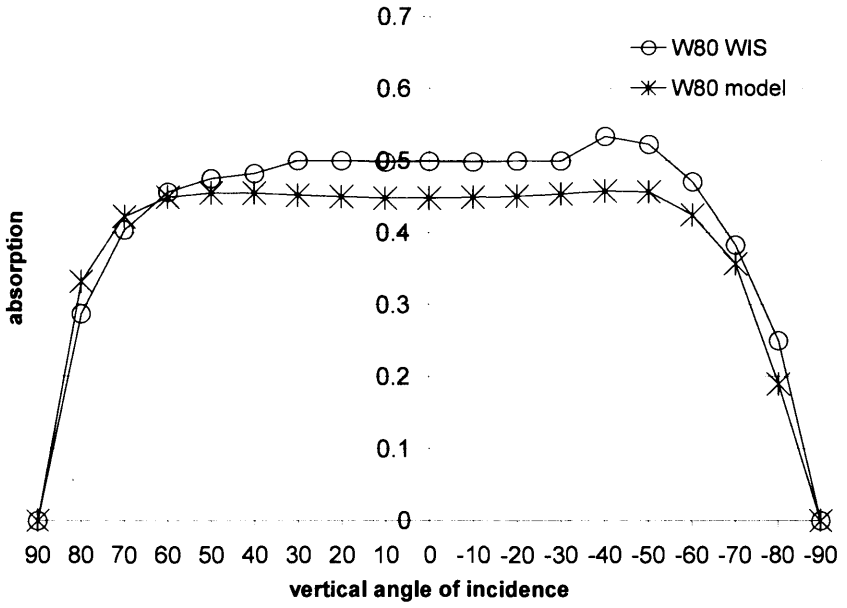


Figure 5.17: Comparison of system absorption of the W80 blind case in a double glazed panel

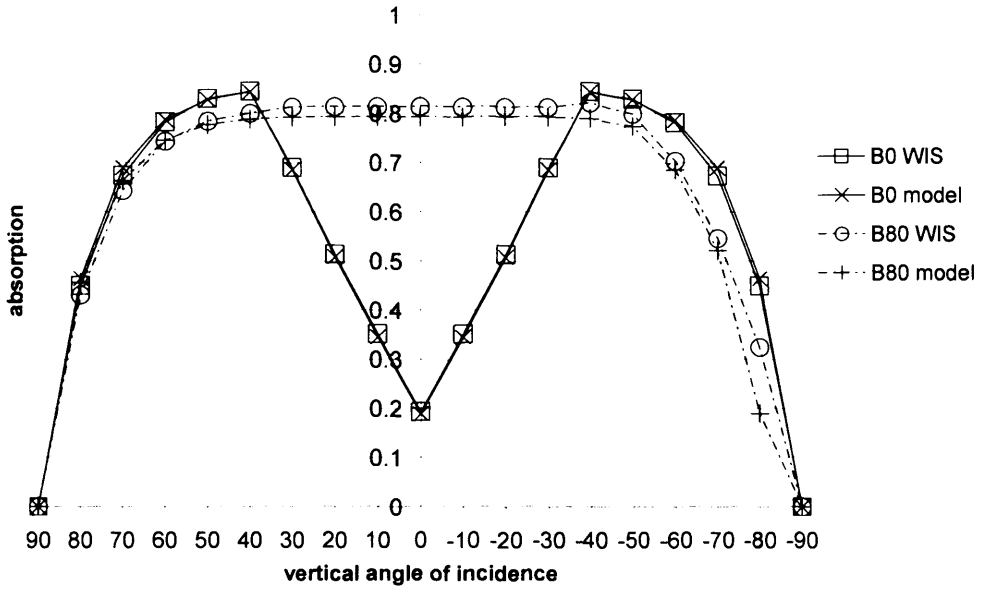


Figure 5.18: Comparison of system absorption of the blue blind cases in a double glazed panel

Table 5.3 summarises the results of the direct and diffuse transmittance and absorption values of the glass-blind-glass configurations under consideration.

| **Blinds in double glazing system** | **WIS mean values for 90 to -90 angle of incidence** | | | **RMSE WIS-Model** | | |
|---|---|---|---|---|---|---|
| | Direct | Diffuse | Absorption | Direct | Diffuse | Absorption |
| W0 (white 0°) | 0.15 | 0.08 | 0.39 | 0.004 | 0.0034 | 0.015 |
| W45 (white 45°) | 0.11 | 0.07 | 0.40 | 0.006 | 0.01 | 0.035 |
| W80 (white 80°) | 0.017 | 0.02 | 0.41 | 0.018 | 0.026 | 0.044 |
| B0 (white 0°) | 0.15 | 0.016 | 0.55 | 0.001 | 0.001 | 0.008 |
| B80 (white 80°) | 0.018 | 0.003 | 0.65 | 0.016 | 0.006 | 0.036 |

Table 5.3: Summary of results from comparison of optical properties of blinds with reference model

### 5.2.3 G-value for Multilayered Glass/Blind Configurations

A comparison against the reference model WIS was undertaken for the prediction, through the whole thermal model, of total solar transmission (G-value) under fixed

boundary conditions. The G-value was determined in the thermal model through the simulation of a test cell, using fixed cell temperatures and transfer coefficients on either side of the glazing panel, and irradiating at normal incidence. The boundary conditions for the tests were examined in Chapter 4 §4.5.1.

These tests were undertaken for a wider range of blind configuration, and included external and internal placements of the blinds, as well as inter-pane ones (figure 5.19). A mid-grey blind (reflectance = 0.5) was assumed for all cases contained between 4mm clear float glass panes in a 30mm unventilated cavity (G-value of the system with no blinds is 0.75; U-value of the system is 2.8 $W/m^2K$). The blind slats were 20mm deep with a 20mm pitch while the parameter varied in the simulation of the three glazing systems was the angle of tilt (20°, 45° and 70°) of the blind's slats. All cavities for these particular tests were assumed to be unventilated since WIS allows currently limited ventilation options (from outside to inside and from inside to inside; ventilation options will be examined on a later stage of this chapter). Results of this comparison are shown in table 5.2.

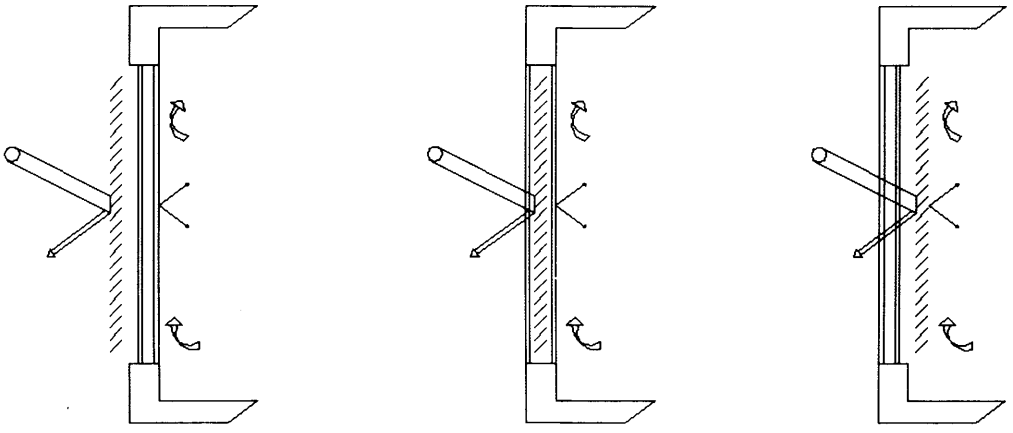

**(a) External** **(b) Inter-pane** **(c) Internal**

Figure 5.19: Illustration of three glazing systems with different shading strategies, indicating convective and radiant heat exchange for (a) external shading, (b) inter-pane shading in sealed cavity and (c) internal shading.

| Glazing Systems | | G-values | |
|---|---|---|---|
| **Slat angle** | **Position** | **WIS** | **Model** |
| 20° | internal | 0.66 | 0.65 |
| | inter-pane | 0.61 | 0.62 |
| | external | 0.57 | 0.59 |
| 45° | internal | 0.55 | 0.51 |
| | inter-pane | 0.43 | 0.43 |
| | external | 0.32 | 0.34 |
| 70° | internal | 0.44 | 0.39 |
| | inter-pane | 0.28 | 0.27 |
| | external | 0.12 | 0.14 |

Table 5.2: Comparison of standard g-values calculated by WIS and by the combined model.

The results showed that the modified model has been able to predict a steady-state G-value to within a mean of ±0.02 of the reference model. Larger discrepancies are noticed in internal blind cases with the lower slat angles (see internal blind of 70° slat angle), which comes to an accordance with the weakness identified in the calculation of the absorption and diffusion values of the blind by the glass simulation program (see §5.2.1).

### 5.2.4 G-value for Glass - Glass - Blind Configuration with Ventilated Cavity

The comparison against the reference model WIS was extended in order to test the applicability of the HTB2 model to the simulation of glazing systems with ventilated cavities. HTB2 model was used this time to predict the G-value of a double glazed system (4mm-12mm-4mm, clear float glass; window area 1.17m x 1.17m; G-value of the system with no shading is 0.75; U-value of the system is 2.8 $W/m^2K$) with various types of roller blinds positioned internally (gap of 12mm between the double glazing and the roller blind; volume of ventilated cavity: 0.016$m^3$) (figure 5.20). The same blind samples (table 5.3) and double glazing-blind systems were used during detailed test-cell measurements during a test programme run by Lund University (Wall & Bülow-Hübe, 2003).

The parameters varied in the simulation of the glazing system were the type of fabric of the roller blind (table 5.3; $R_{diff}$: Diffuse Reflection, $R_{spec}$: Specular Reflection, $T_{diff}$: Diffuse Transmittance and Abs: Absorption) and the ventilation rate through the cavity between the double glazing and the blind. The following fixed ventilation rates were examined; 0.0042m$^3$/s, 0.0085m$^3$/s and 0.016m$^3$/s. These correspond to flow rates due to stack effect, under typical conditions, that would be expected from gaps of 0.01m, 0.02m and 0.04m, respectively, at the top and bottom vents of the roller blind. Also a 0.000 m$^3$/s ventilation rate was examined, which corresponds to a roller blind tightly mounted to the window, not allowing any ventilation through the cavity (figure 5.20 a).

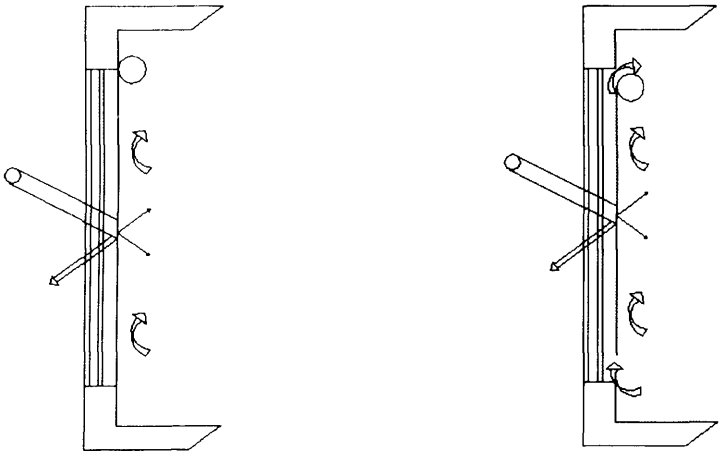

**(a) Unventilated cavity** **(b) Ventilated cavity**

Figure 5.20: Illustration of the glazing system with roller blind (a) tightly mounted to the window not allowing any ventilation, (b) gaps at the top and the bottom of the roller blind allowing ventilation.

| Type of Roller Blind | $R_{diff}$ | $R_{spec}$ | $T_{diff}$ | Abs |
|---|---|---|---|---|
| White Texienne (H 925-90)$^{TM}$ | 0.82 | 0.00 | 0.06 | 0.12 |
| Blue Roller Blind (H 500-54)$^{TM}$ | 0.15 | 0.00 | 0.04 | 0.81 |
| Silver-grey Blind (H981-95)$^{TM}$ | 0.29 | 0.30 | 0.05 | 0.36 |
| White-grey Texienne (H 927-95) | 0.78 | 0.00 | 0.05 | 0.17 |
| White Roller Blind (H 500-90)$^{TM}$ | 0.58 | 0.00 | 0.37 | 0.05 |

Table 5.3: Summary of comparison test data configurations[1].

[1] Roller blind manufacturer: Haglunds I Falköping AB eng., Sweden Reflectance and transmittance values of blinds were also measured with a spectrophotometer at Uppsala University, Uppsala, Sweden

The ventilation rates in the cavity (due to stack effect) were calculated according to ISO 15099 (2003) standard by the equation (3.4). As explained in Chapter 3 §3.2.2, HTB2 is using ventilation factors for the specification of the air flow through the cavity. $C$, being a fixed flow rate due to stack effect in the cavity, was calculated and used here in order to compare results with WIS. In the calculation of $C$, a $T_c$ (the cavity mean temperature in K) of 30°C was used as an approximation.

WIS was used instead of the glazing simulation program, in order to provide HTB2 with the transmission and absorption factors for the angles of incidence from 0° to 90°, in the description of the glazing systems. This choice was based on the fact that roller blind solar transmission characteristics are not as angle dependent as slat-type blinds and also because the glass simulation program expressed a weakness in calculating transmission characteristics for materials with high diffuse transmittance such as the white roller blind case ($T_{diff}$ = 0.37).

The G-values from the steady state simulations are shown in Table 5.4. Both models were set to the same boundary conditions described in Chapter 4 §4.5.1. The G-value has been predicted by HTB2 to within a mean of ±0.01 of the steady-state value across a wide range of blind type and for both the unventilated and ventilated cavities

| **Glazing Systems** | | **G-values** | |
|---|---|---|---|
| Type of blind | Ventilation Rate | WIS | Model |
| White Texienne (H 925-90) | 0.000$m^3/s$ | 0.22 | 0.22 |
| | 0.0042$m^3/s$ | 0.24 | 0.25 |
| | 0.0085$m^3/s$ | 0.25 | 0.26 |
| | 0.016$m^3/s$ | 0.27 | 0.28 |
| Blue Roller Blind (H 500-54) | 0.000$m^3/s$ | 0.51 | 0.49 |
| | 0.0042$m^3/s$ | 0.55 | 0.54 |
| | 0.0085$m^3/s$ | 0.57 | 0.58 |
| | 0.016$m^3/s$ | 0.60 | 0.61 |
| Silver-grey Blind (H981-95) | 0.000$m^3/s$ | 0.33 | 0.32 |
| | 0.0042$m^3/s$ | 0.36 | 0.36 |
| | 0.0085$m^3/s$ | 0.38 | 0.38 |
| | 0.016$m^3/s$ | 0.40 | 0.41 |
| White-grey Texienne (H 927-95) | 0.000$m^3/s$ | 0.24 | 0.24 |
| | 0.0042$m^3/s$ | 0.26 | 0.27 |
| | 0.0085$m^3/s$ | 0.27 | 0.29 |
| | 0.016$m^3/s$ | 0.29 | 0.30 |
| White Roller Blind (H 500-90) | 0.000$m^3/s$ | 0.40 | 0.40 |
| | 0.0042$m^3/s$ | 0.41 | 0.42 |
| | 0.0085$m^3/s$ | 0.42 | 0.43 |
| | 0.016$m^3/s$ | 0.43 | 0.44 |

Table 5.4: Comparison of G-values calculated by WIS and by the combined model in steady-state conditions, ventilated cavity.

Even though test-cell measurements of the g-value of the above configurations were available during a test programme run by Lund University (Wall & Bülow-Hübe, 2003), they were not directly comparable with the results from HTB2 since there were no recorded ventilation rates through the cavity at the time of the measurements.

## *5.3 Comparison to Measurements*

In order to evaluate the performance of the full thermal model, utilising all sub-models and real climatic data, comparison against measured data was considered necessary. The external test cell data were acquired from Lund University and comprised a quality data set of total solar transmission for a number of configurations, made using a "twin-box" facility (Wall & Bülow-Hübe, 2003). Further details regarding the test cell facilities are given in chapter 2, §2.4.4. The five measurement cases (table 5.1, figure 5.21) were each simulated by the HTB2 model, "exposing" each glazing system considered, placed

on a simple enclosure with constant internal temperature, to the recorded climatic data. The glazing dynamic hourly g-value, $\hat{g}_d$, was estimated from the simulation data using the formula 4.1, Chapter 4.

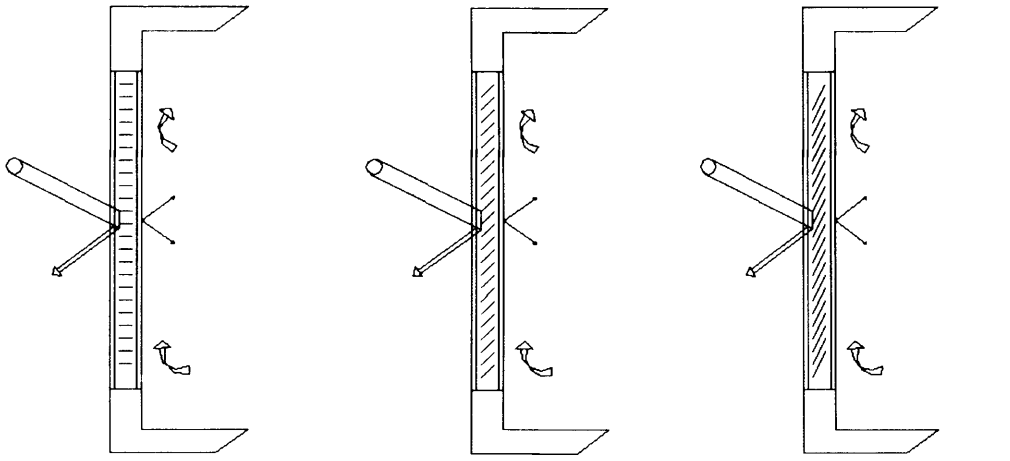

**(a) 0° angle of tilt** **(b) 45° angle of tilt** **(c) 80° angle of tilt**

Figure 5.21: Illustration of three glazing systems with different inter-pane shading strategies, indicating convective and radiant heat exchange for (a) 0° angle of tilt, (b) 45° angle of tilt and (c) 80° angle of tilt.

The authors of the test-cell measurements of total solar transmission indicate their accuracy as better than 5% of the value measured (Bülow-Hübe, Kvist, & Hellstrom, 2003). This seems to be comparable to accuracy's reported by others (e.g. Klems & Warner 1997, Platzer, 2000). Measurements were made on a 10-minute basis. It was noted that, presumably due to varying cloud or wind conditions during a test, the measured values could be seen in some tests to vary rapidly across an hour. Climatic data for simulations was only available in an hourly format, therefore simulation results could only be compared on this time scale. The simulation results would represent the average value over the hour, so the measurement data was averaged to an hourly basis. Any variance over the hour was considered to be a further indication of measurement uncertainty. This typically represented a combined uncertainty in the measured $\hat{g}_d$ values of approximately a mean of ±0.03.

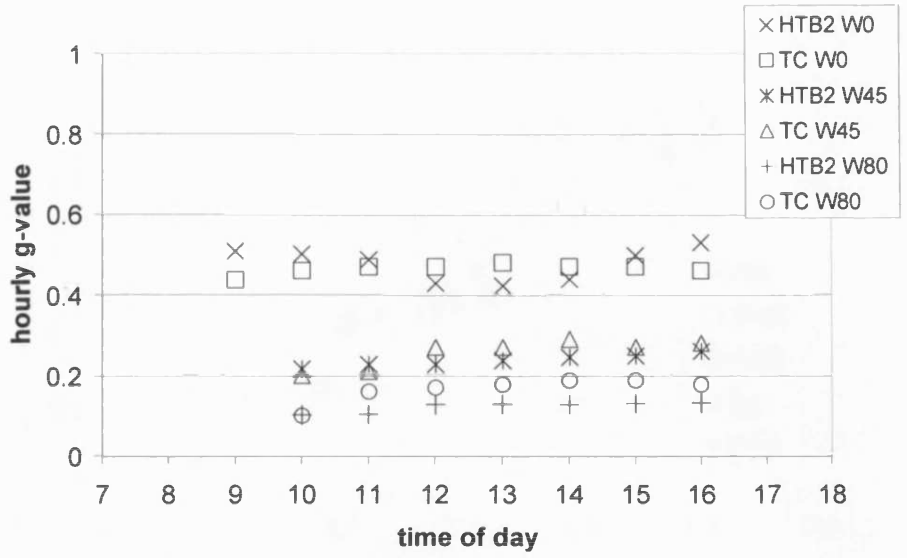


Figure 5.22: Comparison of hourly system $\hat{g}_d$ value for the white blind configurations; TC – test cell measured data, HTB2 – simulations

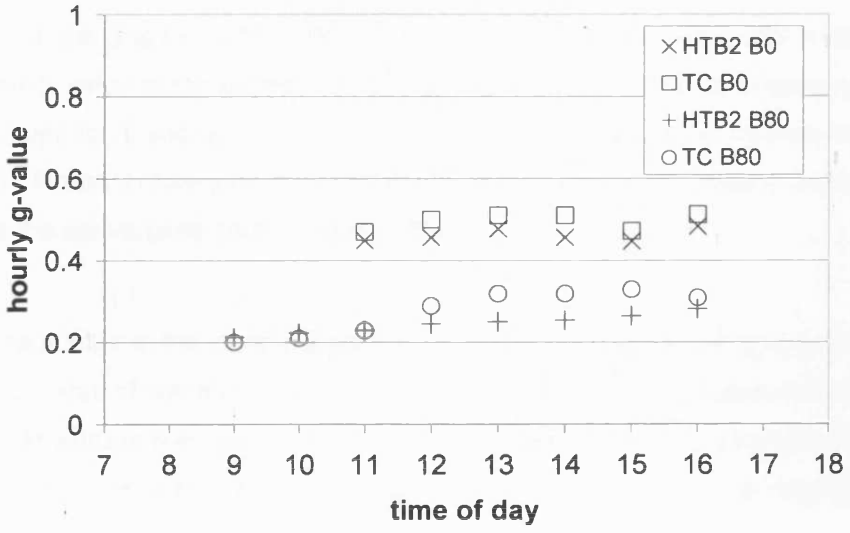


Figure 5.23: Comparison of hourly system $\hat{g}_d$ value for the blue blind configurations; TC – test cell measured data, HTB2 – simulations

Figure 5.24 shows a scatter-gram of all hourly results, as well as the line of ideal agreement. There is a degree of consistency seen between cases, although there is notable scatter within the light 0-degree case (W0).

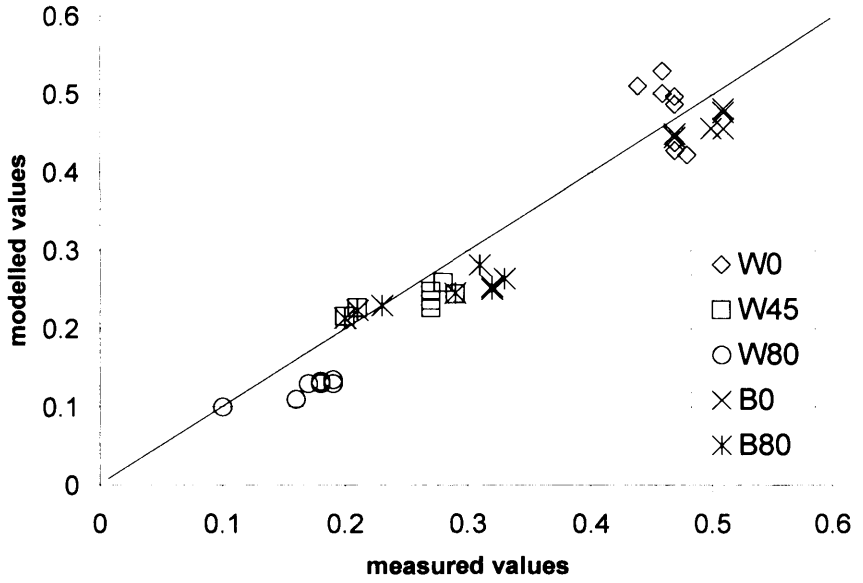


Figure 5.24: Comparison of all hourly system $\hat{g}_d$ values

From the graphs (5.22, 5.23 and 5.24) it is shown that the model mostly underestimates the $\hat{g}_d$ value in comparison to the measurements. The latter is more noticeable in low angles (80°) and light colours of blind material (white) which comes to an agreement with the limitation identified in the model in estimating the absorption and diffusion properties of the above blind configurations (§5.2.1).

The scatter in the comparison of $\hat{g}_d$ of the light 0-degree slat angle case (W0) (figure 5.24) was of some concern. It was noted that during this measurement case, the peak solar altitude was just above the cut-off angle for the blind geometry. It was considered that the relatively coarse 10-degree characteristic table format might be affecting such cases.

Comparisons of the individual hourly results were made with simulations using the heat transfer algorithms (e.g. surface heat transfer coefficients) of HTB2. Typical results are shown in figure 5.22 & 5.23. These tests, comprising 36 hours of measurement across the five configurations tested, showed a RMSE of 0.042 in the predictions, with an indication of an underestimate in $\hat{g}_d$ of a mean of 0.02. Further validation of the modified combined calculation method has been published in the proceedings of the 2005 IBPSA

Conference (Alexander et al, 2005) and in the proceedings of the PLEA2005 Conference (Mylona et al, 2005).

## *5.4 Discussion*

Although absolute accuracy is often desired, a practical model will be required to make some trade-off between accuracy and usability. Detailed specific software solutions may seek to imitate laboratory cases, but in terms of usability in dynamic modelling, limitations in data requirements and speed of calculation are important considerations. Ultimately, however, a model useful to the design industry must show sufficient accuracy to be able to distinguish between design alternatives.

The RMSE results arising from the comparisons would seem to indicate that the error in the total simulation process is of a similar order to the measurements against which it was being compared. The combined HTB2 and glass simulation model would appear to be able to calculate direct, diffuse and re-emitted solar gains, when considered as a $\hat{g}_d$ value, to a band of ±0.04. In practice this should allow the robust differentiation of glazing design alternatives equivalent to differences in g-value of better than 0.1. Although there is scope for improvement, in particular in the calculation of diffusing and absorping effects of blinds, in many applications in the design industry this level of accuracy may be sufficient.

The test cases presented are a case in point. The five configurations (glass-blind-glass) can be ranked by their average measured $\hat{g}_d$ value, in order of increasing solar transmission (e.g. assuming a design intent to minimise solar gains). Table 5.5 compares the rankings made by measurement and made by the modified model in its final configuration. Also indicated in this table are the statistical significance of the difference between a configuration and its next ranked neighbour, as assessed by a t-test on the hourly data for each pair of configurations. Those configurations that are significantly different from their next ranked neighbour are marked with an asterisk (*). Thus for instance the measurements distinguished a significant difference in $\hat{g}_d$ value between the W80 and W45 cases, but not between the W45 and B80 cases.

| Configuration | Mean $g_d$ by measurement | Mean $g_d$ by simulation |
|---|---|---|
| W80 | 0.17 (*) | 0.13 (*) |
| W45 | 0.26 | 0.24 |
| B80 | 0.28 (*) | 0.25 (*) |
| W0 | 0.47 (*) | 0.48 (*) |
| B0 | 0.50 | 0.48 |

Table 5.5: Rankings of the blind configurations, as indicated by measurement and by simulation.

The simulations with the combined method were able to match the resolution of the measurements; the rankings are in the same order, and the same pairs are identified as statistically different. This suggests that the modified combined model HTB2 / glazing simulation program will be able to distinguish between basic design alternatives in the choice of blinds for similar glazing options.

## *5.5 Conclusions*

In order to test the applicability of the prediction tool and calculation method it was considered necessary to compare results with measurements and validated tests, in laboratory facilities and real climate facilities. In the absence of direct access to measurement facilities, the applicability of the combined method was tested against a combination of software standards and previously published laboratory or field trials.

Comparisons were made between the reference model WIS 3.0.1 and the modified model, under steady-state conditions. Initial evaluations were made of the blind transmission model in isolation and in combination with glass panes (glass-blind-glass configurations). The above comparisons showed a very good agreement between the calculations of the direct beam transmission, while some discrepancies were detected in the calculation of the diffusing effects of the blinds, which indicates weakness in the view factor calculation of the model and requires further investigation and development.

A comparison against the reference model WIS has also been undertaken for the prediction of the steady-state total solar transmission (G-value) of various glazing systems with integrated slat-type shading in various positions (internal, external and inter-pane) and of various slat angles. The modified model was able to predict a steady-state G-value to within a mean of ±0.02 of the reference model.

The comparison against the reference model WIS was extended in order to test the applicability of the combined HTB2 and glazing simulation program model to the simulation of glazing systems with ventilated cavities. Internally positioned roller blinds were tested this time with a range of blind material characteristics. Various ventilation rates in the cavity between the internal glass pane and the roller blinds were examined and the G-value was predicted by HTB2 to within a mean of ±0.01 of the standard value.

A final comparison against measured data was considered necessary in order to evaluate the performance of the full thermal model, utilising all sub-models and real climatic data. Measured and calculated data were compared for five blind configurations and showed a good agreement with a RMSE of 0.042. Some concern was drawn to the light 0-degree slat angle case (W0) and so recommendations for future research on the further development of the combined model have been forwarded to the code authors.

Overall comparisons to reference standard software and to test-cell measurements indicate that the software could be expected to predict total solar transmission, as expressed by the g-value, to a band of ±0.04. Although there is scope for further improvements in the calculation of diffused and absorption characteristics of slat-type blind configurations, this level of resolution was considered sufficient to distinguish between glazing options to a degree similar to that available from field measurement.

## *5.6 References*

Alexander, D K, Mylona, A & Jones, P J (2005) 'The Simulation of Glazing Systems in the Dynamic Thermal Model HTB2', Proceedings of the 9th International IBPSA Conference, Montreal, Canada

Bülow-Hübe, H, Kvist, H, & Hellström, B (2003) 'Estimation of the Performance of Sunshades Using Outdoor Measurements and the Software Tool Parasol v2.0', Proceedings ISES Solar World Congress, Gothenburg

Bülow-Hübe, H and Lundh, U (2002) 'Outdoor Measurements of G-values for External, Interpane and Internal Sunshades', Proceedings of EPIC 2002 AIVC Energy Efficienct and Healthy Building in Sustainable Cities, Lyon, 23-26 October, Vol.3, pp.795-800

Dijk, van D & Oversloot, H (2003) 'WIS, the European Tool to Calculate Thermal and Solar Properties of Windows and Window Components' Proceedings of the 8th International IBPSA Conference, Eindhoven, Netherlands

International Standard ISO 15099:2003 (2003) 'Thermal Performance of Windows, Doors and Shading Devices – Detailed Calculations', The International Organization for Standardization

Klems, J H and Warner J L (1997) 'Solar Heat Gain Coefficient of Complex Fenestrations with a Venetian Blind for Differing Slat Tilt Angles', ASHRAE Transactions, Vol.103, Part 1

Mylona, A, Alexander, D and Jones, P (2005) 'Modelling the Thermal Effect of a Ventilated Cavity on the Thermal Performance of Advanced Glazing Systems', Proceedings of PLEA2005 Conference, Beirut, Lebanon

Platzer, W J (2000) 'The ALTSET Project: Measurement of Angular Properties for Complex Glazings', Proceedings of the 3rd International ISES Europe Solar Congress, Copenhagen, Denmark, 19-22 June

Wall, M, and Bülow-Hübe, H (eds) (2001) 'Solar Protection in Buildings', Report TABK--01/3060, Dept. of Construction & Architecture, Lund Institute of Technology, Lund University, Lund, Sweden

Wall, M, and Bülow-Hübe, H (eds) (2003) 'Solar Protection in Buildings. Part 2:2000-2002', Report EBD-R—03/1, Dept. of Construction & Architecture, Lund Institute of Technology, Lund University, Lund, Sweden

# Chapter 6

# Application to Shaded Glazing Systems

## *6.1 Overview*

The combined model, validated in chapter 5, has been applied in this chapter in order to study the influence of various glazing parameters in the G-value calculated under steady-state conditions and also in the dynamically calculated $\hat{g}_d$ value under a more realistic setting.

The following steps were taken in order to examine:

- How the steady-state G-value is varying with the angle of incidence
- How the hourly calculated $\hat{g}_d$ value is varying with time of day and year
- How the $\hat{g}_d$ value compares to the steady-state G-value
- How the $\hat{g}_d$ value varies with location and
- How the $\hat{g}_d$ value depends on ventilation in the cavities formed between glass and blind

## *6.2 Description of Simulations*

The combined model has been used to model a simple space with south-facing window, office volume 54m$^3$ (3m x 6m x 3m) and window area 5.6m$^2$, (2.8m x2m) occupying approximately the 60% of the south-facing wall (figure 6.1). The choice of space was based on two person office occupancy, corresponding to 9 m$^2$/p and to a maximum depth of 6m from the window for the exploitation of the natural daylight (Part L2A, 2006). The modelled space is small enough for it to be influenced by the choice of glazing system. Potentially a larger room, such as an open plan office, would be less influenced by the glazing configuration and more by the properties of the construction material, the occupancy etc.

For the calculation of the steady-state G-value HTB2 was used as a steady-state model in order to model the simple space perfectly heated/cooled to a steady internal temperature and to the boundary conditions (steady solar radiation and external temperature) as further explained in chapter 4, §4.5 and for 10 degree steps of angle of incidence (0° – 90°). The horizontal angle (azimuth) was held at zero (e.g. noon for a South façade) (figure 6.1).

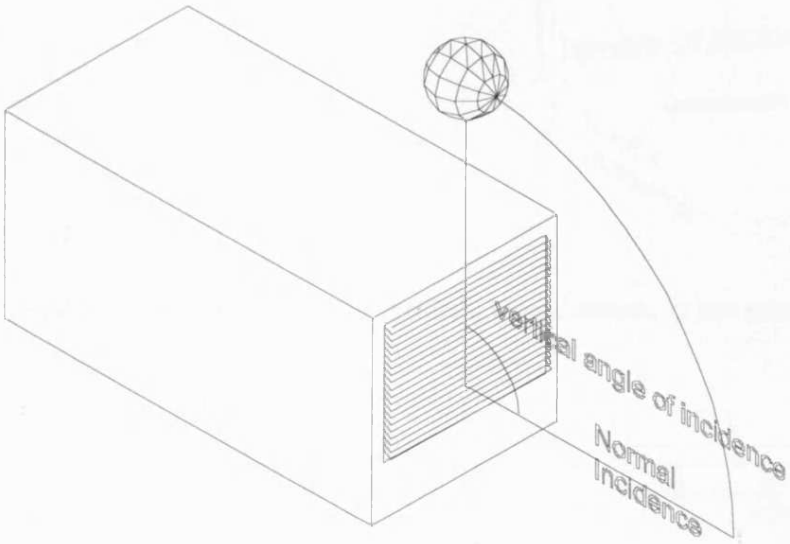


Figure 6.1: 0° - 90° angle of incidence (0° azimuth)

For the calculation of the $\hat{g}_d$ value HTB2 was used as a dynamic thermal model using hourly weather data. This time the sun was allowed to move in both altitude and azimuth (figure 6.2). From annual meteorological data sets (Energy Plus Website) the clearest day for each month was chosen in order to calculate the maximum solar transmittance for every month for three European locations. The space air temperature was kept fixed (by perfect heating and cooling) at 20°C for the winter months and 25°C for the summer months. Ventilation was set to two air changes per hour (CIBSE, 2006). Occupancy levels, lighting and small power sources (e.g. computers) were also considered and kept fixed at 25 W/m$^2$ floor area which correspond to 8 W/m2 occupancy, 9 W/m2 lighting and 8 W/m2/pc for computer equipment (CIBSE, 2006) (figure 6.3). A daily average total solar transmittance $\hat{g}_d$ was calculated from the simulation results using only the daylight hours, for each month.

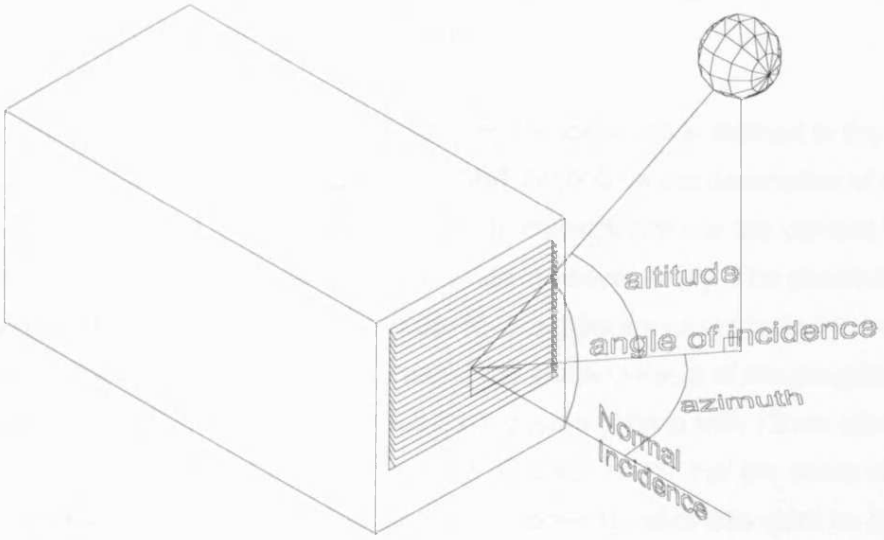


Figure 6.2: Definition of angles: a) angle of incident, b) sun altitude, c) sun azimuth

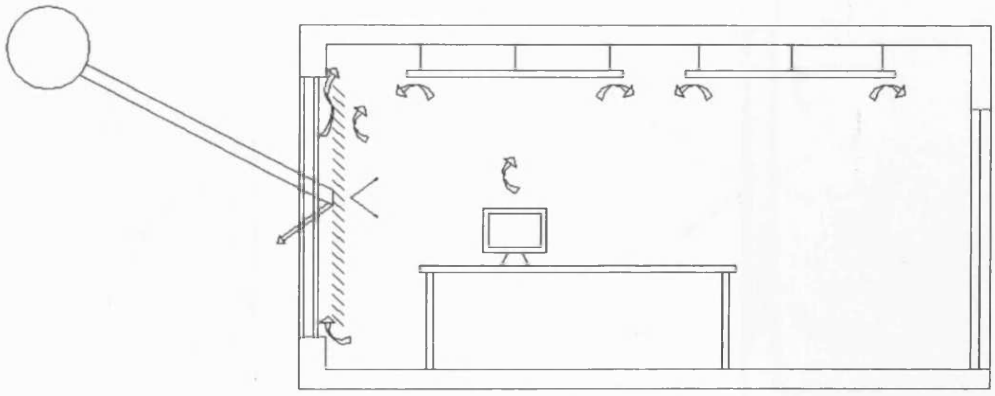

Figure 6.3: Office space illustrated with the internal blind option

Four glazing systems were studied consisted of a double glazing unit with integrated slat-type blinds (e.g. Venetian blinds, 20mm width and 20mm pitch) positioned externally, inter-pane and internally (figure 6.4). The inter-pane option has been studied for both sealed cavity and ventilated cavity. The double glazing unit (2.8m x 2m) in the cases with externally and internally positioned blinds was composed of 4mm float glass panes and 12mm gap between the glass panes, while there was 30mm gap between the double glazing unit and the blind. The cases with inter-pane positioned blinds in a ventilated cavity were composed of 4mm float glass panes, a 30mm gap between

external glass pane and blind (ventilated cavity) and a 12mm gap between the blind and the internal glass pane (non ventilated cavity).

HTB2 is offering a setting of a non standard resistance which is defined in the declared width of the layer as: width = resistance ($m^2$/W/°C)/1000, in the description of the glazing system. The above type of cavity was chosen to characterize the two cavities in the cases with inter-pane positioned slat-type blinds in sealed cavity. The choice for this type of cavity was based on the fact that in order for the different cases tested to be compared in equal terms they had to present the same U-value of double glazed unit, which was 2.8 $m^2$/W/°C, a typical U-value for a double glazing with 12mm spacing between panes according to CIBSE guidance (CIBSE, 2006). For the cases with inter-pane positioned blinds in a ventilated cavity the above U-value was used for the 'blind-non ventilated cavity-glass' part of the glazing system.

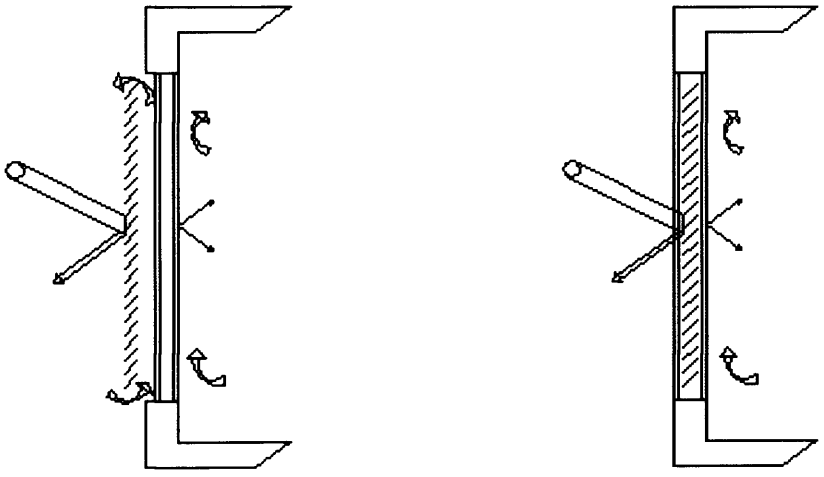

**(a)** **(b)**

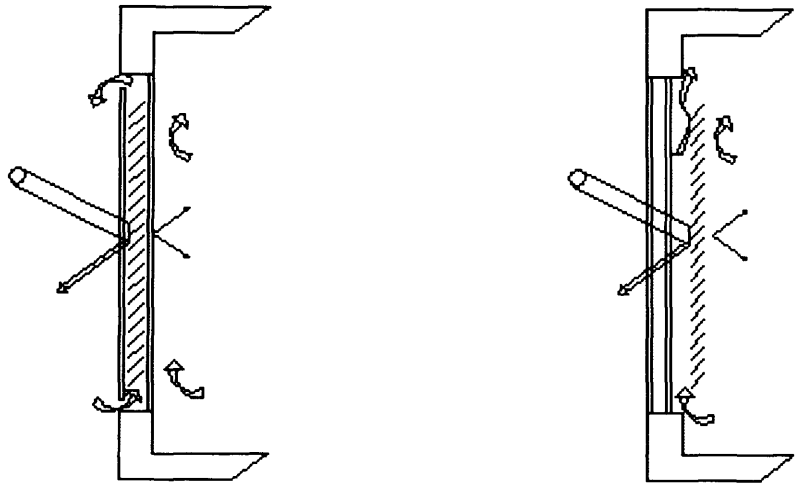

(c) (d)

Figure 6.4: Illustration of four glazing systems with different shading strategies, indicating convective and radiant heat exchange for a) external shading, b) inter-pane shading in sealed cavity, c) inter-pane shading in ventilated cavity, d) internal shading.

The ventilation rates through the ventilated cavities were kept the same through the tests. For the externally positioned slat-type blinds and for the ventilated case of inter-pane positioned blinds the ventilation rate between the blind and the double glazing was kept at 0.07$m^3/s$ which corresponds to air flow due to stuck effect and to wind component, for openings of 4cm at the top and bottom of the system each. Wind speed (u) of 3m/s and mean temperature in the cavity ($T_c$) of 30°C were used as approximations (CIBSE,1999). For the internally positioned slat-type blind the ventilation rate between the double glazing and the blind was only due to stack effect and it was kept at 0.054$m^3/s$ for all internal cases.

The above ventilation options were represented by the ventilation factors described in chapter 3 §3.2.2 and are parameters of the general equation for the flow through the cavity (equation 3.1). For the cases with externally positioned blinds and the ventilated case of inter-pane positioned blinds, B and C ventilation factors were used.

B, being the wind component, was calculated according to CIBSE (CIBSE, 2001-2002) approximations for single sided ventilation by equation (3.5) in Chapter 3 §3.2.2. C,

being the stack effect component, was calculated according to ISO 15099 (2003) standard by the equation (3.4) in Chapter 3 §3.2.2. A, being the force ventilation option, was kept at 0.

In the same way only factor C was used to calculate the ventilation rate in the cases with internally positioned blinds.

## *6.3 Simulations under Steady-State Conditions*

The steady-state simulations run using HTB2 as described in §6.2. The glazing parameters altered in the four glazing systems (figure 6.4) were the angle of tilt (20°, 45° and 70°) and the reflectance (low-0.2, medium-0.5 and high-0.8) of the blind slats. The results of the steady-state simulations are presented in figures 6.5a-e.

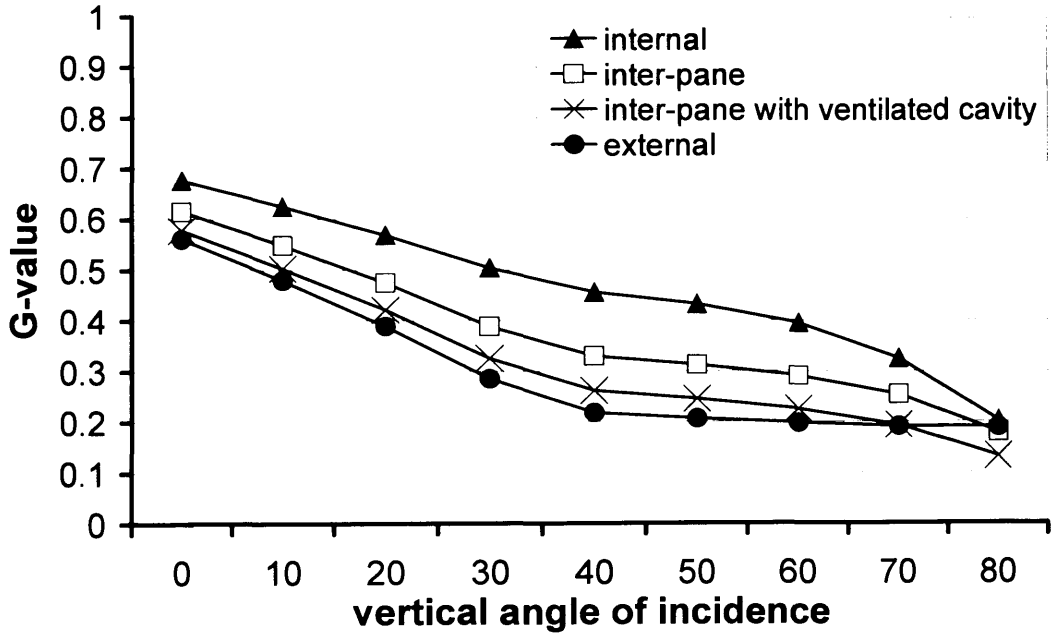


Figure 6.5a: The four cases with slat reflectance 0.5 and slat angle of 20°

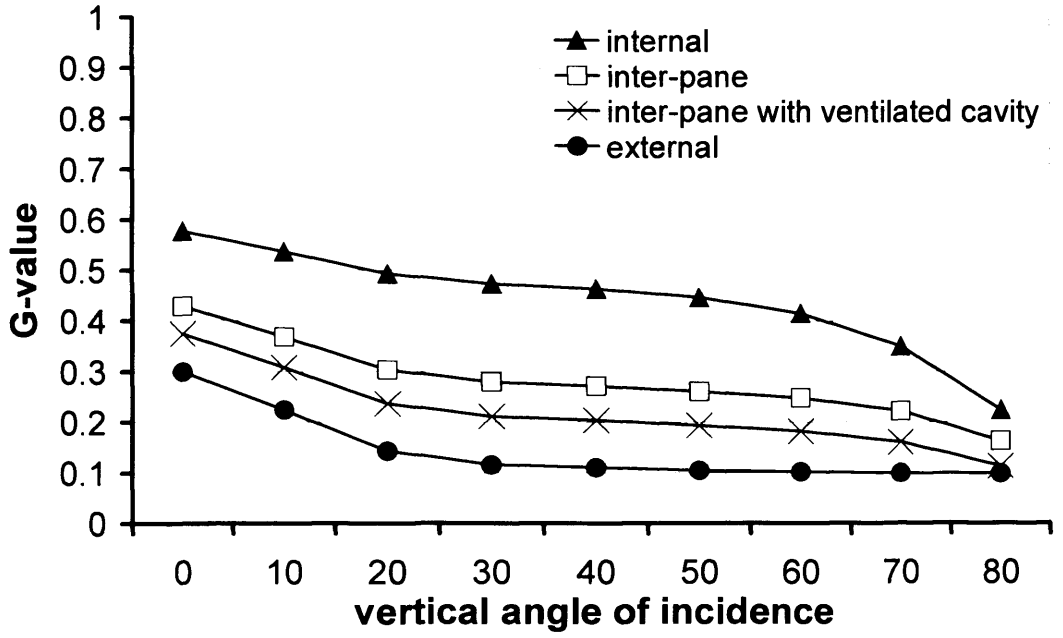


Figure 6.5b: The four cases with slat reflectance 0.5 and slat angle of 45°

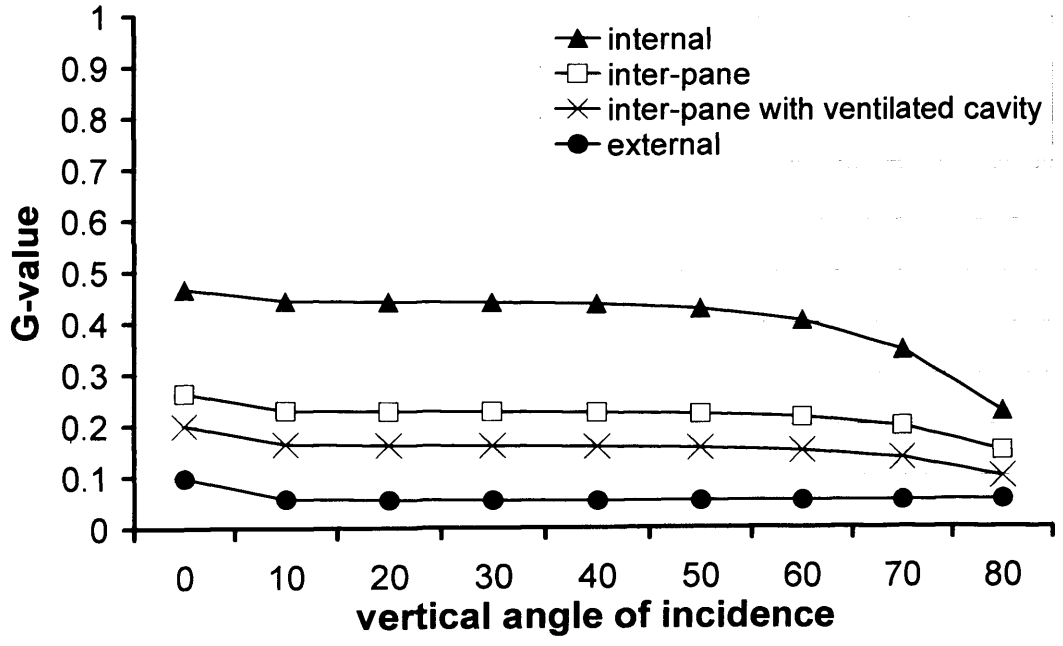


Figure 6.5c: The four cases with slat reflectance 0.5 and slat angle of 70°

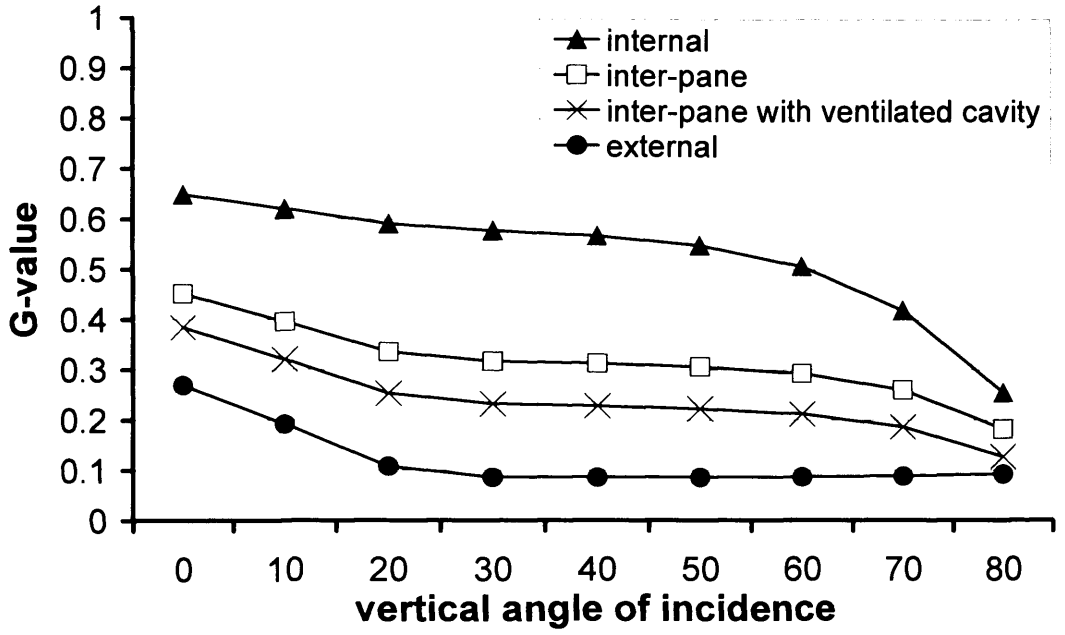


Figure 6.5d: The four cases with slat reflectance 0.2 and slat angle of 45°

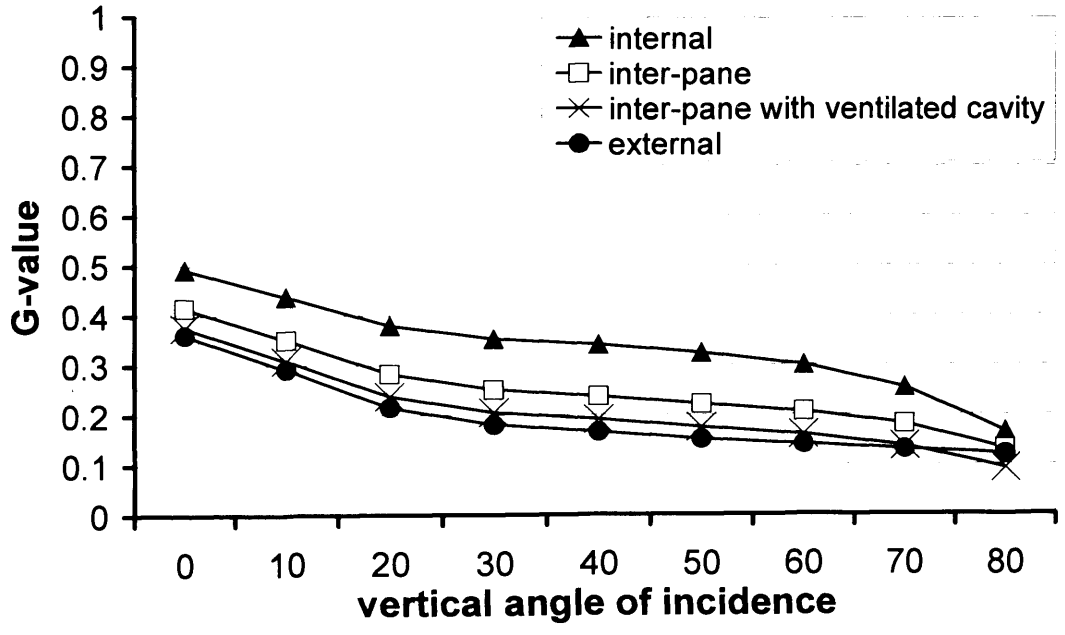


Figure 6.5e: The four cases with slat reflectance 0.8 and slat angle of 45°

These results show that:

- There is wide variation in G-value possible, for essentially the same glazing system (i.e. double glazing with a slat-type blind), depending on the colour and placement of the blind. From the graphs it is shown that it is possible to achieve a G-value as low as 0.10 at normal incidence when blind of 70° slat angle and medium reflectance (0.5) is being used externally, and as high as 0.68 at normal incidence when there is blind of 20° slat angle and medium reflectance (0.5) installed internally.

- In all cases it is shown that the total solar transmittance is not a constant value but depends on the angle of incidence. It reaches its maximum value at normal incident, and its minimum value at 80° angle of incidence.

- The sensitivity of the G's angle dependency in each case examined is directly related to the slat angle. The higher the slat angle (e.g. 70°) the smaller the G variation, while for the cases with 20° slat angle G is widely varying.

- The thermal performance of the various cases also depends on the colour of the blind material with lower G-values achieved by the use of highly reflective material. It is important to notice that while the above is mainly the case for the internally and inter-pane positioned blinds, the reverse effect occurs in the external blind cases. That is low reflectance (0.2) blinds present lower G-values than high reflectance (0.8) blinds, when positioned externally. A possible explanation for the above is that high total solar transmittance in internal and inter-pane cases is caused mainly by long-wave radiation transmitted to the inside (radiation absorbed and re-emitted towards the inside), while for the external blind cases examined the total solar transmittance comes mainly from directly transmitted/directly reflected towards the inside radiation, whereas the long-wave radiation is mostly exhausted to the outside before reaching the glazing unit.

- Also comparing the graphs of different colour cases (reflectance of 0.2, 0.5 and 0.8 – 45° slat angle) it is shown that for high reflectance blinds (0.8) the variation of the thermal performance between the cases is low, especially for external and inter-pane blind cases. For low reflectance blinds (0.2) the difference in the thermal performance is far more noticeable. The above has an immediate relevance to the designer when one has to choose the position of a light or dark colour blind. The

dark blind will require a thorough examination of its placement, while the light blind will perform similarly when positioned externally or inter-pane.

- The externally positioned blind shows, for a consistent surface reflectance and slat angle, the lowest G-value.

- The G-value for external blinds can be higher than for internal or inter-pane blinds, if surface colour and slat angle are not carefully chosen. For example the external blind case with 20° slat angle present higher G-values than the internal blind case with 70° slat angle and the internal blind with 45° of high reflectance (0.8), for low sun altitudes such as 10° and 20°, which represent sunrise and sunset hours and it will be an important factor in the design of east and/or west facades. Also comparing the external blind case with 20° slat angle against the inter-pane blind cases of 45° of high reflectance (0.8) and of 70° of medium reflectance (0.5), it is shown that, for high solar altitudes, similar and, for low sun altitudes, better thermal performance could be achieved by choosing correctly the position, the colour and the slat angle of the blind.

## *6.4 Simulations under Real Climate Conditions, London – UK*

The dynamic simulations run using hourly weather data by HTB2 for the set up described in §6.2. The same glazing parameters were examined; three angles of tilt (20°, 45° and 70°) and three reflectance values (low-0.2, medium-0.5 and high-0.8) of the blind slats. The results of the dynamic simulations are presented in figures 6.6a-e.

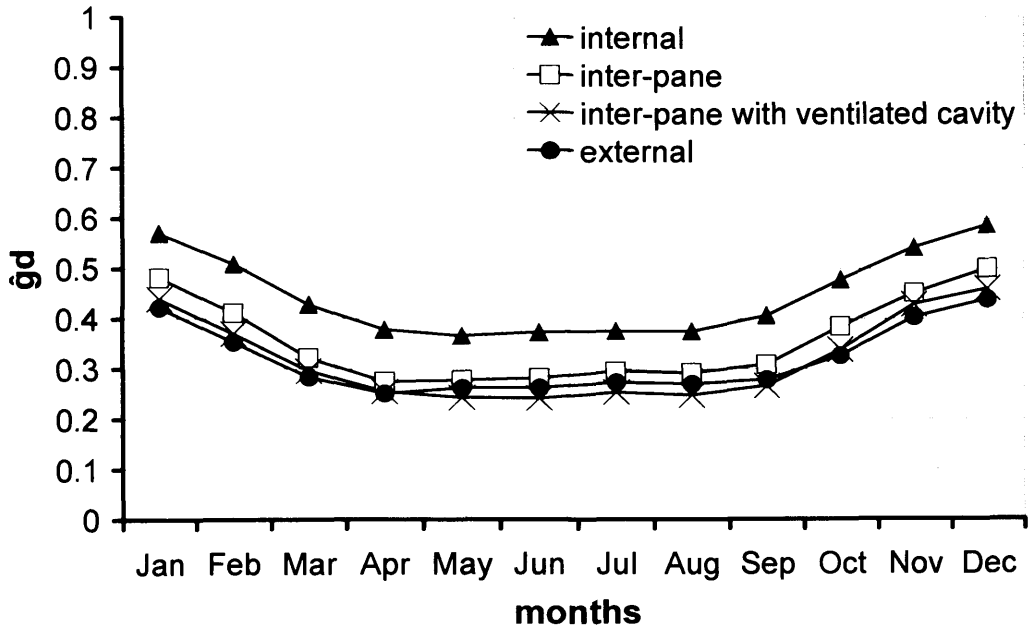


Figure 6.6a: The four cases with slat reflectance 0.5 and slat angle of 20° (London – UK)

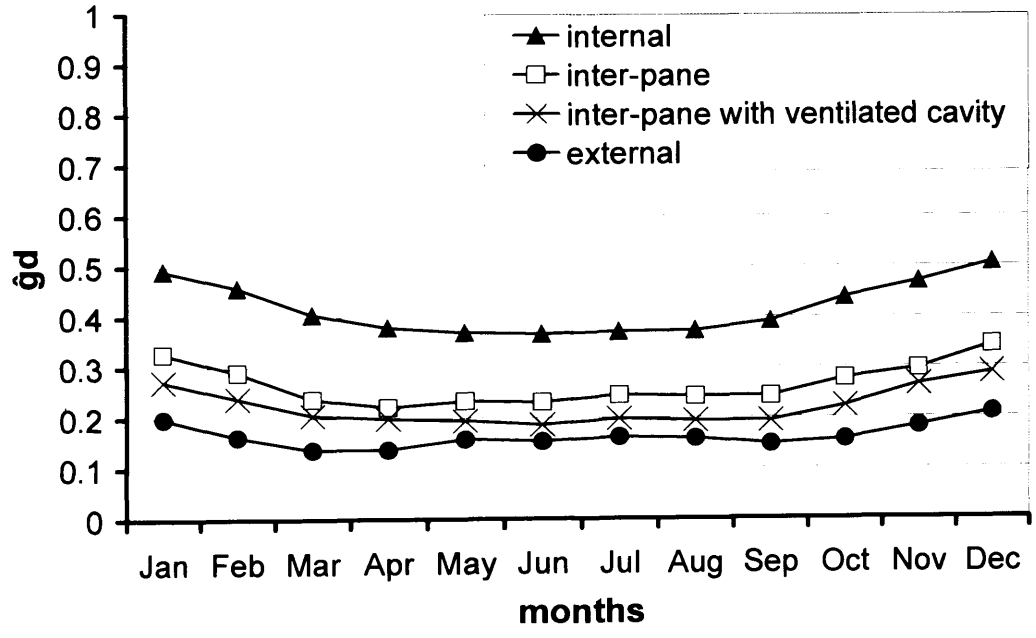


Figure 6.6b: The four cases with slat reflectance 0.5 and slat angle of 45° (London – UK)

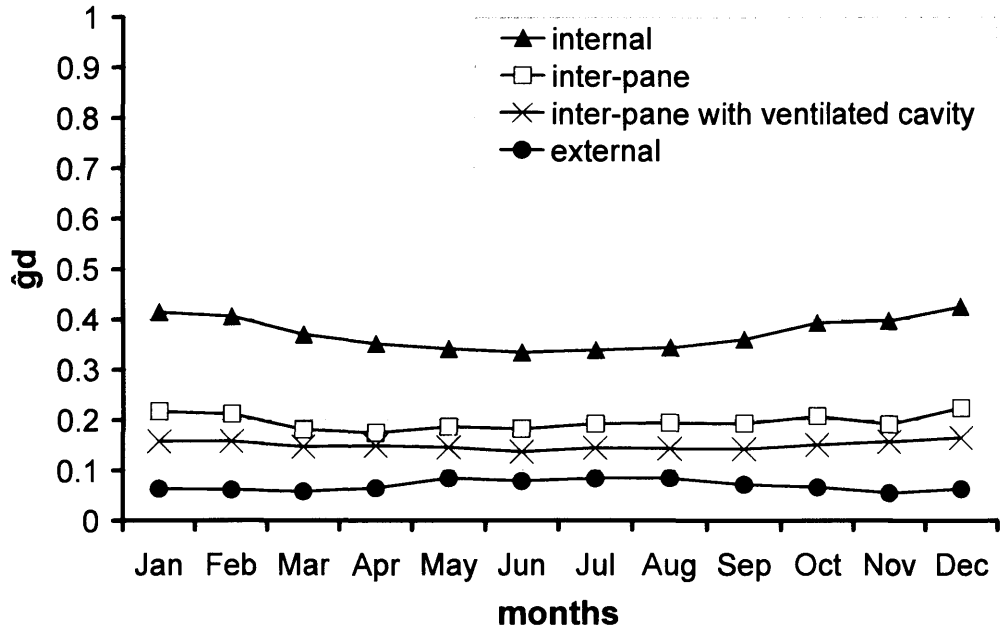


Figure 6.6c: The four cases with slat reflectance 0.5 and slat angle of 70° (London – UK)

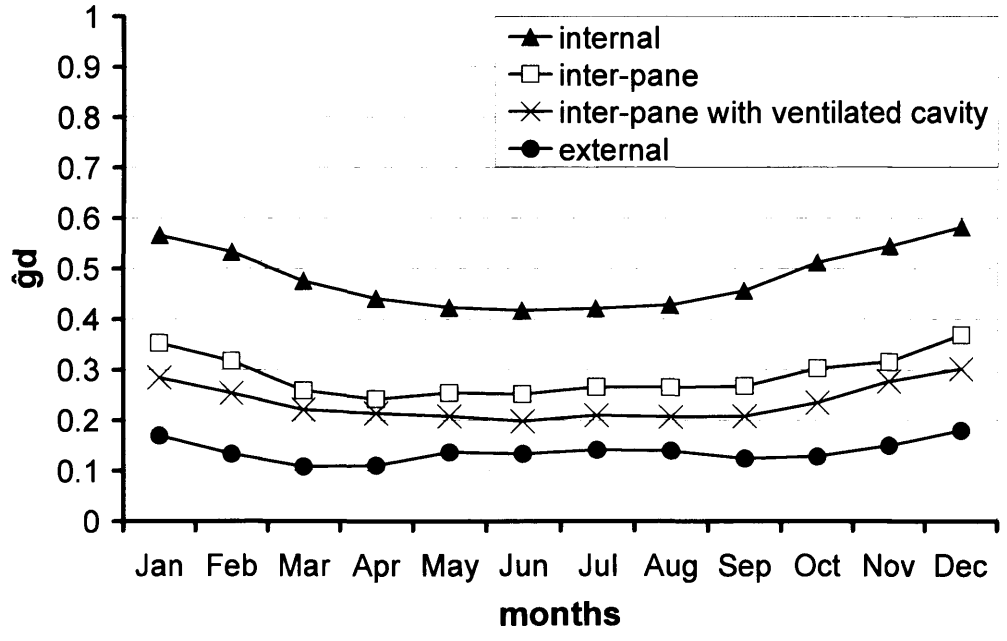


Figure 6.6d: The four cases with slat reflectance 0.2 and slat angle of 45° (London – UK)

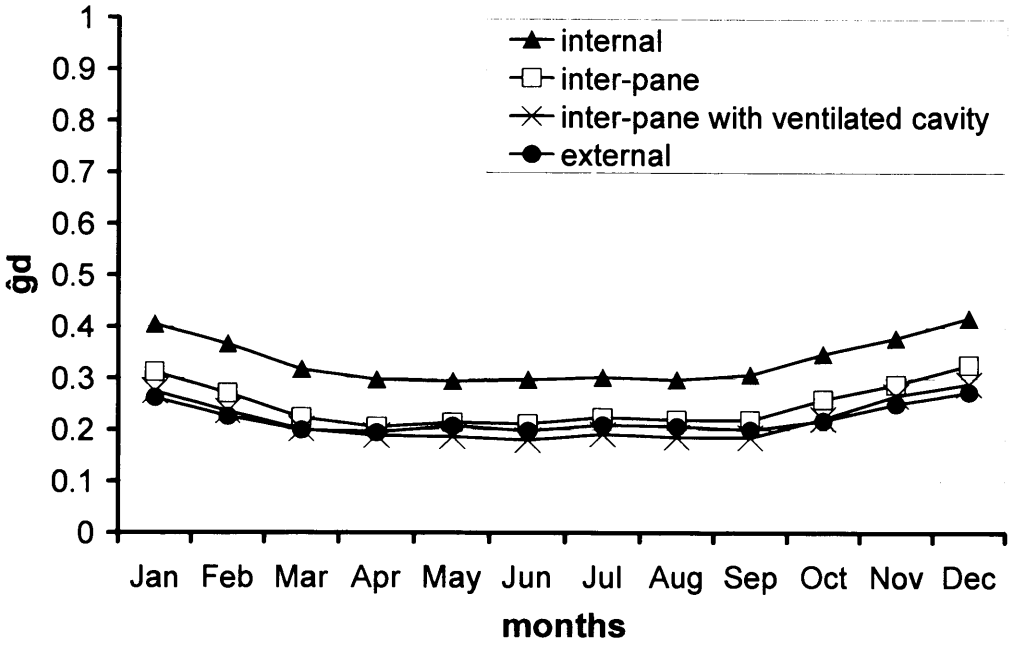


Figure 6.6e: The four cases with slat reflectance 0.8 and slat angle of 45° (London – UK)

Figure 6.6 (a-e) presents the dynamically calculated total solar transmittance $\hat{g}_d$. The results show that:

- $\hat{g}_d$ depends not only on the thermal characteristics of the glazing system but also on the time of the year and solar angles. In most cases $\hat{g}_d$ reaches its maximum value during the winter period when the angle of incidence is low and the direct solar radiation is close to normal incidence for a longer time. Typically $\hat{g}_d$ reaches its minimum value during the summer when the angle of incidence is high and the direct solar radiation is away from normal incidence. The above comes into accordance with the results from the calculations under steady-state conditions (Figure 6.3a-e) where the lower G-values were shown in high angles of incidence and the higher G-values were shown in low angles of incidence.

- The sensitivity of the $\hat{g}_d$ to the seasonal variation in each case examined is directly related to the slat angle. The higher the slat angle (e.g. 70°) the smaller the $\hat{g}_d$ variation, while for the cases with 20° slat angle $\hat{g}_d$ is widely varying.

- Figures 6.6 a, b and c show the $\hat{g}_d$ for the four cases (figure 6.1) with three different slat angles (20°, 45° and 70°) and medium slat reflectance (0.5). A lower total solar

transmittance can be achieved with a higher slat angle. From the graphs it is shown that for the London location it is possible to achieve a $\hat{g}_d$ value as low as 0.08 in the summer and a mean yearly value of 0.07, when blind of 70° slat angle is being used externally, and as high as 0.38 in the summer and a mean yearly value of 0.45, when blind of 20° slat angle is installed internally.

- Also comparing the graphs of different slat angle cases (20°, 45° and 70° - 0.5 reflectance) it is shown that for low slat angles (20°) the variation of the thermal performance between the cases is small, especially for external and inter-pane blind cases. For high slat angles (70°) the difference in the thermal performance is far more noticeable. This has an immediate relevance to the designer, especially when blinds with fixed slat angles are considered as a shading option for a building's facade. Blinds of high slat angles will require a thorough investigation of their placement, while blinds of low slat angles will perform similarly when positioned externally or inter-pane.

- The thermal performance of the various cases also depends on the colour of the blind material with lower $\hat{g}_d$ achieved by the use of highly reflective material. Consistent with the results from the simulations under standard conditions, it is noticed here as well that while the above is mainly the case for the internally and inter-pane positioned blinds, the reverse effect occurs in the external blind cases. That is low reflectance (0.2) blinds present lower $\hat{g}_d$ than high reflectance (0.8) blinds when positioned externally.

- Figures 6.6 b, d and e show the $\hat{g}_d$ for the four cases (figure 6.1) with three different blind colours (reflectance values of 0.2, 0.5 and 0.8) and slat angle of 45°. From the graphs it is shown that for the London location it is possible to achieve a $\hat{g}_d$ value as low as 0.18 in the summer and a mean yearly value of 0.22, when a blind with slat reflectance of 0.8 is being placed in between glass panes in a ventilated cavity, and as high as 0.42 in the summer and a mean yearly value of 0.48, when there is a blind with slat reflectance of 0.2 installed internally. The above ranking is reversed for the external cases where the lowest $\hat{g}_d$ values, as low as 0.13 in the summer and a yearly mean of 0.14, are achieved when there is blind with slat reflectance of 0.2 installed externally.

- Also comparing the graphs of different colour cases (reflectance of 0.2, 0.5 and 0.8 – 45° slat angle) it is shown that for high reflectance blinds (0.8) the variation of the thermal performance between the cases of the same blind characteristics is low, especially for external and inter-pane blind cases. For low reflectance blinds (0.2) the difference in the thermal performance is far more noticeable. As also mentioned before, this has an immediate relevance to the designer when one has to choose the position of a light or dark colour blind. The dark blind will require a thorough examination of its placement, while the light blind will perform similarly when positioned externally of inter-pane.

- The consistency of the lower values presented by externally positioned blinds compared to the cases of the same surface colour and slat angle displayed under steady-state conditions is interrupted here with some of the inter-pane in ventilated cavity blind cases presenting lower $\hat{g}_d$ values to their equivalent external blind cases. The above is noticed for the case of 20° slat angle of medium reflectance (0.5) and 45° slat angle of high reflectance (0.8) (figures 6.6a and 6.6e).

- The $\hat{g}_d$ for external blinds can be similar or higher than for internal or inter-pane blinds, if surface colour and blade angle are not carefully chosen. An example is the external blind case with 20° slat angle which presents similar $\hat{g}_d$ compared to the internal blind case with 70° slat angle and also to the internal blind case with 45° of high reflectance (0.8), all through the year, with small variation noticed during the summer months. Also comparing the external blind case with 20° slat angle to the external and inter-pane blind cases of all other slat angle and reflection blind cases, it is shown that better thermal performance could be achieved by choosing correctly the position, the colour and the slat angle of the blind.

- Under real climate conditions, as well as under steady-state calculations, it is noticed that ventilation in the cavity of inter-pane blind cases can improve the thermal performance of a glazing system. Furthermore, as mentioned previously, ventilation, in the cavity between the glass panes, could even, in some cases, outer perform the equivalent externally positioned blind cases (figures 6.6a & 6.6e).

## *6.5 Comparison between Steady-state G and $\hat{g}_d$ under Real Climate Conditions (London - UK)*

As mentioned in chapter 4, glazing systems are usually characterized, and selected, by their total solar transmittance, for normal incident, as often published by the glazing manufacturers. This paragraph compares the steady-state G-values for normal incident (i.e. values from figure 6.3a-e for 0° sun altitude) with the results from the seasonal variation. The comparison aims to investigate areas where the use of a steady-state value is not enough in order to describe the performance of similar glazing options in practice and could lead to misleading conclusions when choosing the right glazing solution for a building's façade.

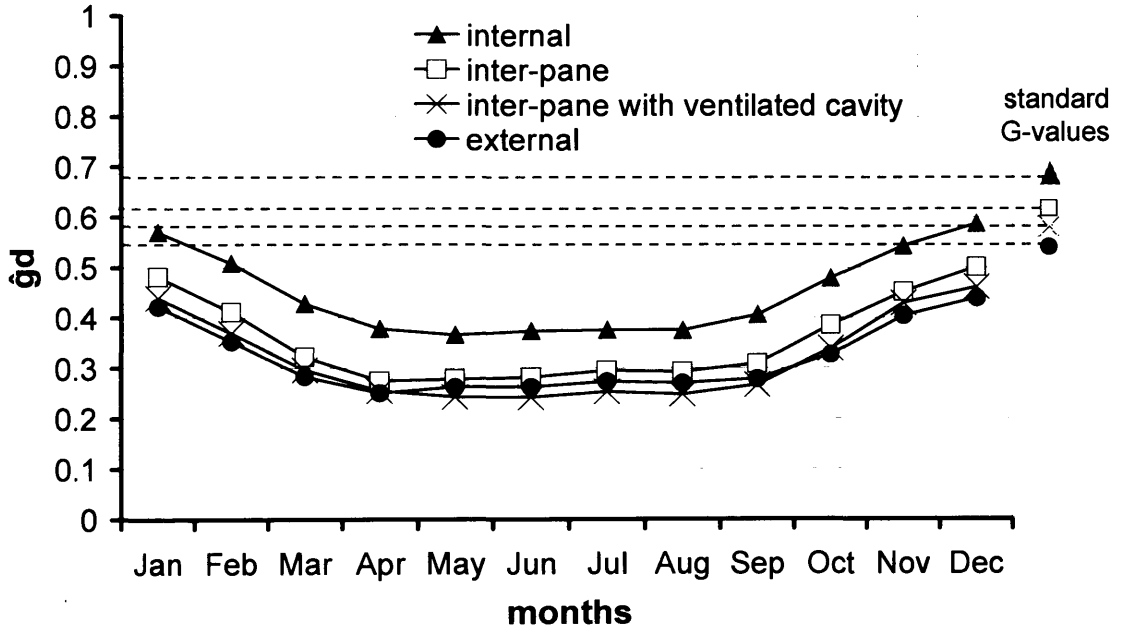


Figure 6.7a: The four cases with slat reflectance 0.5 and slat angle of 20°; real climate against standard G

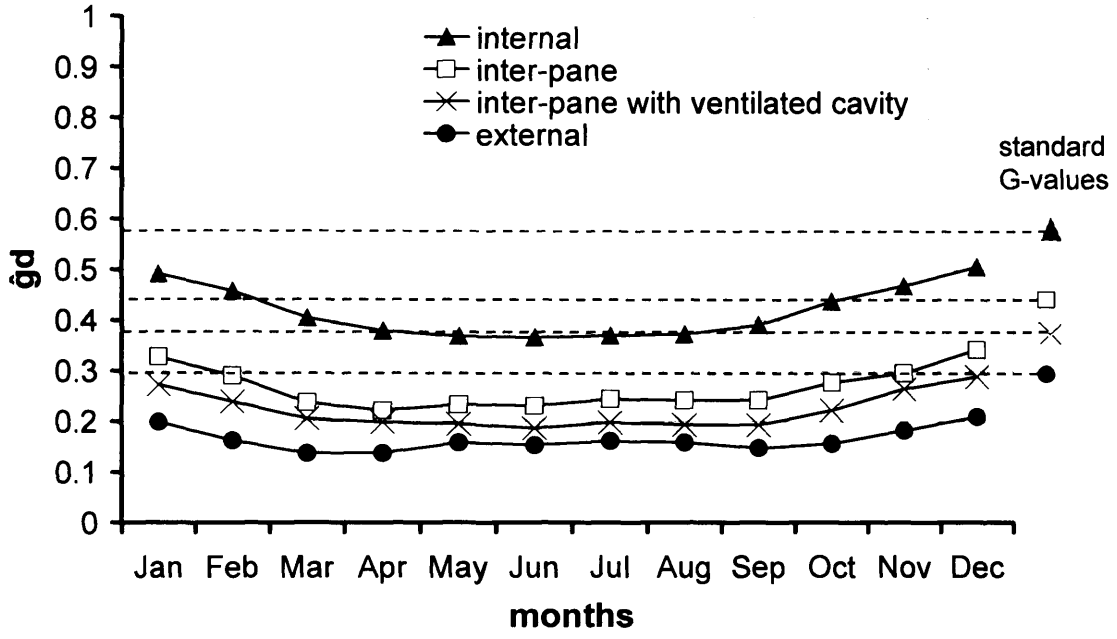


Figure 6.7b: The four cases with slat reflectance 0.5 and slat angle of 45°; real climate against standard G

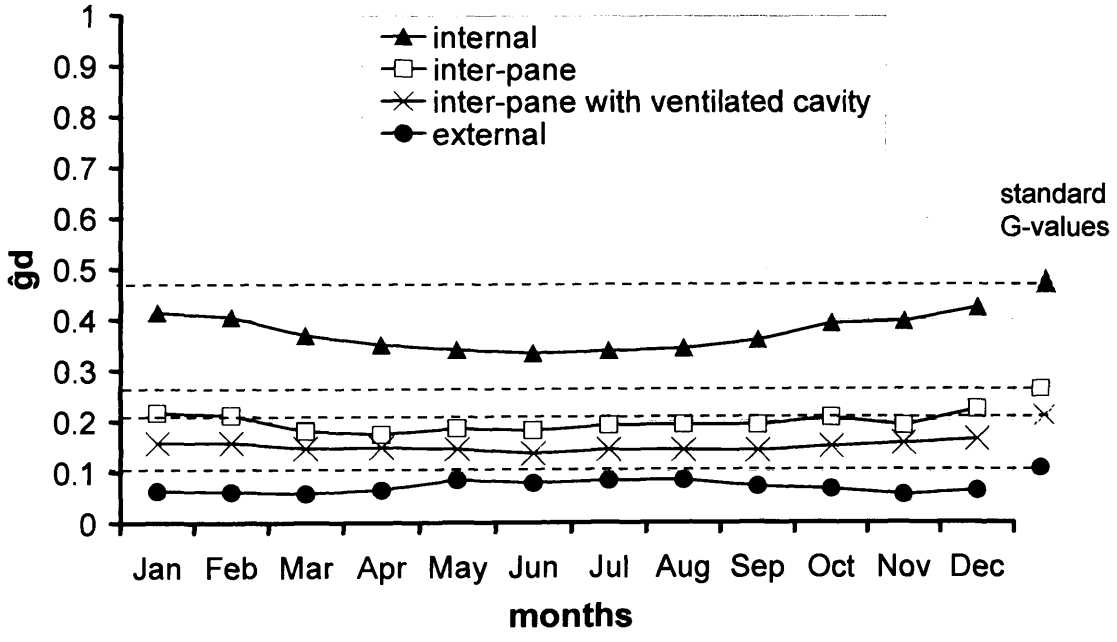


Figure 6.7c: The four cases with slat reflectance 0.5 and slat angle of 70°; real climate against standard G

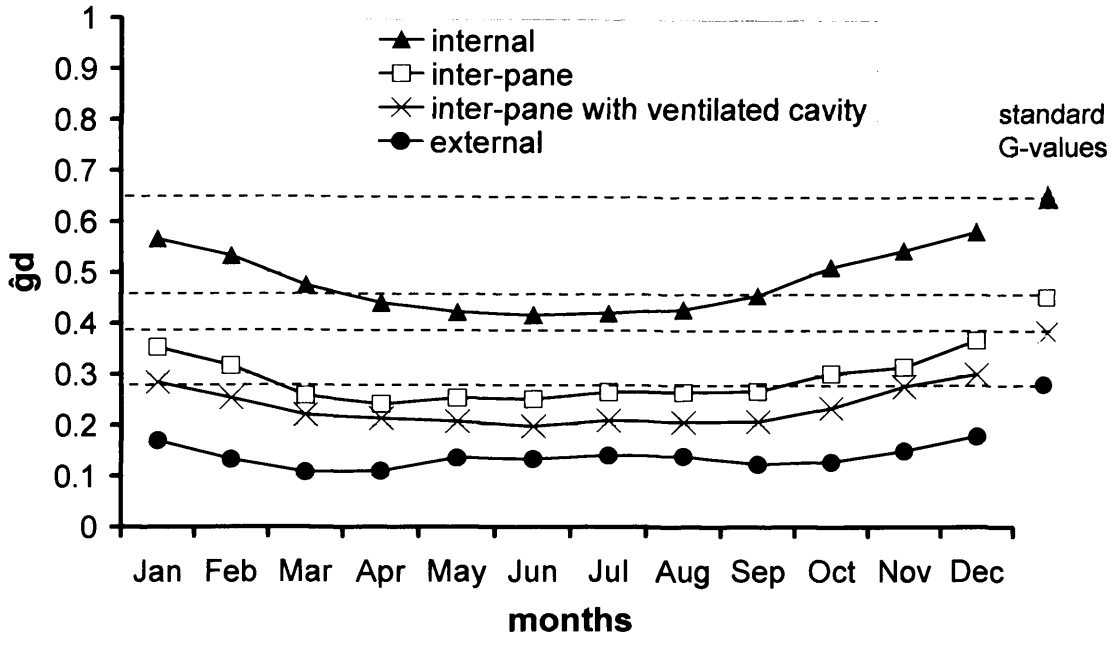


Figure 6.7d: The four cases with slat reflectance 0.2 and slat angle of 45°; real climate against standard G

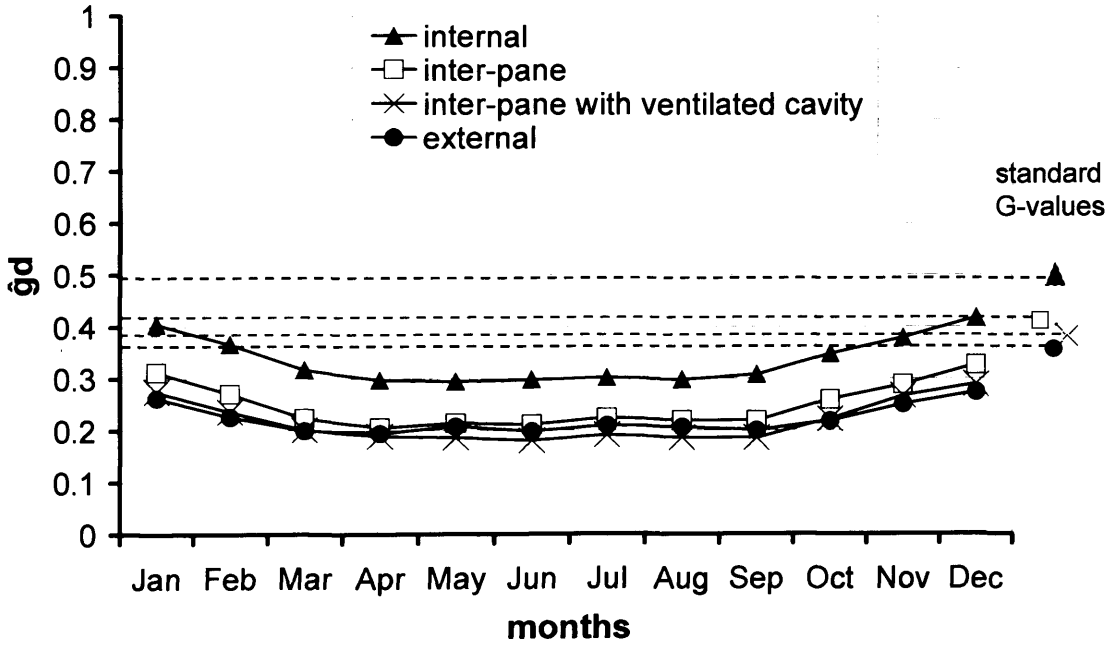


Figure 6.7e: The four cases with slat reflectance 0.8 and slat angle of 45°; real climate against standard G

The G-value under steady-state conditions is calculated for normal incidence, which means it is closer to winter solar incident, when the sun's radiation may be desirable for heating the space. But G-value for normal incidence could be far from the total solar transmittance values occurring during the summer when solar control is needed to avoid overheating. This is especially true for the cases with 20° and 45° angle of slat, presented in figure 6.7a, b, d & e. The $\hat{g}_d$ values during the winter months are apparently much higher than during the summer months. Even in near normal incident, during winter months, the $\hat{g}_d$ does not reach values as high as the G-values predicted under steady-state conditions. The difference between the steady-state G and the dynamically calculated $\hat{g}_d$ and the seasonal variation is less noticed for higher slat angles (figure 6.7c), when the direct transmission is reduced to a minimum.

In comparing glazing options, such as placement of a blind, there is a consistency in the relative rankings between the two calculation methods. The externally positioned blind, in most cases with some seasonal exceptions, show the best performance compared to the other cases, while the internal case shows the poorest thermal performance. However in more detailed comparisons, some rankings alter. Thus, for instance, while the steady-state G-value assessment suggests that the internal (high reflectance of 0.8) blind at 45° should outperform the inter-pane (medium reflectance of 0.5) blind at 20° (0.49 against 0.62 respectively), the dynamically calculated results indicate that they should perform similarly in summer conditions (figure 6.8). As the inter-pane system, with a shallower angle of blade, will allow greater daylight transmission, it should therefore be preferable.

Similar cases can be found in the results, in some cases reversing the rankings suggested by the steady-state G-value. Such examples can be seen by comparing the inter-pane and external blind cases at 20° and the internal blind case at 70°. While at normal incident the first two cases seem to present poor thermal performance in comparison to the third, the dynamically calculated results indicate that their performance in fact reverses, especially during the summer months, when the inter-pane and external blind cases at 20° suggest that outperform the internal blind case at 70° (figure 6.9).

Further analysis of results from the London location is published in the proceedings of the International Conference: Glass in Buildings 2 (Mylona et al, 2005).

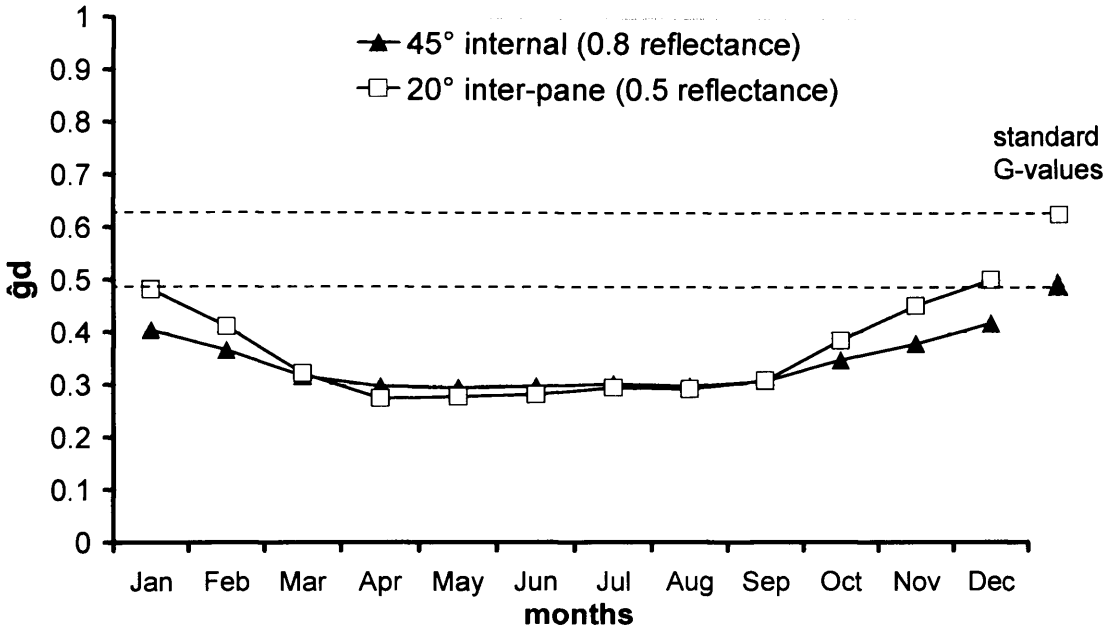


Figure 6.8: G-values against $\hat{g}_d$ for inter-pane blind at 20° and the internal blind at 45°

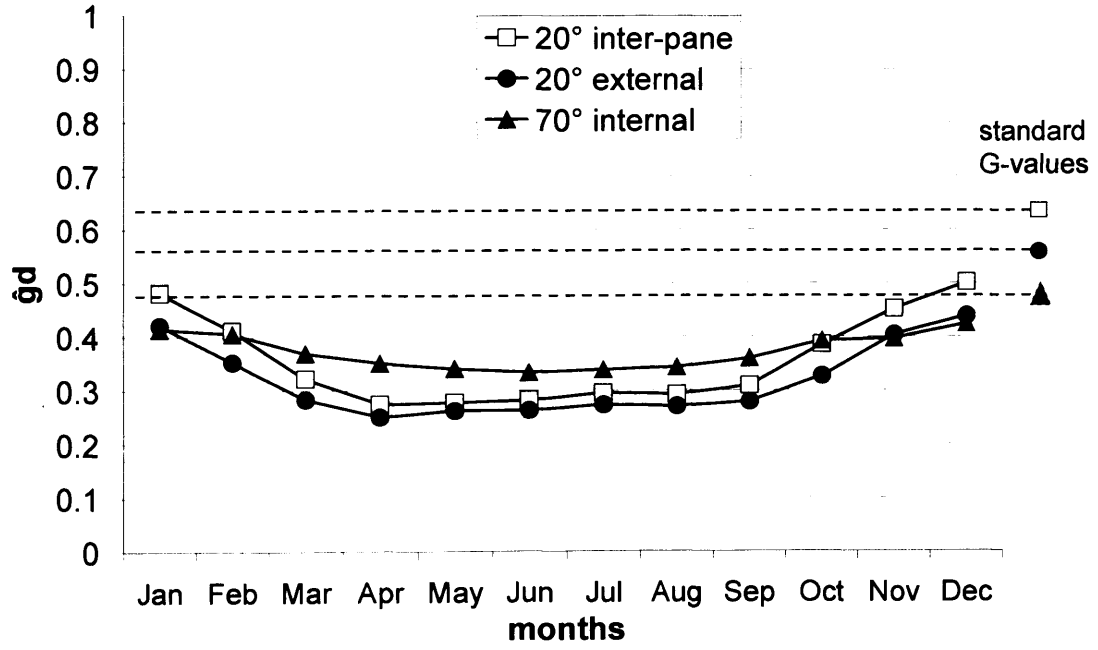


Figure 6.9: G-values against $\hat{g}_d$ for inter-pane & external blind at 20°, and the internal blind at 70°

## 6.6 Simulations under Real Climate Conditions, other Locations: Athens - Greece & Ostersund - Sweden

In order to examine the effect of latitude on the total solar transmittance, the calculation of the dynamic $\hat{g}_d$ for the same four cases (figure 6.1) under real climate conditions, repeated, for the same office space (figure 6.5) and space conditions (see § 6.4), using the same prediction tools, but this time using hourly weather data from annual meteorological data sets measured in Athens - Greece, and Ostersund – Sweden (Energy Plus Website), with latitudes 37° and 63° respectively (figure 6.10). The clearest day for each month of the two data sets was chosen here as well for the calculation of the maximum solar transmittance for each month, for each location. A daily average total solar transmittance $\hat{g}_d$ was calculated from the simulation results using only the daylight hours, for each month.


Figure 6.10: Map of Europe (Google Earth©)

**Athens - Greece**

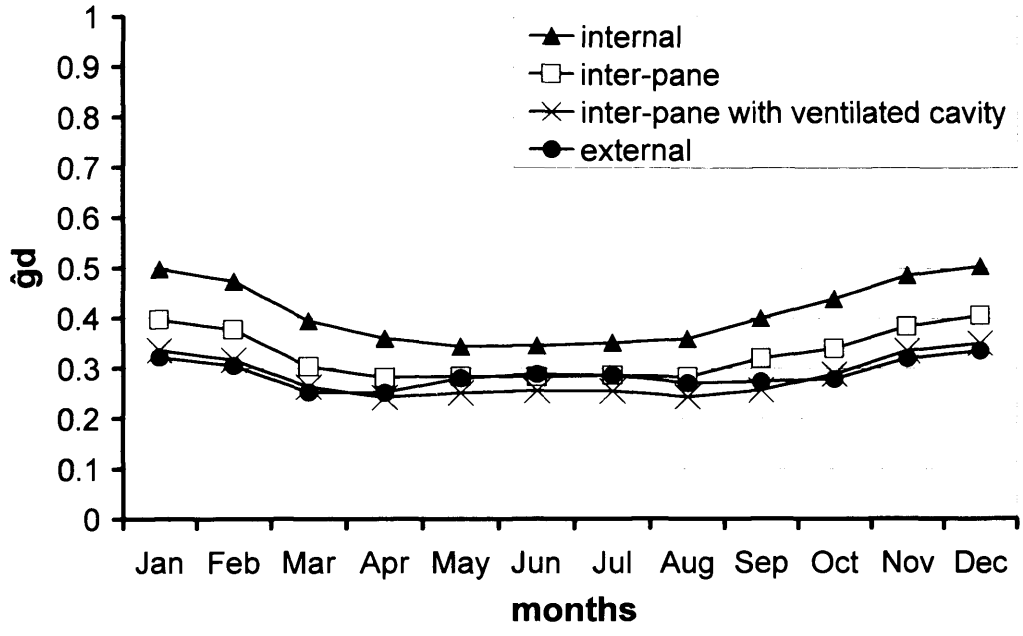


Figure 6.11a: The four cases with slat reflectance 0.5 and slat angle of 20° (Athens – Greece)

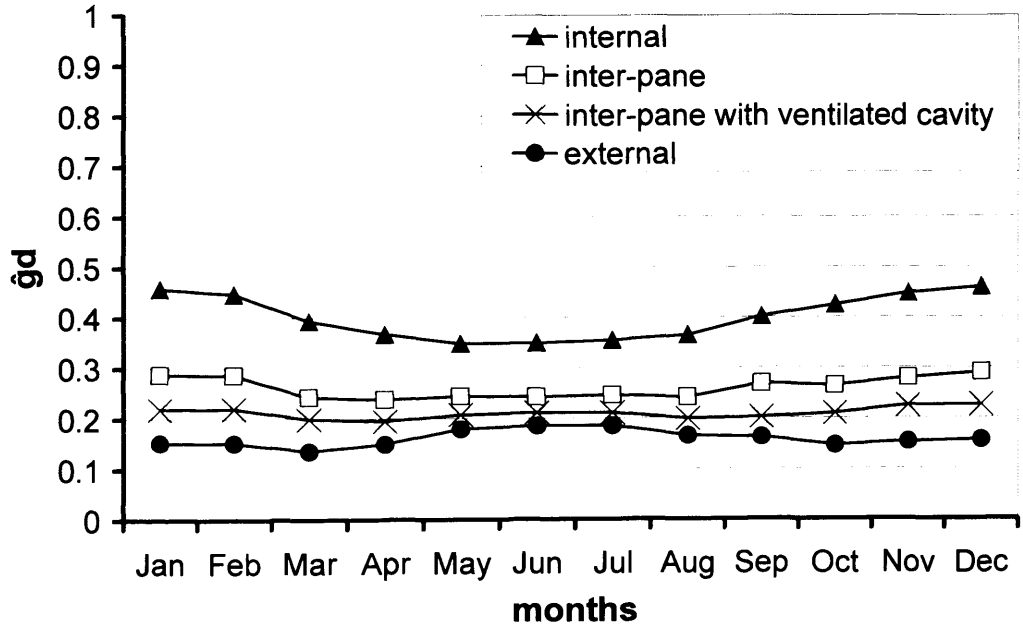


Figure 6.11b: The four cases with slat reflectance 0.5 and slat angle of 45° (Athens – Greece)

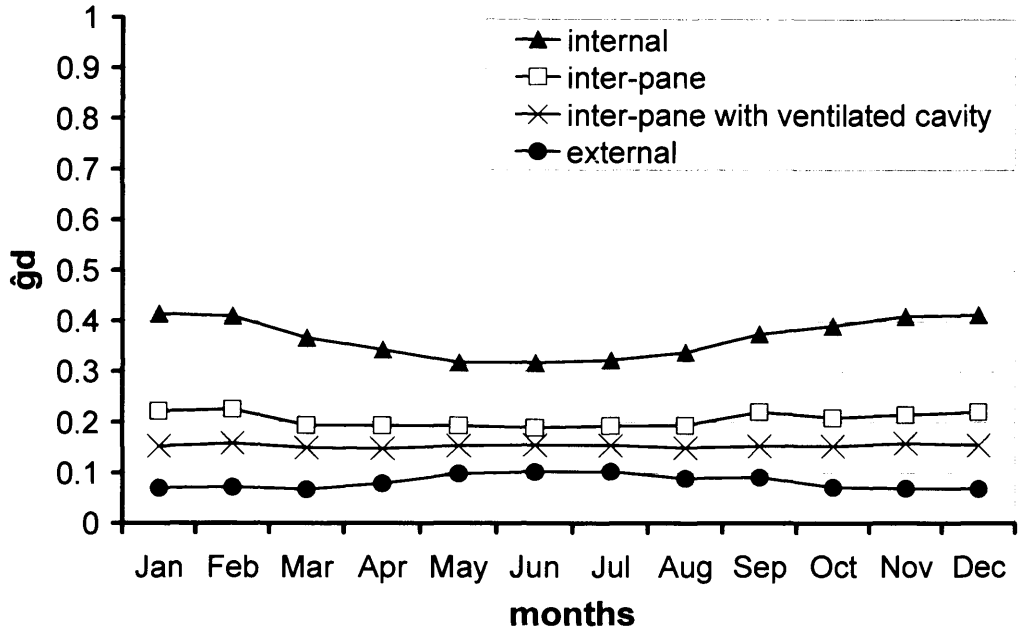


Figure 6.11c: The four cases with slat reflectance 0.5 and slat angle of 70° (Athens – Greece)

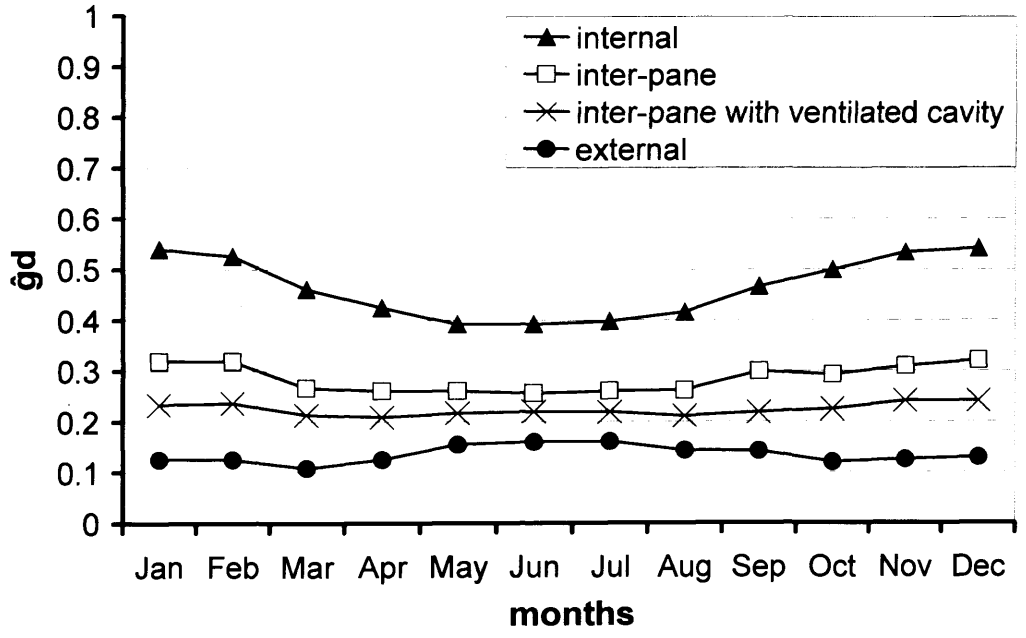


Figure 6.11d: The four cases with slat reflectance 0.2 and slat angle of 45° (Athens – Greece)

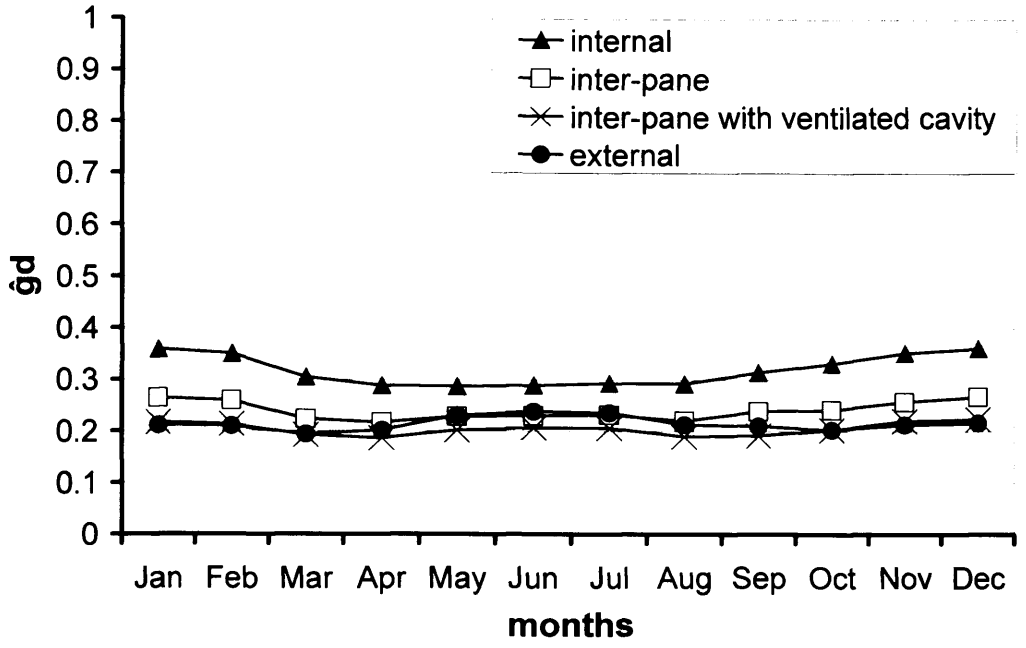


Figure 6.11e: The four cases with slat reflectance 0.8 and slat angle of 45° (Athens – Greece)

**Ostersund - Sweden**

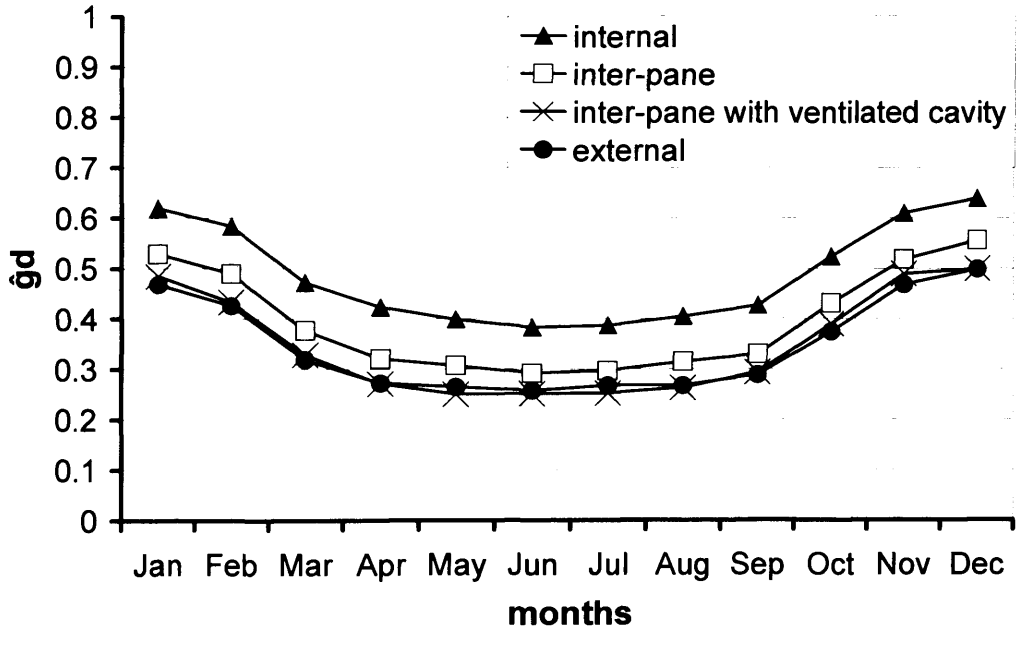


Figure 6.12a: The four cases with slat reflectance 0.5 and slat angle of 20° (Ostersund – Sweden)

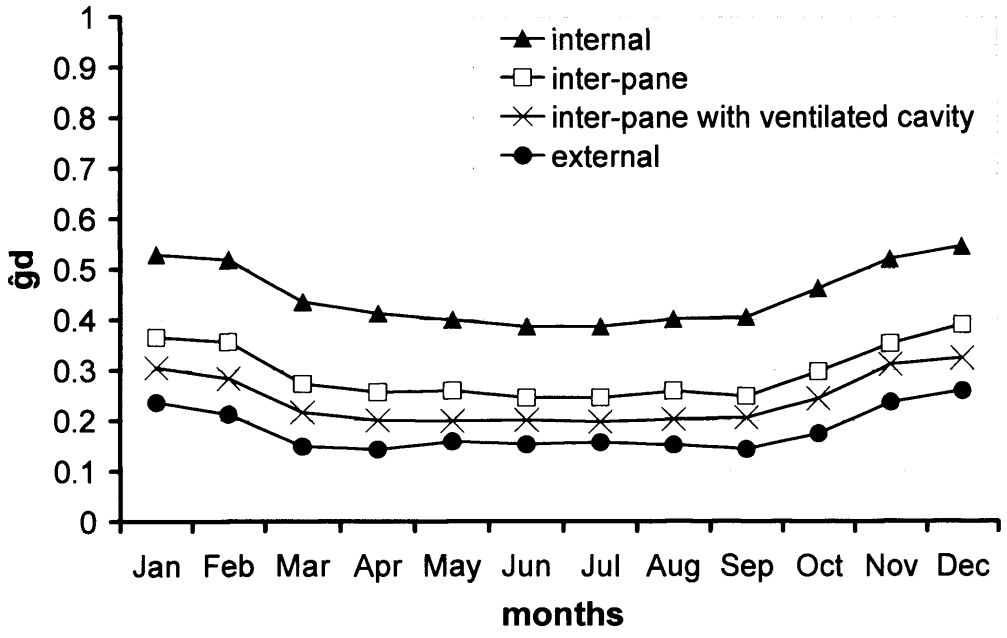


Figure 6.12b: The four cases with slat reflectance 0.5 and slat angle of 45° (Ostersund – Sweden)

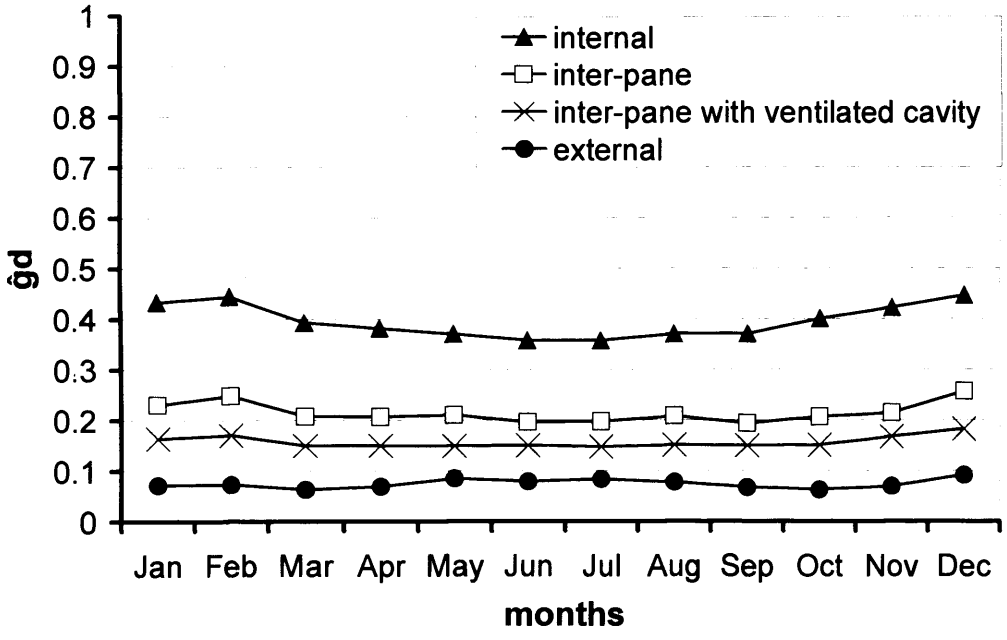


Figure 6.12c: The four cases with slat reflectance 0.5 and slat angle of 70° (Ostersund – Sweden)

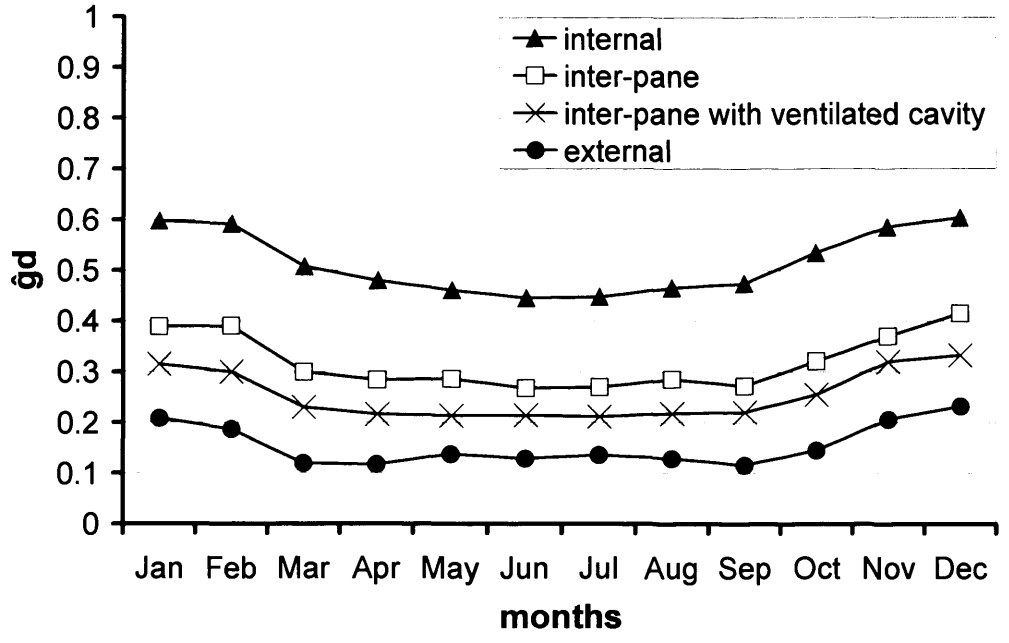


Figure 6.12d: The four cases with slat reflectance 0.2 and slat angle of 45° (Ostersund – Sweden)

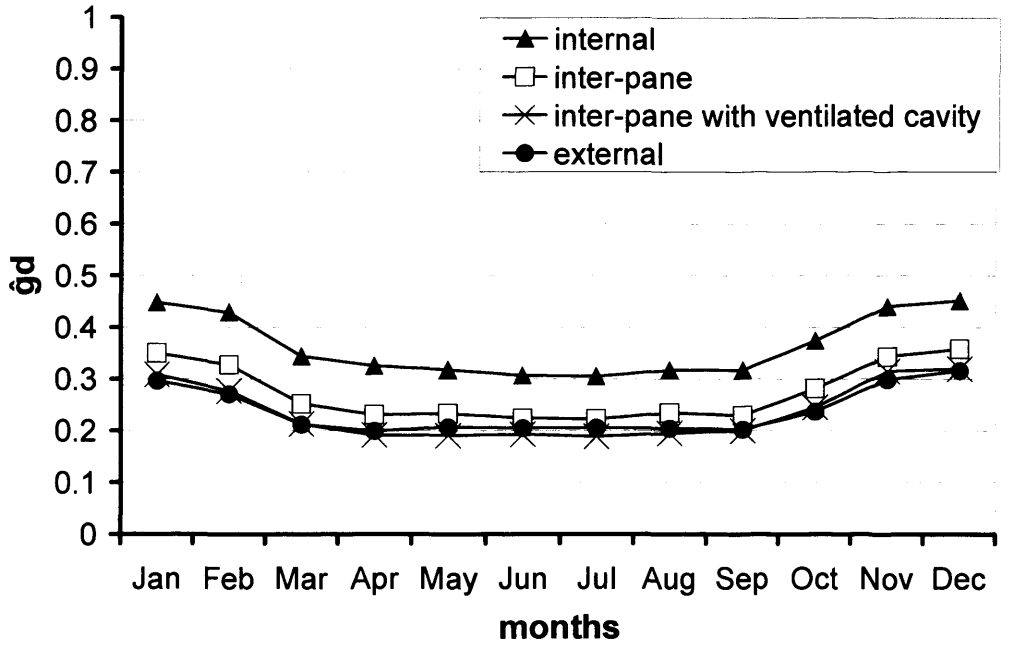


Figure 6.12e: The four cases with slat reflectance 0.8 and slat angle of 45° (Ostersund – Sweden)

Figure 6.11 (a-e) presents the dynamically calculated total solar transmittance $\hat{g}_d$ for Athens and figure 6.12 (a-e) presents the results of $\hat{g}_d$ for Ostersund. The results show that:

- As shown previously, for the London area, $\hat{g}_d$ depends not only on the thermal characteristics of the glazing system but also on the time of the year and solar angles. Most cases, in both areas examined, seem to continue the same pattern, noticeable especially in Ostersund, of maximum $\hat{g}_d$ values during the winter period and minimum values during the summer, while the seasonal variation is less obvious in the results from the Athens area. The lack of the seasonal variation affecting the performance of most of the glazing systems in the Athens area could be explained due to the fact that in south latitudes, even during the winter months, the sun altitude is still far from normal (winter solstice : sun altitude of 30°). Furthermore, the seasonal variation for Ostersund is even more obvious than the one noticed in London, because of the very low, close to normal, winter sun altitude (reaching as low as 3° during the winter solstice).

- The sensitivity of the $\hat{g}_d$ to the seasonal variation in each case examined is directly related to the slat angle and also to the latitude of the location. The higher the slat angle (e.g. 70°) the smaller the $\hat{g}_d$ variation, while for the cases with 20° slat angle $\hat{g}_d$ is widely varying and the variation fluctuates depending on the location's latitude. The connection between seasonal variation and slat angle is more apparent to north locations such as Ostersund and less obvious for south locations such as Athens. For the latter the pattern of lower slat angle (e.g. 20°) - higher $\hat{g}_d$ variation, and vice-versa is still noticeable for the cases of 20° slat angle (and also most of the internal blind cases), but for the rest of the cases and slat angles the above pattern is much less noticed.

- Figures 6.11 (a, b & c) and 6.12 (a, b & c) show the $\hat{g}_d$ for the four cases (figure 6.1) with three different slat angles (20°, 45° and 70°) and medium slat reflectance (0.5), for Athens and Ostersund respectively. In both locations a lower total solar transmittance can be achieved with a higher slat angle (70°). From the graphs (6.11 a, b & c) it is shown that for Athens it is possible to achieve a $\hat{g}_d$ as low as 0.1 in the summer and a mean yearly value of 0.08, when blind of 70° angle slat is being used externally, and as high as 0.35 in the summer and a mean yearly value of 0.38, when

blind of 20° slat angle is installed internally. From the graphs (6.12 a, b & c) it is shown that for the high latitude location of Ostersund it is possible to achieve a $\hat{g}_d$ as low as 0.08 in the summer and a mean yearly value of 0.07, when blind of 70° slat angle is being used externally, and as high as 0.38 in the summer and a mean yearly value of 0.46, when blind of 20° slat angle is installed internally.

- Similarly to the London location, comparing the graphs of different slat angle cases (20°, 45° and 70° - 0.5 reflectance) it is shown that for low slat angles (20°) the variation of the thermal performance between the cases with the same blind characteristics is small, especially for the external and inter-pane blind cases. For high slat angles (70°) the difference in the thermal performance is far more noticeable. As also mentioned earlier for the London area, this has an immediate relevance to the design of a building's facade, especially when blinds with fixed slat angles are considered as a shading option. Blinds of high slat angles will require a thorough investigation of their placement, while blinds of low slat angles will perform similarly when positioned externally or inter-pane.

- The thermal performance of the various cases also depends on the colour of the blind material. In most cases a lower total solar transmittance can be achieved with light colour slats (high reflectance - 0.8). Consistent with the results from the simulations using the London climate, it is noticed here as well that while the above is mainly the case for the internally and inter-pane positioned blinds, the reverse effect occurs in the external blind cases. That is low reflectance (0.2) blinds present lower $\hat{g}_d$ than high reflectance (0.8) blinds when positioned externally, for the same slat angle.

- Figures 6.11 (b, d & e) and 6.12 (b, d & e) show the $\hat{g}_d$ for the four cases (figure 6.1) with three different blind colours (reflectance values of 0.2, 0.5 and 0.8) and slat angle of 45°. From the graphs (6.11 b, c & e) it is shown that in Athens it is possible to achieve a $\hat{g}_d$ as low as 0.2 in the summer and a mean yearly value of 0.2, when blind with slat reflectance of 0.8 is being placed in between glass panes in a ventilated cavity, and as high as 0.40 in the summer and a mean yearly value of 0.47, when there is blind with slat reflectance of 0.2 installed internally. Similarly, from the graphs (6.12 b, c & e) it is shown that in Ostersund it is possible to achieve a $\hat{g}_d$ as low as 0.19 in the summer and a mean yearly value of 0.24, when a blind with slat

reflectance of 0.8 is being placed in between glass panes in a ventilated cavity, and as high as 0.45 in the summer and a mean yearly value of 0.52, when there is a dark blind of 0.2 slat reflectance installed internally. The above effect, of lower $\hat{g}_d$ values achieved with light blinds, is reversed for the external cases. In both Athens and Ostersund locations the lowest $\hat{g}_d$, as low as 0.16 in the summer and a yearly mean of 0.14, in Athens, and as low as 0.13 in the summer and a yearly mean of 0.16, in Ostersund, could be achieved when there is a dark blind of 0.2 slat reflectance installed externally.

- As well as in the results from the simulations using the London climate data, by comparing the graphs of different colour cases (reflectance of 0.2, 0.5 and 0.8 – 45° slat angle) it is shown that for high reflectance blinds (0.8) the variation of the thermal performance between the cases of the same blind characteristics is low, especially for external and inter-pane blind cases, which present almost identical yearly performance. For low reflectance blinds (0.2) the difference in the thermal performance between the cases is far more noticeable. The above has an immediate relevance to the design of a building's facade when choosing the position of a light or dark colour blind. The dark blind will require a thorough examination of its placement, while the light blind will perform similarly when positioned externally of inter-pane.

- The consistency of the lower $\hat{g}_d$ values presented by externally positioned blinds compared to the cases of the same surface colour and slat angle displayed under steady-state conditions is interrupted by the results in Athens and Ostersund locations, as also previously noticed in London area, with some cases of inter-pane blinds in ventilated cavity presenting lower $\hat{g}_d$ values to their equivalent external blind cases. The above is noticed for the cases of 20° slat angle of medium reflectance (0.5) and 45° slat angle of high reflectance (0.8) (figures 6.11a, 6.11e, 6.12a & 6.12e), which is in accordance to the equivalent results from the simulations using the London weather data set (figures 6.6a and 6.6e).

- The $\hat{g}_d$ for external blinds can be similar or higher than for internal or inter-pane blinds, if surface colour and blade angle are not carefully chosen. Examples of the above are noticed in the results from both Athens and Ostersund locations; the external blind case with 20° slat angle presents similar $\hat{g}_d$ compared to the internal blind with 45° of high reflectance (0.8) in Athens (figures 6.11a and 6.11e) and

higher values compared to the internal blind with 45° of any examined reflectance (0.2, 0.5 & 0.8) in Ostersund (figures 6.12a and 6.12b, d & e), especially during the summer months. Also, for the Athens graphs, comparing the external blind case with 20° slat angle to the external and inter-pane blind cases of all other slat angle and reflection blind cases, it is shown that better thermal performance could be achieved by choosing correctly the position, the colour and the slat angle of the blind. Furthermore, in Ostersund the internal cases present constantly the maximum $\hat{g}_d$ values, compared to their equivalent in the other two blind positions, and they never reach values as low as any of the external cases, which makes the external case a better blind position, compared to the internal one, independent to the blind colours and slat angles examined here.

- From the assessment of the thermal performance of the cases under examination (figure 6.1), under different latitudes, it is shown that forced ventilation in the cavity of inter-pane blind cases can improve the thermal performance of a glazing system, independent of the latitude of the building.

- Comparing the equivalent results from the Athens, London and Ostersund simulations it is noticed that most cases present similar thermal performance during the summer months and different during the winter months, when most cases in the Ostersund area present higher $\hat{g}_d$ values than in the London and Athens areas. Only the cases of 70° slat angle present a similar $\hat{g}_d$ throughout the year in all areas. The above refers to the different sun altitudes (the winter sun being lower in Ostersund than in London and Athens) between the locations and how much the position of the sun affects the thermal performance of the glazing system (mostly affected are the low slat angle blinds rather than the high slat angle blinds).

- Generally, from the results under real climate conditions (figures 6.6a-e, 6.11a-e and 6.12a-e), it can be derived that while between the cases of the same blind characteristics (different blind position) the secondary heat is the factor mostly affecting the $\hat{g}_d$ variation, between the same cases in different latitude the factor mostly affecting the $\hat{g}_d$ variation is the sun altitude; differences mostly noticeable during the winter months, depending on how far from normal is the winter sun altitude.

## *6.7 Comparison between Steady-State G and $\hat{g}_d$ under Real Climate Conditions, other Locations: Athens - Greece & Ostersund - Sweden*

Figures 6.13 (a-e) and 6.14 (a-e) show the steady-state G-values, calculated for normal incident and under steady-state conditions (i.e. values from figure 6.3a-e for 0° sun altitude), often used by the manufactures in order to characterise the different glazing types. On the same graphs are also presented the results from the dynamic simulations under real climate for the Athens and Ostersund locations. The comparison aims to investigate areas where the use of a steady-state value is not efficient to describe the performance of similar glazing options in practice and for different latitudes and could lead to misleading conclusions when choosing the right glazing system for a building's façade.

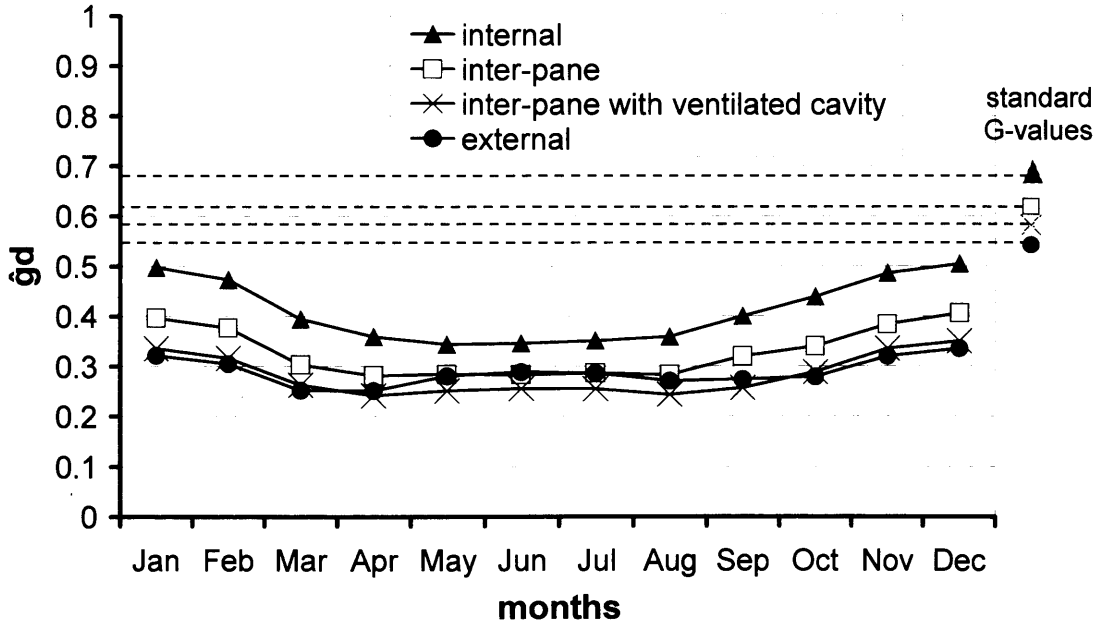


Figure 6.13a: The four cases with slat reflectance 0.5 and slat angle of 20°; real climate (Athens – Greece) against standard G

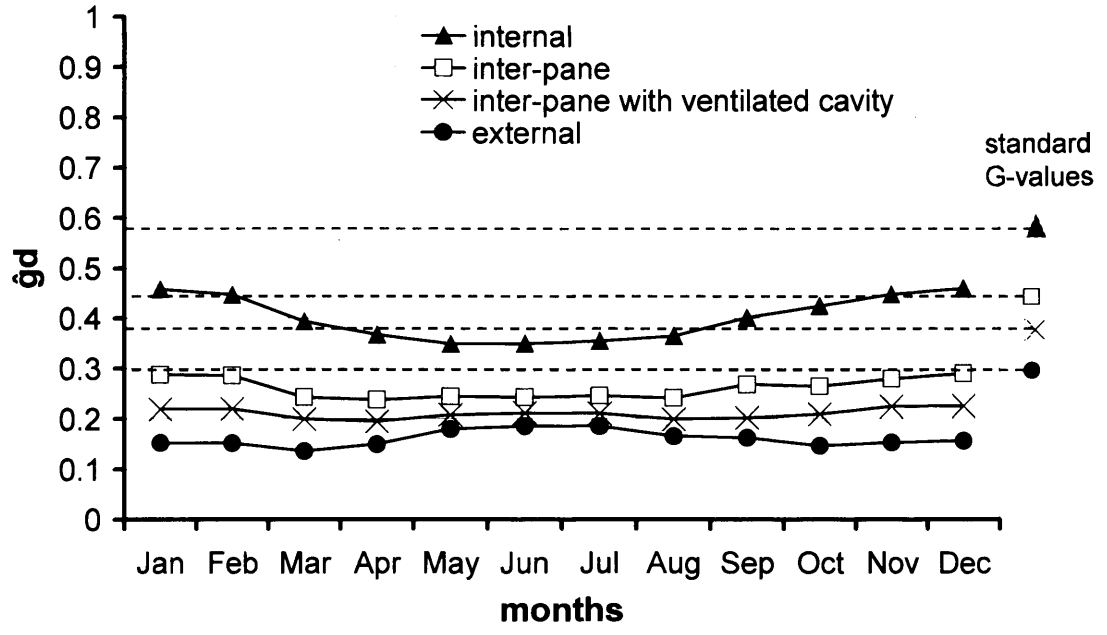


Figure 6.13b: The four cases with slat reflectance 0.5 and slat angle of 45°; real climate (Athens – Greece) against standard G

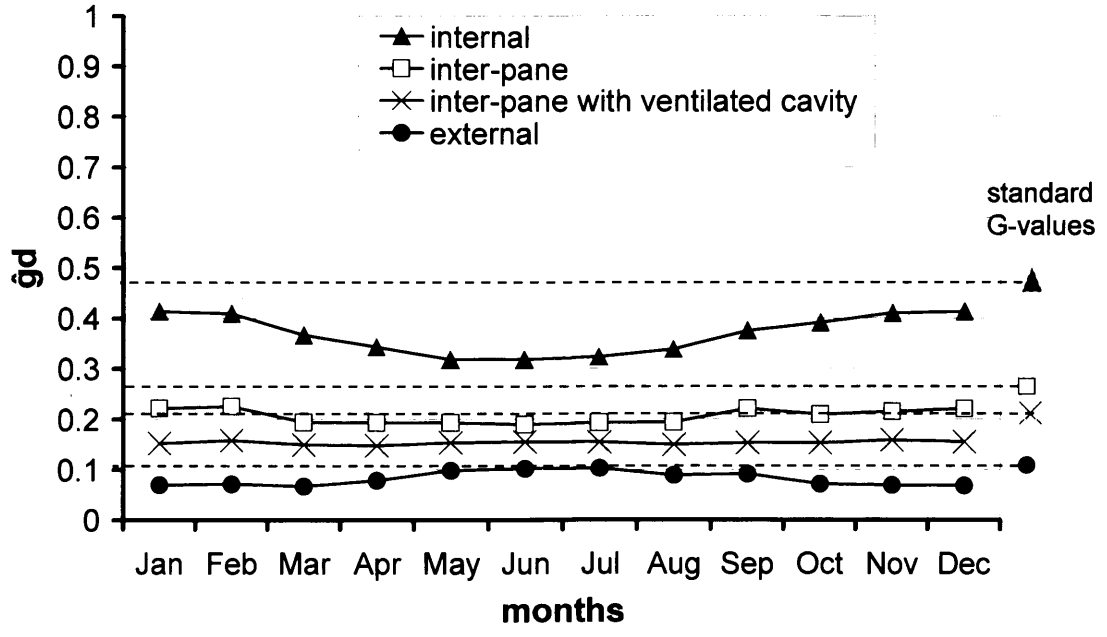


Figure 6.13c: The four cases with slat reflectance 0.5 and slat angle of 70°; real climate (Athens – Greece) against standard G

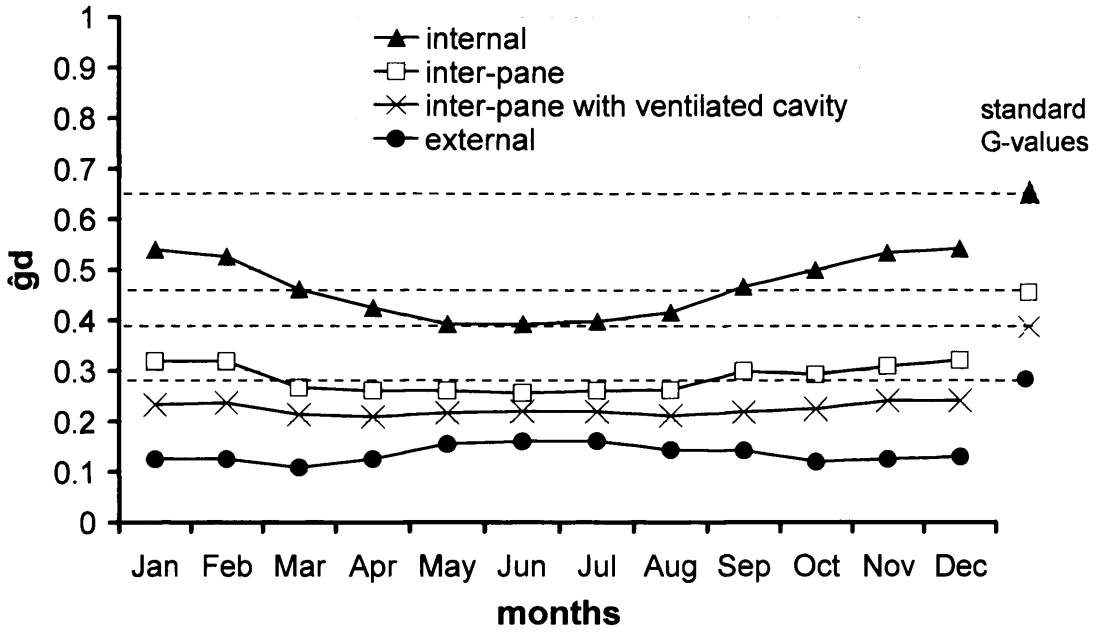


Figure 6.13d: The four cases with slat reflectance 0.2 and slat angle of 45°; real climate (Athens – Greece) against standard G

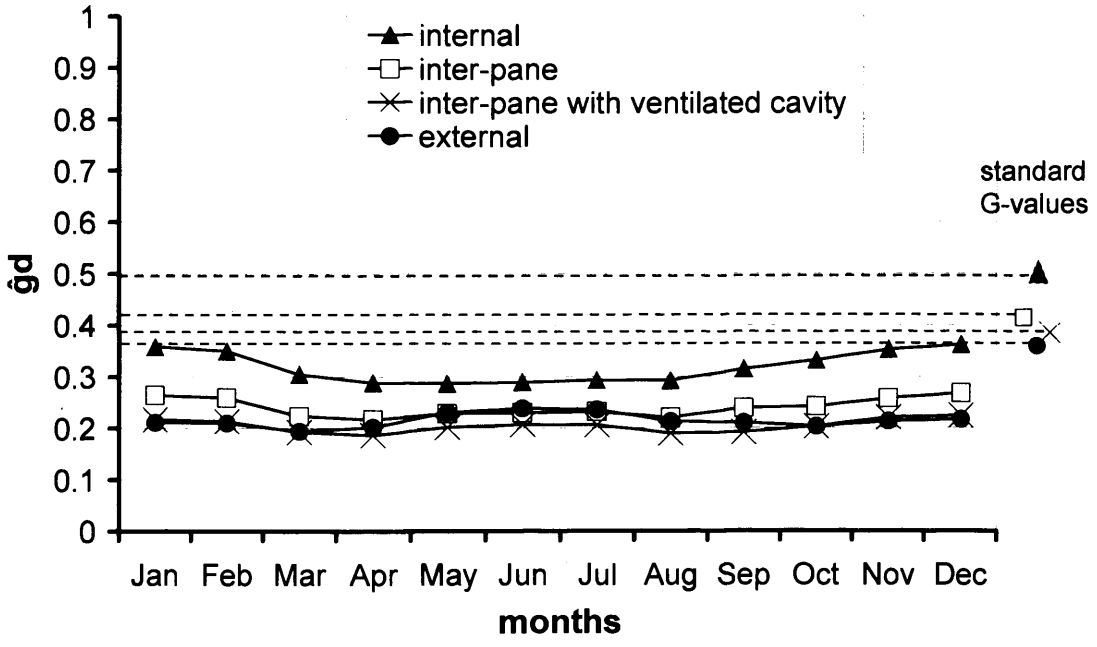


Figure 6.13e: The four cases with slat reflectance 0.8 and slat angle of 45°; real climate (Athens – Greece) against standard G

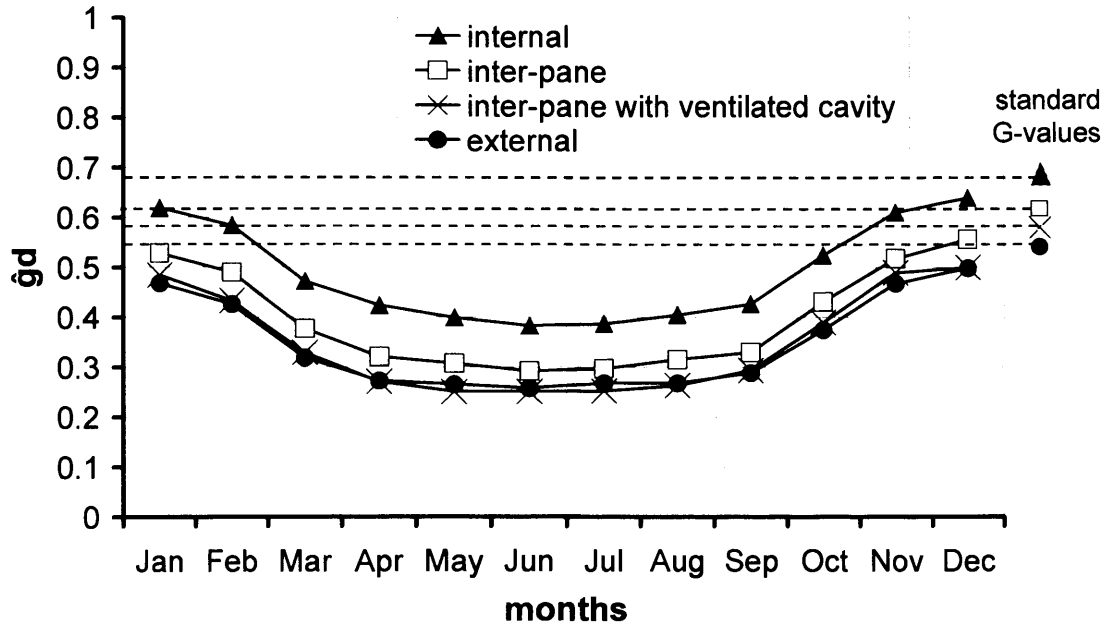


Figure 6.14a: The four cases with slat reflectance 0.5 and slat angle of 20°; real climate (Ostersund – Sweden) against standard G

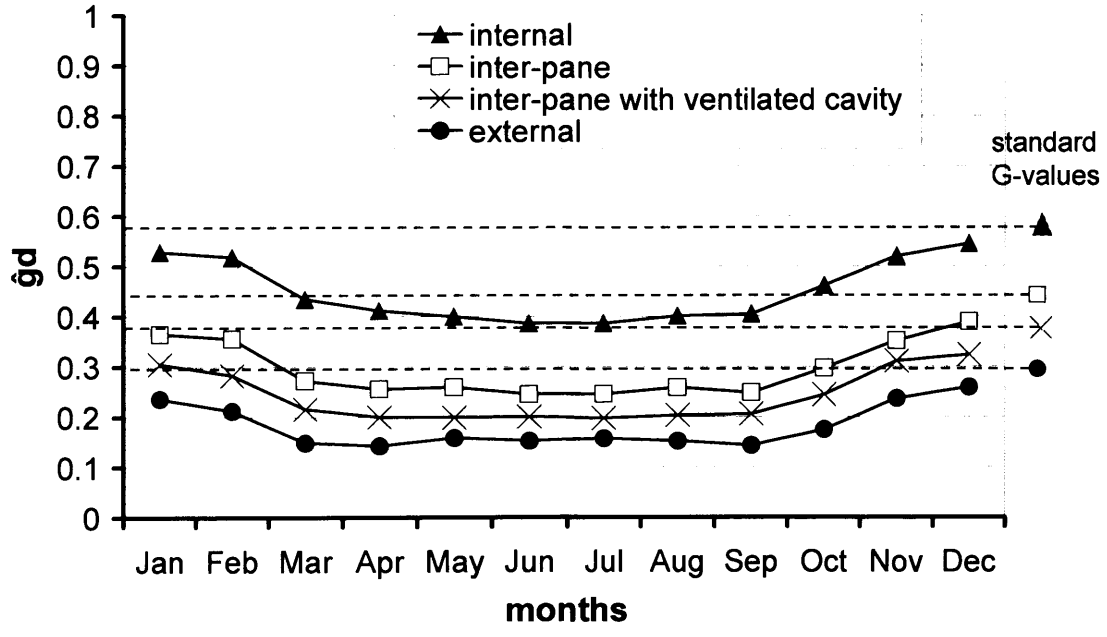


Figure 6.14b: The four cases with slat reflectance 0.5 and slat angle of 45°; real climate (Ostersund – Sweden) against standard G

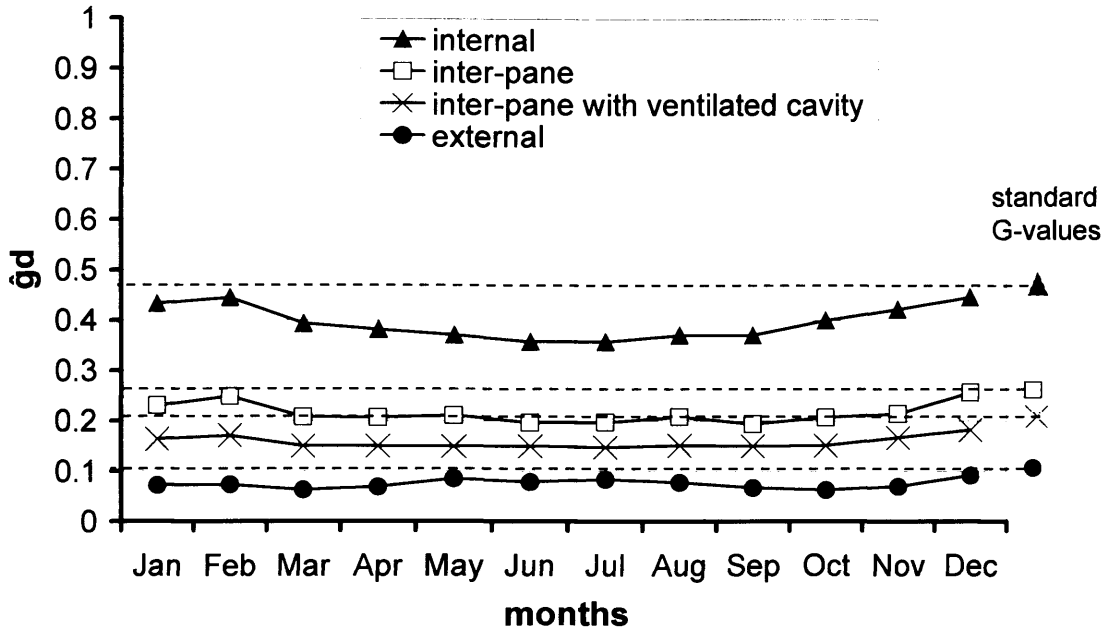


Figure 6.14c: The four cases with slat reflectance 0.5 and slat angle of 70°; real climate (Ostersund – Sweden) against standard G

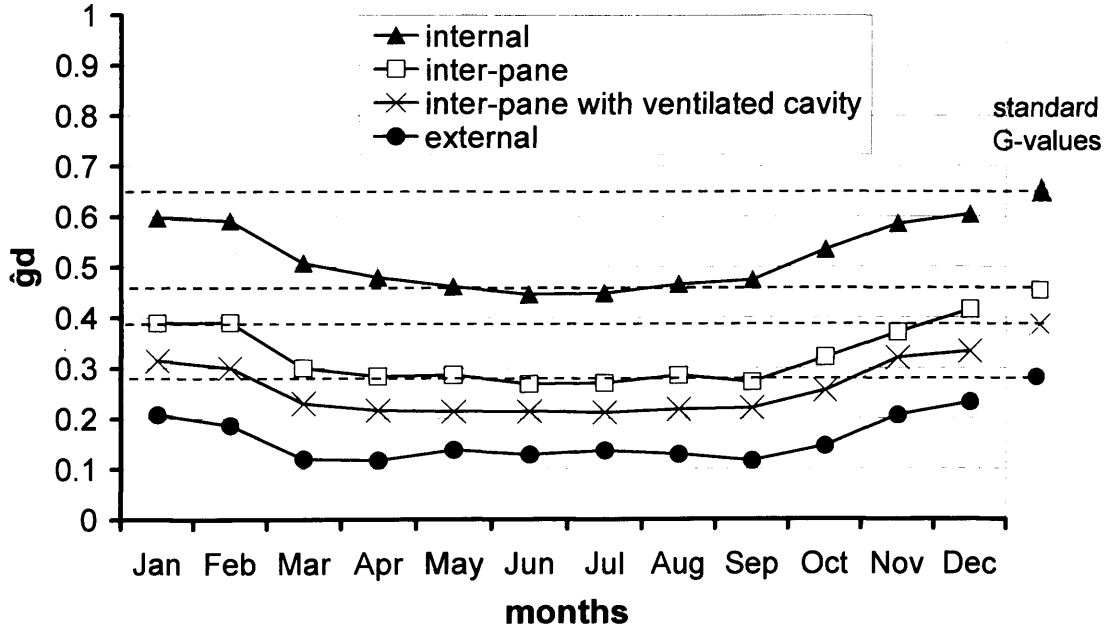


Figure 6.14d: The four cases with slat reflectance 0.2 and slat angle of 45°; real climate (Ostersund – Sweden) against standard G

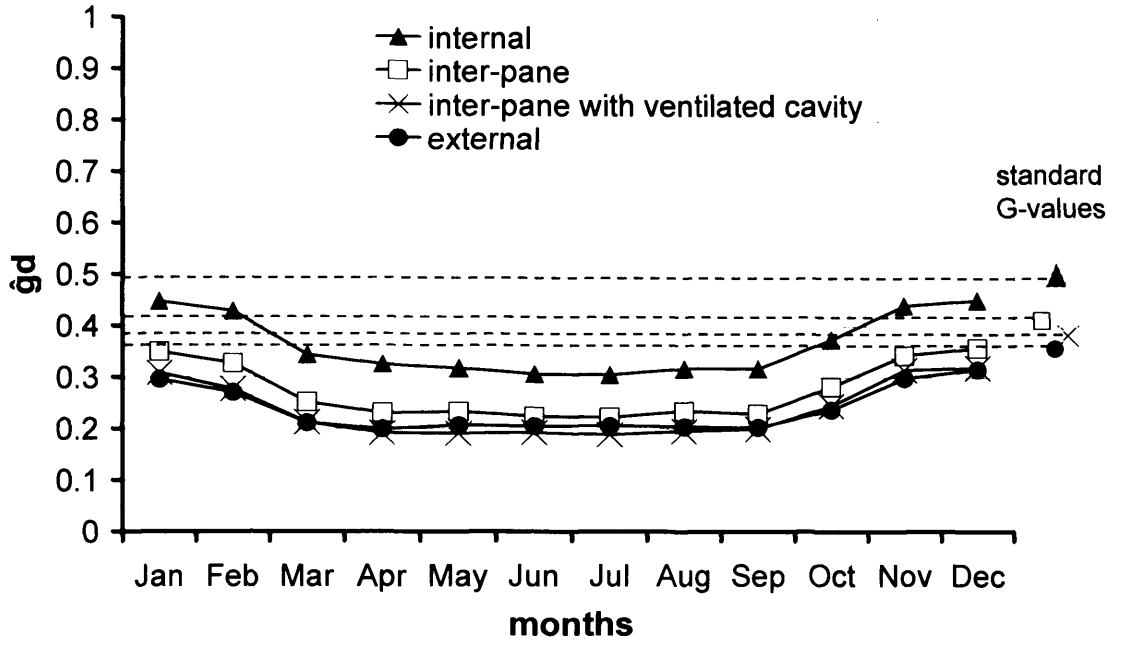


Figure 6.14e: The four cases with slat reflectance 0.8 and slat angle of 45°; real climate (Ostersund – Sweden) against standard G

From the comparison between the dynamically calculated $\hat{g}_d$ in Athens and Ostersund locations and the G calculated for normal incidence under steady-state conditions, it is noticed that most cases, even during the winter months, don't reach values as high as the steady-state predicted values for normal incident. Closer to the steady-state G are some of the winter months in Ostersund where the altitude of the winter sun solstice is 3°, almost normal, while the values in Athens present the maximum difference between G and $\hat{g}_d$ (altitude of the winter sun solstice is 30°, far from normal). The difference between G and $\hat{g}_d$ is maximum for most of the cases examined, in all three locations, during the summer months when solar control is usually considered.

The above is especially true for the cases with 20° and 45° angle of slat, presented in figures 6.13 (a, b, d & e) and 6.14 (a, b, d & e), while the difference between the G and the $\hat{g}_d$ and the variation due to location latitude is less for higher slat angles, such as 70° (figure 6.13c & 6.14c), when the direct solar transmittance is reduced to a minimum.

Also shown for the London location, even though there is a consistency of results between the two calculation methods showing that externally positioned blinds present, in most cases with some seasonal exceptions, the best performance and the internal

blind cases present the poorest thermal performance, more detailed comparisons, show that some rankings alter.

In figure 6.15 and 6.16 it is shown that while the G-value assessment suggests that the internal (high reflectance of 0.8) blind of 45° slat angle should outperform the inter-pane (medium reflectance of 0.5) blind of 20° slat angle (0.49 against 0.62 respectively), the dynamically calculated $\hat{g}_d$ values indicate that they should perform similarly, especially during the summer period, in Ostersund, and most of the year, in Athens. As the inter-pane system, with a shallower angle of blade, will allow greater daylight transmission, it should therefore be preferable.

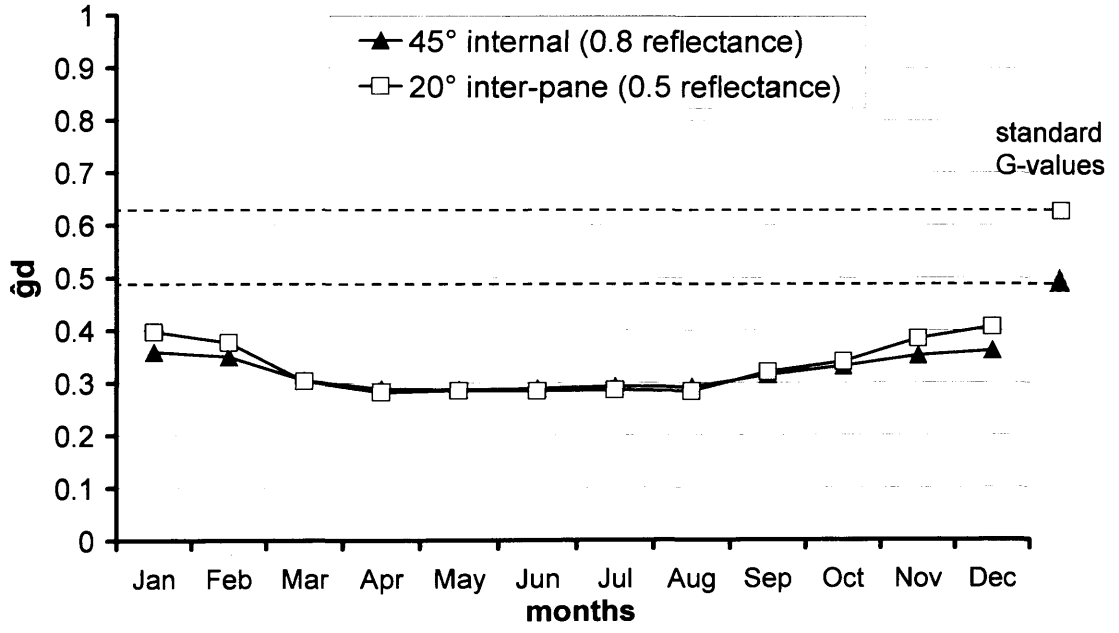


Figure 6.15: G-values against $\hat{g}_d$ for inter-pane blind at 20° and the internal blind at 45° (Athens – Greece)

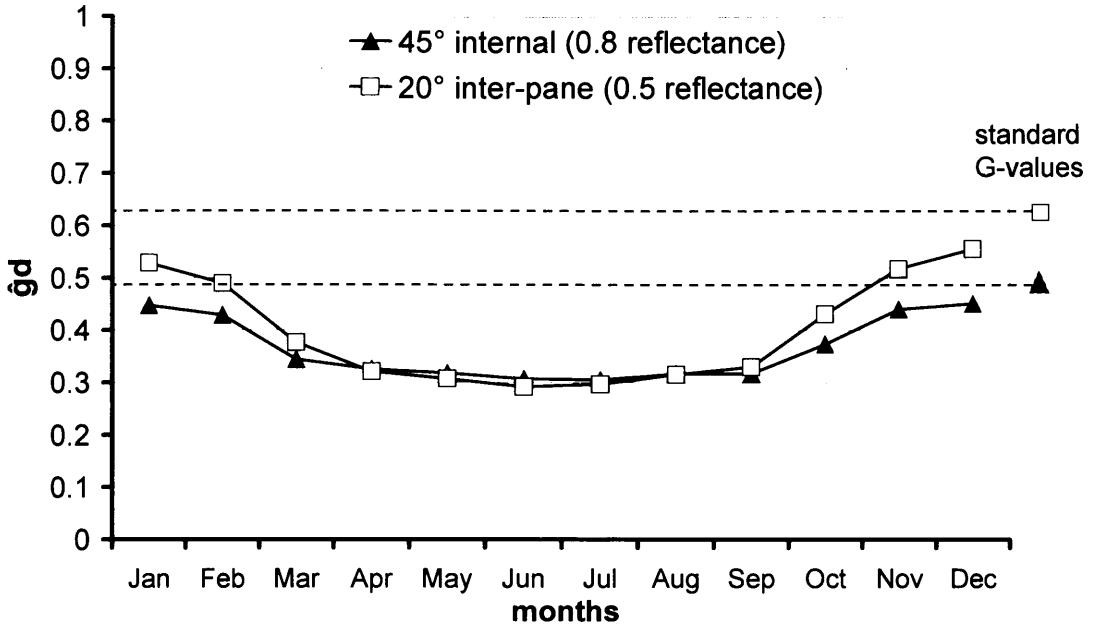


Figure 6.16: G-values against $\hat{g}_d$ for inter-pane blind at 20° and the internal blind at 45° (Ostersund – Sweden)

Figures 6.17 and 6.18 present an example of a case where the rankings suggested by the G calculated under steady-state conditions are reversing when the thermal performance of a glazing is considered under real climate conditions. By comparing the inter-pane and external blind cases of 20° slat angle and the internal blind case of 70° slat angle it is shown that while at normal incident the first two cases seem to present poor thermal performance in comparison to the third, the dynamically calculated results indicate that their yearly performance in fact reverses, and the inter-pane and external blind cases of 20° slat angle seem to outperform the internal blind case of 70° slat angle.

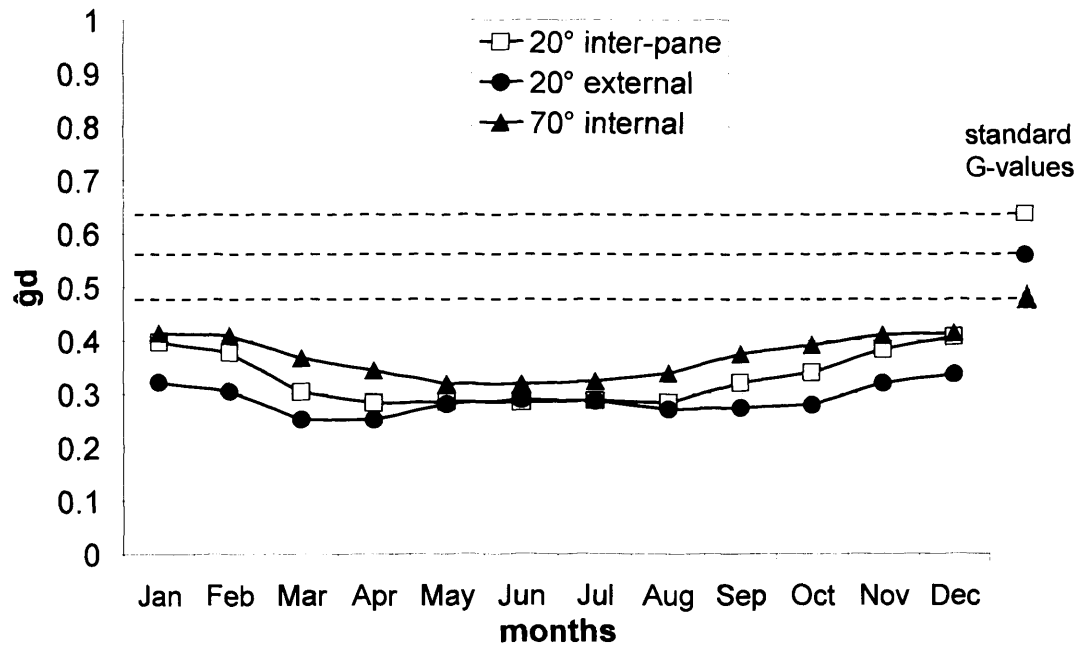


Figure 6.17: G-values against $\hat{g}_d$ for inter-pane & external blind at 20°, and the internal blind at 70° (Athens – Greece)

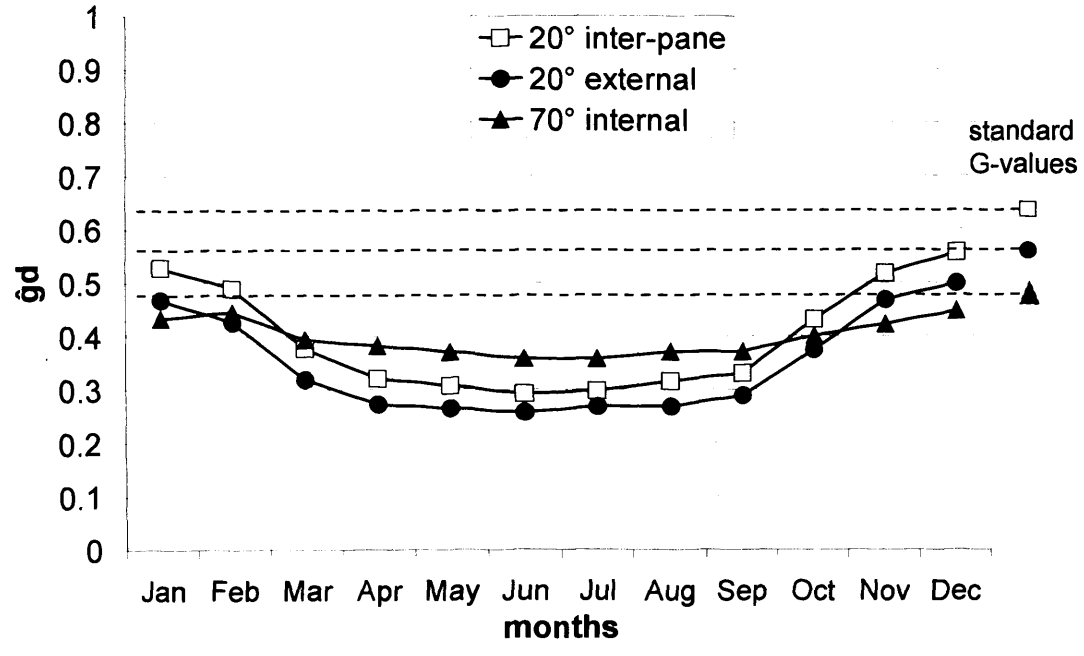


Figure 6.18: G-values against $\hat{g}_d$ for inter-pane & external blind at 20°, and the internal blind at 70° (Ostersund – Sweden)

Table 6.1 summarises the results from the simulations under steady-state and real climate conditions presented in the previous paragraphs.

| **Location** | **Blind** | | **G-value** | **Summer $\hat{g}_d$** | **Winter $\hat{g}_d$** |
|---|---|---|---|---|---|
| | *Slat angle / Reflectance* | *Position* | *Normal incident* | *Average* | *Average* |
| *Athens* | 20° / 0.5 | internal | 0.68 | 0.36 | 0.47 |
| | | inter-pane | 0.62 | 0.29 | 0.37 |
| | | inter-pane ventilated | 0.58 | 0.25 | 0.32 |
| | | external | 0.56 | 0.28 | 0.30 |
| | 45° / 0.5 | internal | 0.58 | 0.36 | 0.44 |
| | | inter-pane | 0.43 | 0.25 | 0.28 |
| | | inter-pane ventilated | 0.37 | 0.20 | 0.22 |
| | | external | 0.30 | 0.15 | 0.17 |
| | 70° / 0.5 | internal | 0.47 | 0.34 | 0.40 |
| | | inter-pane | 0.26 | 0.20 | 0.21 |
| | | inter-pane ventilated | 0.20 | 0.15 | 0.16 |
| | | external | 0.10 | 0.07 | 0.09 |
| | 45°/0.2 | internal | 0.65 | 0.42 | 0.52 |
| | | inter-pane | 0.45 | 0.27 | 0.30 |
| | | inter-pane ventilated | 0.38 | 0.22 | 0.23 |
| | | external | 0.27 | 0.12 | 0.15 |
| | 45°/0.8 | internal | 0.49 | 0.29 | 0.34 |
| | | inter-pane | 0.42 | 0.23 | 0.25 |
| | | inter-pane ventilated | 0.38 | 0.20 | 0.21 |
| | | external | 0.36 | 0.21 | 0.22 |
| *London* | 20° / 0.5 | internal | 0.68 | 0.38 | 0.52 |
| | | inter-pane | 0.62 | 0.29 | 0.43 |
| | | inter-pane ventilated | 0.58 | 0.25 | 0.39 |
| | | external | 0.56 | 0.27 | 0.37 |
| | 45° / 0.5 | internal | 0.58 | 0.38 | 0.46 |
| | | inter-pane | 0.43 | 0.24 | 0.30 |
| | | inter-pane ventilated | 0.37 | 0.19 | 0.25 |
| | | external | 0.30 | 0.15 | 0.18 |

| | | | | | |
|---|---|---|---|---|---|
| | 70° / 0.5 | internal | 0.47 | 0.34 | 0.40 |
| | | inter-pane | 0.26 | 0.19 | 0.21 |
| | | inter-pane ventilated | 0.20 | 0.14 | 0.16 |
| | | external | 0.10 | 0.06 | 0.08 |
| | 45°/0.2 | internal | 0.65 | 0.43 | 0.54 |
| | | inter-pane | 0.45 | 0.26 | 0.32 |
| | | inter-pane ventilated | 0.38 | 0.21 | 0.26 |
| | | external | 0.27 | 0.13 | 0.15 |
| | 45°/0.8 | internal | 0.49 | 0.30 | 0.37 |
| | | inter-pane | 0.42 | 0.22 | 0.28 |
| | | inter-pane ventilated | 0.38 | 0.19 | 0.25 |
| | | external | 0.36 | 0.20 | 0.24 |
| *Ostersund* | 20° / 0.5 | internal | 0.68 | 0.40 | 0.58 |
| | | inter-pane | 0.62 | 0.31 | 0.48 |
| | | inter-pane ventilated | 0.58 | 0.26 | 0.44 |
| | | external | 0.56 | 0.27 | 0.43 |
| | 45° / 0.5 | internal | 0.58 | 0.40 | 0.50 |
| | | inter-pane | 0.43 | 0.25 | 0.34 |
| | | inter-pane ventilated | 0.37 | 0.20 | 0.28 |
| | | external | 0.30 | 0.15 | 0.21 |
| | 70° / 0.5 | internal | 0.47 | 0.37 | 0.42 |
| | | inter-pane | 0.26 | 0.20 | 0.23 |
| | | inter-pane ventilated | 0.20 | 0.15 | 0.16 |
| | | external | 0.10 | 0.07 | 0.08 |
| | 45°/0.2 | internal | 0.65 | 0.46 | 0.57 |
| | | inter-pane | 0.45 | 0.28 | 0.36 |
| | | inter-pane ventilated | 0.38 | 0.22 | 0.29 |
| | | external | 0.27 | 0.13 | 0.18 |
| | 45°/0.8 | internal | 0.49 | 0.32 | 0.41 |
| | | inter-pane | 0.42 | 0.23 | 0.32 |
| | | inter-pane ventilated | 0.38 | 0.19 | 0.28 |
| | | external | 0.36 | 0.20 | 0.27 |

Table 6.1: Summary of graphs presented in paragraphs 6.4-6.7

Further analysis of results from the three locations is published in the proceedings of the International Conference: Transposition of the Energy Performance of Building Directive (Mylona et al, 2006).

## *6.8 Sensitivity of $\hat{g}_d$ value to Ventilation through the Cavity*

The same dynamic set-up described in §6.2 was simulated using hourly weather data by HTB2 in order to study how the choice of material and colour of a blind and the gap size at the top and bottom of the blind effect the ventilation rate through the cavity formed between the glass pane and the blind and how the various ventilation rates in turn effect the $\hat{g}_d$ value.

The choice of internal planar blinds (roller blinds) was based on the fact that no heat transfer would happen due to convection across the blind configuration, as is the case with slat type blinds, while trapped heat in the cavity between the glass and the blind would be transferred in the space through the gaps at the top and bottom of the blind based on gap size. The above set-up would allow a better examination of the effect of gap size and choice of blind colour in the $\hat{g}_d$ value.

Since the planar blinds are less angular dependent than the slat-type blinds and so less affected by the angle of incidence, it was evident that their performance would be mostly dependent on the heat tranfer due to secondary heat transmittance. Based on the above assumption it was decided to examine the $\hat{g}_d$ value of various glazing options for the duration of a clear day (15$^{th}$ of August) for the hours that the sun was shining and for one location using the annual weather data set from London (Energy Plus website). The space air temperature was kept fixed at 25° for all simulations.

The thermal performance of a double glazing system (4mm-12mm-4mm, clear float glass; steady-state G-value of the system with no shading: 0.75; U-value of the double glazing system with no shading: 2.8 $m^2$/W/°C, a typical U-value for a double glazing with 12mm spacing between panes according to CIBSE guidance, 2006) with various types of roller blinds positioned internally (cavity of 30mm between the double glazing and the roller blind; volume of ventilated cavity: 0.168$m^3$, 2mx2.8m window area) (figure 6.19b) was examined. The same blind samples were used during detailed test-cell

measurements during a test programme run by Lund University (Wall & Bülow-Hübe, 2003), and also during the evaluation stage of this work (chapter 5, §5.2.4).

WIS was used instead of the glazing simulation program (modified from GLSIM), in order to provide HTB2 with the transmission and absorption factors for the angles of incidence 0° to 90°, in the description of the glazing systems. This choice was based on the fact that roller blind solar transmission characteristics are not as angle dependent as slat-type blinds and also because the glass simulation program expressed a weakness in calculating transmission characteristics for materials with high diffuse transmittance such as the white roller blind case ($T_{diff}$ = 0.37).

The parameters varied in the simulation of the glazing system were the type of fabric of the roller blind (table 1; Rdiff: Diffuse Reflection, Rspec: Specular Reflection, Tdiff: Diffuse Transmittance and A: Absorption) and the ventilation rate through the cavity between the double glazing and the blind. The ventilation rates examined were 0.012$m^3$/s, 0.025$m^3$/s and 0.054$m^3$/s. These correspond to flow rates, under typical conditions, that would be expected from gaps of 0.01m, 0.02m and 0.04m, respectively, at the top and bottom vents of the roller blind. The ventilation rates in the cavity (due to stack effect) were calculated according to ISO 15099 (2003) standard by the equation 3.2 (chapter 3, §3.4.1), where $T_c$ (the cavity mean temperature in K) of 30°C and $\Delta T$ (the temperature difference between the cavity mean temperature and the entering air) of 10°C were used as approximations for typical conditions (CIBSE, 2006). Also a 0.000 $m^3$/s ventilation rate was examined, which corresponds to a roller blind tightly mounted to the window, not allowing any ventilation through the cavity (figure 6.19a).

For the above simulations, WIS (Dijk & Oversloot, 2003), was used, instead of the glazing simulation program, in order to provide HTB2 with the transmission and absorption factors for the angles of incidence from 0 to 90, in the description of the glazing systems.

| Type of Roller Blind | Rdiff | Rspec | Tdiff | Abs |
|---|---|---|---|---|
| Blue Roller Blind (H 500-54)$^{TM}$ | 0.15 | 0.00 | 0.04 | 0.81 |
| Silver-grey Roller Blind (H981-95)$^{TM}$ | 0.29 | 0.30 | 0.05 | 0.36 |
| White-grey Texienne (H 927-95)$^{TM}$ | 0.78 | 0.00 | 0.05 | 0.17 |

Table 6.2: Summary of comparison test data configurations* (Wall & Bülow-Hübe, 2003)

* Roller blind manufacturer: Haglunds I Falköping AB eng., Sweden

* Reflectance and transmittance values of blinds were also measured with a spectrophotometer at Uppsala University, Uppsala, Sweden

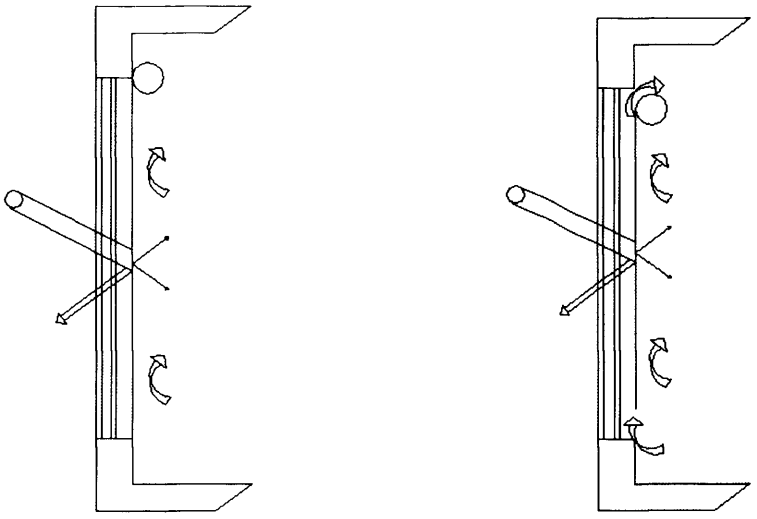

(a) (b)

Figure 6.19: Illustration of the glazing system with roller blind (a) tightly mounted to the window not allowing any ventilation, (b) gaps at the top and the bottom of the roller blind allowing ventilation.

This was achieved by modelling the same "numerical test cell" with dimensions of 3mx6mx3m and with south-facing glazing of 5.6m$^2$ (2.8m x 2m: occupying approximately the 60% of the south-facing wall) also used in the dynamic simulations of the cases with Venetian blinds. The effect of different ventilation rates on the thermal performance of each of the roller blind was calculated, for a clear summer's day (15$^{th}$ of August) from the annual weather data set from London (Energy Plus website). The space air temperature was kept fixed at 25° for all simulations.

Figures 6.20, 6.21 and 6.22 present the calculated $\hat{g}_d$ values for the three different ventilation rates and also a non ventilated cavity option.

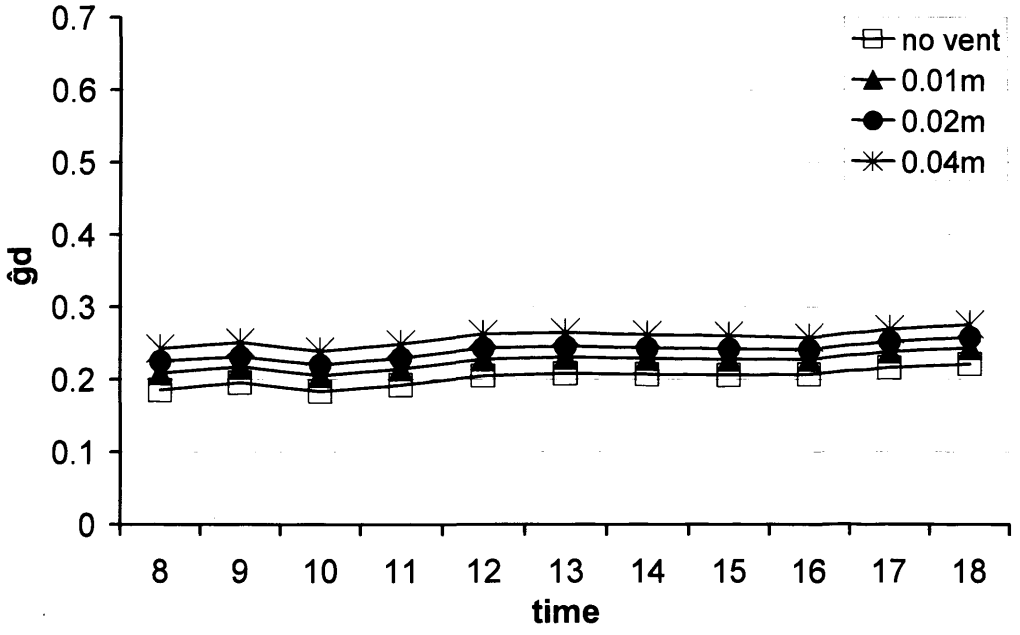


Figure 6.20: Internally positioned white-grey roller blind

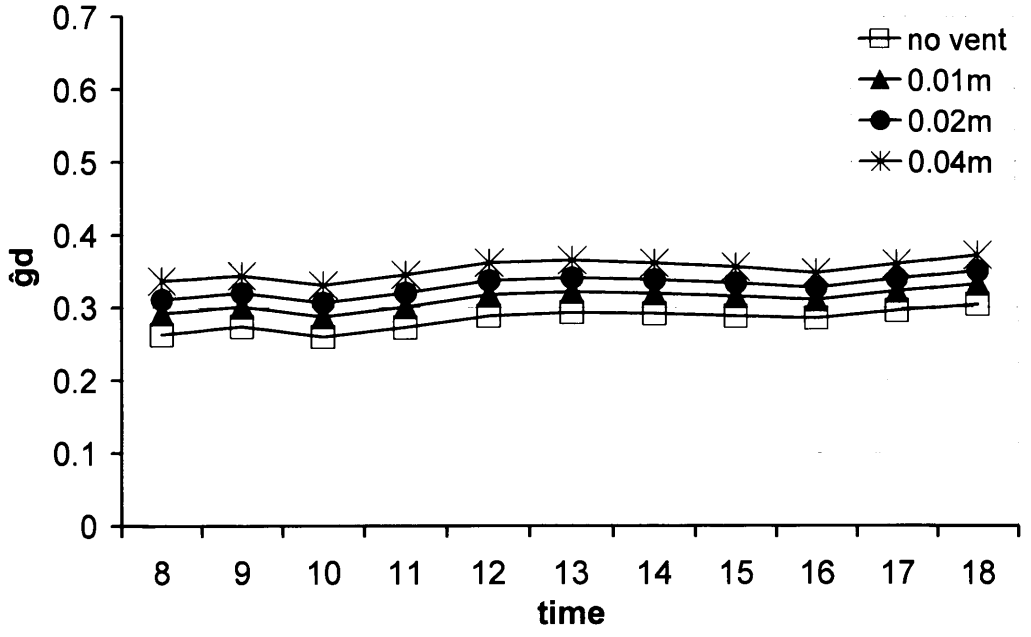


Figure 6.21: Internally positioned silver-grey roller blind

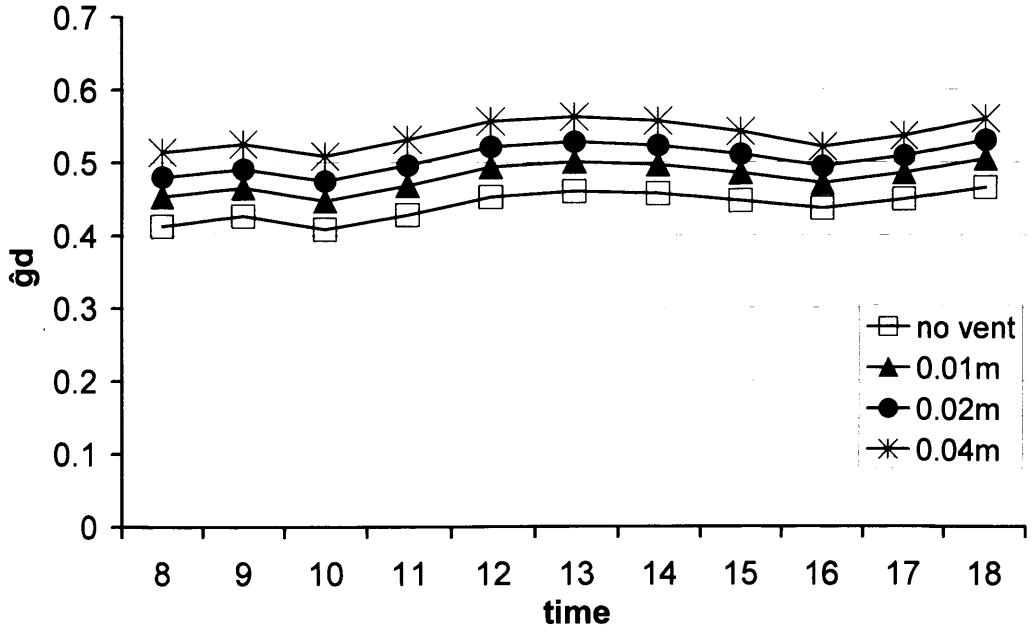


Figure 6.22: Internally positioned blue roller blind

The graphs show that different rates of ventilation can significantly affect the thermal performance of a glazing system depending on the type of the integrated shading device.

As expected, the darker colour materials provide greater thermal gains to the interior. However, the different blinds also reacted differently to the amount of ventilation (or the size of gaps around the blinds) considered.

The light coloured white-grey roller blind (high reflection) is less affected by the change of the ventilation, presenting a maximum difference of 0.05 between the lowest and the highest $\hat{g}_d$ value, varying by the ventilation rate (figure 6.20). The $\hat{g}_d$ of the glazing with the blue roller blind varied by as much as 0.1 (figure 6.22).

Notably, the $\hat{g}_d$ value of the system always increases with an increase in ventilation. Though the surface temperature of the blind material is reduced by increasing ventilation, the reduction of the heat gain from that surface (due to long-wave radiation and convection) is less than the increase of convective heat gain entering the space from the cavity between the window and the blind. Further results are published in the PLEA2005 conference (Mylona et al, 2005). Table 6.3 summarises the results presented in this paragraph.

| **Glazing Systems** | | **G-values** | **Daily average $\hat{g}_d$** |
|---|---|---|---|
| *Type of blind* | *Gap size* | | |
| Blue Roller Blind (H 500-54) | No ventilation | 0.51 | 0.44 |
| | 0.01m | 0.55 | 0.48 |
| | 0.02m | 0.57 | 0.51 |
| | 0.04m | 0.60 | 0.54 |
| Silver-grey Blind (H981-95) | No ventilation | 0.33 | 0.28 |
| | 0.01m | 0.36 | 0.31 |
| | 0.02m | 0.38 | 0.33 |
| | 0.04m | 0.40 | 0.35 |
| White-grey Texienne (H 927-95) | No ventilation | 0.24 | 0.20 |
| | 0.01m | 0.26 | 0.22 |
| | 0.02m | 0.27 | 0.24 |
| | 0.04m | 0.29 | 0.26 |

Table 6.3: Summary of results presented in paragraphs 6.8

## 6.9 Conclusions

The combined model was used to examine the influence of various glazing parameters in the G-value calculated under steady-state conditions and also in the dynamically calculated $\hat{g}_d$ value under a more realistic setting. That was achieved by modelling a simple office space with a south-facing window occupying approximately the 60% of the south-facing wall. Four glazing systems were studied consisted of a double glazing unit with integrated slat-type blinds positioned externally, inter-pane and internally. The inter-pane option has been studied for both sealed cavity and ventilated cavity. Various glazing parameters were examined such as angle of tilt and reflectance value of the blind (Venetian blinds), as well as the impact of ventilation between the glass and blind (roller blinds).

*Steady-state G-value*

The g-value was calculated for both steady-state conditions (G-value) and vertical angle of incidence, and for real climate conditions ($\hat{g}_d$ -value). The results from the calculations under steady-state conditions showed that there is a wide variation in G-value possible, for essentially the same glazing system (i.e. double glazing with a slat-type blind), depending on the colour, the position and the angle of tilt of the blind.
Regarding the colour of the blind material, the lower G-values were achieved by the use of light colour material, with only exception when such blinds were positioned externally and for that position only, low reflectance blinds (dark colour) presented lower G-values than high reflectance blinds (light colour). Furthermore, it was shown that the reflectance of the blind material is affecting the variation of G between the cases of the same blind characteristics, but various positions; the lighter the colour the smaller the G variation and the darker the colour the wider the G variation.

Regarding the slat angle of the blind, lower G-values, for the blinds of the same colour, were achieved with higher slat angles (70°), especially for the near to normal angles of incident. Also, the higher the slat angle the smaller the G variation, while for the cases with low slat angle (20°) G is widely varying. Furthermore, for low slat angles the variation of G between the cases of the same blind characteristics, but various positions, is lower than for high slat angles.

Regarding the position of the blind, the externally positioned blind showed, for a consistent surface reflectance and slat angle, the lowest G-values, but examples also demonstrated that G for externally positioned blinds can be higher than for internally positioned or inter-pane blinds, if surface colour and blade angle are not carefully chosen. Furthermore, it was noticed that ventilation in the cavity of inter-pane blind cases can improve the thermal performance of a glazing system.

Except from the blind characteristics and position of the blind, G showed a high dependence on the angle of incident, with higher values presented at angles of incident close to normal, and lower values at higher angles of incident. Also noticed was that the sensitivity of G's angle dependency is directly related to the slat angle. The higher the slat angle the smaller the G variation, while for the cases with lower slat angles, G is widely varying.

*Dynamically calculated $\hat{g}_d$ value*

The calculations of the g-value of the same glazing systems were repeated under real climate conditions, for the same office specifications, using the same prediction tools, but this time with hourly weather data measured in three European locations; London, Athens and Ostersund. Environmental conditions for the office space were also set, with values for room ventilation, occupancy levels, lighting and small power sources. A daily average $\hat{g}_d$ was calculated from the simulation results using only the daylight hours, for each month.

In accordance with the results from the G calculations, the results of $\hat{g}_d$ showed, that it depends on the blind characteristics and position of the blind, with similar conclusions drawn for the different cases examined. Furthermore, $\hat{g}_d$ also showed that depends on the temperature difference between the external and internal environment, the time of the year and solar angles and the latitude of the location of the building.

The temperature difference between the external and internal environment affects the surface temperature of the glazing system and as a result affects the direction and the rate of heat flow through the glazing system. For the calculation of $\hat{g}_d$ the heat flow fluctuates as opposed to the calculation of G that is steady.

Regarding the seasonal variation, in most cases $\hat{g}_d$ reaches its maximum value during the winter period (low angle of incident) and its minimum value during the summer (high angle of incident). The sensitivity of $\hat{g}_d$ to the seasonal variation is also directly related to the slat angle of the blind. The higher the slat angle the smaller the $\hat{g}_d$ variation, while for the cases with low slat angle, $\hat{g}_d$ is widely varying. The above also comes to accordance with the results from the calculations of G under steady-state conditions.

Regarding the latitude of the location of the building, the seasonal variation of $\hat{g}_d$ is less obvious for south climates and more apparent for north latitudes, which is directly connected to the seasonal variation of the sun's altitude. The connection between seasonal variation and slat angle is less apparent for south latitudes such as Athens and more apparent for north latitudes such as Ostersund.

Furthermore, comparing the equivalent results from the dynamic simulations of the three locations, it was noticed that most cases present similar $\hat{g}_d$ values during the summer months and different $\hat{g}_d$ values during the winter months, and for most cases, the further north the location the higher the winter $\hat{g}_d$ values. The above was more noticeable for low slat angles (20°), while for blind cases with higher slat angle (70°) a similar $\hat{g}_d$ was showed throughout the year in all locations. This seasonal/spatial variation was based on the different solar angles between the locations. The solar angle affects the $\hat{g}_d$ of the various cases, and those affected most are those with low slat angle blinds, rather than the high slat angle blinds.

Generally, from the results under real climate conditions, for three locations of different laltitudes, it was shown that while between the cases of the same blind characteristics (and different blind position), of the same location, the secondary heat was the factor mostly affecting the $\hat{g}_d$ variation, between the same cases (in the same position) of different location the factor mostly affecting the $\hat{g}_d$ variation was the sun altitude; differences mostly noticeable during the winter months, depending on how far from normal is the sun altitude.

*Comparison between G and $\hat{g}_d$*

Comparisons between the G calculated under steady-state conditions and the dynamically calculated $\hat{g}_d$ , for the locations examined, showed that G for normal incident

could be far from the $\hat{g}_d$ values occurring during the summer, since G is calculated for normal incident and so closer to winter solar incident and far from the summer solar incident. This was especially true for the cases with lower slat angles; the $\hat{g}_d$ values during the winter months were much higher than the ones during the summer months. Even in near normal incident, during the winter months, the $\hat{g}_d$ could not reach values as high as the G-values predicted under steady-sate conditions, with some exceptions noticed during some of the winter months in the north location (solar angle very close to normal). The difference between G and $\hat{g}_d$ and the seasonal variation was less obvious for higher slat angles, when the direct transmission was reduced to a minimum.

In comparing glazing options, such as placement of a blind, there was a consistency in the relative rankings between the two calculation methods. The externally positioned blind, in most cases, with some seasonal exceptions, showed the best performance compared to the other cases, while the internal blind case showed the poorest thermal performance. However examples demonstrated that in more detailed comparisons, some rankings alter with cases presenting similar or even better summer, and in some cases yearly, thermal performance, even though their steady-state G suggested otherwise, which could mean compromising on the daylight or result in higher solar gains than originally expected.

*Sensitivity of $\hat{g}_d$ value to ventilation through the cavity*

The $\hat{g}_d$ value of a double glazed window with internally positioned roller blind was also examined using the same prediction tool. The parameters studied for the above system were the choice of material and colour of the roller blind and the gap size at the top and bottom of the roller blind (vents).

The results showed that ventilation rates are sensitive to both colour of the material and size of the vents at the top and bottom of the blind. The darker the colour of the blind and the bigger the size of the gaps the more heat is likely to be transferred, through the cavity, into the room. Following this trend, the $\hat{g}_d$ value of the system is in turn sensitive to the ventilation variations rate formed by the above choices of installation of the shading device to the glazing unit.

Overall, the data presented in this chapter showed that simple choices of shading, usually made after the installation of the glazing panels, could actually prove to be of importance when considering the thermal performance of the system. Location, angle of incidence and seasonal variation are factors that affect the thermal performance of the various glazing systems and should be considered during the early design stage of the building. Thus, the study of different shading options in combination with the location, local climate and environment of the building, is important in order to control the solar gains entering the interior space and avoid overheating in the space.

## *6.10 References*

CIBSE (2001-2002) 'Heating, Ventilation, Air conditioning and Refrigeration', CIBSE Guide, Vol. B, Chartered Institution of Building Services Engineers, London

CIBSE (2006) 'Environmental Design', CIBSE Guide, Vol. A, Chartered Institution of Building Services Engineers, London

Dijk, van D & Oversloot, H (2003) 'WIS, the European Tool to Calculate Thermal and Solar Properties of Windows and Window Components' Proceedings of the 8th International IBPSA Conference, Eindhoven, Netherlands

Energy Plus Website:
http://www.eere.energy.gov/buildings/energyplus/cfm/weather_data.cfm

Flamant, G, Prieus, S, Loncour, X & L'heureux, D (2004) 'Ventilated Double Facades: Real-Scale Testing of Ventilated Double Facades; Energy Performance Assessment', Ministry of Economic Affairs Project, Belgian Building Research Institute (BBRI)

International Standard ISO 15099:2003 (2003) 'Thermal Performance of Windows, Doors and Shading Devices – Detailed Calculations', The International Organization for Standardization

Mylona, A, Alexander, D and Jones, P (2005) 'Modelling the Thermal Effect of a Ventilated Cavity on the Thermal Performance of Advanced Glazing Systems', Proceedings of PLEA2005 Conference, Beirut, Lebanon

Mylona, A, Alexander, D and Jones, P (2005) 'Modelling the Thermal Performance of Advanced Glazing Systems in Office Buildings', Proceedings of the International Conference: Glass in Buildings 2, Bath

Mylona, A, Alexander, D and Jones, P (2006) 'Modelling the Thermal Performance of Advanced Glazing Systems in Three European Locations', Proceedings of the International Conference: Transposition of the Energy Performance of Building Directive, Budapest, Hungary

Part L2A (2006) 'Conservation of Fuel and Power in the New buildings other than Dwellings', Office of the Deputy Prime Minister

Wall, M, and Bülow-Hübe, H (eds) (2003) 'Solar Protection in Buildings. Part 2:2000-2002', Report EBD-R—03/1, Dept. of Construction & Architecture, Lund Institute of Technology, Lund University, Lund, Sweden

# Chapter 7

# Efficiency of the G-value and the $\hat{g}_d$ value as Indicators of Cooling Demand

## *7.1 Overview*

Chapter 7 will examine the efficiency of the steady-state G-value and the dynamically calculated $\hat{g}_d$ value as indicators of the cooling demand in a simple office space. This will be achieved by comparing the G values and $\hat{g}_d$ values of various glazing systems, already calculated in chapter 6, against the average cooling load demand in order to keep desirable space air temperatures in an office space, for a clear day and for the three locations also examined in the previous chapter.

## *7.2 Cooling Loads against Total Solar Transmittance*

HTB2 was used in a dynamic mode (figure 6.2, chapter 6) to model the same simple office described in §6.2 (figure 6.3, chapter 6) in order to calculate the sensible cooling loads for keeping acceptable temperature levels in the office space when coupled with various glazing systems. The same office space was chosen for the calculation of the cooling loads as its size was considered to be sensitive to the choice of glazing system. Potentially a larger room, such as an open plan office, would be less influenced by the glazing configuration and more by the properties of the construction material, the occupancy etc.

For the dynamic calculations of $\hat{g}_d$ in chapter 6 the space air temperature was fixed at 20°C for the winter months and 25°C for the summer months for 24 hours a day. This was done to allow an easier comparison to the steady-state G-value. For the calculation

of the cooling loads the space air temperature was allowed to vary between 18°C (the heating set point) and 25°C (the cooling set point), which is the recommended maximum temperature for office buildings during the summer by CIBSE guidance (CIBSE, 2006). This adjustment was expected to provide a more realistic environment for the calculation of the cooling loads.

The average cooling loads were calculated over a clear summer day during the hours of solar radiation, for the same three locations also examined in chapter 6 ($14^{th}$ - Athens, $15^{th}$ - London and $8^{th}$ - Ostersund).

The same glazing systems (figure 6.4) and glazing parameters (6.2) were examined and results were compared with the results of G-value and $\hat{g}_d$ value calculated in chapter 6, in order to examine the efficiency of the above values as indicators of the cooling demand in a space.

Figures 7.1 a, b & c show the average cooling loads predicted plotted against the G-values of the same glazing options simulated under steady-state conditions (chapter 6, §6.3) (the case codes used in the graphs are described in table 7.1)

| *Case Code* | *Blind position* | *Blind slat angle* | *Blind reflectance* |
|---|---|---|---|
| a | internal | 20° | 0.5 |
| b | inter-pane | 20° | 0.5 |
| c | inter-pane with ventilated cavity | 20° | 0.5 |
| d | external | 20° | 0.5 |
| e | internal | 45° | 0.5 |
| f | inter-pane | 45° | 0.5 |
| g | inter-pane with ventilated cavity | 45° | 0.5 |
| h | external | 45° | 0.5 |
| i | internal | 70° | 0.5 |
| j | inter-pane | 70° | 0.5 |
| k | inter-pane with ventilated cavity | 70° | 0.5 |
| l | external | 70° | 0.5 |

| | | | |
|---|---|---|---|
| m | internal | 45° | 0.2 |
| n | inter-pane | 45° | 0.2 |
| o | inter-pane with ventilated cavity | 45° | 0.2 |
| p | external | 45° | 0.2 |
| q | internal | 45° | 0.8 |
| r | inter-pane | 45° | 0.8 |
| s | inter-pane with ventilated cavity | 45° | 0.8 |
| t | external | 45° | 0.8 |

Table 7.1: Reference codes of the cases examined

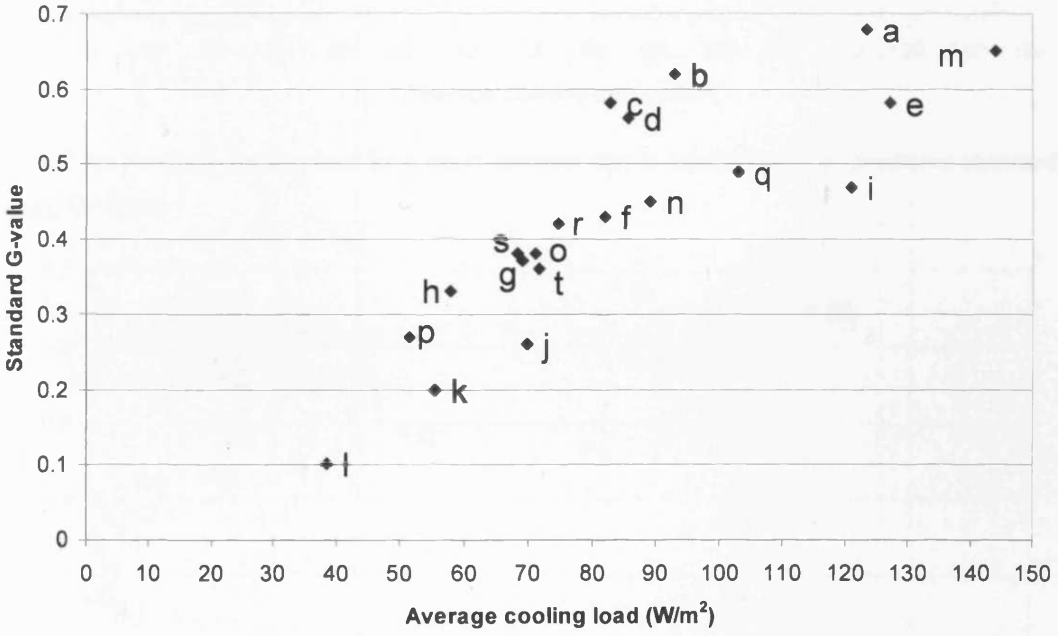


Figure 7.1a: Average cooling load for a clear summer day in Athens against predicted standard glazing G-values

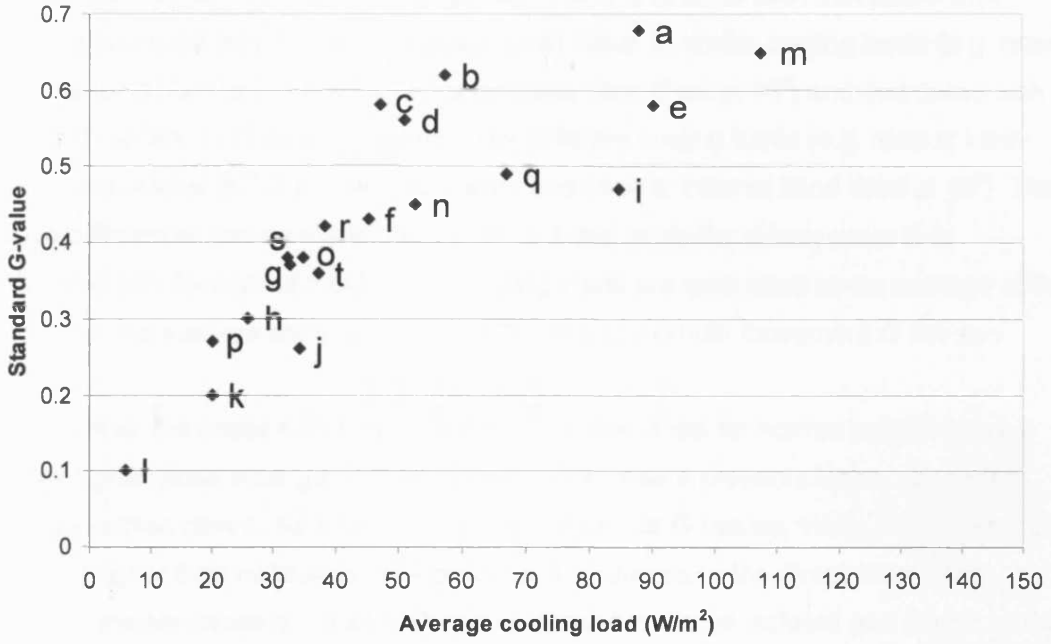


Figure 7.1b: Average cooling load for a clear summer day in London against predicted standard glazing G-values

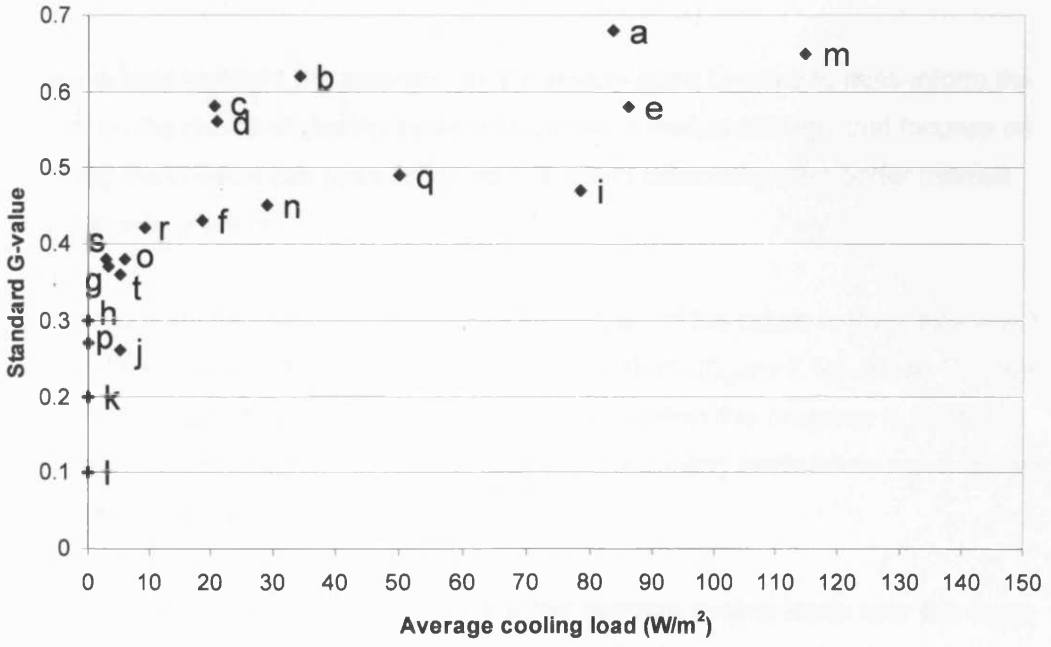


Figure 7.1c: Average cooling load for a clear summer day in Ostersund against predicted standard glazing G-values

The results from all three locations (figures 7.1 a, b & c) show both that cases with different predicted steady-state G-values could result in similar cooling loads (e.g. case d: external blind tilted at 20° and case f: inter-pane blind tilted at 45°) and that cases with similar G-values could result in significantly different cooling loads (e.g. case c: inter-pane blind tilted at 20° in a ventilated cavity and case e: internal blind tilted at 45°). The above differences can be explained by the fact that while the steady-state G is calculated only for normal incident the cooling loads are calculated as an average of the hours that the sun was shining, for both altitude and azimuth movement of the sun.

For example, the cases c and e present similar G because for normal incident case c shows higher direct solar gains than case e, while case e presents higher secondary heat gains than case c. As a result they present similar G-values. When the summer sun altitude (higher than normal) is considered, the difference of the direct solar gains between the two cases is not as high as predicted for normal incident and the secondary heat gain becomes the main contributor to the space temperature rise. That means that the internal case (e) will require higher cooling loads in order to keep desirable temperature levels in the space.

The above data highlight the potential for the steady-state G-value to miss-inform the designer on the choice of glazing system solutions; a design strategy that focuses on minimizing the G-value can miss solutions that could potentially offer better thermal performance in practice.

Also noticed from the graphs is the parallel movement of the cases to the y axis which represents the progress from South (figure 7.1a) to North (figure 7.1c). Since G is the same for each glazing system independently of its location this progress is restricted only to the x axis and represents the decrease of the cooling loads when move towards the northern locations.

Figures 7.2 a, b & c present the same predicted average cooling loads over the same hot day previously examined for each location but this time against the dynamically calculated $\hat{g}_d$ values, for the various cases under consideration (table 7.1).

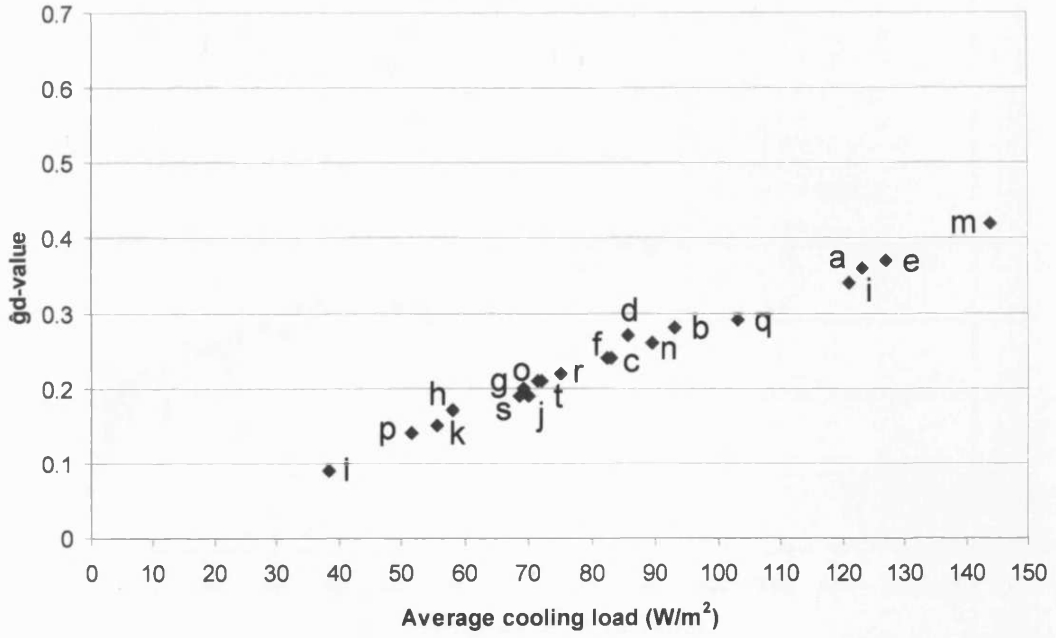


Figure 7.2a: Average cooling load for a clear summer day in Athens against average $\hat{g}_d$ –values calculated for the same day

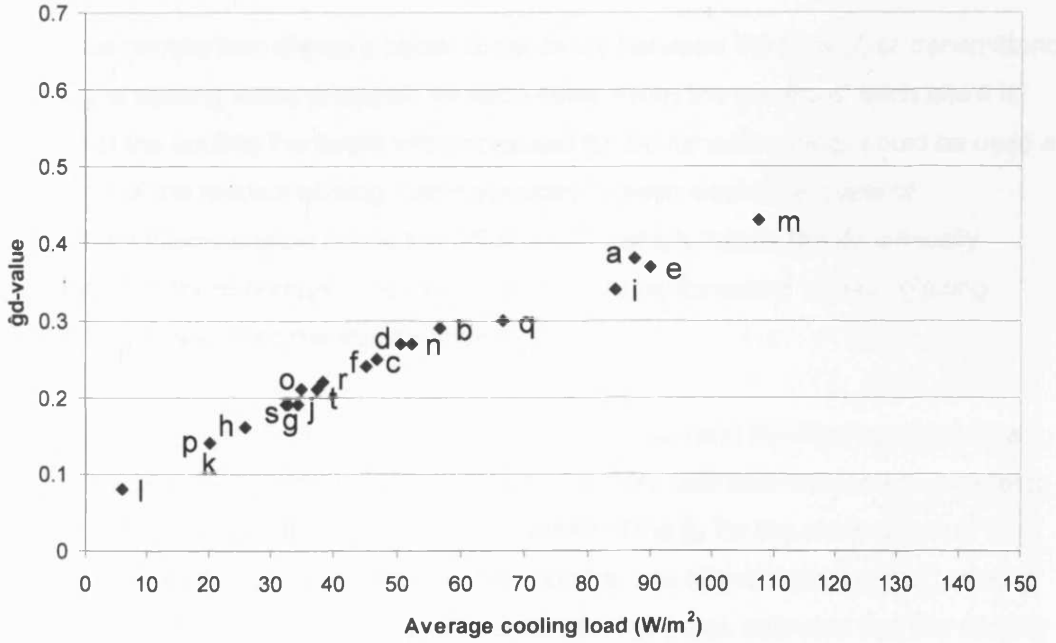


Figure 7.2b: Average cooling load for a clear summer day in London against average $\hat{g}_d$ –values calculated for the same day

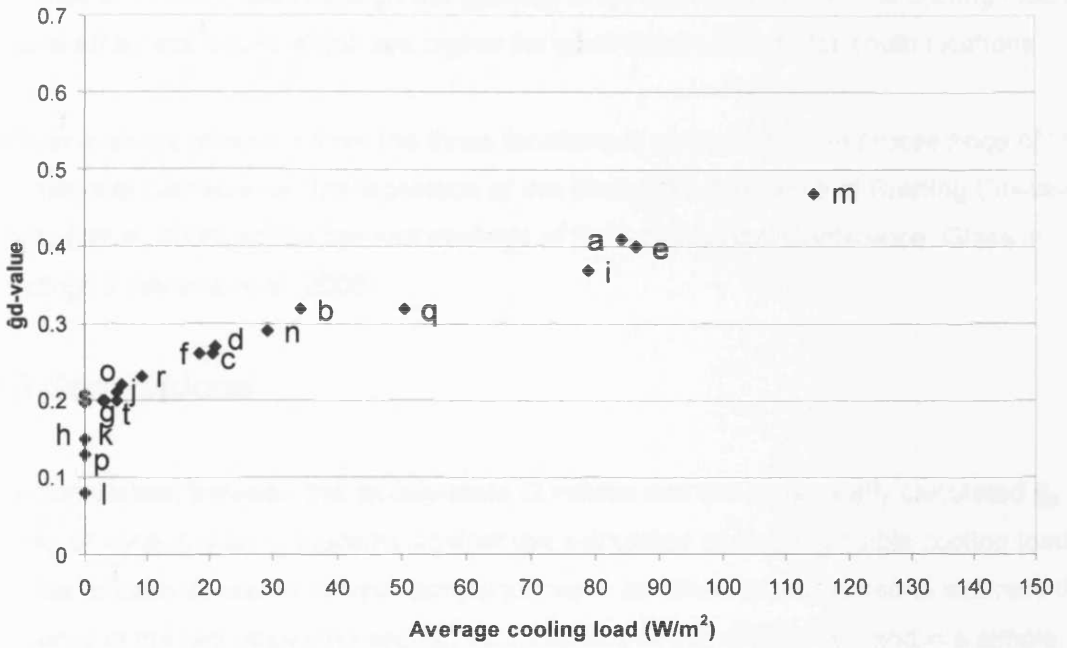


Figure 7.2c: Average cooling load for a clear summer day in Ostersund against average $\hat{g}_d$ – values calculated for the same day

The above comparison shows a better consistency between the total solar transmittance ($\hat{g}_d$) and the cooling loads predicted for each case. From the graphs of each site it is shown that the cooling increases with increased $\hat{g}_d$. So for each site $\hat{g}_d$ could be used as a predictor of the relative cooling load necessary to keep desirable levels of environmental temperature inside the office space, which makes the dynamically calculated $\hat{g}_d$ a more reliable indicator of the thermal performance of each glazing system, in practice, than the steady-state G.

Comparing the results from all three locations there is a trend manifesting which is a small or no movement parallel to the x axis and a more definable movement parallel to the y axis. The first indicates small or no increase of the $\hat{g}_d$ for the same cases in the three different locations during the summer months (see also chapter 6 §6.5), moving towards the north location, while the movement on the y axis indicates that the cooling loads significantly increase while moving towards the south location. The above contradiction of results is due to the nature of the total solar transmittance $\hat{g}_d$ which

excludes any heat losses through the glazing, while the calculation of the cooling loads includes the heat losses which are higher for north locations than for south locations.

Further analysis of results from the three locations is published in the proceedings of the International Conference: Transposition of the Energy Performance of Building Directive (Mylona et al, 2006) and in the proceedings of the International Conference: Glass in Buildings 2 (Mylona et al, 2005).

## *7.3 Conclusions*

The comparison between the steady-state G values and the dynamically calculated $\hat{g}_d$ values of various glazing systems against the calculated average sensible cooling loads in order to keep desirable internal temperatures in an office space, aimed to examine the efficiency of the two values (G and $\hat{g}_d$) as indicators of the cooling demand in a simple office space.

The comparison between the cooling loads and G showed both that cases with different predicted G-values could result in similar cooling loads and that cases with similar G-values could result in significantly different cooling loads, since G is calculated only for normal incident while the cooling loads are calculated as an average of the hours that the sun was shining, for both altitude and azimuth movement of the sun.

Also noticed from the comparison between the G and the cooling loads is the parallel to the y axis movement of the cases, which represent the progress from South to North. Based on the fact that the G is calculated independent of location, this progress is restricted to only the x axis and represents the decrease of the cooling loads when moving towards the north.

The comparison between the cooling loads and the dynamically calculated $\hat{g}_d$ values showed a better consistency between the results. The graphs of each site demonstrated that the cooling increases with increased $\hat{g}_d$, and the opposite.

Also comparing the results from all three locations there was a trend formulated, which was a small or no movement on the y axis and a more definable movement on the x axis. The first indicates small or no increase of the $\hat{g}_d$ of the same cases in the three different locations during the summer months when moving towards the north location, whereas the movement on the x axis indicates that the cooling loads significantly increase when moving towards the south location, due to the nature of the $\hat{g}_d$ which excludes any heat losses through the glazing, as opposed to the calculation of the cooling loads which includes the heat losses that are higher for north locations than for south locations.

Overall, the two comparisons highlighted the potential for the steady-state G-value to miss-inform the designer on the choice of glazing system, while $\hat{g}_d$ could be used as a predictor of the relative cooling load necessary to keep desirable levels of air temperature inside the office space, which makes the dynamically calculated $\hat{g}_d$ a more reliable indicator of the thermal performance of each glazing system, in practice, than the steady-state G-value.

## 7.4 References

CIBSE (2006) 'Environmental Design', CIBSE Guide, Vol. A, Chartered Institution of Building Services Engineers, London

Mylona, A, Alexander, D and Jones, P (2005) 'Modelling the Thermal Performance of Advanced Glazing Systems in Office Buildings', Proceedings of the International Conference: Glass in Buildings 2, Bath

Mylona, A, Alexander, D and Jones, P (2006) 'Modelling the Thermal Performance of Advanced Glazing Systems in Three European Locations', Proceedings of the International Conference: Transposition of the Energy Performance of Building Directive, Budapest, Hungary

# Chapter 8

# Application to a Case Study

## *8.1 Overview*

This chapter will study the influence of various glazing systems on the performance of an energy efficient cooling system in a case study application. Examined will be the way different window arrangements influence the internal temperature and condensation levels when coupled with a fixed capacity cooling system, for three locations.

## *8.2 Effect of Various Glazing Systems on the Performance of a Chilled Ceiling System*

A case study application of an office space with an already installed cooling system of fixed capacity was used here in order to examine the effect the various glazing configurations would have in the internal conditions. HTB2 was used in a dynamic mode (figure 6.2, chapter 6) to model the same simple office described in §6.2 (figure 6.3, chapter 6). The same office space was used here as the case study, as this single/double-occupancy office size was considered to be sensitive to the choice of glazing system. Potentially the temperature and condensation levels in a larger room, such as an open plan office, would be less influenced by the glazing configuration and more by the properties of the construction material, the occupancy, the type of cooling system etc.

In the previous chapter an ideal on/off system was examined in combination with the various glazing systems. In reality, cooling systems could be much more sophisticated than the above system, with various temperature, humidity and time controls to be taken

under consideration in order to provide indoor thermal comfort and air quality to the occupants. Therefore, prediction tools should be able to model such systems as closely to reality as possible in order to give an accurate indication of their performance in conjunction with various glazing options and provide designers with the best possible solution.

Chilled surface systems are currently often used in highly glazed buildings because they provide sensible cooling in order to remove sensible heat gains through the glass surfaces. Although such systems were first used in cold Scandinavian countries, their positive features (chilled surface systems can achieve high levels of comfort by providing uniform room temperatures with minimal noise and air movement), made them popular in the rest of the European countries and soon in the rest of the world with applications to temperate or hot and humid climates.

A downside of their application to temperate or hot and humid countries is the risk of high condensation levels presented on the chilled surfaces (CIBSE, 2001-2002), especially where high infiltration levels are occurring (e.g. due to loose glazing fittings). In the summer the outside air is warm and can therefore be high in moisture content. The incoming air is added to the internal air and moisture content and when it gets in contact with the chilled surface condensation might occur if the surface is cooler than the dew-point temperature of the space air.

The simple office case study modelled in HTB2 with a chilled ceiling installation to provide sensible cooling to the space by means of radiant exchange or a combination of radiation and convection. An imbedded pipe network in the concrete slab is used in order to cool the ceiling surface (figure 8.1). Such a cooling system is thermally heavyweight with the thermal capacity to store cooling but at the same time is slow in responding to load changes. During the simulations the system's maximum power output was set to a fixed 35W/m$^2$, where 25W/m$^2$ are the internal loads and 10W/m$^2$ are the design solar loads (CIBSE, 2006) for the weekdays between 6.30am-6.30pm. Occupancy and computers were kept switched on for weekdays, 8am-6pm, while lighting was kept switched on for a longer period, 6.30am-8pm. All systems were switched off during weekends.

Since the chilled ceiling could provide only sensible cooling, parallel mechanical ventilation system must be used to remove latent loads and to ensure acceptable air quality and humidity levels in the space. An air supply with humidity control system was introduced in the model.

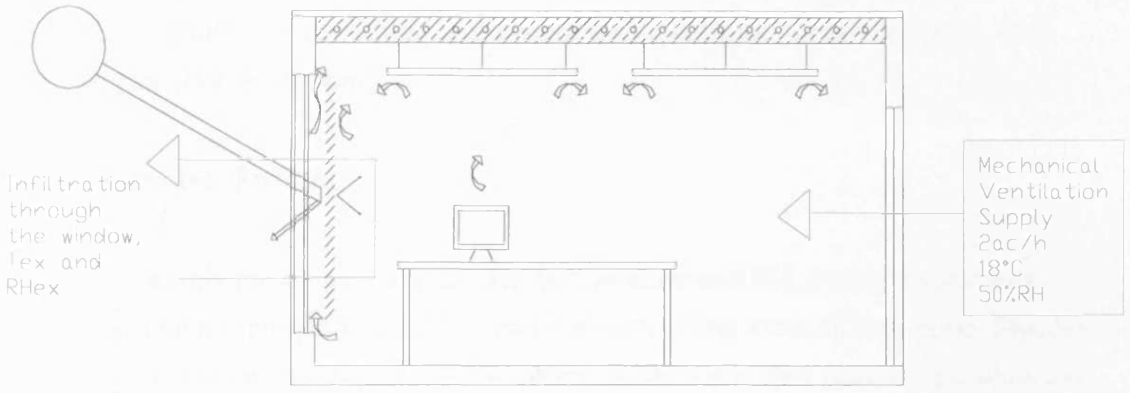


Figure 8.1: Case study application with cooling pipe network in structural concrete slab and ventilation supply

The supply ventilation was kept at 2ac/h at 18°C at 50% RH, for the weekdays only and for the hours between 6.30am and 6.30pm, which is air demand equivalent to 10 l/s/p for two occupants in 18m$^2$ per floor area. According to CIBSE guidance (CIBSE, 2001-2002) 8l/s/p of air is needed for non smoking office, ASHRAE Standard 62 (ASHRAE, 20001) recommends min 9.4 l/s/p, while European Guidelines for air quality (CEN CR 1752,1998) suggest 10l/s/p for low occupant dissatisfaction in a non smoking office. Since this research is concentrating in various European locations the latest CEN recommendation, on demand for natural ventilation in an office, was adopted. Outside the above mentioned hour limits and during weekends ventilation was occurred only by infiltration. Various infiltration levels were examined ranging from a relatively tight glazing fitting to a relatively loose glazing fitting. Infiltration rates examined were 0.1, 0.2, 0.5 and 1.0 ac/h.

The same glazing systems (figure 6.4) and glazing parameters (as described in §6.2, Chapter 6) were examined with the above described cooling system but this time a low U-value of 1.4 was chosen for the double glazing unit in order to represent the attempt to control heat losses through the window with the use of an advanced rather than a typical double glazing unit (U-value of 2.8).

Environmental and ceiling surface temperatures and dew point levels in the office space were examined over a hot summer week for the three locations (Ostersund, London and Athens). Internal environmental temperature was calculated as 1/3 radiant temperature and 2/3 air temperature, according to CIBSE guidance (CIBSE, 1999), and maximum acceptable temperature, before occupant dissatisfaction occurred, was considered to be 25°C (CIBSE, 1999). Condensation levels were also calculated, where occurred, over the whole year (hours per year).

### 8.2.1 Ostersund, Sweden

Figure 8.2 presents the external conditions, temperature and RH, during a summer's week chosen for the presentation of the thermal state of the room in Ostersund, Sweden. Figures 8.3 (a-d) show the environmental, ceiling surface and dew point temperatures in the office space with a blind of 45° slat angle and 0.5 reflectance positioned externally, inter-pane and internally, tested for 0.1ac/h infiltration rate. The first and last days presented are weekend days when all systems are switched off.

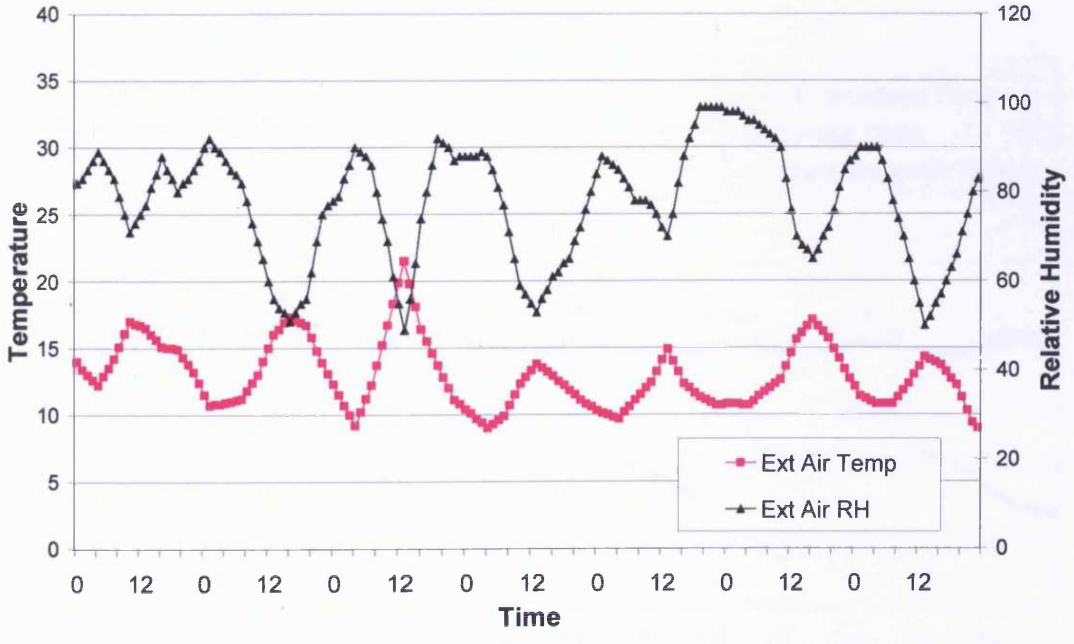


Figure 8.2: External conditions, temperature and relative humidity for the week examined in Ostersund, Sweden

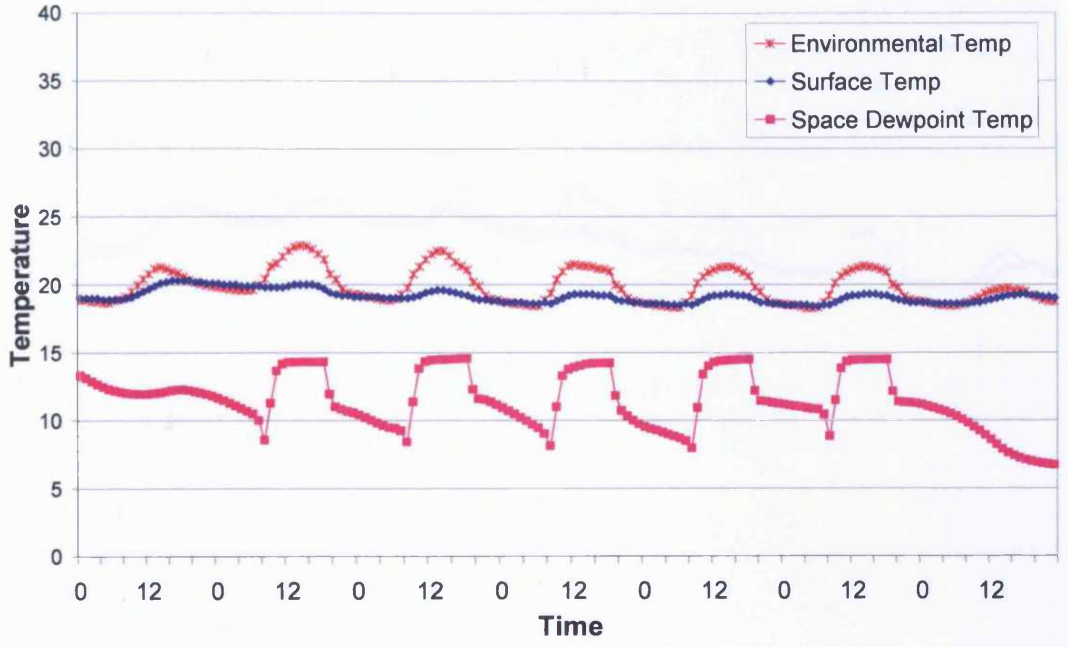


Figure 8.3a: Blind of 45° slat angle and 0.5 reflectance positioned externally (Ostersund – Sweden)

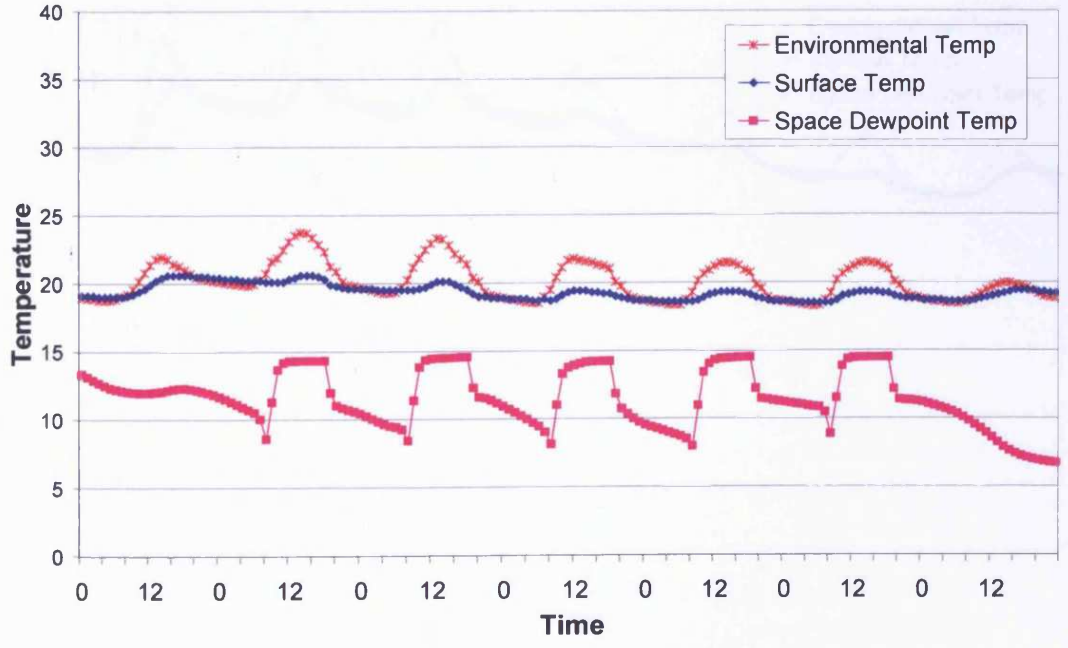


Figure 8.3b: Blind of 45° slat angle and 0.5 reflectance positioned in a ventilated cavity (Ostersund – Sweden)

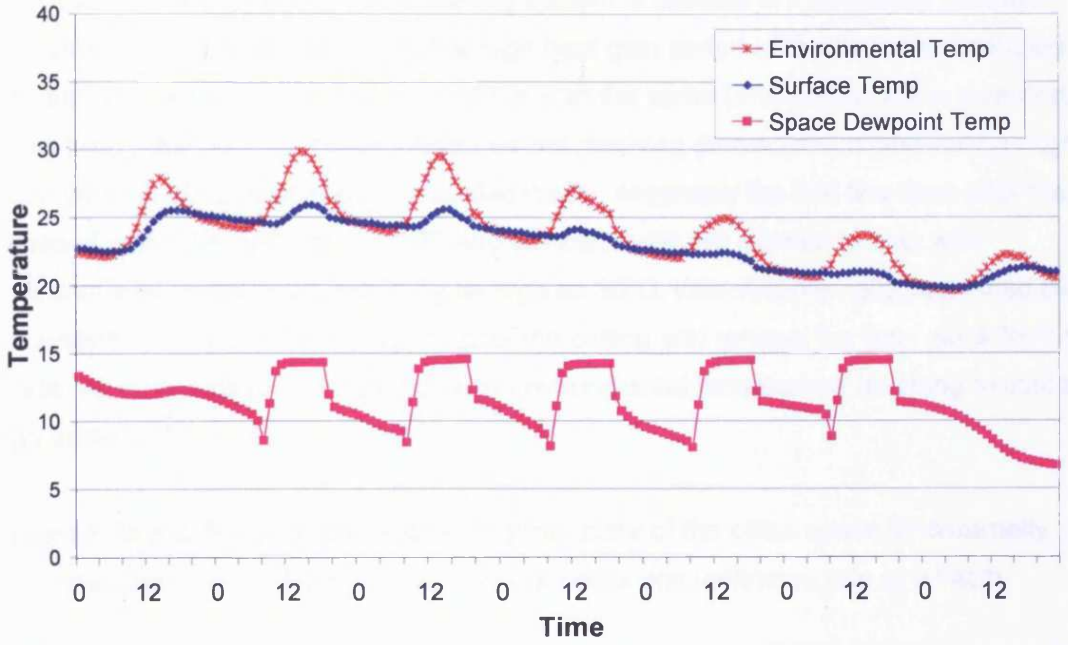


Figure 8.3c: Blind of 45° slat angle and 0.5 reflectance positioned in a sealed cavity (Ostersund – Sweden)

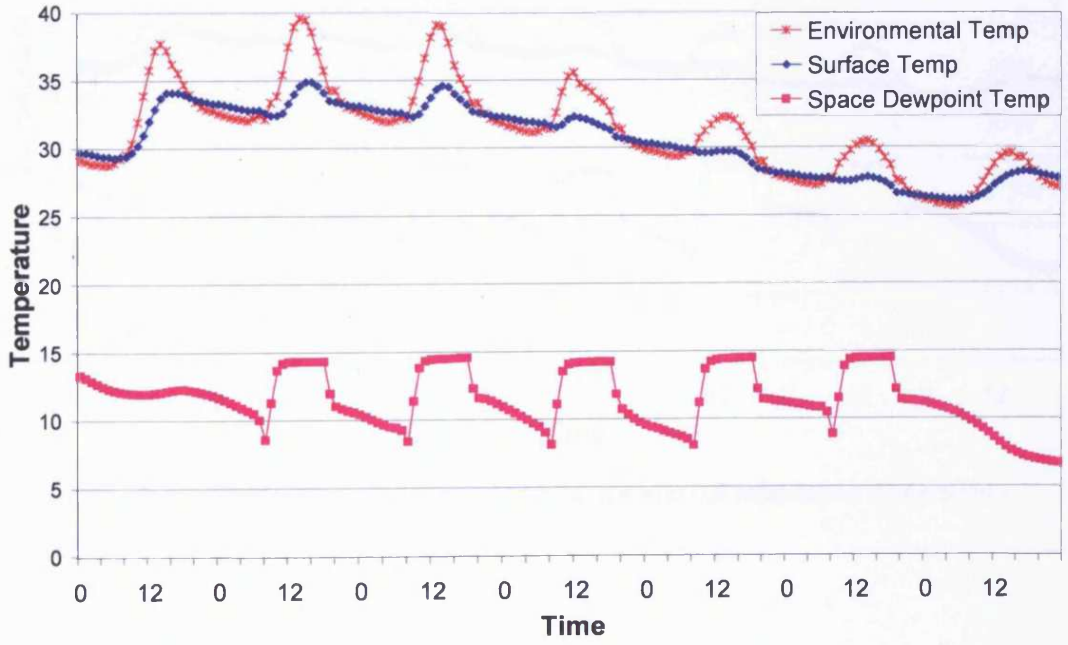


Figure 8.3d: Blind of 45° slat angle and 0.5 reflectance positioned internally (Ostersund – Sweden)

The results showed that the chilled ceiling system is capable of maintaining desired environmental temperature, during the high heat gain period of the day, when coupled with an externally positioned blind of 45° or with the same blind positioned in a ventilated cavity, with maximum space temperatures not reaching above 24°C. Overheating might occur with the blind positioned in a sealed cavity, especially the first few days after the weekend when the systems are "off" and temperatures are allowed to rise, with environmental temperature reaching as high as 30°C. With the internally positioned blind the system is not powerful enough to cool the ceiling and remove the heat gains from the space, which results in overheating, with environmental temperature reaching almost as high as 40°C.

Graphs 8.3a and 8.4 (a-d) present the thermal state of the office space for externally positioned blinds with different blind characteristics and infiltration rate of 0.1ac/h.

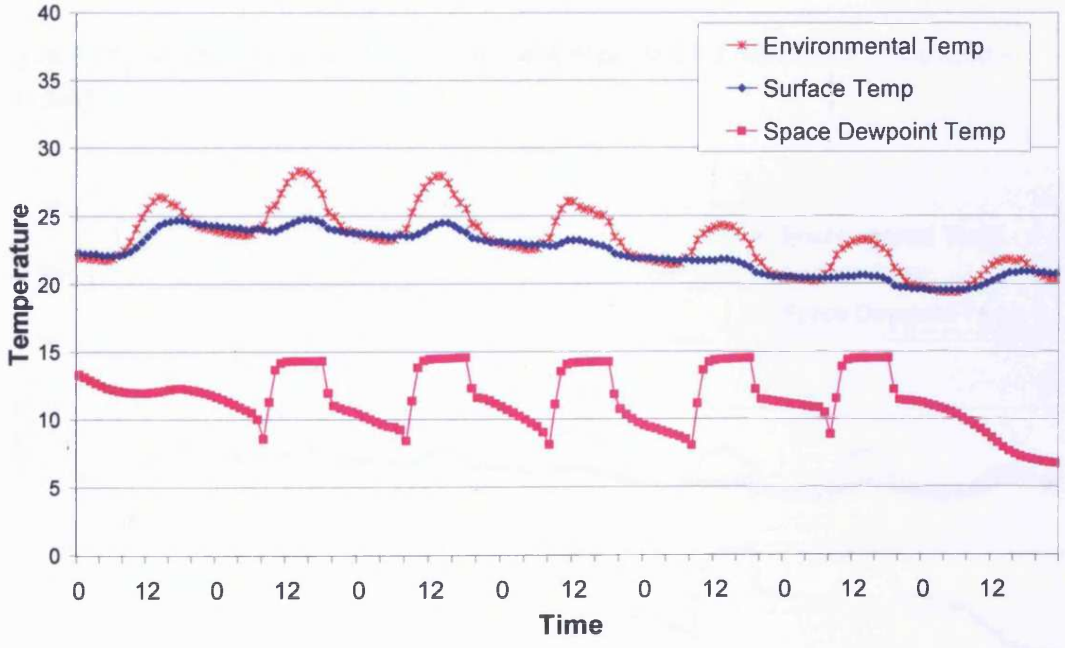


Figure 8.4a: Externally positioned blind of 20° slat angle and 0.5 reflectance (Ostersund – Sweden)

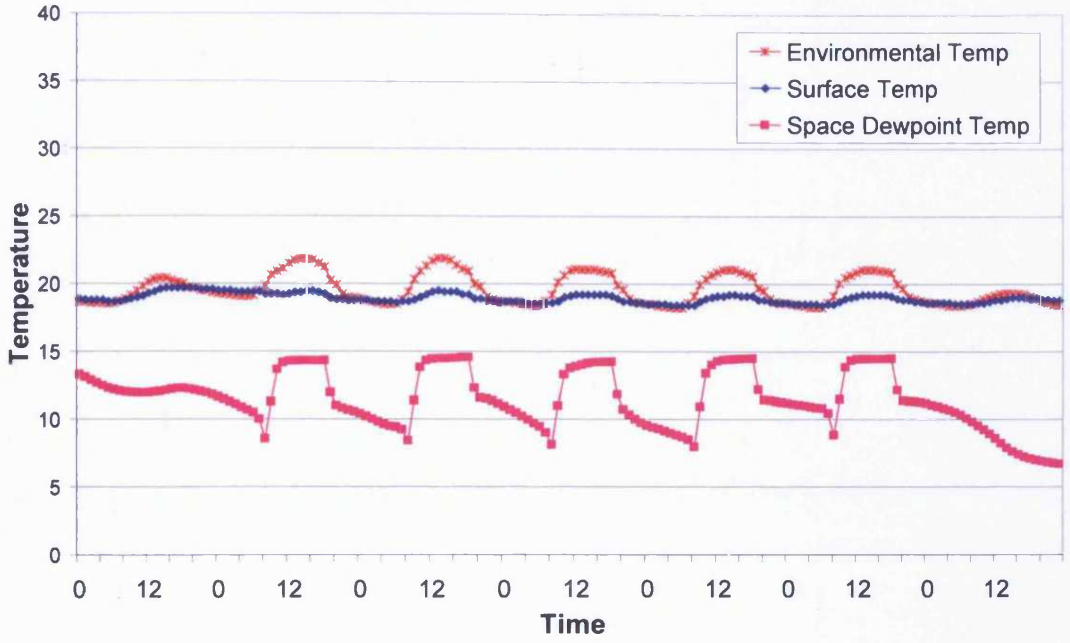


Figure 8.4b: Externally positioned blind of 45° slat angle and 0.2 reflectance (Ostersund – Sweden)

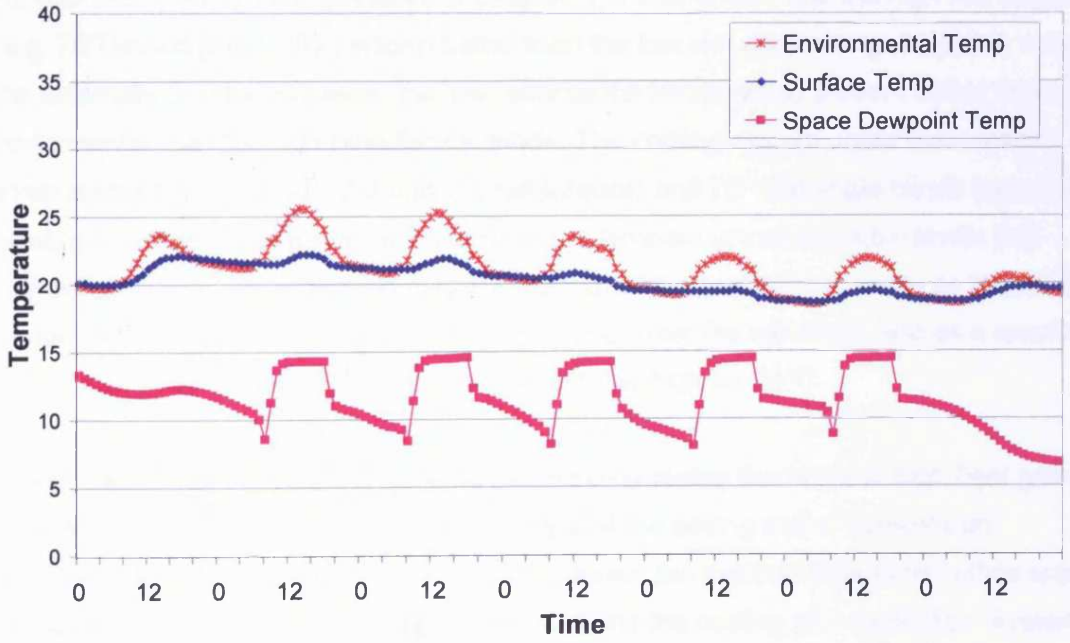


Figure 8.4c: Externally positioned blind of 45° slat angle and 0.8 reflectance (Ostersund – Sweden)

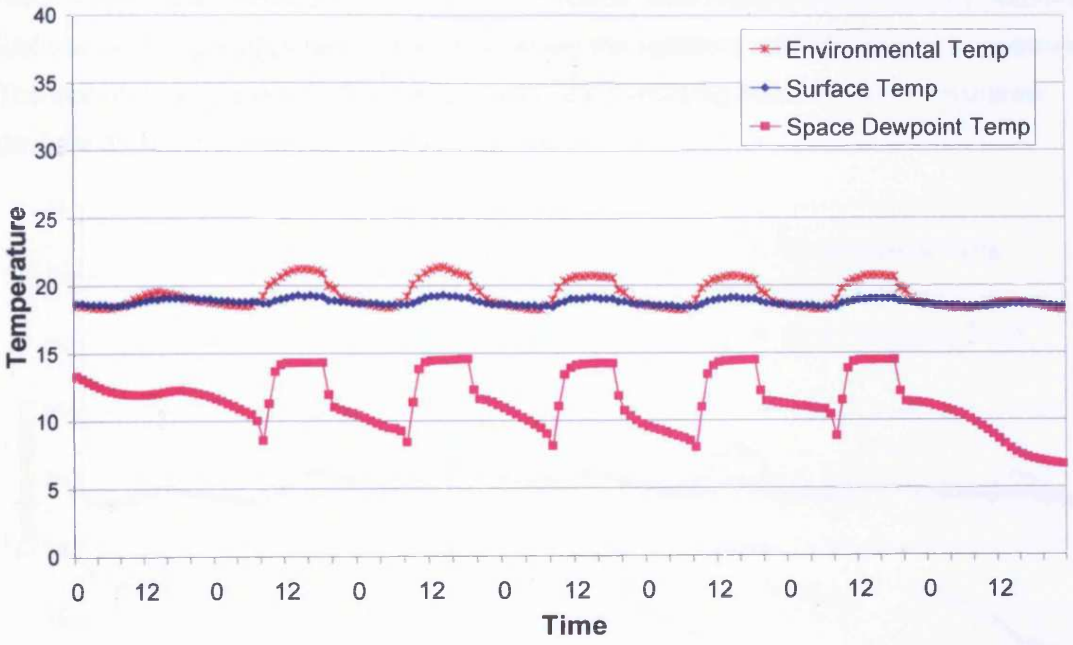


Figure 8.4d: Externally positioned blind of 70° slat angle and 0.5 reflectance (Ostersund – Sweden)

As also predicted by their $\hat{g}_d$ values in chapter 6, it was shown that the high slat angles (e.g. 70°) would potentially perform better than the low slat angles (e.g. 20°) and, only for the externally positioned cases, the low reflectance blinds would present better thermal performance than the high reflectance blinds. The cooling system under examination when coupled with the 45° (0.2 and 0.5 reflectance) and 70° slat angle blinds seems to be able to remove heat gains and keep internal temperature at desirable levels (no higher than 23°C), while overheating could occur with a low 20° slat angle as the cooling system is not able to cool down the ceiling in time, after the weekend, and as a result the space, with environmental temperature reaching as high as 28°C.

Cases that are on the verge of causing overheating during the hours of high heat gains could potentially benefit from the thermal mass of the ceiling and a "systems on" arrangement during the weekend. Figure 8.5 shows the thermal state of the office space with externally positioned 20°C slat angle blind and the cooling and ventilation "systems on" during weekends as well as weekdays. Comparing the above with the results from when the systems are "off" during the weekend (figure 8.4a) it is shown that due to the thermal mass of the ceiling the surface temperature is kept low (max 21°C), and as a

result the environmental temperature of the space, with highest temperatures reaching just below 25°C as opposed to the 28°C when the systems are "off" during the weekend. The above arrangement in this case would help in making the most of the available daylight during the hours of high solar gains.

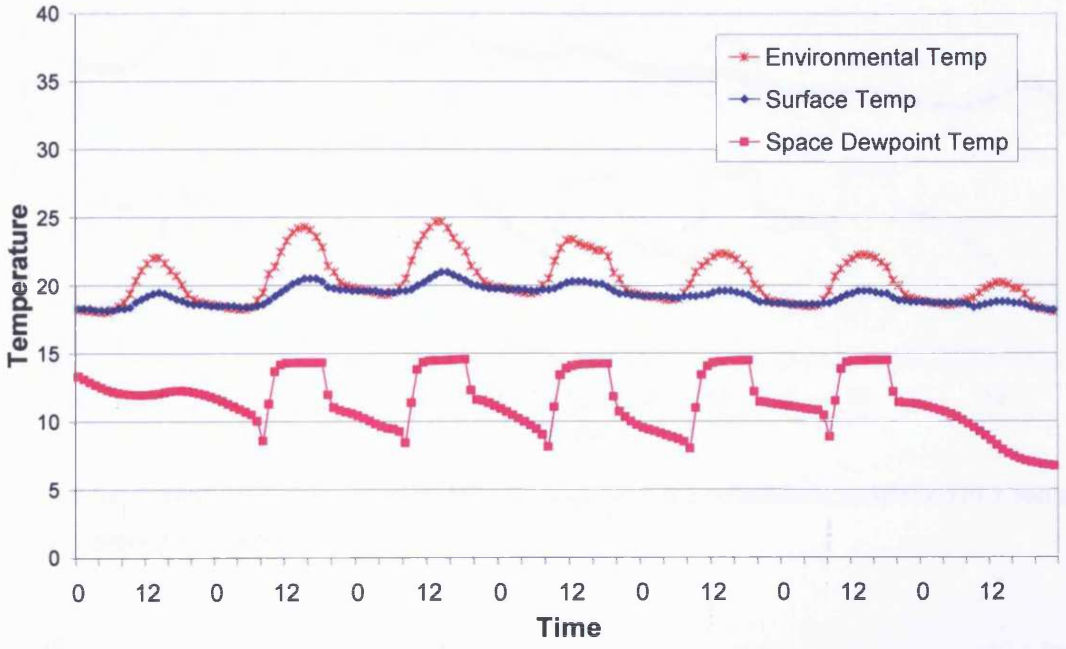


Figure 8.5: Externally positioned blind of 20° slat angle and 0.5 reflectance; cooling and ventilation systems "on" during weekends (Ostersund – Sweden)

There was no condensation noticed in the Ostersund location as shown in the summary table 8.1, even with high infiltration rates. The surface temperature was always above the dew point of the space air temperature and so no condensation occurred on the ceiling surface.

Figures 8.3c and 8.6 (a-c) present different infiltration rates for the blind of 45° slat angle and 0.5 reflectance positioned in a sealed cavity.

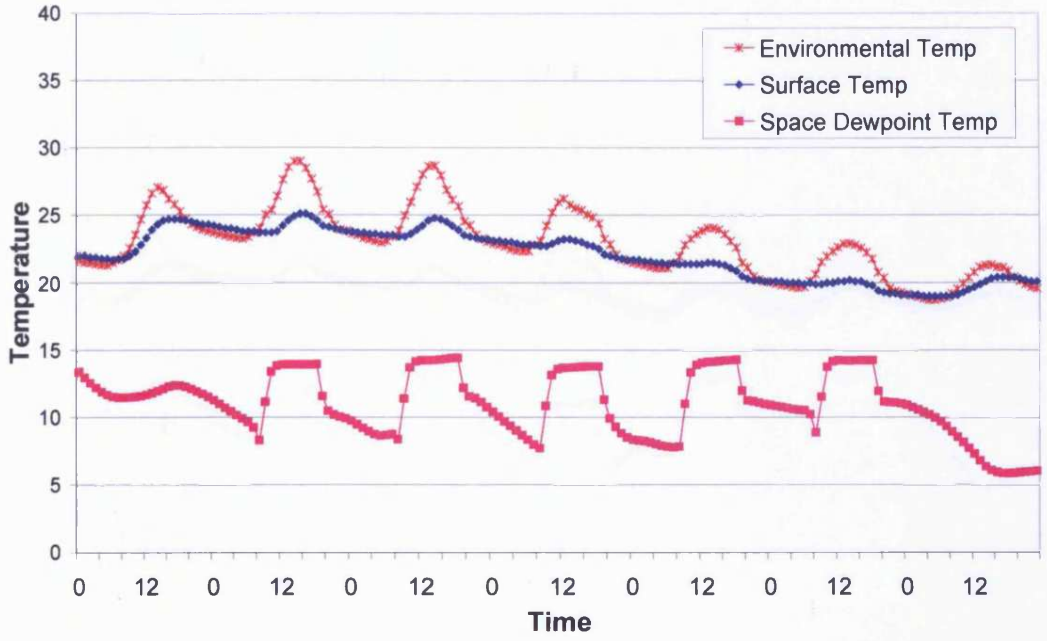


Figure 8.6a: 0.2ac/h infiltration, blind of 45° slat angle and 0.5 reflectance positioned in a sealed cavity (Ostersund – Sweden)

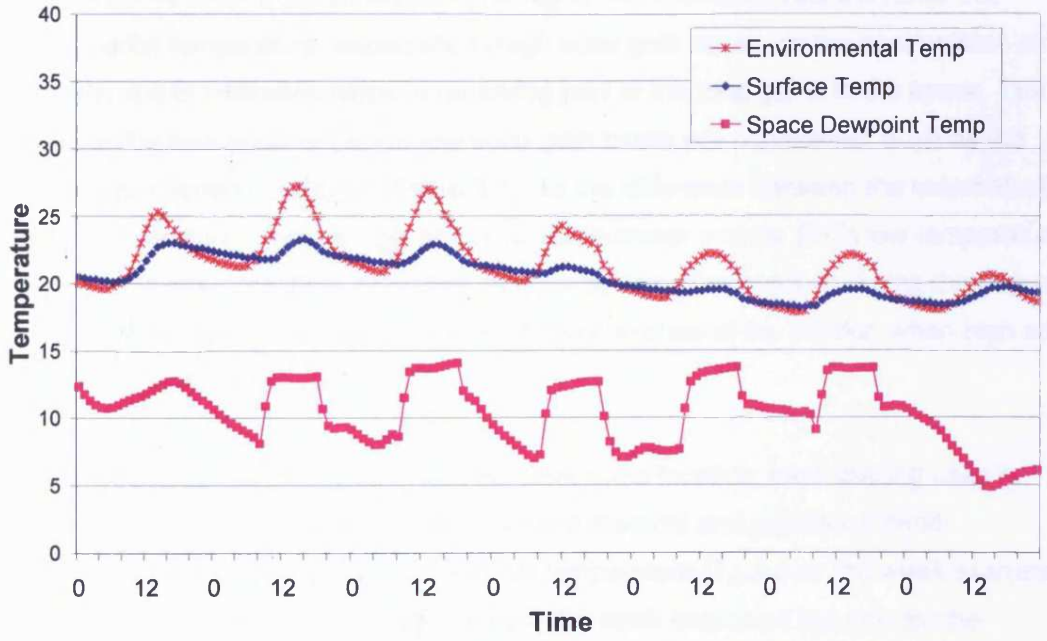


Figure 8.6b: 0.5ac/h infiltration, blind of 45° slat angle and 0.5 reflectance positioned in a sealed cavity (Ostersund – Sweden)

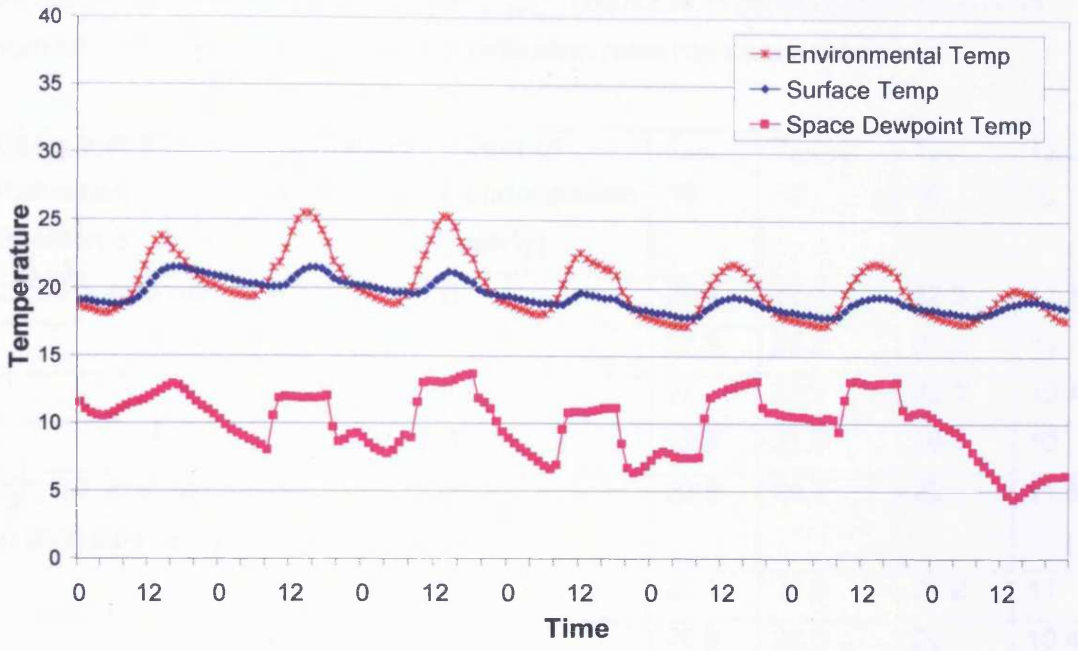


Figure 8.6c: 1.0ac/h infiltration, blind of 45° slat angle and 0.5 reflectance positioned in a sealed cavity (Ostersund – Sweden)

From the above results it is shown that the higher the infiltration rate the lower the environmental temperature, especially in high solar gain cases, as the cool outside air brought in due to infiltration helps in removing part of the heat gains in the space. The above trend is less apparent when low solar gain cases are considered, such as the externally positioned blind case (Table 8.1), as the difference between the external and internal temperature is not as high and less heat transfer occurs. So in low temperature climate conditions intentional infiltration (e.g. by opening the window) during the pick of the solar gains could potentially improve the thermal state of the interior, when high solar gain glazing systems are used.

Table 8.1 summarises the results from the Ostersund location; each glazing case is described by the angle of slat, reflection of blind material and position of blind. Summarised are the average environmental temperature ($T_{env}$) over the week examined, the average environmental temperature over the week examined but only for the weekdays and occupancy hours (8am-6pm) ($T_{env\ 8\text{-}6}$), the average chilled ceiling temperature over the week examined ($T_{surf}$) and the average space dew point

temperature over the week examined ($T_{dew}$). The hours of condensation have been summarised over a year and various infiltration rates have been examined.

| **Case: Slat angle/ Reflection/ Position of blind** | **Infiltration Ac/h** | **Hours of Condensation (yearly)** | **$T_{env}$ °C** | **$T_{env\ 8\text{-}6}$ °C** | **$T_{surf}$ °C** | **$T_{dew}$ °C** |
|---|---|---|---|---|---|---|
| 20°, 0.5, external | 0.1 | 0 | 23.2 | 25.1 | 22.3 | 11.5 |
| | 0.2 | 0 | 22.3 | 24.2 | 21.5 | 11 |
| | 0.5 | 0 | 21 | 22.7 | 20.1 | 10.4 |
| | 1.0 | 0 | 19.8 | 21.7 | 19.1 | 10 |
| 20°, 0.5, inter-pane in ventilated cavity | 0.1 | 0 | 22.8 | 24.7 | 22 | 11.5 |
| | 0.2 | 0 | 22.1 | 23.9 | 21.2 | 11 |
| | 0.5 | 0 | 20.8 | 22.6 | 20 | 10.4 |
| | 1.0 | 0 | 19.8 | 21.6 | 19.1 | 10 |
| 20°, 0.5, inter-pane in sealed cavity | 0.1 | 0 | 26.8 | 28.8 | 25.9 | 11.5 |
| | 0.2 | 0 | 25.6 | 27.7 | 24.8 | 11 |
| | 0.5 | 0 | 23.2 | 25.4 | 22.4 | 10.4 |
| | 1.0 | 0 | 21.2 | 23.3 | 20.4 | 10 |
| 20°, 0.5, internal | 0.1 | 0 | 31.4 | 33.6 | 30.6 | 11.5 |
| | 0.2 | 0 | 29.8 | 32 | 29 | 11 |
| | 0.5 | 0 | 26.4 | 28.7 | 25.6 | 10.4 |
| | 1.0 | 0 | 23.1 | 25.5 | 22.3 | 10 |
| 45°, 0.5, external | 0.1 | 0 | 19.9 | 21.3 | 19.1 | 11.5 |
| | 0.2 | 0 | 19.7 | 21.1 | 19 | 11 |
| | 0.5 | 0 | 19.4 | 20.9 | 18.8 | 10.4 |
| | 1.0 | 0 | 18.9 | 20.5 | 18.5 | 10 |
| 45°, 0.5, inter-pane in ventilated cavity | 0.1 | 0 | 20.1 | 21.5 | 19.3 | 11.5 |
| | 0.2 | 0 | 19.9 | 21.4 | 19.2 | 11 |
| | 0.5 | 0 | 19.5 | 21 | 18.9 | 10.4 |
| | 1.0 | 0 | 19 | 20.6 | 18.6 | 10 |

| | | | | | | |
|---|---|---|---|---|---|---|
| 45°, 0.5, inter-pane in sealed cavity | 0.1 | 0 | 23.8 | 25.7 | 22.9 | 11.5 |
| | 0.2 | 0 | 22.9 | 24.9 | 22.1 | 11 |
| | 0.5 | 0 | 21.3 | 23.2 | 20.5 | 10.4 |
| | 1.0 | 0 | 20 | 22 | 19.4 | 10 |
| 45°, 0.5, internal | 0.1 | 0 | 31.3 | 33.4 | 30.5 | 11.5 |
| | 0.2 | 0 | 29.7 | 31.9 | 28.9 | 11 |
| | 0.5 | 0 | 26.2 | 28.6 | 25.5 | 10.4 |
| | 1.0 | 0 | 23 | 25.3 | 22.2 | 10 |
| 45°, 0.2, external | 0.1 | 0 | 19.6 | 20.9 | 18.9 | 11.5 |
| | 0.2 | 0 | 19.5 | 20.8 | 18.9 | 11 |
| | 0.5 | 0 | 19.1 | 20.6 | 18.7 | 10.4 |
| | 1.0 | 0 | 18.7 | 20.2 | 18.4 | 10 |
| 45°, 0.2, inter-pane in ventilated cavity | 0.1 | 0 | 19.9 | 21.3 | 19.2 | 11.5 |
| | 0.2 | 0 | 19.8 | 21.2 | 19.1 | 11 |
| | 0.5 | 0 | 19.4 | 20.9 | 18.8 | 10.4 |
| | 1.0 | 0 | 18.9 | 20.5 | 18.5 | 10 |
| 45°, 0.2, inter-pane in sealed cavity | 0.1 | 0 | 25.3 | 27.3 | 24.5 | 11.5 |
| | 0.2 | 0 | 24.3 | 26.3 | 23.5 | 11 |
| | 0.5 | 0 | 22.2 | 24.2 | 21.4 | 10.4 |
| | 1.0 | 0 | 20.5 | 22.6 | 19.9 | 10 |
| 45°, 0.2, internal | 0.1 | 0 | 34.5 | 36.8 | 33.8 | 11.5 |
| | 0.2 | 0 | 32.6 | 34.9 | 31.9 | 11 |
| | 0.5 | 0 | 28.5 | 31 | 27.8 | 10.4 |
| | 1.0 | 0 | 24.6 | 27.2 | 23.9 | 10 |
| 45°, 0.8, external | 0.1 | 0 | 21.1 | 22.7 | 20.2 | 11.5 |
| | 0.2 | 0 | 20.7 | 22.3 | 19.8 | 11 |
| | 0.5 | 0 | 20 | 21.6 | 19.2 | 10.4 |
| | 1.0 | 0 | 19.3 | 21.1 | 18.8 | 10 |
| 45°, 0.8, inter-pane in ventilated cavity | 0.1 | 0 | 20.5 | 22.1 | 19.7 | 11.5 |

| | | | | | | |
|---|---|---|---|---|---|---|
| | 0.2 | 0 | 20.3 | 21.9 | 19.5 | 11 |
| | 0.5 | 0 | 19.8 | 21.4 | 19.1 | 10.4 |
| | 1.0 | 0 | 19.2 | 20.9 | 18.7 | 10 |
| 45°, 0.8, inter-pane in sealed cavity | 0.1 | 0 | 22.5 | 24.3 | 21.6 | 11.5 |
| | 0.2 | 0 | 21.8 | 23.7 | 21 | 11 |
| | 0.5 | 0 | 20.6 | 22.4 | 19.8 | 10.4 |
| | 1.0 | 0 | 19.7 | 21.6 | 19.1 | 10 |
| 45°, 0.8, internal | 0.1 | 0 | 27.1 | 29.1 | 26.2 | 11.5 |
| | 0.2 | 0 | 25.9 | 27.9 | 25 | 11 |
| | 0.5 | 0 | 23.3 | 25.4 | 22.5 | 10.4 |
| | 1.0 | 0 | 21.1 | 23.2 | 20.4 | 10 |
| 70°, 0.5, external | 0.1 | 0 | 19.3 | 20.5 | 18.8 | 11.5 |
| | 0.2 | 0 | 19.2 | 20.4 | 18.7 | 11 |
| | 0.5 | 0 | 18.8 | 20.2 | 18.5 | 10.4 |
| | 1.0 | 0 | 18.4 | 19.8 | 18.2 | 10 |
| 70°, 0.5, inter-pane in ventilated cavity | 0.1 | 0 | 19.5 | 20.8 | 18.9 | 11.5 |
| | 0.2 | 0 | 19.4 | 20.7 | 18.8 | 11 |
| | 0.5 | 0 | 19 | 20.4 | 18.6 | 10.4 |
| | 1.0 | 0 | 18.5 | 20.1 | 18.3 | 10 |
| 70°, 0.5, inter-pane in sealed cavity | 0.1 | 0 | 21.4 | 23.1 | 20.6 | 11.5 |
| | 0.2 | 0 | 21 | 22.6 | 20.1 | 11 |
| | 0.5 | 0 | 20.1 | 21.8 | 19.4 | 10.4 |
| | 1.0 | 0 | 19.4 | 21.2 | 18.9 | 10 |
| 70°, 0.5, internal | 0.1 | 0 | 29.8 | 31.9 | 29 | 11.5 |
| | 0.2 | 0 | 28.3 | 30.4 | 27.5 | 11 |
| | 0.5 | 0 | 25.1 | 27.4 | 24.4 | 10.4 |
| | 1.0 | 0 | 22.2 | 24.5 | 21.5 | 10 |

Table 8.1: Summary of results for Ostersund

### 8.2.2 London, UK

Figure 8.7 presents the external conditions, temperature and RH, during a summer's week chosen for the presentation of the thermal state of the room in London, UK. Figure 8.8 (a-d) presents the environmental, ceiling surface and air dew point temperatures for the same office space, but this time for London, with a blind of 45° slat angle and 0.5 reflectance positioned externally, inter-pane and internally, tested for 0.1ac/h infiltration rate. A hot summer's week was chosen to demonstrate the thermal state of the room. The first and last days presented are weekend days when all systems are "off".

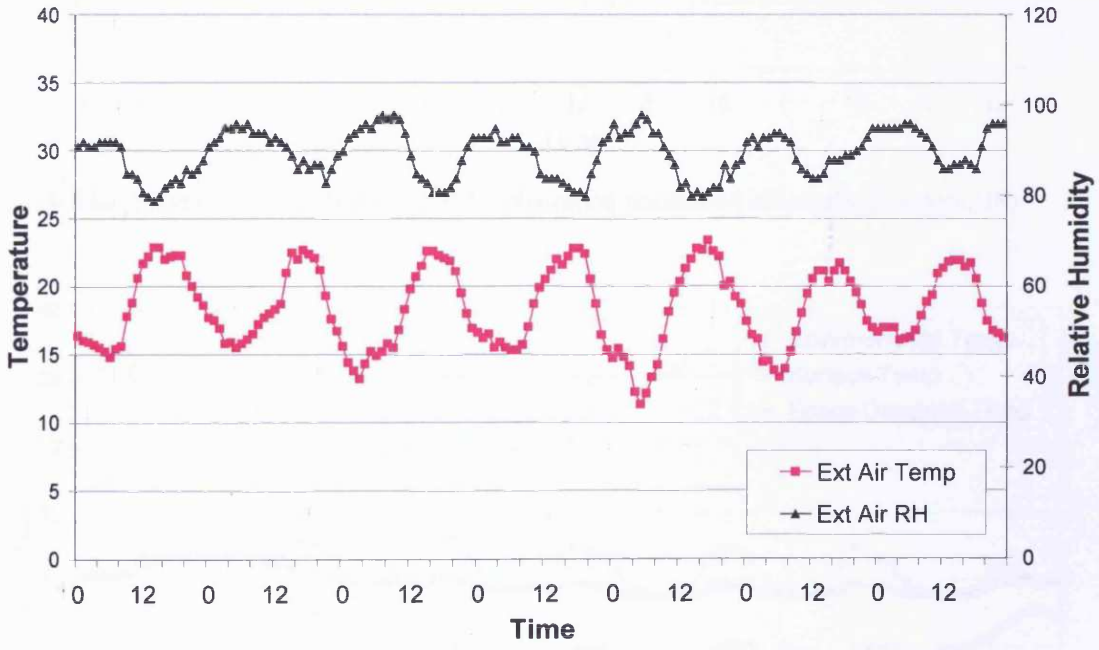


Figure 8.7: External conditions, temperature and relative humidity for the week examined in London, UK

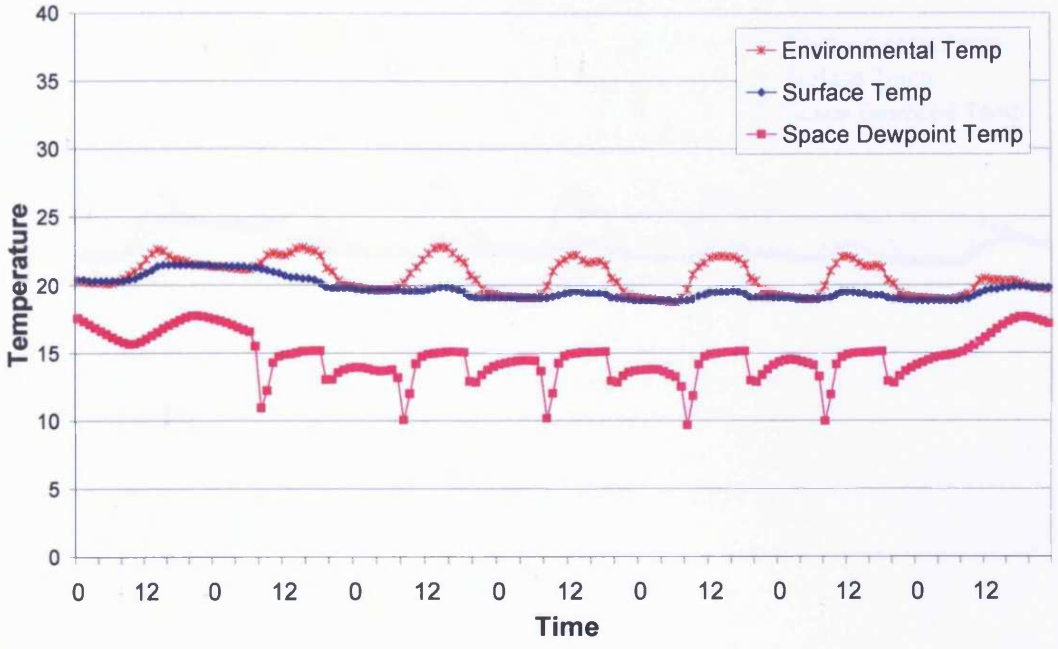


Figure 8.8a: Blind of 45° slat angle and 0.5 reflectance positioned externally (London, UK)

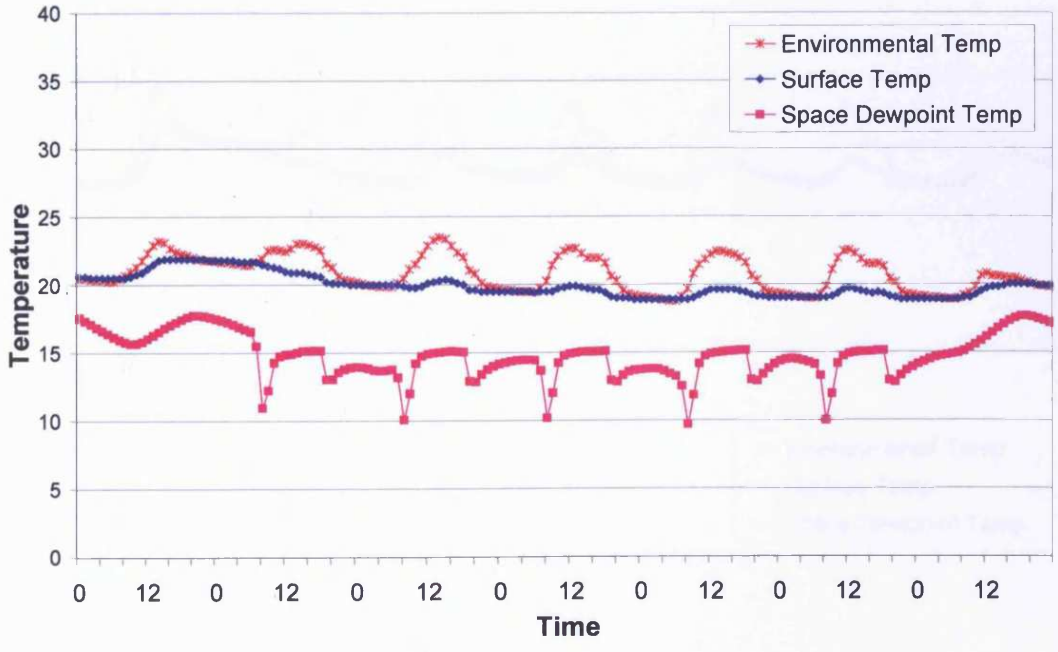


Figure 8.8b: Blind of 45° slat angle and 0.5 reflectance positioned in a ventilated cavity (London, UK)

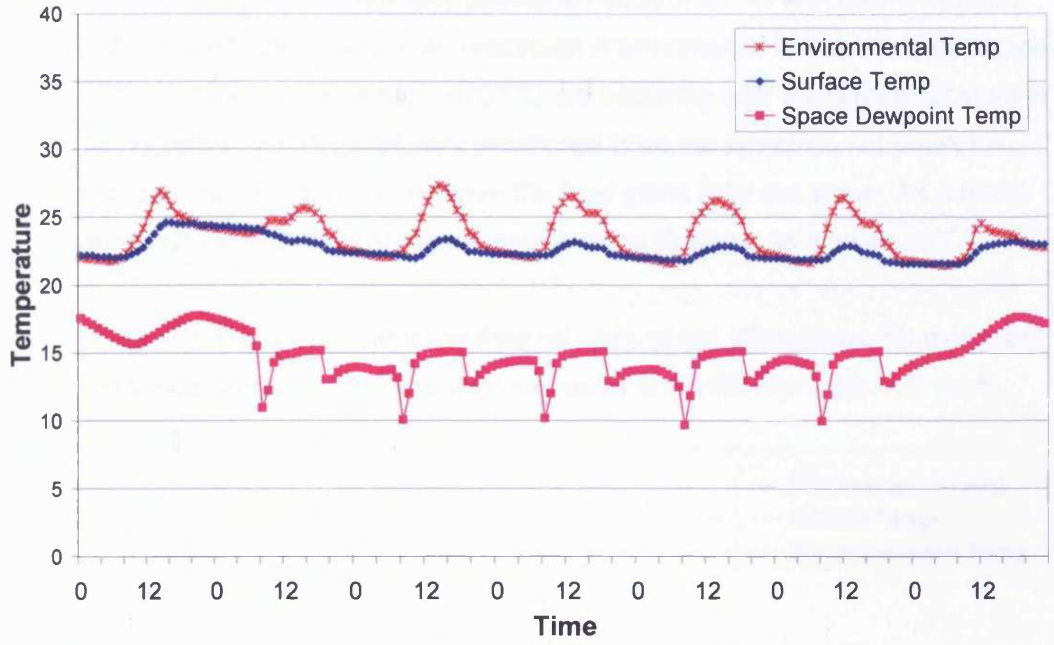


Figure 8.8c: Blind of 45° slat angle and 0.5 reflectance positioned in a sealed cavity (London, UK)

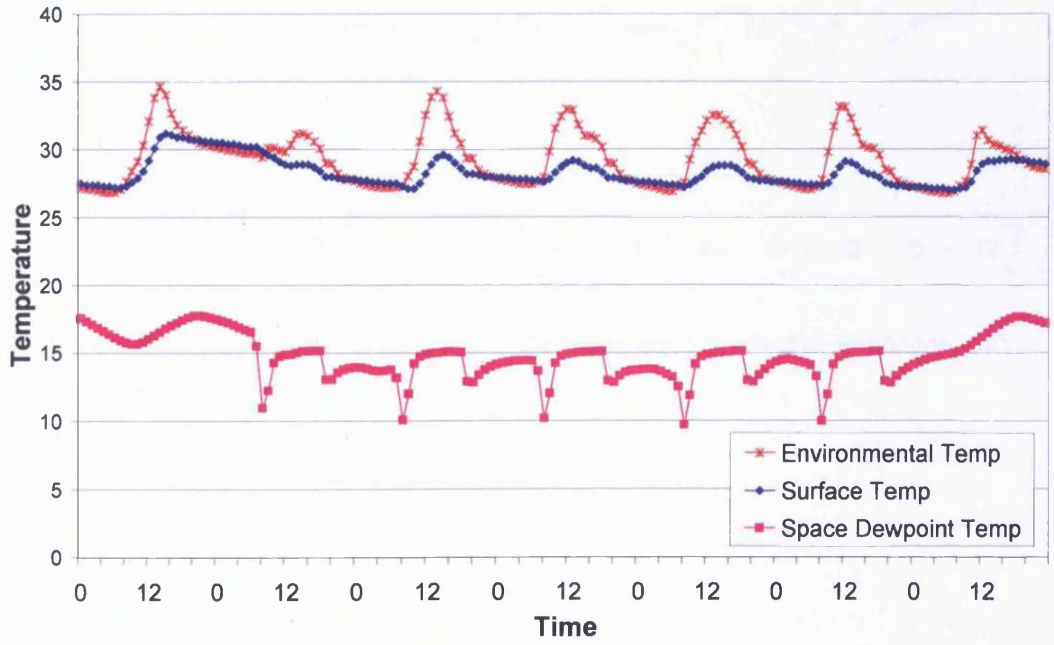


Figure 8.8d: Blind of 45° slat angle and 0.5 reflectance positioned internally (London, UK)

The results showed that the chilled ceiling system under examination is capable of maintaining desired environmental temperature, during the high solar gain period of the

day, when coupled with an externally positioned blind of 45° or with the same blind positioned in a ventilated cavity, with maximum environmental temperature not reaching above 23°C. Temperatures as high as 27°C are occurring with the blind positioned in a sealed cavity, while with the internally positioned blind the system is not powerful enough to cool the ceiling and to remove the heat gains from the space. As a result overheating occurs, with environmental temperature reaching as high as 35°C.

Graphs 8.8a and 8.9 (a-d) present the thermal state of the office space for externally positioned blinds with different blind characteristics and infiltration rate of 0.1ac/h.

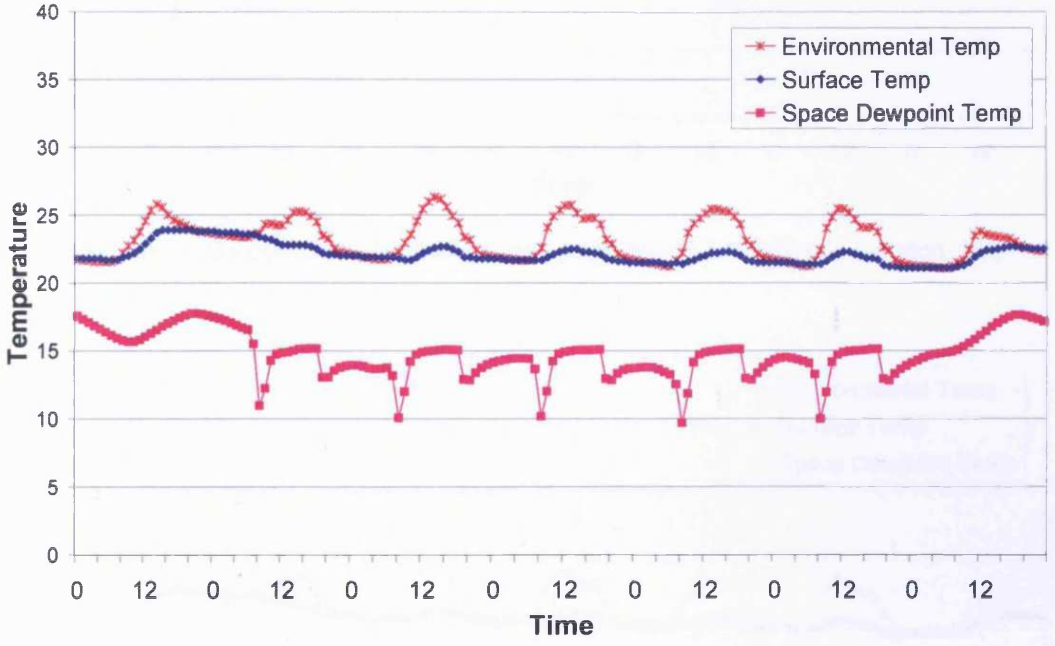


Figure 8.9a: Externally positioned blind of 20° slat angle and 0.5 reflectance (London, UK)

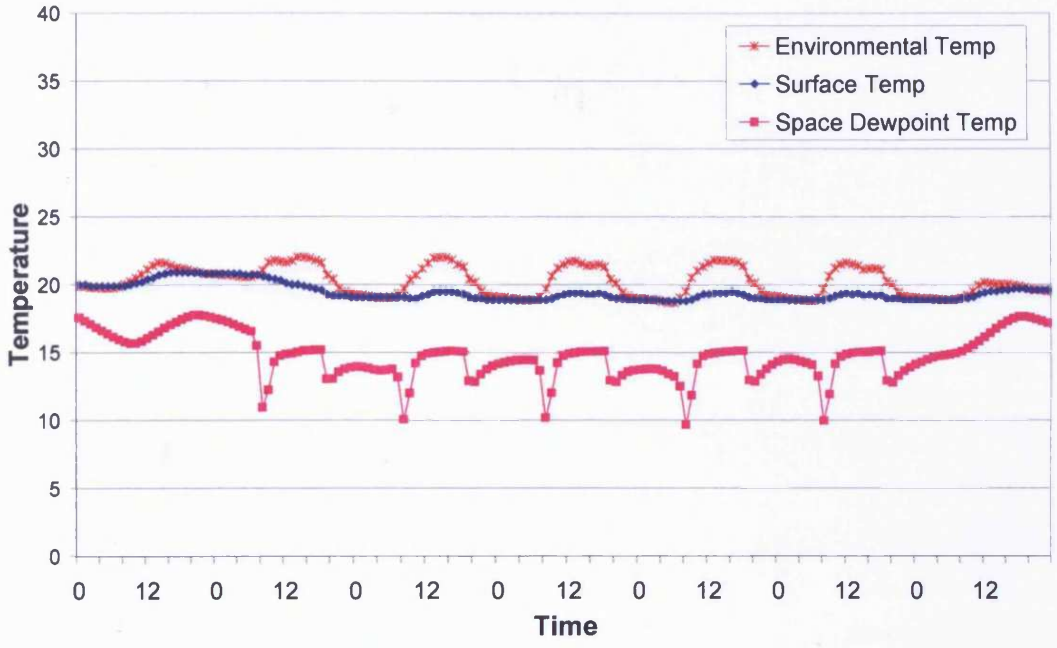


Figure 8.9b: Externally positioned blind of 45° slat angle and 0.2 reflectance (London, UK)

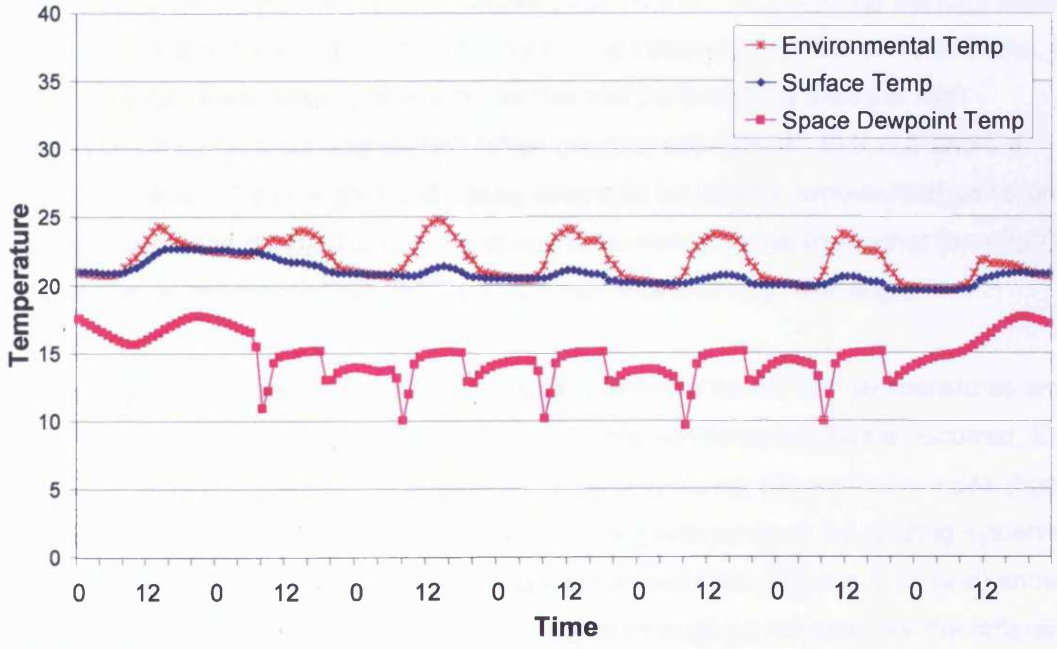


Figure 8.9c: Externally positioned blind of 45° slat angle and 0.8 reflectance (London, UK)

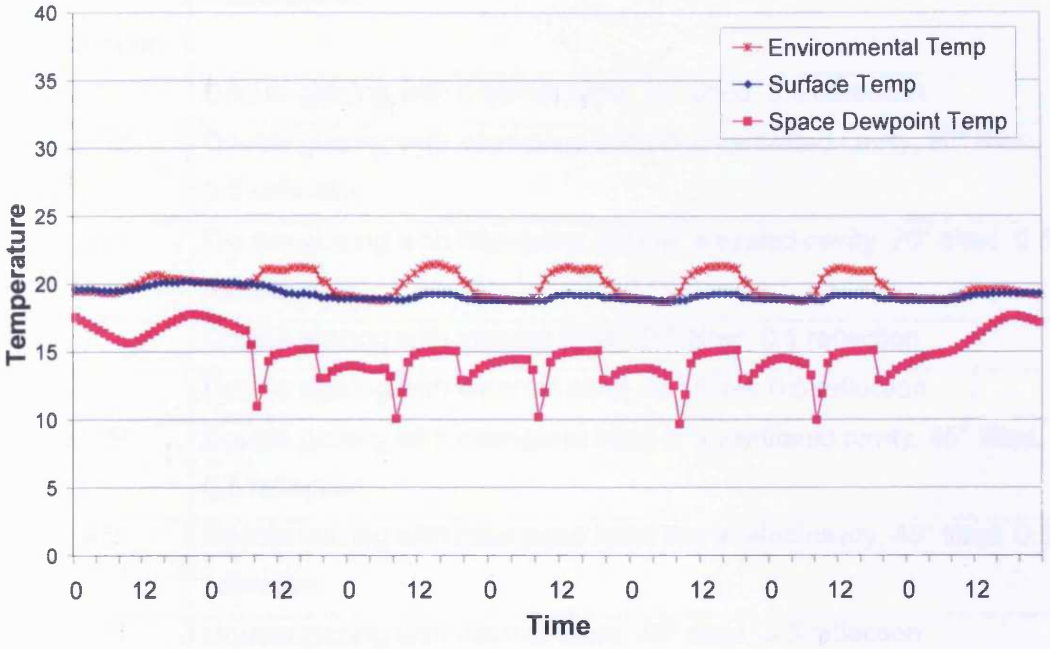


Figure 8.9d: Externally positioned blind of 70° slat angle and 0.5 reflectance (London, UK)

The results showed that the high slat angles (e.g. 70°) would potentially perform better than the low slat angles (e.g. 20°) and, only for the externally positioned blind cases, the low reflectance blinds would present better thermal performance than the high reflectance blinds. The cooling system when coupled with the 45° (0.2, 0.5 and 0.8 reflectance) and 70° slat angle blind cases seems to be able to remove heat gains and keep environmental temperature in the space at desirable levels (no higher than 25°C), while temperatures higher than 25°C could occur with a low 20° slat angle.

The choice of week examined for London was mainly based on high temperatures and high solar radiation availability and not based on the condensation levels occurred. Even though the results showed no condensation occurring during this particular week (figures 8.8, 8.9 and 8.13) there was condensation occurring with some of the glazing systems examined (table 8.3 and figure 8.11) during the summer time. Figures 8.10 (a-e) show the number of hours when condensation occurred throughout the year, for the different glazing systems examined. Table 8.2 describes the abbreviations used for each case in the graphs presented.

| Case abbreviation | Description |
|---|---|
| dgex 20° | Double glazing with external blind, 20° tilted, 0.5 reflection |
| dgvent 20° | Double glazing with inter-pane blind in a ventilated cavity, 20° tilted, 0.5 reflection |
| dgmid 20° | Double glazing with inter-pane blind in a sealed cavity, 20° tilted, 0.5 reflection |
| dgin 20° | Double glazing with internal blind, 20° tilted, 0.5 reflection |
| dgex 45° | Double glazing with external blind, 45° tilted, 0.5 reflection |
| dgvent 45° | Double glazing with inter-pane blind in a ventilated cavity, 45° tilted, 0.5 reflection |
| dgmid 45° | Double glazing with inter-pane blind in a sealed cavity, 45° tilted, 0.5 reflection |
| dgin 45° | Double glazing with internal blind, 45° tilted, 0.5 reflection |
| dgex 45°, 0.2 | Double glazing with external blind, 45° tilted, 0.2 reflection |
| dgvent 45°, 0.2 | Double glazing with inter-pane blind in a ventilated cavity, 45° tilted, 0.2 reflection |
| dgmid 45°, 0.2 | Double glazing with inter-pane blind in a sealed cavity, 45° tilted, 0.2 reflection |
| dgin 45°, 0.2 | Double glazing with internal blind, 45° tilted, 0.2 reflection |
| dgex 45°, 0.8 | Double glazing with external blind, 45° tilted, 0.8 reflection |
| dgvent 45°, 0.8 | Double glazing with inter-pane blind in a ventilated cavity, 45° tilted, 0.8 reflection |
| dgmid 45°, 0.8 | Double glazing with inter-pane blind in a sealed cavity, 45° tilted, 0.8 reflection |
| dgin 45°, 0.8 | Double glazing with internal blind, 45° tilted, 0.8 reflection |
| dgex 70° | Double glazing with external blind, 70° tilted, 0.5 reflection |
| dgvent 70° | Double glazing with inter-pane blind in a ventilated cavity, 70° tilted, 0.5 reflection |
| dgmid 70° | Double glazing with inter-pane blind in a sealed cavity, 70° tilted, 0.5 reflection |
| dgin 70° | Double glazing with internal blind, 70° tilted, 0.5 reflection |

Table 8.2: Description of case abbreviation

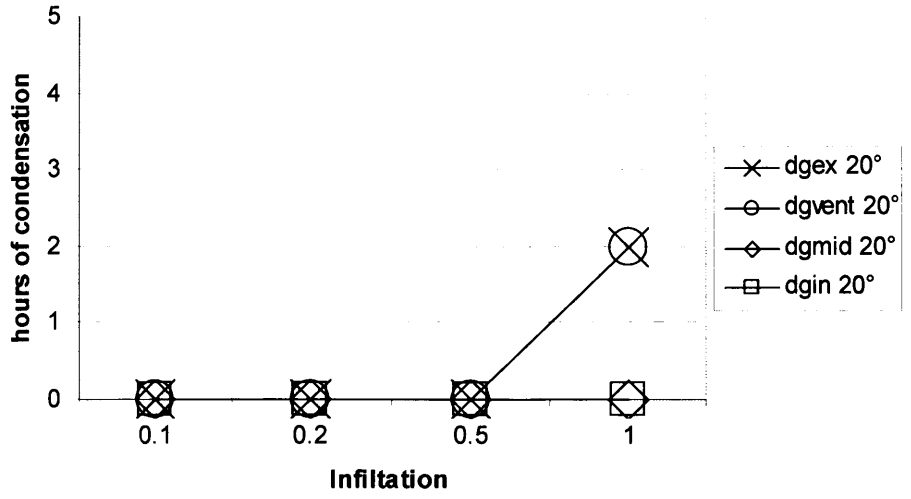


Figure 8.10a: Condensation levels for a 20° slat angle blind of 0.5 reflectance (London, UK)

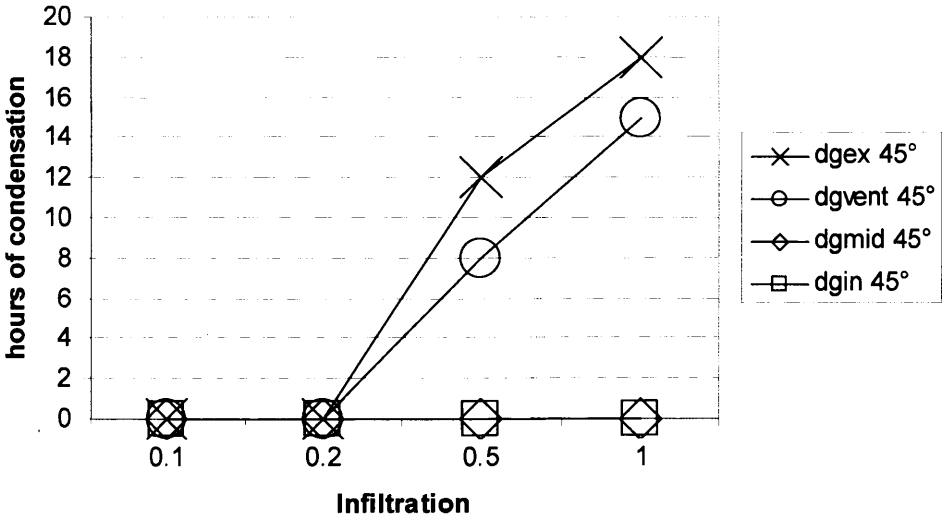


Figure 8.10b: Condensation levels for a 45° slat angle blind of 0.5 reflectance (London, UK)

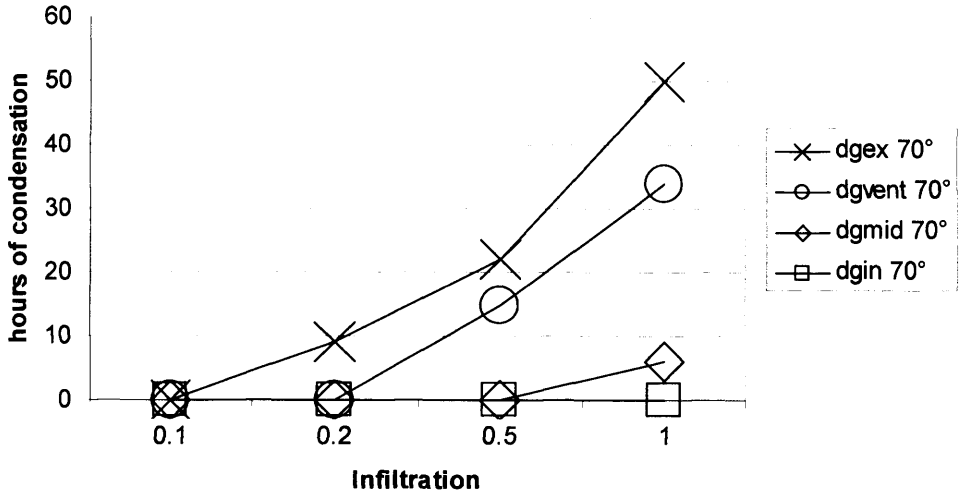


Figure 8.10c: Condensation levels for a 70° slat angle blind of 0.5 reflectance (London, UK)

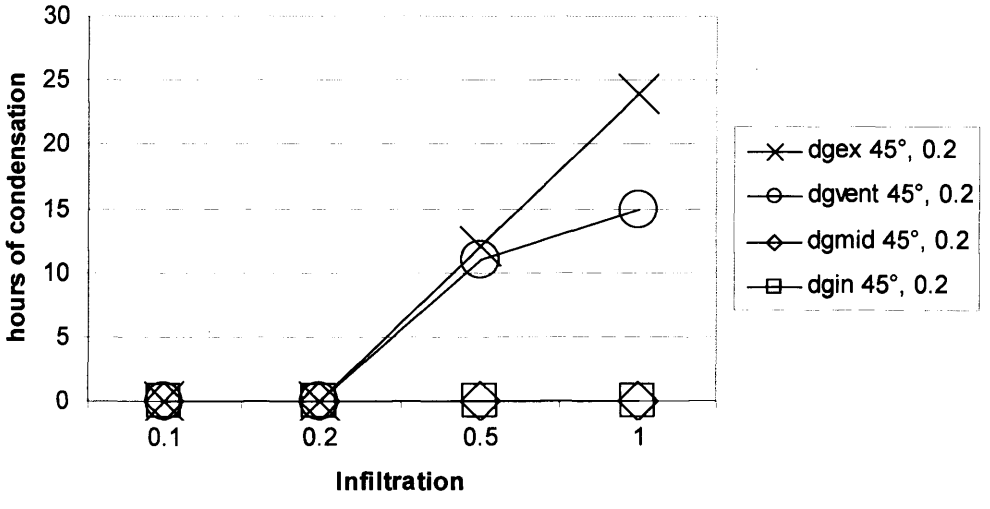


Figure 8.10d: Condensation levels for a 45° slat angle blind of 0.2 reflectance (London, UK)

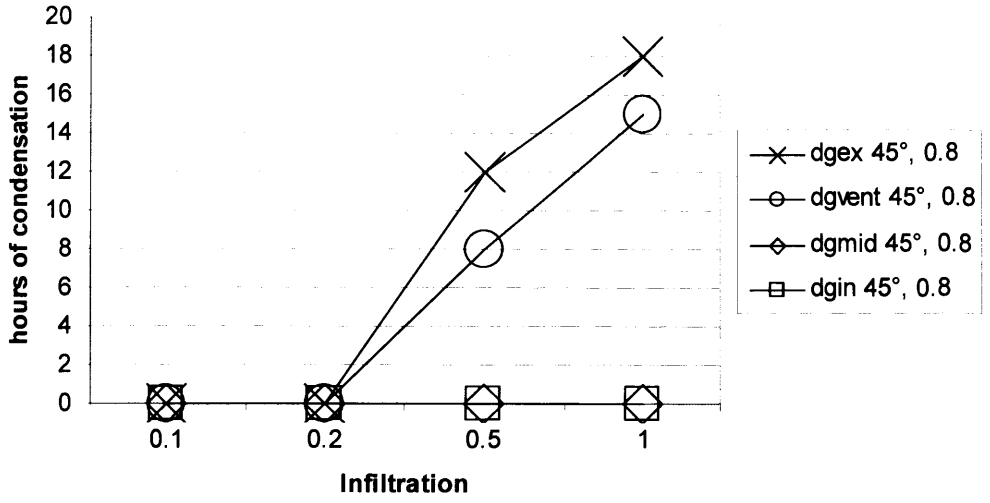


Figure 8.10e: Condensation levels for a 45° slat angle blind of 0.8 reflectance (London, UK)

From the graphs it is shown that the higher solar gain cases (internal and inter-pane) would potentially present less condensation, while lower solar gain cases (external and inter-pane with ventilated cavity) would potentially present higher condensation levels when combined with the specific cooling system under consideration. The above contradictory results are noticed because in the summer the low power cooling system ($35W/m^2$) is unable to cope with the heat load of the room when coupled with high solar gain glazing systems and so the space and surface temperatures rise above air dew point. The same cooling system is working efficiently when coupled with lower solar gain cases and so space and surface temperatures might fall below the air dew point and condensation could happen (figure 8.11).

It is also noticed from the same graphs that for almost sealed buildings (infiltration of 0.1ac/h) there is no condensation, while condensation levels start to rise with increased infiltration. Moisture content increases with increased humid air coming into the space due to infiltration and the higher the moisture content of the air the higher its dew point temperature and so the higher the possibility of the surface temperature falling below the air dew point temperature.

It is important to notice here that the above condensation levels were all occurred during weekends and night time when the humidity control of the air supply system was

switched off. Due to the ceilings thermal mass the surface temperatures stay low during the night and weekends which implies that the "systems off" period could be important for the prevention of condensation.

Figure 8.11 and 8.12 present the same case but the second graph with the mechanical ventilation system switched on during weekends (for the daytime hours only as for weekdays). It is shown that even with high infiltration rates (0.5ac/h) condensation could be avoided if there is a control of space moisture content.

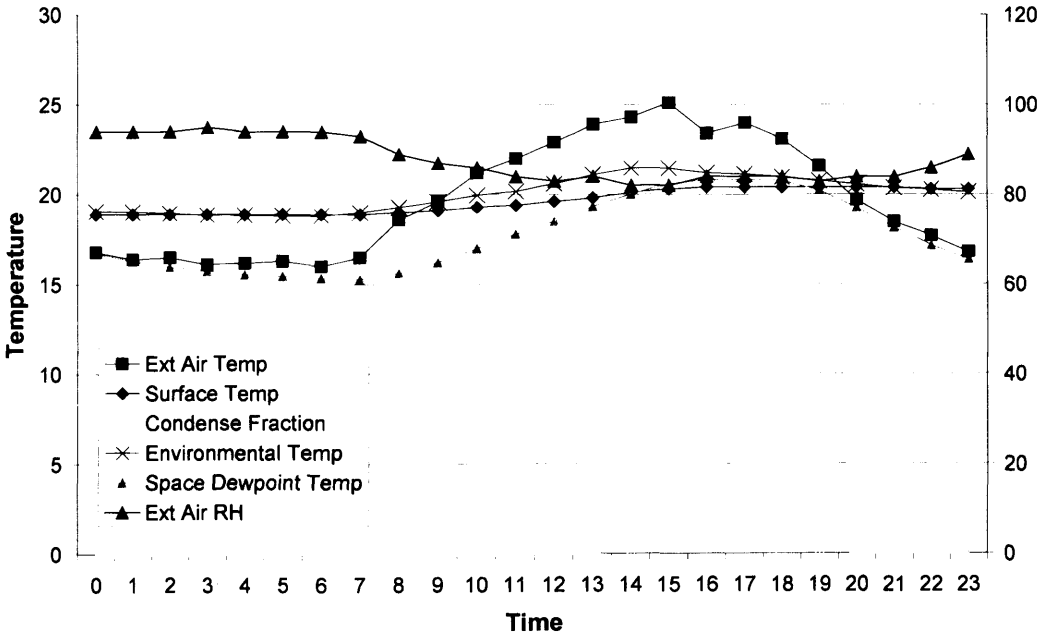


Figure 8.11: Internal conditions with a 45° tilted blind (0.5 reflectance) positioned externally and 0.5ac/h infiltration rate. Ventilation "off" during weekends (London, UK)

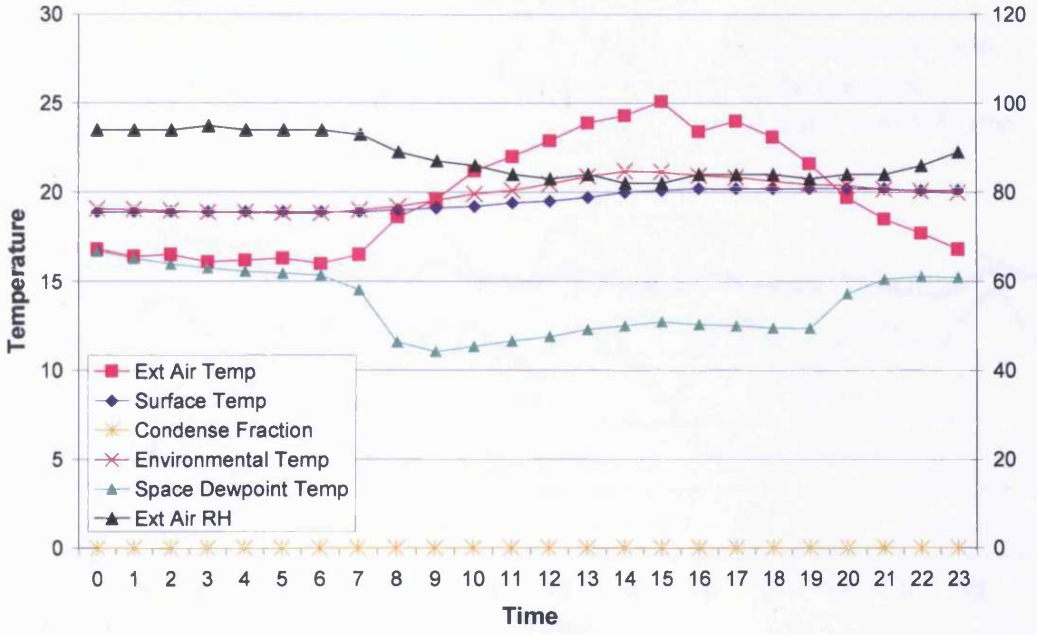


Figure 8.12: Internal conditions with a 45° tilted blind (0.5 reflectance) positioned externally and 0.5ac/h infiltration rate. Ventilation "on" during weekends (London, UK)

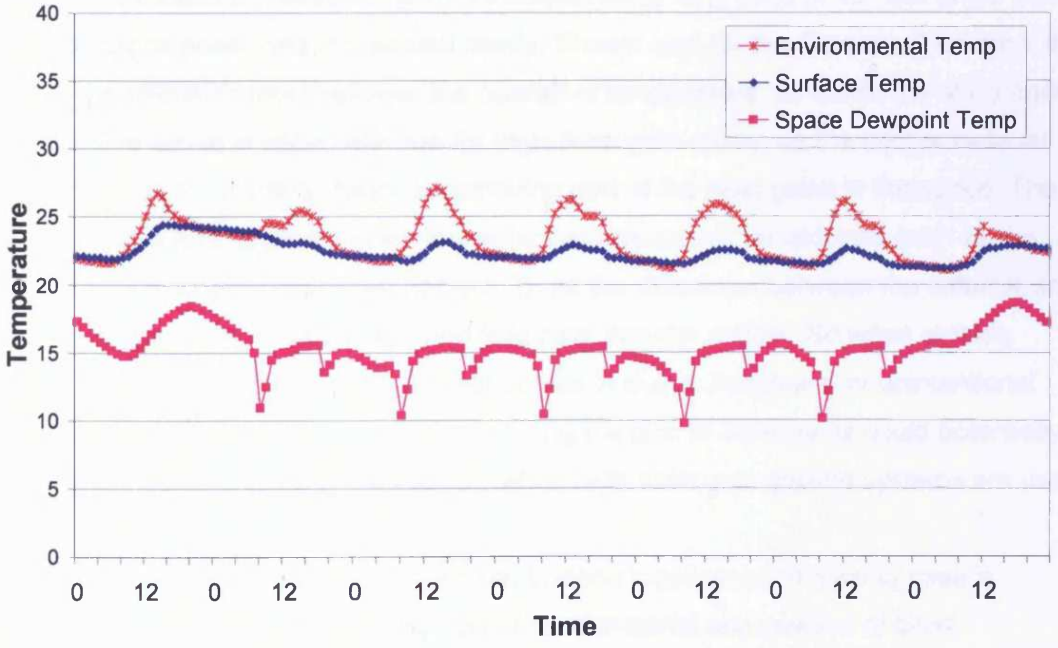


Figure 8.13a: 0.2ac/h infiltration, blind of 45° slat angle and 0.5 reflectance positioned in a sealed cavity (London, UK)

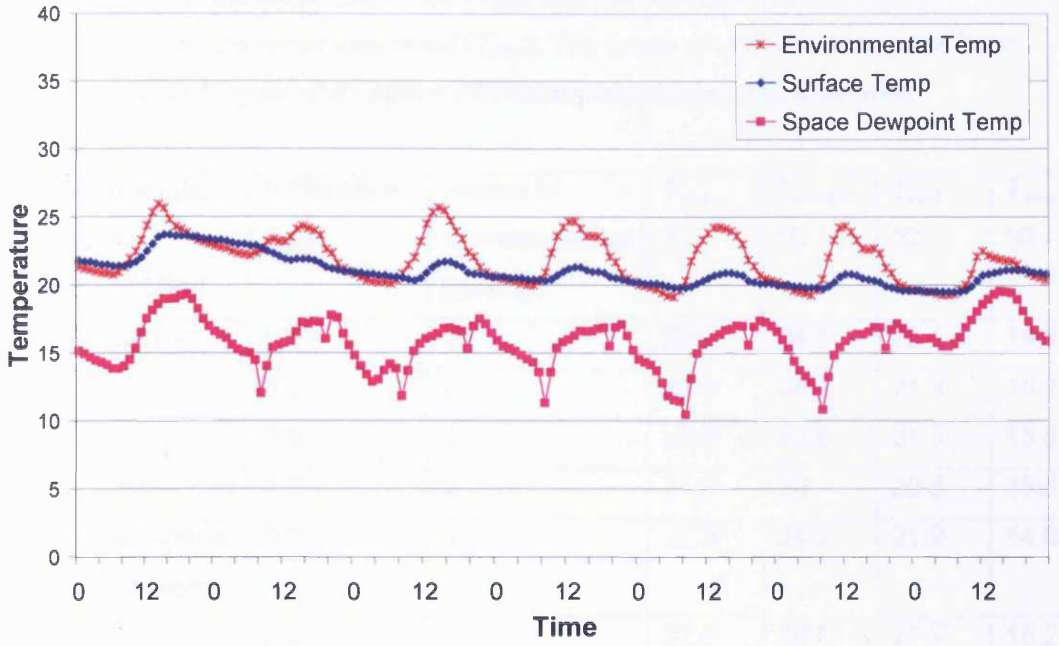


Figure 8.13b: 1.0ac/h infiltration, blind of 45° slat angle and 0.5 reflectance positioned in a sealed cavity (London, UK)

Figures 8.13 a and b present different infiltration rates for a blind of 45° slat angle and 0.5 reflectance positioned in a sealed cavity. Shown also for the Ostersund location, the higher the infiltration rate the lower the operative temperature, as London is still a cool climate. The above is especially true for high solar gain cases, as the cool outside air brought in due to infiltration helps in removing part of the heat gains in the space. The above trend is less apparent when low solar gain cases are considered, such as the externally positioned blind cases (table 8.3), as the difference between the external and internal temperature is not as high and less heat transfer occurs. So when outside temperature is lower than inside, air that comes in due to intentional or unintentional ventilation (e.g. by opening the window) during the pick of solar gains could potentially improve the thermal state of the interior, when high solar gain glazing systems are used.

Table 8.3 summarises the results from the London location; each glazing case is described by the angle of slat, reflection of blind material and position of blind. Summarised are the average environmental temperature ($T_{env}$) over the week examined, the average environmental temperature over the week examined but only for the weekdays and occupancy hours (8am-6pm) ($T_{env\ 8\text{-}6}$), the average chilled ceiling

temperature over the week examined ($T_{surf}$) and the average space dewpoint temperature over the week examined ($T_{dew}$). The hours of condensation have been summarised over a year and various infiltration rates have been examined.

| **Case: Slat angle/ Reflection/ Position of blind** | **Infiltration Ac/h** | **Hours of Condensation (yearly)** | **$T_{env}$ °C** | **$T_{env\ 8\text{-}6}$ °C** | **$T_{surf}$ °C** | **$T_{dew}$ °C** |
|---|---|---|---|---|---|---|
| 20°, 0.5, external | 0.1 | 0 | 23.2 | 24.6 | 22.1 | 14.8 |
| | 0.2 | 0 | 22.9 | 24.4 | 21.9 | 15.2 |
| | 0.5 | 0 | 22.3 | 23.8 | 21.3 | 15.6 |
| | 1.0 | 2 | 21.6 | 23 | 20.6 | 15.8 |
| 20°, 0.5, inter-pane in ventilated cavity | 0.1 | 0 | 22.9 | 24.3 | 21.9 | 14.8 |
| | 0.2 | 0 | 22.6 | 24.1 | 21.7 | 15.2 |
| | 0.5 | 0 | 22.1 | 23.5 | 21.1 | 15.6 |
| | 1.0 | 2 | 21.4 | 22.8 | 20.5 | 15.8 |
| 20°, 0.5, inter-pane in sealed cavity | 0.1 | 0 | 25.8 | 27.4 | 24.8 | 14.8 |
| | 0.2 | 0 | 25.2 | 26.8 | 24.2 | 15.2 |
| | 0.5 | 0 | 24 | 25.7 | 23 | 15.6 |
| | 1.0 | 0 | 23 | 24.7 | 22.1 | 15.8 |
| 20°, 0.5, internal | 0.1 | 0 | 29.3 | 30.9 | 28.3 | 14.8 |
| | 0.2 | 0 | 28.4 | 30 | 27.4 | 15.2 |
| | 0.5 | 0 | 26.4 | 28.1 | 25.4 | 15.6 |
| | 1.0 | 0 | 24.6 | 26.4 | 23.7 | 15.8 |
| 45°, 0.5, external | 0.1 | 0 | 20.6 | 21.8 | 19.7 | 14.8 |
| | 0.2 | 0 | 20.5 | 21.7 | 19.7 | 15.2 |
| | 0.5 | 12 | 20.4 | 21.5 | 19.6 | 15.6 |
| | 1.0 | 18 | 20.2 | 21.4 | 19.5 | 15.8 |
| 45°, 0.5, inter-pane in ventilated cavity | 0.1 | 0 | 20.8 | 22 | 19.9 | 14.8 |
| | 0.2 | 0 | 20.7 | 21.9 | 19.8 | 15.2 |
| | 0.5 | 8 | 20.6 | 21.8 | 19.7 | 15.6 |

| | | | | | | |
|---|---|---|---|---|---|---|
| | 1.0 | 15 | 20.4 | 21.6 | 19.6 | 15.8 |
| 45°, 0.5, inter-pane in sealed cavity | 0.1 | 0 | 23.6 | 25.2 | 22.6 | 14.8 |
| | 0.2 | 0 | 23.3 | 24.9 | 22.3 | 15.2 |
| | 0.5 | 0 | 22.7 | 24.2 | 21.7 | 15.6 |
| | 1.0 | 0 | 21.9 | 23.4 | 21 | 15.8 |
| 45°, 0.5, internal | 0.1 | 0 | 29.3 | 30.9 | 28.3 | 14.8 |
| | 0.2 | 0 | 28.4 | 30 | 27.4 | 15.2 |
| | 0.5 | 0 | 26.3 | 28 | 25.4 | 15.6 |
| | 1.0 | 0 | 24.5 | 26.3 | 23.6 | 15.8 |
| 45°, 0.2, external | 0.1 | 0 | 20.2 | 21.3 | 19.4 | 14.8 |
| | 0.2 | 0 | 20.2 | 21.3 | 19.4 | 15.2 |
| | 0.5 | 12 | 20.1 | 21.2 | 19.4 | 15.6 |
| | 1.0 | 24 | 20 | 21.1 | 19.3 | 15.8 |
| 45°, 0.2, inter-pane in ventilated cavity | 0.1 | 0 | 20.6 | 21.8 | 19.8 | 14.8 |
| | 0.2 | 0 | 20.6 | 21.7 | 19.7 | 15.2 |
| | 0.5 | 11 | 20.5 | 21.6 | 19.7 | 15.6 |
| | 1.0 | 15 | 20.3 | 21.4 | 19.5 | 15.8 |
| 45°, 0.2, inter-pane in sealed cavity | 0.1 | 0 | 24.7 | 26.3 | 23.7 | 14.8 |
| | 0.2 | 0 | 24.2 | 25.8 | 23.2 | 15.2 |
| | 0.5 | 0 | 23.4 | 25 | 22.5 | 15.6 |
| | 1.0 | 0 | 22.5 | 24 | 21.6 | 15.8 |
| 45°, 0.2, internal | 0.1 | 0 | 31.8 | 33.5 | 30.9 | 14.8 |
| | 0.2 | 0 | 30.7 | 32.4 | 29.7 | 15.2 |
| | 0.5 | 0 | 28.2 | 30 | 27.3 | 15.6 |
| | 1.0 | 0 | 25.8 | 27.7 | 24.9 | 15.8 |
| 45°, 0.8, external | 0.1 | 0 | 21.8 | 23.2 | 20.8 | 14.8 |
| | 0.2 | 0 | 21.6 | 23 | 20.7 | 15.2 |
| | 0.5 | 12 | 21.2 | 22.6 | 20.3 | 15.6 |
| | 1.0 | 18 | 20.8 | 22.1 | 19.9 | 15.8 |
| 45°, 0.8, inter-pane | 0.1 | 0 | 21.3 | 22.7 | 20.4 | 14.8 |

| in ventilated cavity | | | | | | |
|---|---|---|---|---|---|---|
| | 0.2 | 0 | 21.2 | 22.5 | 20.3 | 15.2 |
| | 0.5 | 8 | 20.9 | 22.2 | 20 | 15.6 |
| | 1.0 | 15 | 20.6 | 21.9 | 19.7 | 15.8 |
| 45°, 0.8, inter-pane in sealed cavity | 0.1 | 0 | 22.8 | 24.2 | 21.8 | 14.8 |
| | 0.2 | 0 | 22.5 | 24 | 21.5 | 15.2 |
| | 0.5 | 0 | 22 | 23.5 | 21 | 15.6 |
| | 1.0 | 0 | 21.3 | 22.8 | 20.4 | 15.8 |
| 45°, 0.8, internal | 0.1 | 0 | 25.9 | 27.5 | 24.9 | 14.8 |
| | 0.2 | 0 | 25.3 | 26.9 | 24.3 | 15.2 |
| | 0.5 | 0 | 24 | 25.6 | 23.1 | 15.6 |
| | 1.0 | 0 | 23 | 24.6 | 22.1 | 15.8 |
| 70°, 0.5, external | 0.1 | 0 | 19.9 | 20.9 | 19.2 | 14.8 |
| | 0.2 | 9 | 19.9 | 20.9 | 19.2 | 15.2 |
| | 0.5 | 22 | 19.8 | 20.8 | 19.1 | 15.6 |
| | 1.0 | 50 | 19.7 | 20.7 | 19 | 15.8 |
| 70°, 0.5, inter-pane in ventilated cavity | 0.1 | 0 | 20.1 | 21.2 | 19.4 | 14.8 |
| | 0.2 | 0 | 20.1 | 21.1 | 19.3 | 15.2 |
| | 0.5 | 15 | 20 | 21 | 19.3 | 15.6 |
| | 1.0 | 34 | 19.9 | 20.9 | 19.2 | 15.8 |
| 70°, 0.5, inter-pane in sealed cavity | 0.1 | 0 | 22.1 | 23.5 | 21.1 | 14.8 |
| | 0.2 | 0 | 21.9 | 23.3 | 20.9 | 15.2 |
| | 0.5 | 0 | 21.4 | 22.8 | 20.5 | 15.6 |
| | 1.0 | 8 | 20.9 | 22.3 | 20 | 15.8 |
| 70°, 0.5, internal | 0.1 | 0 | 28.1 | 29.7 | 27.1 | 14.8 |
| | 0.2 | 0 | 27.2 | 28.9 | 26.3 | 15.2 |
| | 0.5 | 0 | 25.5 | 27.1 | 24.5 | 15.6 |
| | 1.0 | 0 | 24 | 25.7 | 23.1 | 15.8 |

Table 8.3: Summary of results for London

### 8.2.3 Athens, Greece

Figure 8.14 presents the external conditions, temperature and RH, during a summer's week chosen for the presentation of the thermal state of the office space in Athens, Greece. Figure 8.15 (a-d) presents the environmental, ceiling surface and space air dew point temperatures for the same office space, but this time for the Athens location, with a blind of 45° slat angle and 0.5 reflectance positioned externally, inter-pane and internally, tested for 0.1ac/h infiltration rate. A hot summer's week was chosen to demonstrate the thermal state of the room. The first and last days presented are weekend days when all systems are "off".

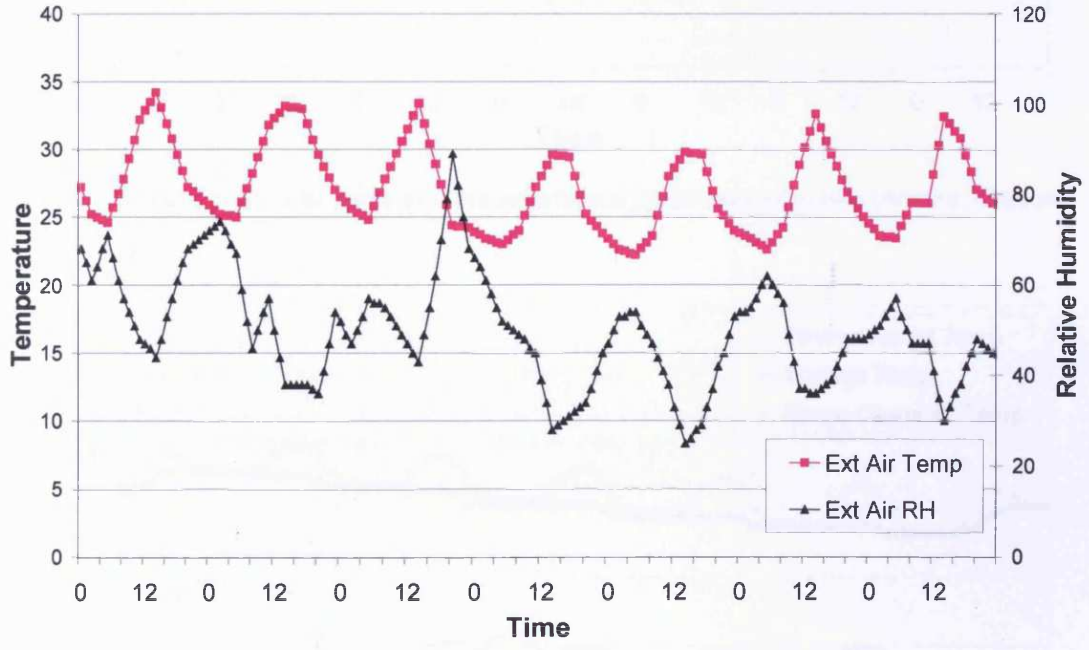


Figure 8.14: External conditions, temperature and relative humidity for the week examined in Athens, Greece

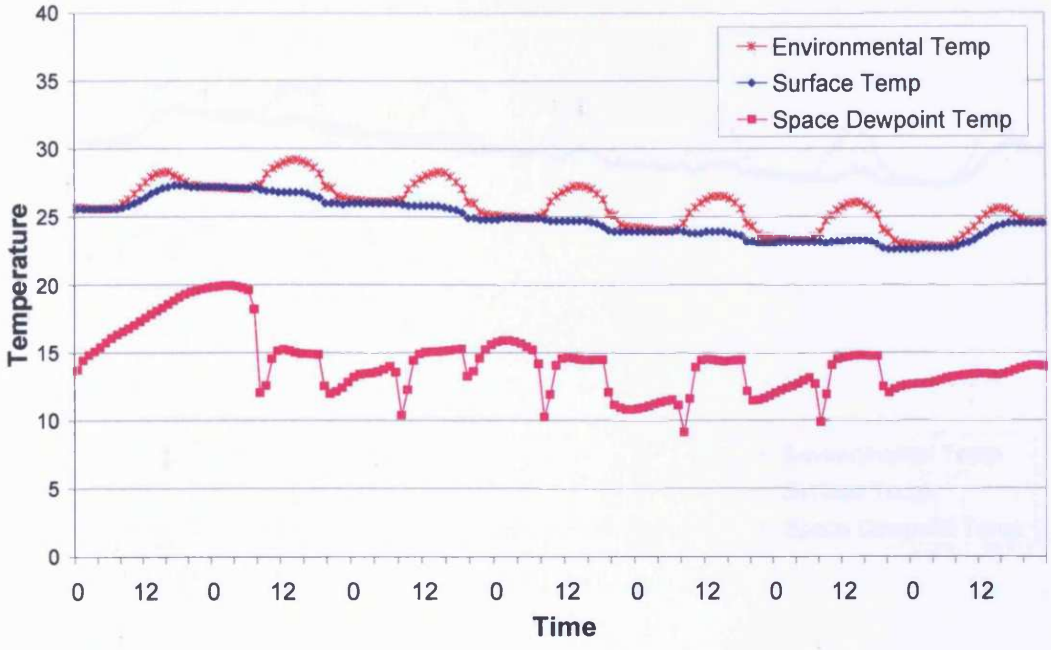


Figure 8.15a: Blind of 45° slat angle and 0.5 reflectance positioned externally (Athens, Greece)

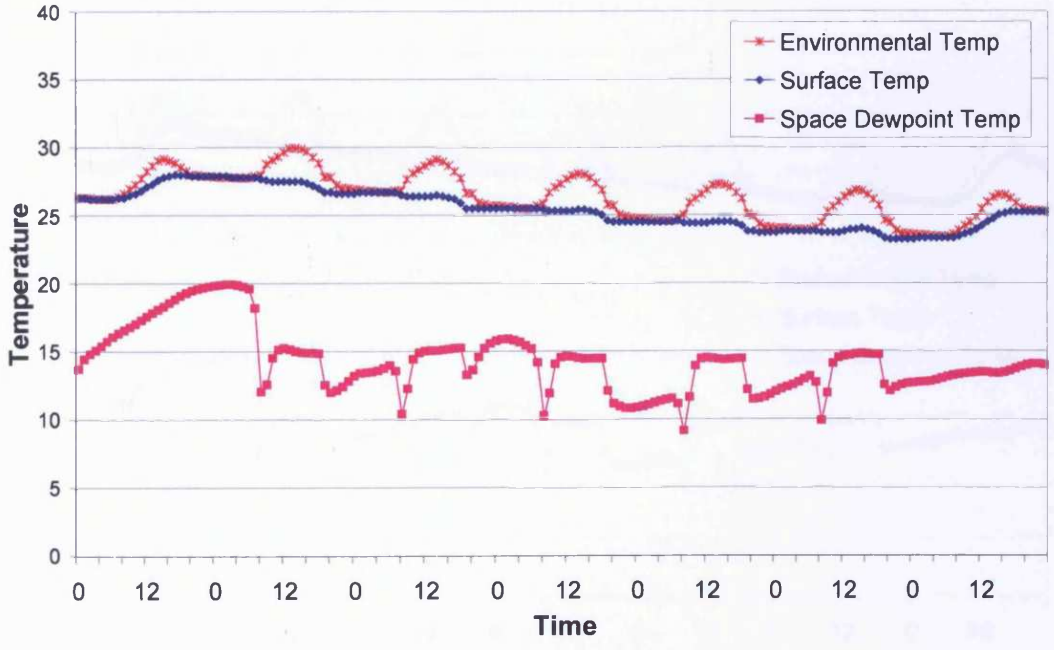


Figure 8.15b: Blind of 45° slat angle and 0.5 reflectance positioned in a ventilated cavity (Athens, Greece)

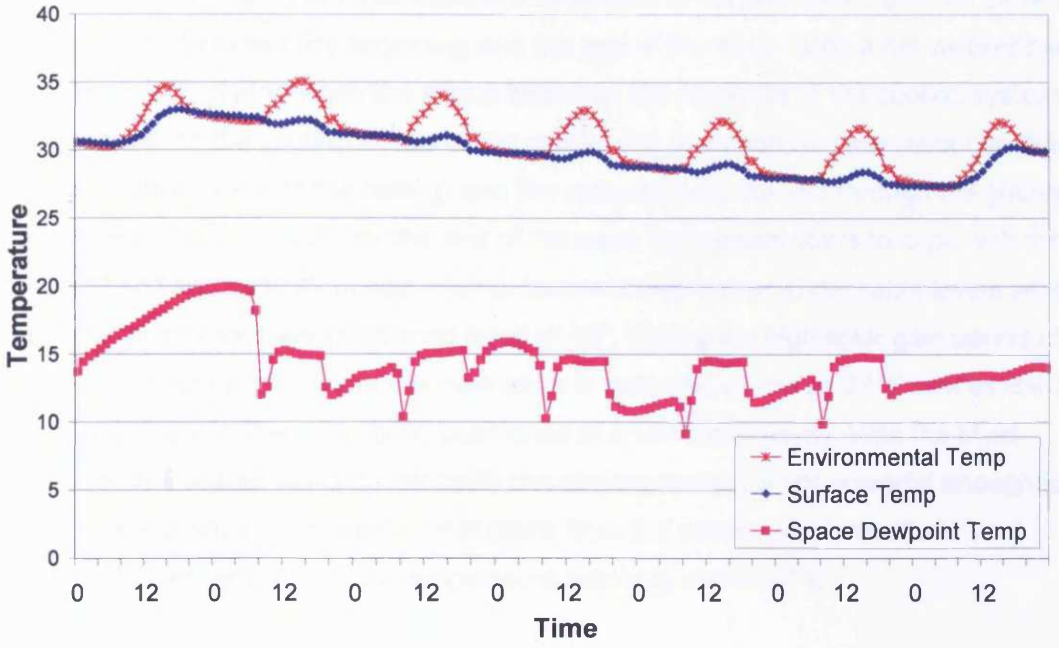


Figure 8.15c: Blind of 45° slat angle and 0.5 reflectance positioned in a sealed cavity (Athens, Greece)

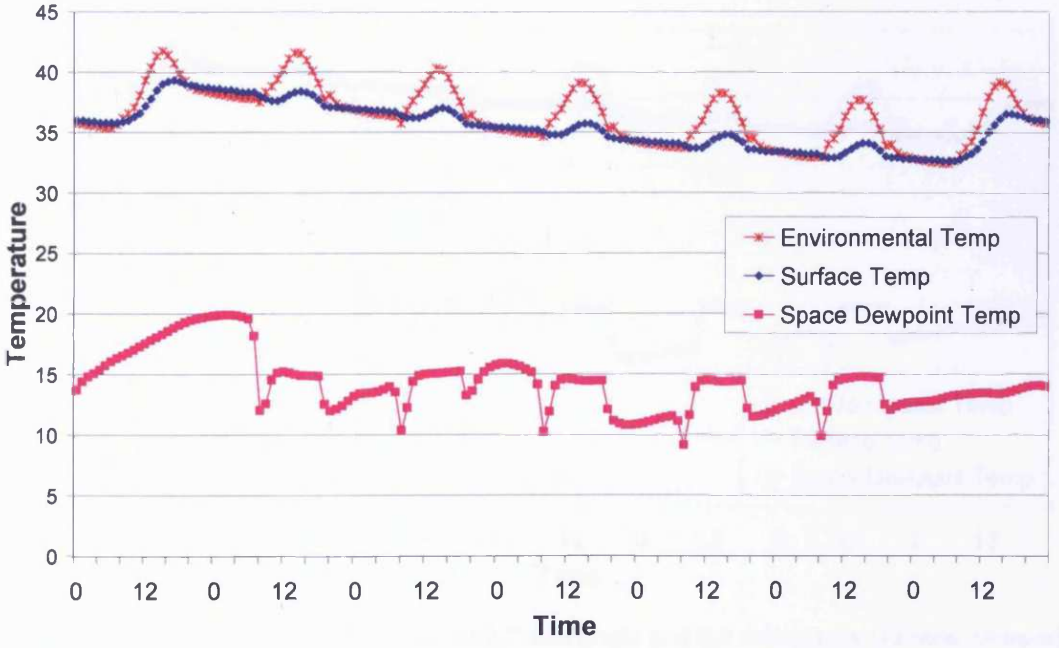


Figure 8.15d: Blind of 45° slat angle and 0.5 reflectance positioned internally (Athens, Greece)

From the graphs it is shown that there is a difference in the performance of the chilled ceiling system between the beginning and the end of the week. After a hot weekend with all systems "off", during when the space heats up, the response of the cooling system is not immediate to the cooling needs of the space, due to its nature (slow response due to the high thermal mass of the ceiling) and the reduced heat transfer through the glazing system (low U-value). Towards the end of the week the system starts to cope with the heat load and successfully brings internal temperatures closer to desirable levels when coupled with an externally positioned blind of 45°. During the high solar gain period of the day maximum environmental temperature is reaching as low as 26°C and as low as 27°C occurring with the same blind positioned in a ventilated cavity. With the blind positioned in a sealed cavity or internally the cooling system is not powerful enough to cool the ceiling and to remove the heat gains from the space, which results in overheating, with environmental temperature reaching above 40°C.

Graphs 8.15a and 8.16 (a-d) present the thermal state of the office space for externally positioned blinds with different blind characteristics and infiltration rate of 0.1ac/h.

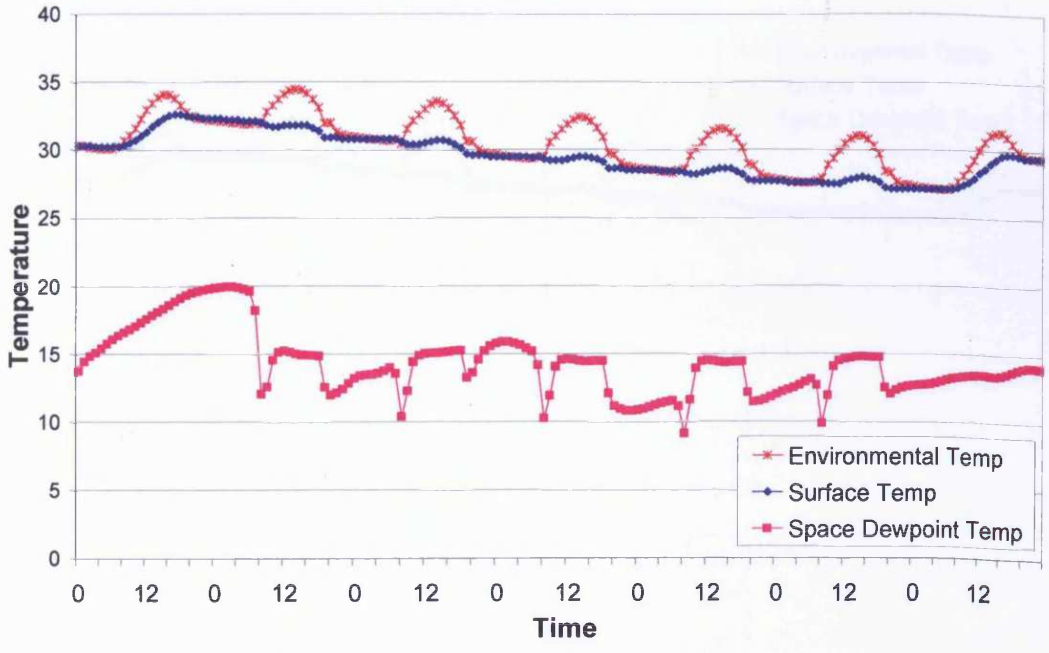


Figure 8.16a: Externally positioned blind of 20° slat angle and 0.5 reflectance (Athens, Greece)

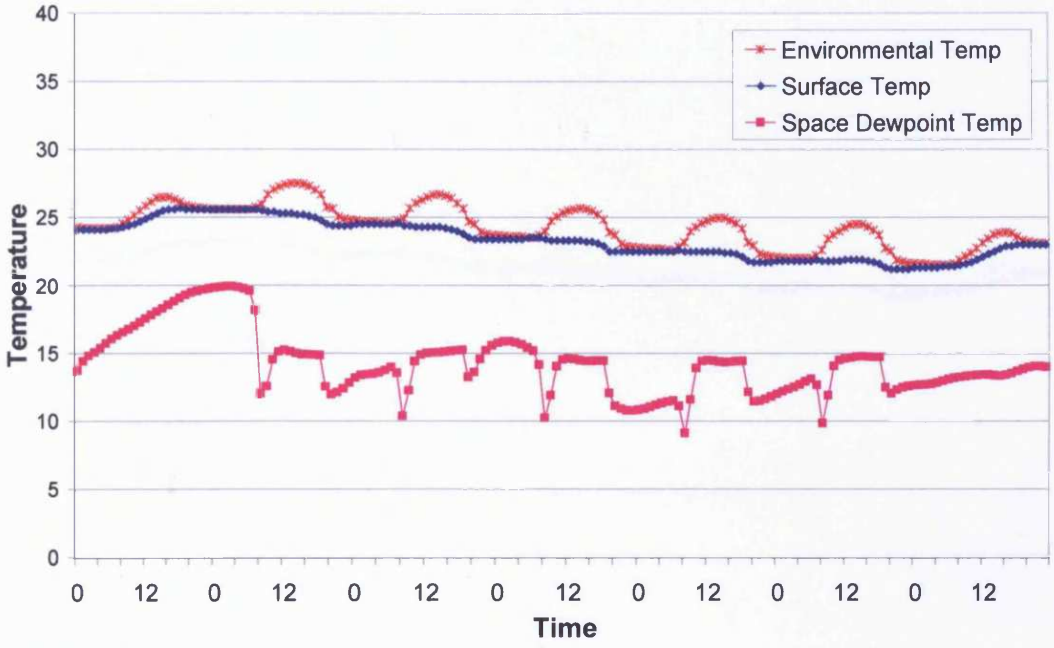


Figure 8.16b: Externally positioned blind of 45° slat angle and 0.2 reflectance (Athens, Greece)

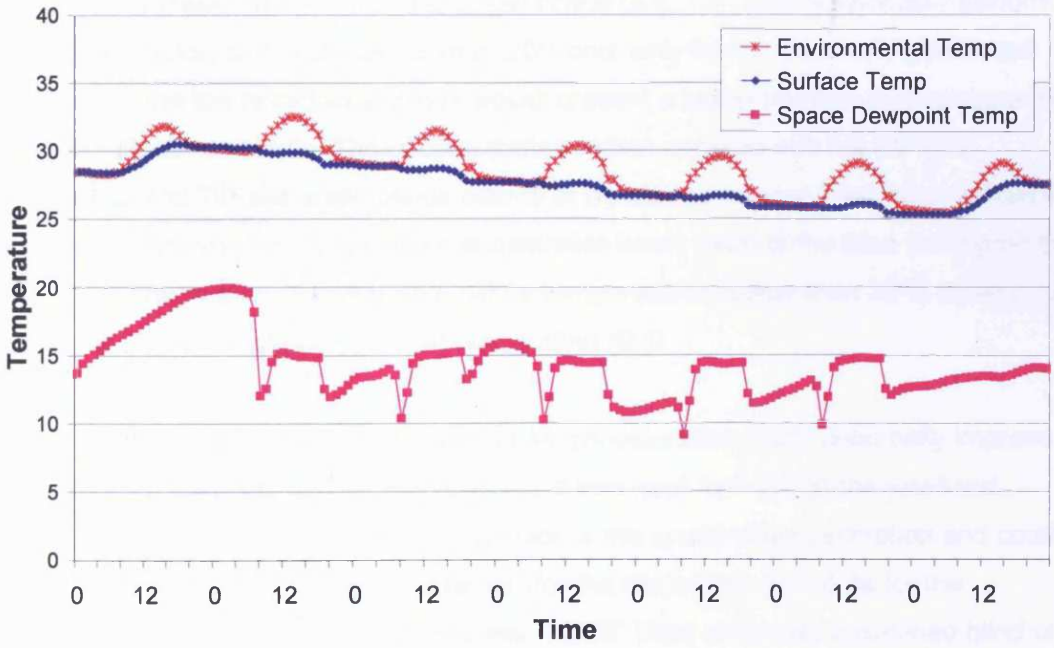


Figure 8.16c: Externally positioned blind of 45° slat angle and 0.8 reflectance (Athens, Greece)

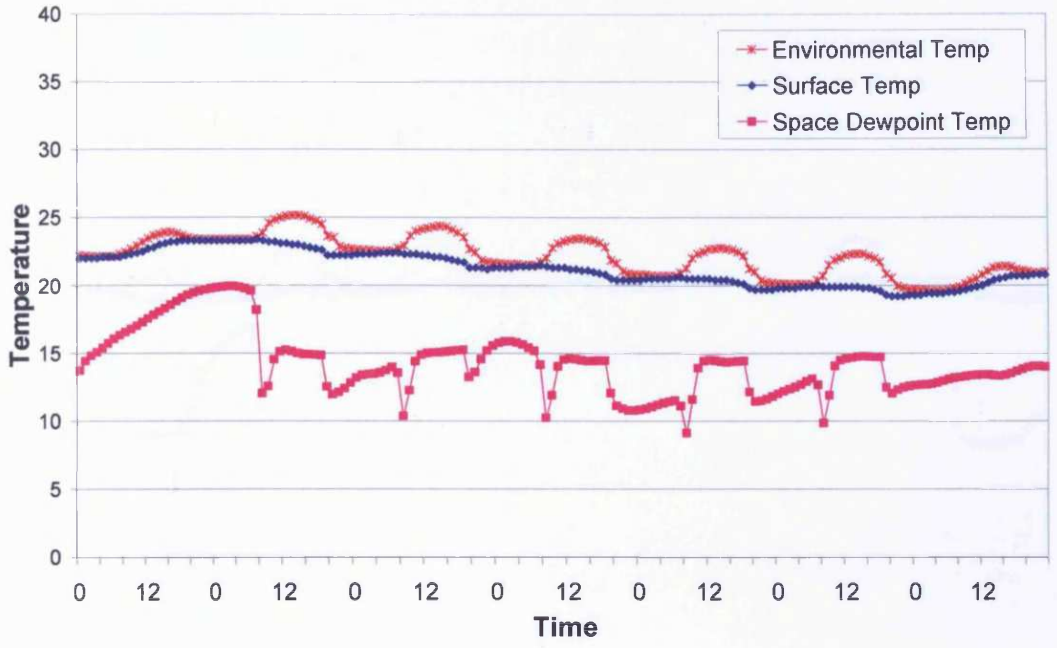


Figure 8.16d: Externally positioned blind of 70° slat angle and 0.5 reflectance (Athens, Greece)

The results showed that the high slat angle blinds (e.g. 70°) would potentially perform better than the low slat angle blinds (e.g. 20°) and, only for the externally positioned blind cases, the low reflectance blinds would present a better thermal performance than the high reflectance blinds. The cooling system when coupled with the 45° (0.2 reflectance) and 70° slat angle blinds seems to be able to remove heat loads efficiently and keep environmental temperature at desirable levels most of the time (no higher than 27°C immediately after the weekend), while temperatures higher than 30°C could occur with a low 20° slat angle or highly reflective blind (0.8).

The performance of the cooling system under consideration could potentially improve when coupled with higher solar gain cases if it was kept "on" during the weekend. Figure 8.17 (a & b) presents the thermal state of the space when ventilation and cooling systems are left "on" during the weekends (for the same time period as for the weekdays). The glazing system tested was the 45° tilted externally positioned blind of 0.5 reflectance and the 20° tilted externally positioned blind of 0.5 reflectance.

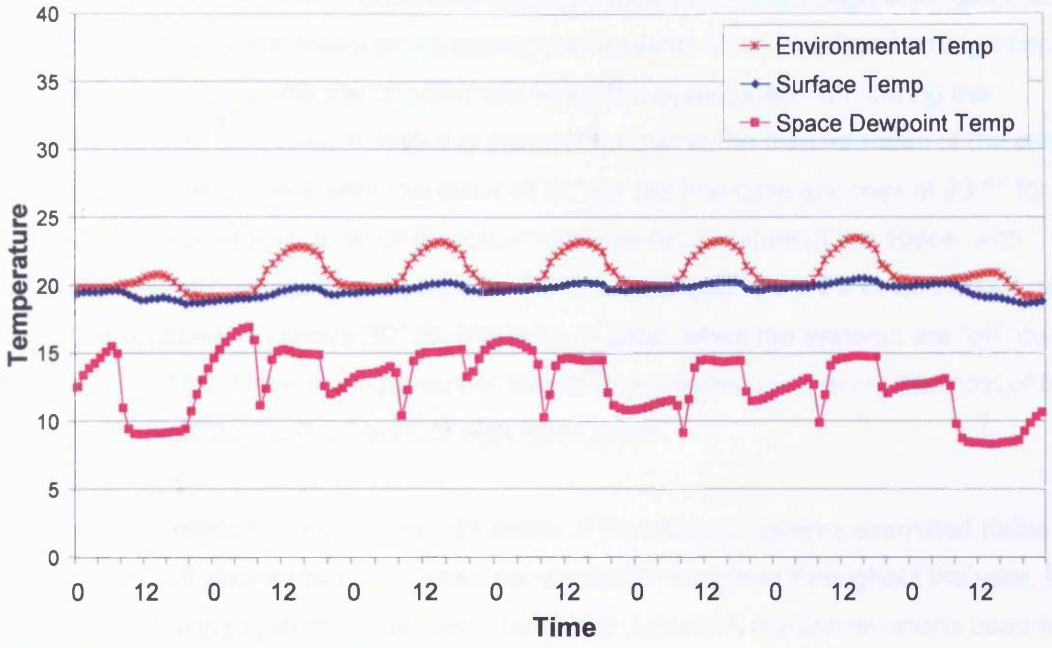


Figure 8.17a: Internal conditions with a 45° tilted blind (0.5 reflection) positioned externally and 0.1ac/h infiltration rate. Systems "on" during weekends (Athens, Greece)

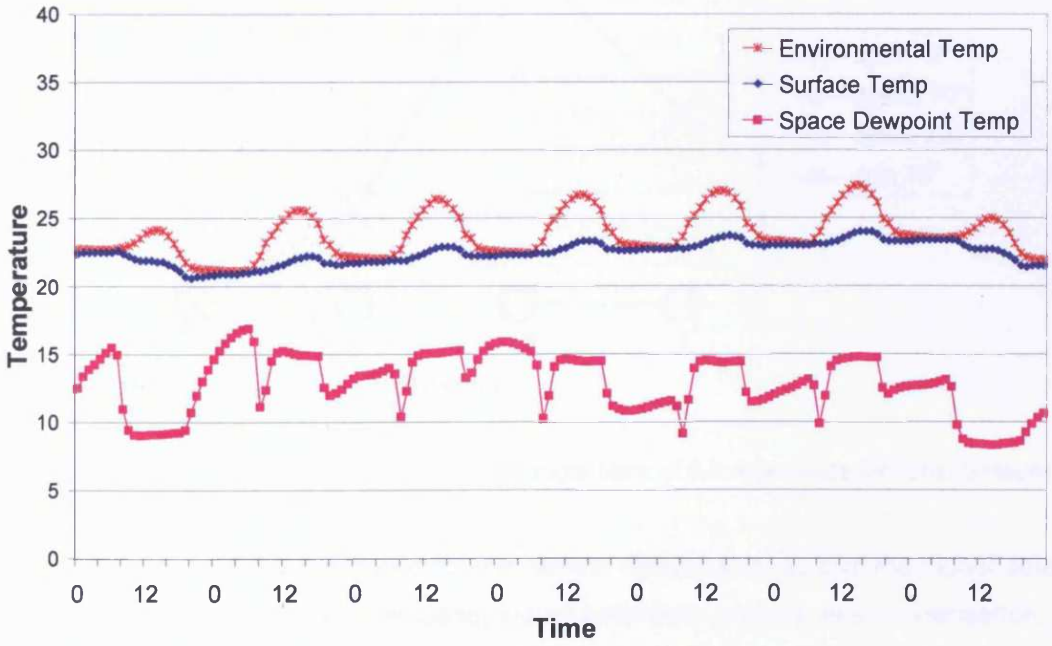


Figure 8.17b: Internal conditions with a 20° tilted blind positioned externally and 0.1ac/h infiltration rate. Systems "on" during weekends (Athens, Greece)

Cases that could potentially cause overheating during the hours of high solar gains could benefit from the thermal mass of the ceiling and a systems "on" weekend arrangement. Comparing the above with the results from when the systems are "off" during the weekend (figures 8.15a and 8.16a) it is shown that due to the thermal mass of the ceiling the surface temperature is kept low (max of 21° for the first case and max of 23.5° for the second case), and as a result the environmental temperature of the space, with highest temperatures reaching as high as 23°C as opposed to the 29°C for the first case and 27° as opposed to above 30° for the second case, when the systems are "off" during the weekend. The above arrangement in this case would help in making the most of the available daylight during the hours of high solar gains.

There was condensation occurring with some of the glazing systems examined (table 8.4). Figure 8.18 shows the hours when condensation occurred throughout the year, for the different glazing systems examined. Table 8.2 describes the abbreviations used for each case in the graphs presented.

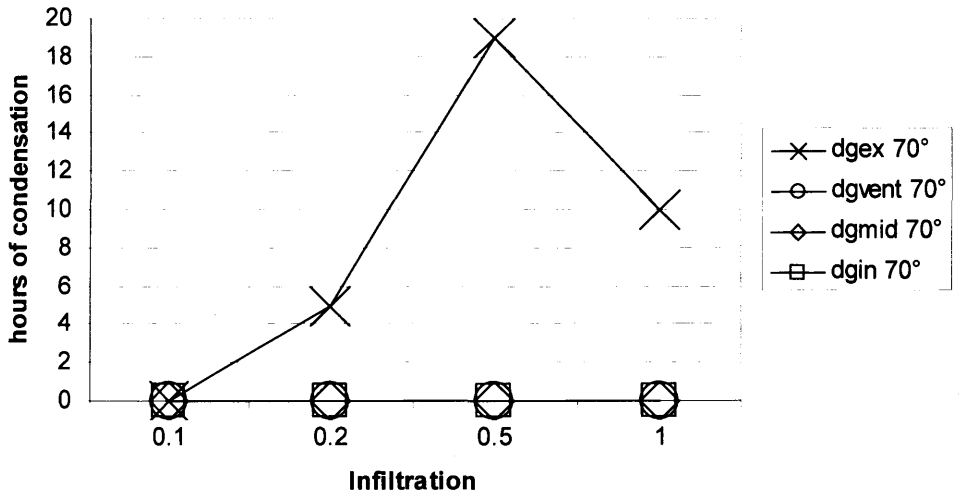


Figure 8.18: Condensation levels for a 70° slat angle blind of 0.5 reflectance (Athens, Greece)

The condensation levels examined for the Athens climate showed that the higher solar gain cases (e.g. internal and inter-pane) would potentially present less condensation, while lower solar gain cases (e.g. external) would potentially present higher condensation levels when combined with the specific cooling system under consideration. The above contradictory results are noticed because in the summer the

low power cooling system (35W/m$^2$) is unable to cope with the heat load of the room when coupled with high solar gain glazing systems and so the space and surface temperatures rise above the air dew point. The same cooling system is working efficiently when coupled with lower solar gain cases and so space and surface temperatures might fall below the air dew point and condensation could happen (figure 8.18).

It is also noticed from the same graph that for almost sealed buildings (infiltration of 0.1ac/h) there is no condensation, while condensation levels start to rise with increased infiltration. Moisture content increases with increased humid air coming into the space due to infiltration and the higher the moisture content of the air the higher its dew point temperature and so the higher the possibility of the surface temperature falling below the air dew point temperature.

It is important to notice here that the above condensation levels were all occurred during weekends and night time when the humidity control was switched off. Due to the ceilings thermal mass the surface temperatures stay low during the night and weekends which implies that the "systems off" period could be important for the prevention of condensation.

Figure 8.18 also shows that condensation levels for the externally positioned blind of 70° slat angle increase up to a 0.5ac/h of infiltration rate and decrease again for 1.0ac/h of infiltration rate. The above is caused because the increased warm air coming in the space due to increased infiltration raises the air temperature in the space above its dew point and less condensation occurs. The above is shown in a graphical way in figures 8.19 a & b where the internal conditions are presented for a night time in September between a weekday and a weekend (16$^{th}$ – 17$^{th}$ September).

It should be noted here that the condensation levels for the various glazing systems could potentially change with alterations in the cooling system's operation or/and capacity e.g. when systems are staying switched on during weekends as well as weekdays, during hot periods of the summer. Glazing options that seem not to cause condensation (e.g. 20° and 45° slat angle blinds) could potentially present condensation by increased efficiency of the cooling system's operation.

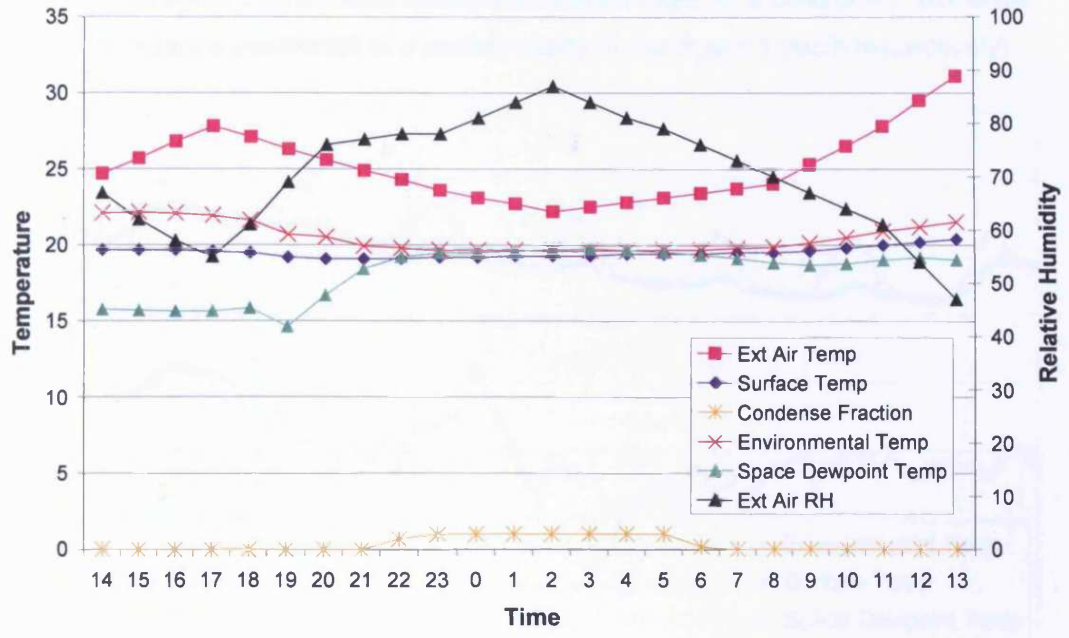


Figure 8.19a: Condensation levels for 0.5ac/h infiltration rate, 70° slat angle blind of 0.5 reflection positioned externally (Athens, Greece)

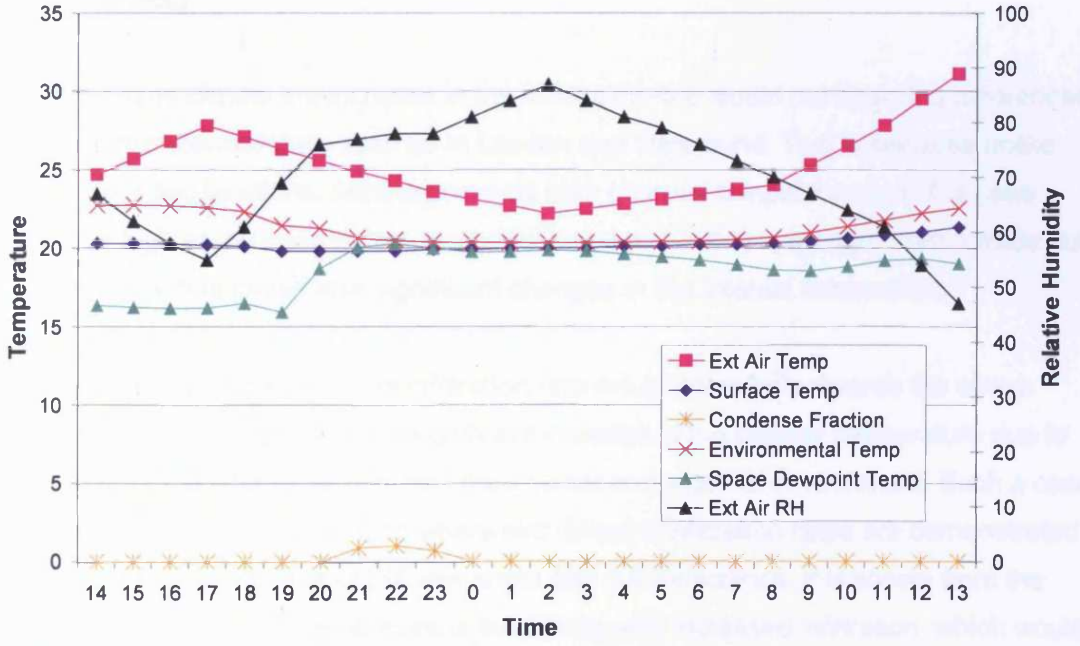


Figure 8.19b: Condensation levels for 1.0ac/h infiltration rate, 70° slat angle blind of 0.5 reflection positioned externally (Athens, Greece)

Figures 8.15c and 8.20a present different infiltration rates for a blind of 45° slat angle and 0.5 reflectance positioned in a sealed cavity (0.1ac/h and 1.0ac/h respectively).

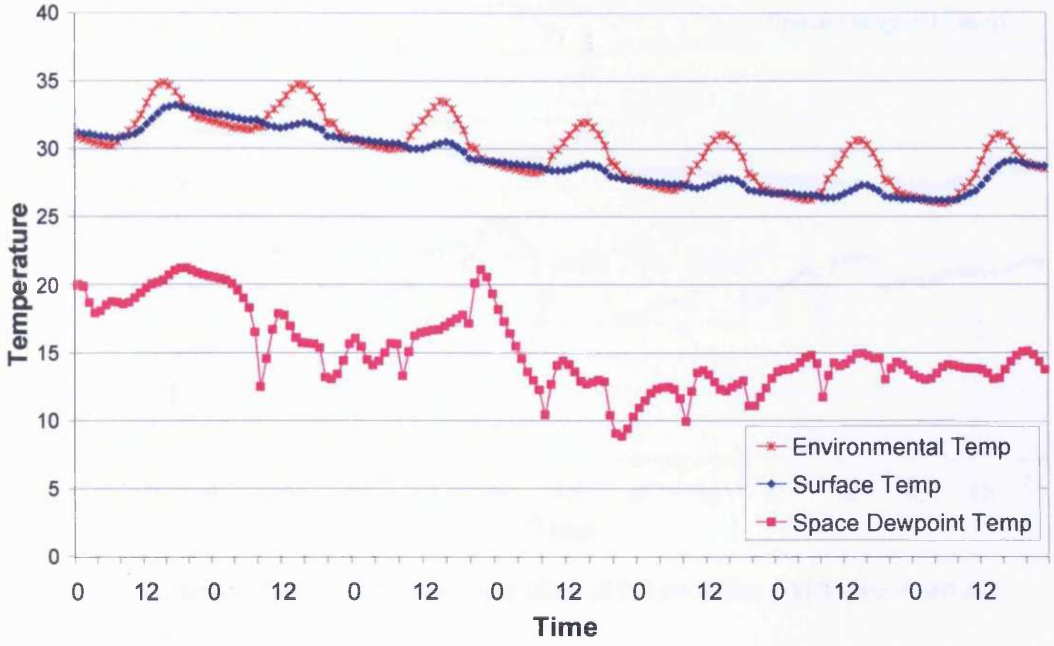


Figure 8.20c: 1.0ac/h infiltration, 45° slat angle blind of 0.5 reflection positioned in sealed cavity (Athens, Greece)

For the Athens climate the increase in the infiltration rate would not show big differences in the internal thermal state such as in London and Ostersund. That is because unlike the previous two locations, Athens presents high external temperatures, in this case almost as high as the internal temperatures, so warm air that is brought from outside due to infiltration would cause less significant changes in the internal temperature.

In low gain cases increase in the infiltration rate would potentially reverse the above phenomenon and would cause a significant increase in the internal temperature due to high temperature difference between the internal and external environment. Such a case is presented in figure 8.21 (a & b) where two different infiltration rates are demonstrated for the double glazing case of 70° slat angle and 0.5 reflectance. It is shown from the graphs that the internal temperature is increasing with increased infiltration, which would be an undesirable effect during the hours of high solar gains.

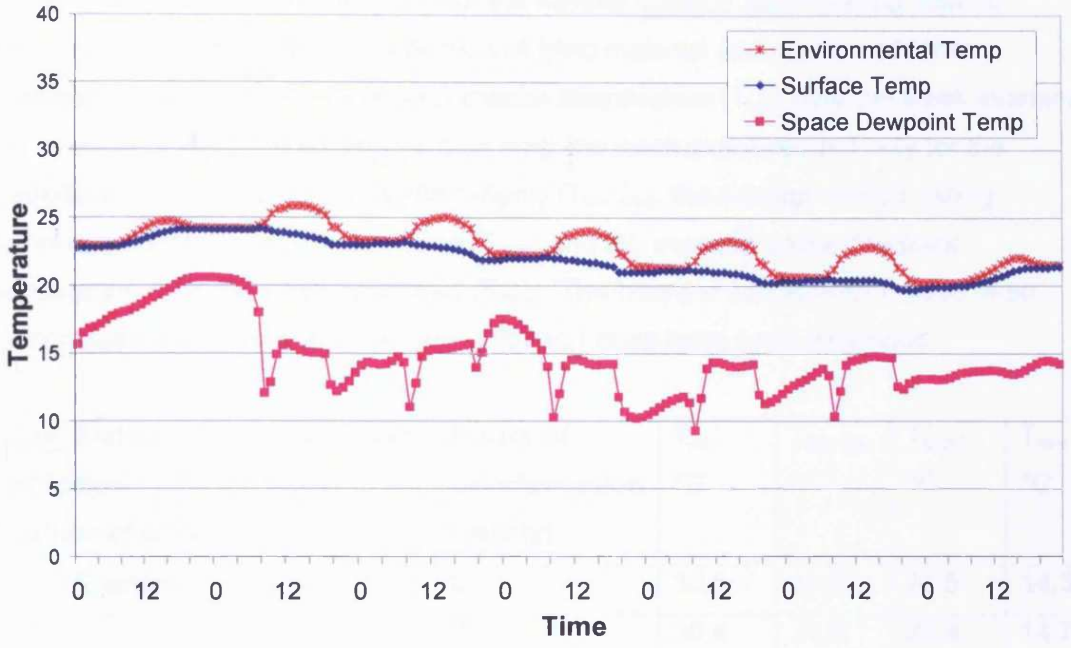


Figure 8.21a: 0.2ac/h infiltration, 70° slat angle blind of 0.5 reflection positioned externally (Athens, Greece)

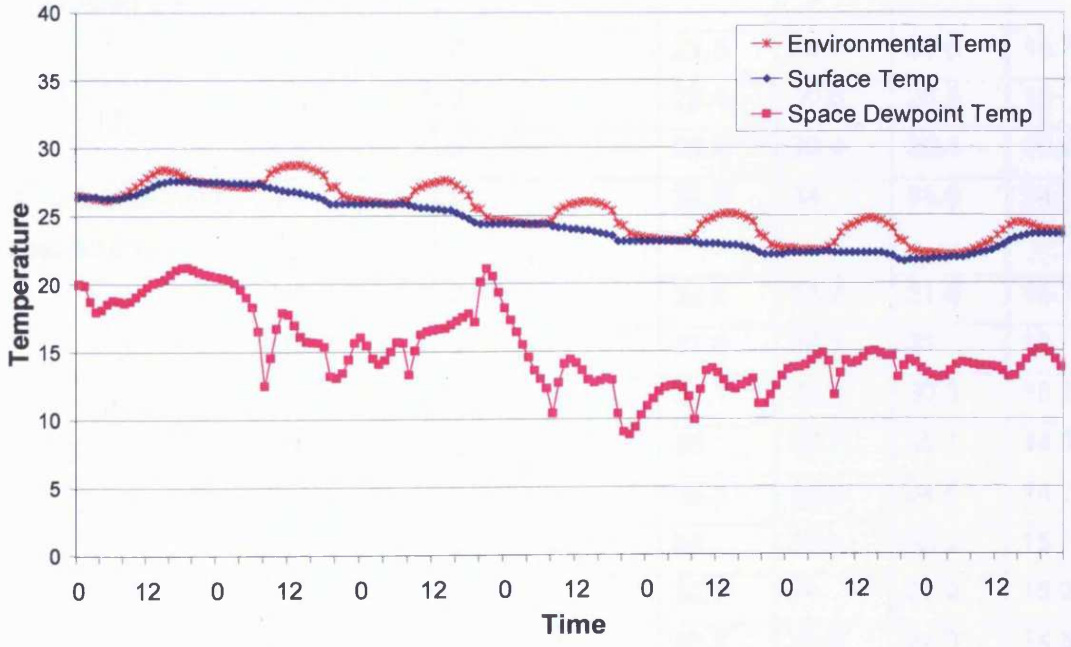


Figure 8.21b: 1.0ac/h infiltration, 70° slat angle blind of 0.5 reflection positioned externally (Athens, Greece)

Table 8.4 summarises the results from the Athens location; each glazing case is described by the angle of slat, reflection of blind material and position of blind. Summarised are the average environmental temperature ($T_{env}$) over the week examined, the average environmental temperature over the week examined but only for the weekdays and occupancy hours (8am-6pm) ($T_{env\ 8\text{-}6}$), the average chilled ceiling temperature over the week examined ($T_{surf}$) and the average space dewpoint temperature over the week examined ($T_{dew}$). The hours of condensation have been summarised over a year and various infiltration rates have been examined.

| **Case: Slat angle/ Reflection/ Position of blind** | **Infiltration Ac/h** | **Hours of Condensation (yearly)** | **$T_{env}$ °C** | **$T_{env\ 8\text{-}6}$ °C** | **$T_{surf}$ °C** | **$T_{dew}$ °C** |
|---|---|---|---|---|---|---|
| 20°, 0.5, external | 0.1 | 0 | 30.5 | 31.6 | 29.5 | 14.3 |
| | 0.2 | 0 | 30.4 | 31.5 | 29.4 | 14.7 |
| | 0.5 | 0 | 30.1 | 31.2 | 29.2 | 15 |
| | 1.0 | 0 | 29.7 | 30.9 | 28.9 | 15.2 |
| 20°, 0.5, inter-pane in ventilated cavity | 0.1 | 0 | 29.5 | 30.7 | 28.6 | 14.3 |
| | 0.2 | 0 | 29.5 | 30.7 | 28.6 | 14.7 |
| | 0.5 | 0 | 29.4 | 30.6 | 28.5 | 15 |
| | 1.0 | 0 | 29.2 | 30.4 | 28.4 | 15.2 |
| 20°, 0.5, inter-pane in sealed cavity | 0.1 | 0 | 32.8 | 34 | 31.9 | 14.3 |
| | 0.2 | 0 | 32.5 | 33.7 | 31.6 | 14.7 |
| | 0.5 | 0 | 31.8 | 33.1 | 31 | 15 |
| | 1.0 | 0 | 31.1 | 32.4 | 30.3 | 15.2 |
| 20°, 0.5, internal | 0.1 | 0 | 36 | 37.2 | 35.1 | 14.3 |
| | 0.2 | 0 | 35.4 | 36.6 | 34.5 | 14.7 |
| | 0.5 | 0 | 34 | 35.4 | 33.2 | 15 |
| | 1.0 | 0 | 32.7 | 34 | 31.9 | 15.2 |
| 45°, 0.5, external | 0.1 | 0 | 25.7 | 26.8 | 24.8 | 14.3 |
| | 0.2 | 0 | 26 | 27.1 | 25.1 | 14.7 |
| | 0.5 | 0 | 26.7 | 27.7 | 25.8 | 15 |

| | | | | | | |
|---|---|---|---|---|---|---|
| | 1.0 | 0 | 27.2 | 28.1 | 26.3 | 15.2 |
| 45°, 0.5, inter-pane in ventilated cavity | 0.1 | 0 | 26.4 | 27.5 | 25.4 | 14.3 |
| | 0.2 | 0 | 26.6 | 27.7 | 25.7 | 14.7 |
| | 0.5 | 0 | 27.1 | 28.1 | 26.2 | 15 |
| | 1.0 | 0 | 27.5 | 28.5 | 26.6 | 15.2 |
| 45°, 0.5, inter-pane in sealed cavity | 0.1 | 0 | 30.8 | 32 | 29.9 | 14.3 |
| | 0.2 | 0 | 30.7 | 31.8 | 29.7 | 14.7 |
| | 0.5 | 0 | 30.3 | 31.5 | 29.4 | 15 |
| | 1.0 | 0 | 29.9 | 31.1 | 29.1 | 15.2 |
| 45°, 0.5, internal | 0.1 | 0 | 36.4 | 37.6 | 35.5 | 14.3 |
| | 0.2 | 0 | 35.7 | 37 | 34.8 | 14.7 |
| | 0.5 | 0 | 34.3 | 35.6 | 33.5 | 15 |
| | 1.0 | 0 | 32.9 | 34.2 | 32.1 | 15.2 |
| 45°, 0.2, external | 0.1 | 0 | 24.3 | 25.4 | 23.3 | 14.3 |
| | 0.2 | 0 | 24.7 | 25.4 | 23.8 | 14.7 |
| | 0.5 | 0 | 25.6 | 26.6 | 24.7 | 15 |
| | 1.0 | 0 | 26.3 | 27.2 | 25.5 | 15.2 |
| 45°, 0.2, inter-pane in ventilated cavity | 0.1 | 0 | 25.8 | 26.9 | 24.9 | 14.3 |
| | 0.2 | 0 | 26.1 | 27.2 | 25.2 | 14.7 |
| | 0.5 | 0 | 26.7 | 27.7 | 25.8 | 15 |
| | 1.0 | 0 | 27.2 | 28.1 | 26.3 | 15.2 |
| 45°, 0.2, inter-pane in sealed cavity | 0.1 | 0 | 32 | 33.2 | 31.1 | 14.3 |
| | 0.2 | 0 | 31.7 | 32.9 | 30.8 | 14.7 |
| | 0.5 | 0 | 31.2 | 32.4 | 30.3 | 15 |
| | 1.0 | 0 | 30.6 | 31.8 | 29.8 | 15.2 |
| 45°, 0.2, internal | 0.1 | 0 | 38.7 | 39.9 | 37.8 | 14.3 |
| | 0.2 | 0 | 37.8 | 39.1 | 37 | 14.7 |
| | 0.5 | 0 | 36 | 37.4 | 35.2 | 15 |
| | 1.0 | 0 | 34.1 | 35.5 | 33.4 | 15.2 |

| | | | | | | |
|---|---|---|---|---|---|---|
| 45°, 0.8, external | 0.1 | 0 | 28.6 | 29.8 | 27.7 | 14.3 |
| | 0.2 | 0 | 28.7 | 29.8 | 27.7 | 14.7 |
| | 0.5 | 0 | 28.8 | 29.9 | 27.9 | 15 |
| | 1.0 | 0 | 28.9 | 30.1 | 28.1 | 15.2 |
| 45°, 0.8, inter-pane in ventilated cavity | 0.1 | 0 | 27.5 | 28.6 | 26.5 | 14.3 |
| | 0.2 | 0 | 27.6 | 28.7 | 26.7 | 14.7 |
| | 0.5 | 0 | 27.9 | 29 | 27 | 15 |
| | 1.0 | 0 | 28.1 | 29.1 | 27.2 | 15.2 |
| 45°, 0.8, inter-pane in sealed cavity | 0.1 | 0 | 29.5 | 30.7 | 28.6 | 14.3 |
| | 0.2 | 0 | 29.5 | 30.7 | 28.6 | 14.7 |
| | 0.5 | 0 | 29.4 | 30.6 | 28.5 | 15 |
| | 1.0 | 0 | 29.2 | 30.4 | 28.4 | 15.2 |
| 45°, 0.8, internal | 0.1 | 0 | 33 | 34.2 | 32 | 14.3 |
| | 0.2 | 0 | 32.6 | 33.8 | 31.7 | 14.7 |
| | 0.5 | 0 | 31.9 | 33.1 | 31 | 15 |
| | 1.0 | 0 | 31 | 32.3 | 30.2 | 15.2 |
| 70°, 0.5, external | 0.1 | 0 | 22.2 | 23.2 | 21.2 | 14.3 |
| | 0.2 | 5 | 22.8 | 23.8 | 21.9 | 14.7 |
| | 0.5 | 19 | 24.1 | 25 | 23.2 | 15 |
| | 1.0 | 10 | 25.2 | 26 | 24.3 | 15.2 |
| 70°, 0.5, inter-pane in ventilated cavity | 0.1 | 0 | 23.6 | 24.6 | 22.7 | 14.3 |
| | 0.2 | 0 | 24.1 | 25.1 | 23.2 | 14.7 |
| | 0.5 | 0 | 25.1 | 26 | 24.2 | 15 |
| | 1.0 | 0 | 25.9 | 26.8 | 25.1 | 15.2 |
| 70°, 0.5, inter-pane in sealed cavity | 0.1 | 0 | 28.4 | 29.5 | 27.5 | 14.3 |
| | 0.2 | 0 | 28.5 | 29.6 | 27.6 | 14.7 |
| | 0.5 | 0 | 28.6 | 29.7 | 27.7 | 15 |
| | 1.0 | 0 | 28.6 | 29.6 | 27.7 | 15.2 |
| 70°, 0.5, internal | 0.1 | 0 | 35.2 | 36.3 | 34.3 | 14.3 |

| | | | | | | |
|---|---|---|---|---|---|---|
| | 0.2 | 0 | 34.6 | 35.8 | 33.7 | 14.7 |
| | 0.5 | 0 | 33.4 | 34.7 | 32.6 | 15 |
| | 1.0 | 0 | 32.2 | 33.5 | 31.4 | 15.2 |

Table 8.4: Summary of results for Athens

## *8.3 Conclusions*

An energy efficient cooling system was studied regarding its ability to keep acceptable internal environmental temperatures when coupled with the various glazing systems under consideration and for three locations. Condensation levels were also examined for various infiltration rates.

It was found that the different glazing systems could have an effect on the performance of the cooling system, in particular in the ability of the system to control environmental temperature and in the potential for condensation occurring on the chilled ceiling surface.

Internal temperatures

Regarding the position of the blind, it was shown that the cases with externally positioned blind or blind in a ventilated cavity presented lower environmental temperatures than the cases with blind in a sealed cavity and internally positioned blind, for the same blind characteristics.

Regarding the slat angle, it was shown that the higher the slat angle the lower the environmental temperature. Overheating could occur with the blind positioned in a sealed cavity or internally and mostly during the first few days after the weekend when the systems were "off" and temperatures were allowed to rise.

Regarding the blind colour, it was shown that the lighter the colour the lower the internal temperatures, except from the externally positioned blinds where the darker blind presented the lower internal temperatures.

Regarding the location of the building, it was shown that some higher solar gain cases could perform efficiently in cold climates (e.g. Ostersund), due to low external

temperatures, but are being on the verge of causing or even causing overheating in the warmer climates (e.g. Athens). It was also shown that such cases could improve their performance in warmer climates with a "systems on" approach during the weekends. Such approach is keeping control of the space temperature during the weekends and so the cooling system is able to cope with the extra heat gains coming in the space with higher solar gain cases, during occupancy.

Condensation levels

Condensation events on the chilled ceiling were also examined and expressed by the amount of hours that condensation occurred, for the yearly weather data used, for the three locations. The results showed no condensation levels for the Ostersund location, while high levels were noticed in the London climate due to the nature of the incoming air (warmer and more humid) due to infiltration, causing condensation when getting in touch with the cool ceiling surface. In Athens due to high internal heat gains in most of the cases the cooling system was not powerful enough to lower the internal temperatures in levels where condensation could occur, so only the very low solar gain cases presented condensation risk.

Overall, the higher solar gain cases (e.g. internal and inter-pane) would potentially present less condensation, while lower solar gain cases (e.g. external) would potentially present higher condensation levels when combined with the specific cooling system under consideration. The above contradictory results were noticed because in the summer the low power cooling system ($35W/m^2$, a practical limit of chilled ceiling approach based on internal loads of $25W/m^2$ and design solar loads of $10W/m^2$) was unable to cope with the heat load of the room when coupled with high solar gain glazing systems and so the space and surface temperatures rise above air dew point. The same cooling system was working efficiently when coupled with lower solar gain cases and so surface temperatures fell below the air dew point and condensation occurred.

It should be noted here that in some cases when condensation was not a problem, the system was not working satisfactorily (e.g. the temperature rise above desirable levels). In that case an alternative or supplementary cooling system might be used, which could potentially change the condensation events occurring on the chilled surface.

The cooling system worked efficiently, and with no condensation events occurring, with external and inter-pane in ventilated cavity blind cases of 45° and 70° slat angle, in Ostersund and London, but for London only when infiltration rates were minimised. The above glazing cases showed increased occurrence of condensation with increased infiltration, in London, while for Ostersund there was no condensation occurring even with increased infiltration. In Athens the system worked efficiently only with the very low solar gain blind cases (e.g. externally positioned 70° slat angle blind) and condensation occurred with increased infiltration.

From the above it is implied that the chilled ceiling cooling system is more suitable for cooler drier climates while lack of cooling effectiveness or condensation occurrence could be a problem in warm and/or humid climates. The above results also imply that even though the choice of glazing could affect the condensation levels in a room the control of infiltration rates is the parameter most important for the prevention of condensation in the space.

It is important to notice here that all condensation events occurred during weekends and night time when the humidity control in the mechanical air supply was switched off. Due to the ceilings thermal mass the surface temperatures stay low during the night and weekends which implies that "systems off" periods could be important. An example in London climate demonstrated that with a ventilation system "on" approach, even with high infiltration rates, condensation could be avoided if there is a humidity control in the space.

Infiltration rates

Comparing different infiltration rates for the same glazing systems it was shown that for outside temperatures cooler than inside the higher the infiltration rates the lower the environmental temperature, especially in high solar gain cases, because the cool outside air brought in due to infiltration is helping to remove part of the heat gains in the space (e.g. London and Ostersund). The above trend was less obvious for low solar gain cases, as the difference between the external and internal temperature is not as high and less heat transfer occurred.

When external temperatures are as high as the internal temperatures (e.g. Athens) the warm air brought from outside due to infiltration would cause less significant changes in the internal temperatures. In low gain cases increase in the infiltration rate would potentially reverse the above phenomenon and would cause a significant increase in the internal temperatures due to high temperature difference between the internal and external environment, which would be an undesirable effect during the hours of high solar gains.

So when outside temperatures are lower than inside, air that comes in due to intentional or unintentional ventilation (e.g. by opening the window) during the pick of the internal heat gains could potentially improve the thermal state of the interior, when high solar gain glazing systems are used. When outside temperatures are higher than inside temperatures, a sealed building / closed windows approach could be beneficial in order to keep low internal temperatures.

Overall, the performance of the chilled ceiling cooling system showed to be affected by the choice of glazing/blind option, but greater, in terms of both condensation and temperature control, was the effect of infiltration rates.

## 8.4 References

CIBSE (2006) 'Environmental Design', CIBSE Guide, Vol. A, Chartered Institution of Building Services Engineers, London

CIBSE (2001-2002) 'Heating, Ventilation, Air conditioning and Refrigeration', CIBSE Guide, Vol. B, Chartered Institution of Building Services Engineers, London

ASHRAE Standard 62 (2001) 'Ventilation for Acceptable Indoor Air Quality', American Society of Heating, Refrigerating and Air conditioning Engineer, Atlanta

CEN CR 1752 (1998) 'Ventilation for Buildings: Design Criteria for the Indoor Environment', European Organisation for Standardisation, Brussels

# Chapter 9

# Research Outcome and Recommendations for Future Research

## *9.1 Overview*

This chapter will summarise the findings of this research and conclusions will be drawn based on the objectives set in the first chapter. Recommendations for further research will also be presented based on the further development of the tools and for their application to other research projects.

## *9.2 Chapter by Chapter Research Outcome*

### *1. Research overview*

Glass is a material widely used in office buildings because it offers visual contact with the outside and maximise the use of the available daylight during the working hours of the day, creating a healthy and pleasant environment for the occupants. Due to recent technological advances, glass has also become a popular material towards energy efficient buildings. Large window areas are being increasingly introduced and fully glazed facades are being designed as the building's external skin in order to make the most of the natural daylight and minimise electricity costs. Furthermore, low U-values of advanced glazing systems minimise heat losses and make possible the exploitation of the winter sun for passive heating, allowing low heating costs during the winter months.

However, there are still problems associated with highly glazed buildings such as high solar gains, often resulting in overheating and excessive use of mechanical cooling. This work aimed to minimise the solar gains entering the space through the transparent

elements of a building's façade, by investigating the thermal performance of various shaded glazing options, through the use of thermal modelling.

## *2. Origins of Research*

Research on the transportation of solar radiation through glazing systems, with slat-type shading, gradually developed from one considering only the direct solar radiation transfer to one including also the secondary heat transfer. Both elements are used in order to characterise the thermal performance of a glazing system and its individual components, as embodied by a single value, the g-value, usually calculated under steady-state conditions and for normal angle of incident.

Starting with oversimplified calculation methods research gradually developed complex mathematical calculation models and experimental measurement methods, in controlled environment or in real climate, in order to calculate the g-value of various glazing options and provide the designer with general guidelines for the use of such systems.

All above calculation methods proved to be time consuming and impractical, restricting the performance predictions to the research community, when one had to take under consideration a wide variety of material and shading options or when technology introduced advanced or new materials that needed description.

Most recent research recognised the need for flexible prediction tools that would calculate the thermal performance of various multilayered glazing options at an early design stage, also taking under consideration the location, the orientation and the environmental conditions of the individual building. Furthermore, identified was the importance of the angle of solar incident, not only the vertical but also the sun altitude and azimuth dependant, in the thermal performance of the various angle dependant glazing options (i.e. with slat-type blinds).

To address the above issues, flexible computer models were developed that would calculate the g-value and the solar properties of different glazing systems, with the possibility of integrated shading options, under steady-state conditions or under more

realistic scenarios and with the prospect of updating the material library when new technological advances directed it.

WIS and WINDOW5 are the two prediction tools currently used to calculate the g-value (or SHGC) of various glazing systems with and without shading (there is no shading option in the WINDOW5 software) for normal incidence and under steady-state conditions. Output data produced by these two computer models can be used as input data in subroutines in more detailed energy simulation programs in order to calculate the energy use in a building, while the g-value (or SHGC) produced can be used for comparing different glazing options.

ParaSol is a tool for designers to predict the thermal performance of different glazing systems with integrated shading techniques, during the early design stage of a building. This prediction tool is producing a g-value for both normal incident, under steady-state conditions, and a monthly average for local climate conditions and for various locations, but for a limited range of options.

The prediction tool review identified the need for a tool that would be able to provide a comparable value calculated under steady-state conditions as well as a more realistic value, dynamically calculated under more realistic scenarios, for the description of a wide variety of glazing systems currently in the market, and at the same time flexible enough to incorporate future technological advances.

## ***3. Description of Prediction Tools Used in this Research***

Two existing simulation packages were chosen and modified in order to be used in this work for the study of the thermal performance of various multilayered glazing systems. HTB2 was chosen because of its flexibility in use and further development, offering various options for the calculation environment (under steady-state or real climate conditions) and various options of building form, fabric and building systems. Modifications to the model involved the more accurate representation of the different glazing systems and their treatment of optical and thermal properties.

The glass simulation program calculates the solar properties, which vary in relative altitude and azimuth, of various glazing systems, composed by a series of layers, each layer being either glass or blind. The glass simulation program was chosen for this research because of its flexibility in calculating a wide range of glazing options and its compatibility with the thermal model HTB2. Modifications to the program were undergone in order to further widen the options of glazing to be calculated and also produce a more realistic representation of their solar properties.

### *4. Solar Radiation Transfer through Glazing & Review of Total Solar Transmittance Theory and Practice*

The review of the calculation of the g-value revealed that even though some differences are expressed in the way the g-value is measured or calculated, depending on the availability of resources and calculation methods used, the variables that influence the g-value and so the thermal performance of a glazing system are the same; i.e. the incident solar radiation, the optical and thermal properties of the glazing system and its components, and the temperature difference between internal and external environment (for the calculations/measurements under real climate conditions), while it excludes any heat losses through the system.

As a result of the investigation a distinction was made between the steady-state G-value and the dynamically calculated $\hat{g}_d$ value under real climate conditions. Taking under consideration all the variables that influence the total solar transmittance a calculation method was suggested for both G-value and $\hat{g}_d$ value and also the boundary conditions for the calculation of steady-state G-value.

### *5. Evaluation of Prediction Tools*

Comparisons of results were presented between the reference model WIS 3.0.1 and the modified prediction tools, under steady-state conditions, and between the prediction tools and measurements, under real climate conditions. Examined under steady-state conditions were the blind transmission characteristics in isolation and in combination with glass panes and the G-values of various glazing systems with integrated slat-type shading in various positions (internal, external and inter-pane) and of various slat angles.

Internally positioned roller blinds were also examined for a range of blind material characteristics and various ventilation rates in the cavity between the internal glass pane and the roller blinds. The $\hat{g}_d$ value of various glass-shading combinations was also compared with results from real climate measurements, made independently at a test facility in Sweden.

The results from the above comparisons showed that although there is scope for further improvements in the calculation of diffused and absorption characteristics of slat-type blind configurations, the prediction tools will be able to distinguish between basic design alternatives, in the choice of similar shaded glazing options, in a sufficient to many applications in the design industry level of accuracy.

## ***6. Application to Shaded Glazing Systems***

The prediction tools were used to predict the relative performance of four different glazing systems consisted of a double glazing unit with integrated slat-type blinds, of various slat angles and reflection characteristics, positioned externally, inter-pane and internally. The inter-pane option has been studied for both sealed cavity and ventilated cavity. The g-value of each of the above systems was calculated for both steady-state conditions (G-value) and vertical angle of incidence, and for real climate conditions ($\hat{g}_d$ - value). All systems were simulated for a simple office space in order to enable their relative thermal performance to be assessed.

### *Steady-state G-value*

The results from the calculations under steady-state conditions showed that G-value depends on the blind characteristics, colour and angle of tilt of the blind, the position of the blind and the angle of incident of solar radiation.

Light colour blinds result in lower G-values with exception only when such blinds are positioned externally; for that position only low reflectance blinds (dark colour) present lower G-values than high reflectance blinds (light colour). Furthermore, for light blinds the variation of G between the cases of the same blind characteristics, but various positions, is smaller than for dark blinds.

Lower G-values, for the blinds of the same colour, were achieved with higher slat angles, especially for near to normal angles of incident. Also, the higher the slat angle the smaller the G variation, while for the cases with low slat angle G is widely varying. Furthermore, for low slat angles the variation of G between the cases of the same blind characteristics, but various positions, is smaller than for high slat angles.

Externally positioned blinds showed, for a consistent surface reflectance and slat angle, the lowest G-values, but examples also demonstrated that G for externally positioned blinds can be higher than for internally positioned or inter-pane blinds, if surface colour and blade angle are not carefully chosen. Furthermore, ventilation in the cavity of inter-pane blind cases can improve the thermal performance of a glazing system.

In addition to the blind characteristics and position of the blind, G showed a high dependency on the angle of incidence, with higher values presented at angles of incident close to normal, and lower values at higher angles of incident. Also noticed was that the sensitivity of the G-value's angle dependency is directly related to the slat angle. The higher the slat angle the smaller the G variation, while for the cases with lower slat angles, G is widely varying.

*Dynamically calculated $\hat{g}_d$ value*

Hourly weather data from three European locations were used in order to examine the thermal performance of the same shaded glazing options. Environmental conditions for the office space were also set, with values for room ventilation, occupancy levels, lighting and small power sources. A daily average $\hat{g}_d$ was calculated from the simulation results using only the daylight hours, for each month.

The results showed that except from the slat-type blind characteristics and position of the blind $\hat{g}_d$ also depends on the temperature difference between the external and internal environment, the solar angles and the location of the building.

The temperature difference between the external and internal environment affects the surface temperature of the glazing system and as a result affects the heat transfer to and

from the surface of the glazing system. For the calculation of $\hat{g}_d$ the surface heat flow fluctuates as opposed to the calculation of G that is steady.

For most cases $\hat{g}_d$ reaches its maximum value during the winter period and its minimum value during the summer. The sensitivity of $\hat{g}_d$ to the seasonal variation is also directly related to the slat angle of the blind. The higher the slat angle the smaller the $\hat{g}_d$ variation, while for the cases with low slat angle, $\hat{g}_d$ is widely varying.

The seasonal variation of $\hat{g}_d$ is less obvious for south climates and more apparent for north climates, which is directly connected to the seasonal variation of the sun's altitude. The connection between seasonal variation and slat angle is less apparent for south locations and more apparent for north climates.

Furthermore, most cases present similar $\hat{g}_d$ values during the summer months and different $\hat{g}_d$ values during the winter months, and for most cases, the further north the location the higher the winter $\hat{g}_d$ values. The above was more noticeable for low slat angles, while for blind cases with higher slat angle a similar $\hat{g}_d$ was showed throughout the year in all locations.

Generally, from the results under real climate conditions, for three locations of different altitudes, it was shown that while between the cases of the same blind characteristics (and different blind position), of the same location, the secondary heat was the factor mostly affecting the $\hat{g}_d$ variation, between the same cases (in the same position) of different location the factor mostly affecting the $\hat{g}_d$ variation was the sun altitude; for the latter, differences mostly noticeable during the winter months, depending on how far from normal is the sun altitude.

*Comparison between G and $\hat{g}_d$*

Comparisons between the G calculated under steady-state conditions and the dynamically calculated $\hat{g}_d$ showed that G for normal incident could be far from the $\hat{g}_d$ values occurring during the summer, since G is calculated for normal incident and is closer to the winter solar incident rather than the summer one. The above difference was more noticeable for the cases with lower slat angles, with winter $\hat{g}_d$ values much higher

than the summer. Similarly, the difference between G and $\hat{g}_d$ and the seasonal variation was less obvious for higher slat angles, when the direct transmission was reduced to a minimum.

In comparing glazing options, such as the placement of a blind, there was a consistency in the relative rankings between the two calculation methods. The externally positioned blind, in most cases, with some seasonal exceptions, showed the best performance compared to the other cases, while the internal blind case showed the poorest thermal performance. However examples demonstrated that in more detailed comparisons, some rankings alter with cases presenting similar or even better summer and in some cases yearly, thermal performance, even though their steady-state G suggested otherwise.

*Sensitivity of $\hat{g}_d$ value to ventilation through the cavity*

The sensitivity of the $\hat{g}_d$ value to the ventilation rate through a cavity was examined for a variety of internally positioned roller blinds of different material and colour and for a variety of vent size at the top and bottom of the roller blind.

The results showed that ventilation rates are sensitive to both colour of the material and size of the vents at the top and bottom of the blind. The darker the colour of the blind and the bigger the size of the gaps the more heat is likely to be transferred through the cavity into the room. Following this trend, the $\hat{g}_d$ value of the system is in turn sensitive to the ventilation variations formed by the above choices of installation of the shading device to the glazing unit.

## *7. Efficiency of the G-value and the $\hat{g}_d$ value as Indicators of Cooling Demand*

The comparison between the cooling loads needed to keep desirable internal temperatures in an office space, for the three locations, and G showed both that cases with different predicted G-values could result in similar cooling loads and that cases with similar G-values could result in significantly different cooling loads, since G is calculated only for normal incident while the cooling loads are calculated as an average of the

hours that the sun was shining, for both altitude and azimuth movement of the sun. Furthermore, results showed that while G is independent of location, the predicted cooling load depends on the location. For the above reasons G is not a good indicator of the relative cooling loads.

The comparison between the cooling loads and the dynamically calculated $\hat{g}_d$ values showed a better consistency between the results. The graphs of each site demonstrated that the cooling increases with increased $\hat{g}_d$, and the opposite. Also noticed was a small or no movement on the y axis ($\hat{g}_d$ values) and a more definable movement on the x axis (cooling loads). This non linear advance of the $\hat{g}_d$ values compared to the cooling loads is due to the way the $\hat{g}_d$ is calculated excluding any heat losses through the glazing, as opposed to the calculation of the cooling loads which includes the heat losses; i.e. higher for north locations than for south locations.

Overall, the two comparisons highlighted the potential for the standard G-value to miss-inform the designer on the choice of glazing system, while $\hat{g}_d$ could be used as a predictor of the relative cooling load demand, which makes the dynamically calculated $\hat{g}_d$ a more reliable indicator of the thermal performance of each glazing system, in practice, than the steady-state G.

## ***8. Application to a Case Study***

An energy efficient cooling system was examined regarding its ability to keep acceptable internal environmental temperatures when coupled with the various glazing systems under consideration and for three locations. Condensation levels were also examined for various infiltration rates.

Internal temperatures

Cases with externally positioned blind or blind in a ventilated cavity presented lower internal temperatures than the cases with blind in a sealed cavity and internally positioned blind, for the same blind characteristics. Higher slat angles presented lower temperatures, while the lighter the colour of the blind the lower the internal temperatures, except from the externally positioned blinds where the darker blind presented the lower internal temperatures.

Overheating mostly occurred during the first few days after the weekend when the systems were "off" and temperatures were allowed to rise. The thermally heavyweight cooling system was operating more efficiently during the end of the week. Also, higher internal temperatures were presented during the middle of the day, when external temperatures were also at pick. Furthermore, cases performing efficiently in the northern location were being on the verge of causing or even causing overheating in the southern location. It was also shown that such cases could benefit from a "systems on" approach during the weekends.

Condensation levels

The operation of the cooling system at the north location presented no condensation levels, while high levels were noticed in the humid London climate. High external summer temperatures and high internal heat gains for most of the cases in Athens presented failure of the cooling system to keep low internal temperatures and so only low solar gain cases presented condensation risk.

The higher solar gain cases (e.g. internal and inter-pane) would potentially present less condensation, while lower solar gain cases (e.g. external) would potentially present higher condensation levels when combined with the specific cooling system under consideration. The above contradictory results were noticed because in the summer the low power cooling system (35W/m$^2$, a practical limit of chilled ceiling approach based on internal loads of 25W/m$^2$ and design solar loads of 10W/m$^2$) was unable to cope with the heat load of the room when coupled with high solar gain glazing systems and so the space and surface temperatures rise above air dew point. The same cooling system was working efficiently when coupled with lower solar gain cases and so surface temperatures fell below the air dew point and condensation occurred.

It should be noted here that in some cases when condensation was not a problem, the system was not working satisfactorily (e.g. the temperature rise above desirable levels). In that case an alternative or supplementary cooling system might be used, which could potentially change the condensation events occurring on the chilled surface.

The cooling system worked efficiently, and with no condensation events occurring, with external and inter-pane in ventilated cavity blind cases of 45° and 70° slat angle, in

Ostersund and London, but for London only when infiltration rates were minimised. The above glazing cases showed increased occurrence of condensation with increased infiltration, in London, while for Ostersund there was no condensation occurring even with increased infiltration. In Athens the system worked efficiently only with the very low solar gain blind cases (e.g. externally positioned 70° slat angle blind) and condensation occurred with increased infiltration.

From the above it is implied that the chilled ceiling cooling system is more suitable for cooler drier climates while lack of cooling effectiveness or condensation occurrence could be a problem in warm and/or humid climates. The above results also imply that even though the choice of glazing could affect the condensation levels in a room the control of infiltration rates is the parameter most important for the prevention of condensation in the space.

Infiltration rates

Comparing different infiltration rates for the same glazing systems it was shown that non intentional ventilation could affect the thermal state of the space. When outside temperatures are lower than inside, air that comes in the room, due to intentional or unintentional ventilation (e.g. by opening the window), during the pick of the internal heat gains, could potentially improve the thermal state of the space, especially when high solar gain glazing systems are used. When outside temperatures are higher than inside temperatures, a sealed building / closed windows approach could be beneficial in order to keep low internal temperatures, especially when low solar gain glazing systems are in operation.

## *9.3 Recommendations for Future Research*

### 9.3.1 Further Development of the Prediction Tools

As demonstrated in this research and especially in chapter 5, the glass simulation tool presents some weaknesses. The need for further research and development related to the view factor of the program has been recognised since the current version seems to be underestimating the transmittance characteristics of highly reflective blinds with low angle tilted slats (see case study W80 chapter 5), and as a result of the glazing systems that integrate such slat-type devices. Furthermore, more weaknesses have been identified in the pre-processor when it was asked to calculate the transmittance characteristics of highly diffusive material, such as semi-transparent roller blind material.

The data produced by the glazing simulation program is currently transferred manually in the thermal model HTB2, which makes the combined tool less user friendly and time consuming. The embedment of the pre-processor in the interface of the thermal model HTB2 would create a more flexible and user friendly tool. Some work towards the above has already been considered (Alexander et al, 2005), but further research is needed.

The introduction of an anisotropic sky as opposed to the isotropic currently used to the HTB2 thermal model would also help in resolving problems related to "cut off" solar angles. Such problem was identified for the white blind of 0° slat angle during the comparison of results with real climate data (§5.3, chapter 5), where the prediction tool seem to overestimate the $\hat{g}_d$ during sunrise and sunset.

The development of the thermal model could be also related to the integration of extra features in order to enhance its area of application and validity of results. Such features could include a window frame choice that would allow the input of frame characteristics and would calculate the thermal exchanges with the glazing system, the integration of a CFD model in order to achieve a more realistic approach on the airflow in the ventilated cavities and in the space, especially for naturally ventilated buildings or for buildings of more complex geometry. Finally, the tool could be enhanced with a $CO_2$ emissions calculation model that could allow the designer to examine the implications of each possible design solution to the environment.

### 9.3.2 Use of the Tool in other Related Research

The tool developed and applied in this research could potentially be used towards exploring the use of various shading devices in real case studies where occupants are allowed to modify the shading position and tilt according to their own comfort. Such an investigation could be extended to visual as well as thermal comfort and could help understand how occupants' control affect the seasonal performance of the building, find an optimum control strategy that would be based on occupants' comfort and minimise at the same time energy consumption for cooling and lighting and further validate the prediction tool by comparing results with measurements.

Further research could be fused on the effect of ventilated cavities in multilayered glazing systems with the use of a CFD model along with the prediction tool used for this research. As briefly shown in chapter 6 the performance of the ventilated cavity depends on the airflow rate as well as on the properties and position of the shading device. As a result such a feature could influence the performance of the glazing system and of the building. Little information is currently available on the effect of ventilated cavities in the energy use of the building and a research based on a combination of thermal modelling and measurements would help in identifying the influence of such an effect.

Finally, the performance of various complex glazing systems could be investigated for future climate scenarios currently available by UKCIP (2002). The above future scenarios could be downscaled by the use of morphing techniques in order to produce hourly weather data (CIBSE, 2005 and Hacker et al, 2005). A risk assessment approach could be used in order to estimate how different glazing solutions could affect the energy performance of highly glazed buildings and help towards preparing a contingency plan for longer periods of hot cloudless days and high temperatures.

## *9.4 Conclusions*

This work aimed to solve the problem of high solar gains in highly glazed buildings which could cause overheating, by examining the thermal performance of various shading

options through the use of thermal modelling. The above was achieved through a series of steps: identify the elements most important in shaping the thermal performance of glazing systems and the current needs in the calculation of such performance; select the right prediction tools modifying them where needed; identify the thermal performance representation and its calculation; validate the prediction tools; apply the prediction tools to calculate the thermal performance of various representative shaded glazing systems, under both steady-state and real climate conditions; apply the prediction tools to examine how the various glazing options effect the thermal state of the space.

The above steps identified the complexity of the currently used g-value as a representation of the thermal performance of glazing options and drawbacks of its use as a steady-state value. Examples demonstrated that the steady-state G could potentially give misleading information about the seasonal thermal performance of a glazing system and also the potential to miss-inform the designer on the relative cooling load necessary to keep acceptable temperature levels in a space. A more dynamic approach in the calculation of the thermal performance of glazing options, by the use of appropriate computerised prediction tools, could result in more robust choices that minimise solar gains and reduce energy consumption for cooling in the building.

## *9.5 References*

Alexander, D K, Mylona, A & Jones, P J (2005) 'The Simulation of Glazing Systems in the Dynamic Thermal Model HTB2', Proceedings of the 9th International IBPSA Conference, Montreal, Canada

Hacker, J N, Belcher, S E and Connell, RK (2005) 'Beating the Heat: Keeping UK Buildings Cool in a Warming Climate', UKCIP Briefing Report, UKCIP, Oxford

Hacker, J N, Holmes, M, Belcher, S E and Davies G (2005) 'Climate Change and the Indoor Environment: Impacts and Adaptation', CIBSE TM 36, Chartered Institution of Building Services Engineers, London